

https://dspace.org/

Mineralogical and geochemical studies of some witwatersrand gold ores with special reference to the nature of the phyllosilicates

Von Rahden, Herbert, Valentin, Richard

1970
http://hdl.handle.net/10539/22042

Downloaded from a DSpace repository. https://dspace.org/

MINERALOGICAL AND GEOCHEMICAL STUDIES OF SOME WITWATERSRAND GOLD ORES WITH SPECIAL REFERENCE TO THE NATURE OF THE PHYLLOSILICATES.

A thesis submitted for the degree of Doctor of Philosophy in the Faculty of Science at the University of the Witwatersrand

by

Herbert Valentin Richard von Rahden B. Sc. Hons. (Cape Town), M. Sc.

November 1970.

DECLARATION.

I, Herbert Valentin Richard von Rahden, do hereby declare that this work is my own and that it has not been submitted previously for any degree at any University.

HVR von Rahden

November 1970.

ABSTRACT.

The present thesis is divided into three parts. The study described in Part I arose out of a request by the Chamber of Mines Mining Research Laboratory to the National Institute for Metallurgy to undertake a preliminary study of whether it would be feasible, in Witwatersrand conglomerates, to carry out rapid delimitation of areas rich in gold and/or uranium at the rock face, a procedure which would permit areas of rich ore to be removed selectively by means of the "rock-cutter". The approach adopted in this study was essentially geochemical, while conventional mineralogical techniques (macro-autoradiographs, thin section and polished section analyses) provided a control. The samples were drawn from the Vaal Reef at Hartebeestfontein and Zandpan and from the Ventersdorp Contact Reef at Venterspost, and were analysed quantitatively for gold, silver, uranium, pyrite, muscovite, pyrophyllite, chlorite, quartz, iron, potassium, nickel, titanium, zirconium and chromium. The intensity of the interrelationships between the elements and minerals analysed for was examined statistically by means of correlation covariance and factor analysis programmes written for an IBM 360/50 digital computer. A sympathetic relationship -- defined as significant positive correlation (with a correlation coefficient $r > 0.7$) -- was found to exist between gold and uranium in both the Vaal Reef and Ventersdorp Contact Reef samples. These findings suggest that gold and uranium can be removed simultaneously by means of the rock-cutter, and that radioactivity can be used as an indicator for on-site delimitation of areas rich in gold.

In the course of the study described in Part I, it became evident that little detailed mineralogical work had ever been done on the phyllosilicates occurring in the Witwatersrand System. Accordingly, certain phyllosilicates from Witwatersrand conglomerate bands and other sources were examined in detail, this study being described in Part II of the present thesis. This study called for detailed chemical, optical, X-ray crystallographic, infra-red, differential thermal and thermogravimetric analyses, the results of which are presented. The findings were examined in the light of various classification schemes that have been proposed for the phyllosilicates. This investigation revealed the need for a universally acceptable system of classification for the phyllosilicates, which should preferably be drawn up under the auspices of the International Mineralogical Association to avoid the confusion that exists at present.

Part III of the present thesis is devoted to a discussion and description of various analytical techniques that had to be modified or developed to meet the requirements of the studies described in Parts I and II. The techniques described include:

(1) An X-ray diffraction method which was developed for the quantitative analysis of pyrite, muscovite, pyrophyllite, chlorite and quartz in crushed ore from Witwatersrand conglomerates. This method makes use of novaculite as an external standard and of binary mixtures as analytical standards, and had a mean absolute error of 1.1%. This method may be expanded to permit analysis of an n-component mixture.

(2) A whole rock pressed powder technique of X-ray fluorescence analysis which was used for the quantitative determination of iron, potassium, nickel, titanium, zirconium and chromium. This method makes use of international rock standards as external standards.

Six computer programmes used for the computation of the analytical results and in the statistical and crystallographic calculations are also presented in Part III.

CONTENTS.

		Page
	PART I	
1.	INTRODUCTION	1
1.1.	Reasons for Undertaking the Present Investigation	1
1.2.	The Aims of the Present Study	2
1.3.	Source of Samples for the Present Study	4
1.4.	Geological Setting	5
1.4.1.	The Witwatersrand System	5
1.4.2.	Vaal Reef	6
1.4.3.	Ventersdorp Contact Reef	7
1.5.	Previous Work	7
1.5.1.	Vaal Reef	7
1.5.2.	Ventersdorp Contact Reef	9
1.5.3.	Quantitative Studies	10
1.6.	Techniques Adopted in the Present Study	12
2.	SAMPLING TECHNIQUES	14
2.1.	Collection of Bulk Samples from the Mines	14
2.2.	Subdivision of Individual Bulk Samples	14
3.	OPTICAL STUDIES	16
3.1.	Macroscopic Studies	16
3.2	Microscopic Studies	18
3.2.1.	Thin section studies	19
3.2.2.	Polished section studies	21
3.2.2.1.	Gold	21
3.2.2.2.	Uraninite	22
3.2.2.3.	The alteration products of uraninite	23
3.2.2.4.	Thucholite	24
3.2.2.5.	Pyrite	26
3.2.2.6.	Rare sulphides	27
3.2.2.6.1.	Pyrrhotite	27
3.2.2.6.2.	Cobaltian-gersdorffite and cobaltite	27
3.2.2.6.3.	Molybdenite	28
3.2.2.7.	Titanium minerals	28
3.2.2.8.	Zircon	28

		Page
3.2.2.9	Chromite	29
3.3.	Optical Studies -- Conclusions	29
4.	STATISTICAL EVALUATION OF RESULTS OF QUANTITATIVE ANALYSES	32
4.1.	Introduction	32
4.2.	Statistical Concepts	33
4.2.1.	Product-moment correlation coefficient	33
4.2.2.	Factor analysis	34
4.3	Logarithmic Transformation of Data	37
4.4.	Results of Statistical Treatment of Analytical Data	37
4.5.	Discussion of Results	38
4.5.1.	Means, standard deviations and coefficients of variation for the three mines examined	38
4.5.2.	Correlation studies	38
4.5.2.1.	Correlation coefficient matrix	45
4.5.2.2.	Factor analysis	46
4.5.2.3.	Summary of results of correlation studies	49
5.	DISCUSSION OF RESULTS AND CONCLUSIONS	52
5.1.	Introduction	52
5.2.	Comparison of Results of Mineralogical and Geochemical Studies	53
5.3.	Relationships between Minerals in the Vaal Reef and Ventersdorp Contact Reef	54
5.3.1.	Gold and uranium	55
5.3.2.	Pyrite, gold and uranium	56
5.3.3.	Zircon, chromite and other heavy minerals	57
5.3.4.	Phyllosilicates	59
5.4.	Conclusions	59
	PART II	
6.	PHYLLOSILICATE MINERALOGY	62
6.1.	Introduction	62
6.2	Chlorite	65
6.2.1.	Chlorite in Witwatersrand conglomerates	65
6.2.2.	Chlorite in the Ventersdorp Contact Reef and Vaal Reef	66

		Page
6.2.3.	The identification of minerals of the chlorite group	67
6.2.3.1.	The structure of chlorite	67
6.2.3.2.	Proposed systems of classification of chlorites -- a review	67
6.2.3.2.1.	Optical methods	67
6.2.3.2.2.	Chemical composition as a basis for the classification of chlorites	67
6.2.3.3.	Analytical techniques used as aids in the characterization of chlorites	68
6.2.3.3.1.	X-ray diffraction as an aid in the classification of the chlorites	68
6.2.3.3.2.	Infra-red spectroscopy as an aid to the classification of the chlorites	69
6.2.3.3.3.	Differential thermal analysis and thermogravimetric analysis as aids to the classification of the chlorites	69
6.2.3.3.4.	Electron microscopy and electron diffraction as aids to the study of the chlorites	70
6.2.3.4.	The characterization of chlorite from the Venters-dorp Contact Reef at Venterspost, and of two other chlorites	70
6.2.3.4.1.	Optical studies	71
6.2.3.4.2.	Sample preparation for X-ray diffraction, and other, studies on chlorites	72
6.2.3.4.3.	X-ray diffraction studies on the three chlorites	72
6.2.3.4.4.	Infra-red spectroscopy studies on the three chlorites	75
6.2.3.4.5.	Chemical analyses of the three chlorites	75
6.2.3.4.6.	Structural formulae of the three chlorites	75
6.2.3.4.7.	Differential thermal analysis and thermogravimetric analysis of the three chlorites	77
6.2.3.4.8.	Subsequent heat treatment of the chlorites from Vermont, Venterspost and New Mexico	78
6.2.3.5.	Discussion of results of analyses carried out on the three chlorites from Vermont, Venterspost and New Mexico	78
6.2.3.5.1.	X-ray diffraction	78
6.2.3.5.2.	Infra-red spectroscopy	82
6.2.3.5.3.	Differential thermal and thermogravimetric analyses (D.T.A. and T.G.A.)	84

		Page
6.2.3.5.4.	The varietal classification of the three chlorites examined	85
6.2.3.5.5.	The characterization of chlorites -- conclusions	88
6.3.	Pyrophyllite	89
6.3.1.	Occurrence and genesis of pyrophyllite in the Witwatersrand	89
6.3.2.	Characterization of pyrophyllites from Loraine and Gestoptefontein	90
6.3.2.1.	Introduction	90
6.3.2.2.	Chemical analyses	92
6.3.2.3.	Structure and structural formulae of pyrophyllite from Gestoptefontein and Loraine Gold Mine	93
6.3.2.4.	X-ray diffraction	93
6.3.2.5.	Infra-red spectroscopy	93
6.3.2.6.	Discussion of results	94
6.4.	Muscovite	97
6.4.1.	Introduction	97
6.4.2.	A review of the structure and nomenclature of the muscovites	98
6.4.2.1.	Muscovite	99
6.4.2.2.	Sericite	101
6.4.2.3.	Hydro(us)-muscovites	101
6.4.2.4.	Illites	102
6.4.2.5.	Properties of the muscovite minerals -- a summary	104
6.4.3.	Experimental studies on muscovites, hydromuscovite and illite	105
6.4.3.1.	X-ray diffraction studies on muscovite, hydromuscovite and illite	106
6.4.3.2.	Infra-red spectroscopy studies on muscovites, hydromuscovite and illite	106
6.4.3.3.	Chemical analyses of muscovites, hydromuscovite and illite	109
6.4.3.4.	Structural formulae for two muscovites, hydromuscovite and illite	111
6.4.3.5.	Discussion of results	111
6.4.3.5.1.	X-ray diffraction	111
6.4.3.5.2.	Infra-red spectroscopy	112

		Page
6.4.3.5.3.	Chemical composition of the micas	113
6.4.3.5.4.	The usefulness and limitations of X-ray diffraction analysis and infra-red spectroscopy in the study of the micas	114
6.4.3.6.	The nature of the mica present in samples from the Vaal Reef at Hartebeestfontein and Zandpan and from the Ventersdorp Contact Reef at Venterspost	114
	PART III	
7.	PREPARATION OF SAMPLES FOR QUANTITATIVE ANALYSIS	116
7.1.	Introduction	116
7.2.	Sample Preparation	116
8.	ANALYTICAL TECHNIQUES USED IN THE PRESENT STUDY	118
8.1.	Introduction	118
8.2.	Chemical Analysis	118
8.3.	Atomic Absorption Spectrophotometry	118
8.4.	Quantitative X-ray Fluorescence Analysis	118
8.4.1.	Sample preparation for X-ray fluorescence analysis	119
8.4.1.1.	Reasons for choice of pressed powder briquette technique for X-ray fluorescence analysis	119
8.4.1.2.	Preparation of pressed powder briquettes	119
8.4.2.	Matrix effects	120
8.4.2.1.	Mass absorption coefficient	120
8.4.2.2.	Development of a method for the determination of the mass absorption coefficient of a sample by direct measurement	122
8.4.2.3.	Verification of analytical procedure for determination of mass absorption coefficient	126
8.4.3.	Methods of quantitative X-ray fluorescence analysis	127
8.4.3.1.	The internal standard method	127
8.4.3.2.	The external standard method -- international rock standards	128
8.4.4.	Method of quantitative X-ray fluorescence analysis adopted in the present study	128

		Page
8.4.4.1.	Instrumental variables in X-ray fluorescence analysis	129
8.4.4.1.1.	X-ray tube target	129
8.4.4.1.2.	Analysing crystals	129
8.4.4.1.3.	Choice of counter	129
8.4.4.1.4.	Counting losses	130
8.4.4.1.5.	Counting times	130
8.4.4.2.	Calculation of results of quantitative X-ray fluorescence analysis	131
8.4.4.3.	Check on the self-consistency of the method of X-ray fluorescence analysis used in the present study	131
8.5.	Quantitative X-ray Diffraction Analysis	132
8.5.1.	Introduction	132
8.5.2.	Fundamental concepts and techniques in quantitative X-ray diffraction analysis	133
8.5.2.1.	Choice of radiation	133
8.5.2.2.	Detection limit	133
8.5.2.3.	Peak position	134
8.5.2.4.	The measurement of intensity	134
8.5.2.5.	Techniques used in integration	135
8.5.2.5.1.	Triangulation	135
8.5.2.5.2.	Planimetry	136
8.5.2.5.3.	Height times width at half peak height	136
8.5.2.5.4.	Cut and weigh	136
8.5.2.5.5.	Disc Integrator	136
8.5.2.6.	The choice of divergence slits	137
8.5.3.	Factors affecting the intensity of reflections in X-ray diffraction analysis	138
8.5.3.1.	Intensity and sample particle size	138
8.5.3.2.	Intensity and the effect of background	140
8.5.3.3.	Intensity and sample thickness	141
8.5.3.4.	Sample holders and their effect on intensity measurements	142
8.5.3.4.1.	Rotary sample holders	142
8.5.3.4.2.	Stationary sample holders	143
8.5.3.5.	Preferred orientation and intensity measurements	146
8.5.3.6.	Mass absorption and peak intensities	147

		Page
8.5.4.	Methods of quantitative X-ray diffraction analysis	148
8.5.5.	Method of X-ray diffraction analysis adopted for the present study	151
8.5.5.1.	General considerations	151
8.5.5.2.	The preparation of binary-mixture standards	153
8.5.5.3.	The determination of mass absorption coefficients for Witwatersrand samples and for binary-mixture standards	155
8.5.5.4.	Procedure adopted for quantitative X-ray diffraction analysis	156
8.5.5.4.1.	Instrument settings	156
8.5.5.4.2.	Choice of analytical peaks	156
8.5.5.4.3.	Detection limits	157
8.5.5.4.4.	Precision of measurement	158
8.5.5.4.5.	Procedure for the determination of diffracted intensities in Witwatersrand samples and binary-mixture standards	158
8.5.5.5.	Calculation of results of quantitative X-ray diffraction analyses	159
8.5.5.5.1.	Preparation of calibration curves for binary-mixture standards	159
8.5.5.5.2.	Evaluation of equation 10	160
8.5.5.6.	Check on the accuracy of the method of quantitative X-ray diffraction analysis adopted in the present study	161
8.6.	The High-precision Determination of the Cell Parameters of Phyllosilicates	163
8.6.1.	General considerations	163
8.6.2.	Sample preparation for cell parameter determinations	164
8.6.3.	Measurement of angular position and intensity of peaks	164
8.7.	Infra-red Spectroscopy	165
9.	COMPUTER PROGRAMMES	166
10.	ACKNOWLEDGEMENTS	168
11.	REFERENCES	169

PART I

MINERALOGICAL AND GEOCHEMICAL STUDIES OF THREE WITWATERSRAND GOLD MINES.

1. INTRODUCTION.

1.1. Reasons for Undertaking the Present Investigation.

In the years that have elapsed since the discovery of gold on the Witwatersrand in 1886, mining operations have had to be carried out at ever-increasing depths, and the recovery of the gold has accordingly become an increasingly complex and expensive process. Traditional mining methods involve drilling, blasting with explosives and the removal to the surface of large amounts of broken rock. As a considerable portion of this may be barren or "waste" rock, the cost of extraction is high. Furthermore, this unselective procedure demands an extremely large labour force, which in turn leads to high mine-ventilation costs and adds to the cost of extraction. The stage has now been reached where it is desirable to investigate the possibility of alternative mining methods that will be more selective with regard to the excavation of barren rock.

The Mining Research Laboratory of the Chamber of Mines of South Africa has already carried out considerable research into the development of a prototype rock-cutting device that makes it possible to cut and remove relatively narrow parallel-sided slabs of rock from the rock face (Cook et. al., 1968). This makes the selective mining of ore feasible and thus offers an opportunity of reducing the amount of "waste" or barren rock to a minimum, with a consequent reduction in many handling, transport, hoisting and milling tasks. The rock-cutter has other potential advantages, including the possibility of better strata control because of the reduction in effective stoping width. This, coupled with the fact that blasting would be eliminated, should greatly reduce the likelihood of rockfalls and rockbursts. Yet another advantage of the rock-cutting method is the ease with which parallel-sided slabs of waste rock can be cut for use as packs to support the roofs of the drives.

Thus, in theory, the rock-cutter offers considerable advantages over conventional mining techniques. However, gold-bearing conglomerate bands in the Witwatersrand can vary in thickness from a few centimetres to six metres or more (as described in Section 1.4), and the advantages of the rock-cutter would be greatly reduced if all six metres of the conglomerate band had to be cut and moved to the surface. Some method for the delimitation of those particular areas of thick conglomerate bands that are most likely to contain gold or uranium or

both, so that only relatively narrow slabs of ore rich in gold or uranium need be removed, is obviously a prerequisite for the successful utilization of the rock-cutter. Reliance on normal gold assays for guidance in positioning the rock-cutter would, however, lead to delays in mining operations because of the time-consuming nature of the gold assay procedure itself and because of the laborious daily sampling programme that would become necessary. As it is, a total of some 300 underground samples is already taken per day in a mine of average size, since chip samples taken at regular intervals along exposed faces usually provide the basic data for all valuation purposes (Munro, 1966, p.4).

In view of these problems, the Chamber of Mines Mining Research Laboratory requested the National Institute for Metallurgy to undertake an investigation as to whether, in the Witwatersrand conglomerate bands at present being exploited, it would be feasible to carry out rapid delimitation of gold- and uranium-rich areas at the rock face. This investigation is described in Part I of this thesis.

1.2. The Aims of the Present Study.

The primary aim of the present study was, therefore, to carry out a preliminary investigation of the feasibility of rapid on-site delimitation of areas of high gold and uranium content in Witwatersrand conglomerate bands. Since some visual or rapid instrumental method of delimitation was envisaged, it was apparent that the following features would have to be investigated:

(1) The spatial distribution of gold and uranium in Witwatersrand conglomerate layers, to see whether the gold and uranium do in fact occur in localized areas within the conglomerate beds, as would be most desirable for the successful application of the rock-cutting technique.

(2) The relation between gold and uranium, because it would indicate whether these elements (in their mineral form) could be removed simultaneously, and whether radioactivity (from the uranium-bearing minerals) could be used as an indicator of gold.

(3) The relationship between the distribution of gold and uranium and the distribution of certain other easily-recognizable minerals in the conglomerate beds, as these other minerals (if they were found to vary sympathetically with gold and uranium) might provide clues whereby gold- and uranium-rich layers of ore could be identified. As pyrite is, generally, a very conspicuous component of most conglomerate beds, the distribution of gold and uranium relative to the distribution of pyrite was thought to be worth investigating. Similarly, as certain

phyllosilicates (such as chlorite, muscovite and pyrophyllite) are known to be generally present in various gold-bearing conglomerate beds, and to modify the colours of such beds in specific areas, it was decided that the relation of chlorite, muscovite and pyrophyllite to gold and uranium should be examined quantitatively. In addition, it was decided that geochemical correlation studies should be carried out, and that for this purpose the following elements should be analysed for quantitatively: Au, Ag, U, Ni, Ti, Zr, Cr, K and Fe.

If meaningful conclusions regarding these relationships were to be reached, it was clear that the qualitative and subjective techniques often used in the past would have to be abandoned. It was apparent that an objective, quantitative approach was called for, and that the results obtained should be evaluated by strict statistical methods. It was therefore decided that the following experimental programme should be adopted:

(a) Samples should be obtained from several Witwatersrand horizons, so that the validity of conclusions could be double-checked on more than one conglomerate band.

(b) These samples should be taken in such a way that each would represent a complete cross-section of the conglomerate band.

(c) The samples should first be investigated by optical techniques. Macroscopic studies, thin section and polished section studies should be carried out in order to gain some idea of the spatial distribution of various minerals across the whole conglomerate band.

(d) Quantitative analyses, which would be capable of undergoing rigorous statistical examination, should then be carried out on samples obtained by subdivision of the original samples. Comparison of the results of these analyses with the results of the optical studies should permit an objective assessment of the spatial distribution of elements and minerals across the complete conglomerate band to be made. It was decided that the following 14 variables should be analysed for quantitatively: gold, silver, uranium, pyrite, muscovite, pyrophyllite, chlorite, quartz, iron, potassium, nickel, titanium, zirconium and chromium.

As the present investigation proceeded, its aims were expanded to include the examination of certain phyllosilicates occurring in Witwatersrand conglomerate bands. This study was undertaken when it became clear that comparatively few detailed mineralogical studies had previously been carried out on phyllosilicates occurring specifically in the gold-bearing conglomerates of the Witwatersrand System, although the phyllosilicates as a group constitute a major part of the

non-quartz mineral assemblage of these conglomerates. Various phyllosilicates from the Witwatersrand banket were subjected to detailed mineralogical examination in the course of the present study, and the results of these examinations are reported in Part II of this thesis.

1.3. Source of Samples for the Present Study.

As the present investigation into the practicability of rapid on-site delimitation of areas of high gold and uranium content in Witwatersrand conglomerate bands was intended to be only a pilot study, sampling was restricted to three mines: Hartebeestfontein and Zandpan, where the Vaal Reef was sampled, and Venterspost, where samples were taken from the Ventersdorp Contact Reef. The locations of these mines are shown in the location map (Figure 1), and the geological features of the Vaal Reef and the Ventersdorp Contact Reef are discussed in Section 1.4.

These particular mines were selected as sample sources for the following reasons:

(1) Samples were taken from the Vaal Reef at both Hartebeestfontein and Zandpan in view of the fact that, although the two mines are in close proximity to one another, Zandpan, unlike Hartebeestfontein, is characterized by areas in which low and unpay values are encountered (Wilson, Oosthuizen, Brink and Toens, 1964, p. 409). It was therefore thought that it would be interesting to compare the nature of the mineralization of the Vaal Reef at the two mines.

(2) The Ventersdorp Contact Reef at Venterspost mine was chosen because its mineralogy (examined by von Rahden in 1964) appeared to be different from that of the Vaal Reef (examined by Jacob at the Vaal Reefs gold mine in 1966). It was therefore thought that it would be interesting to compare the geochemistry of the Ventersdorp Contact Reef with that of the Vaal Reef, and to see whether conclusions regarding the feasibility of on-site delimitation of areas of rich gold and uranium mineralization derived from work on Vaal Reef samples would in fact be substantiated by work on Ventersdorp Contact Reef samples.

(3) Another reason for investigating samples from the Ventersdorp Contact Reef was provided by the fact that it attains a much greater thickness than the Vaal Reef and would therefore present a far greater challenge to the successful operation of the rock-cutter.

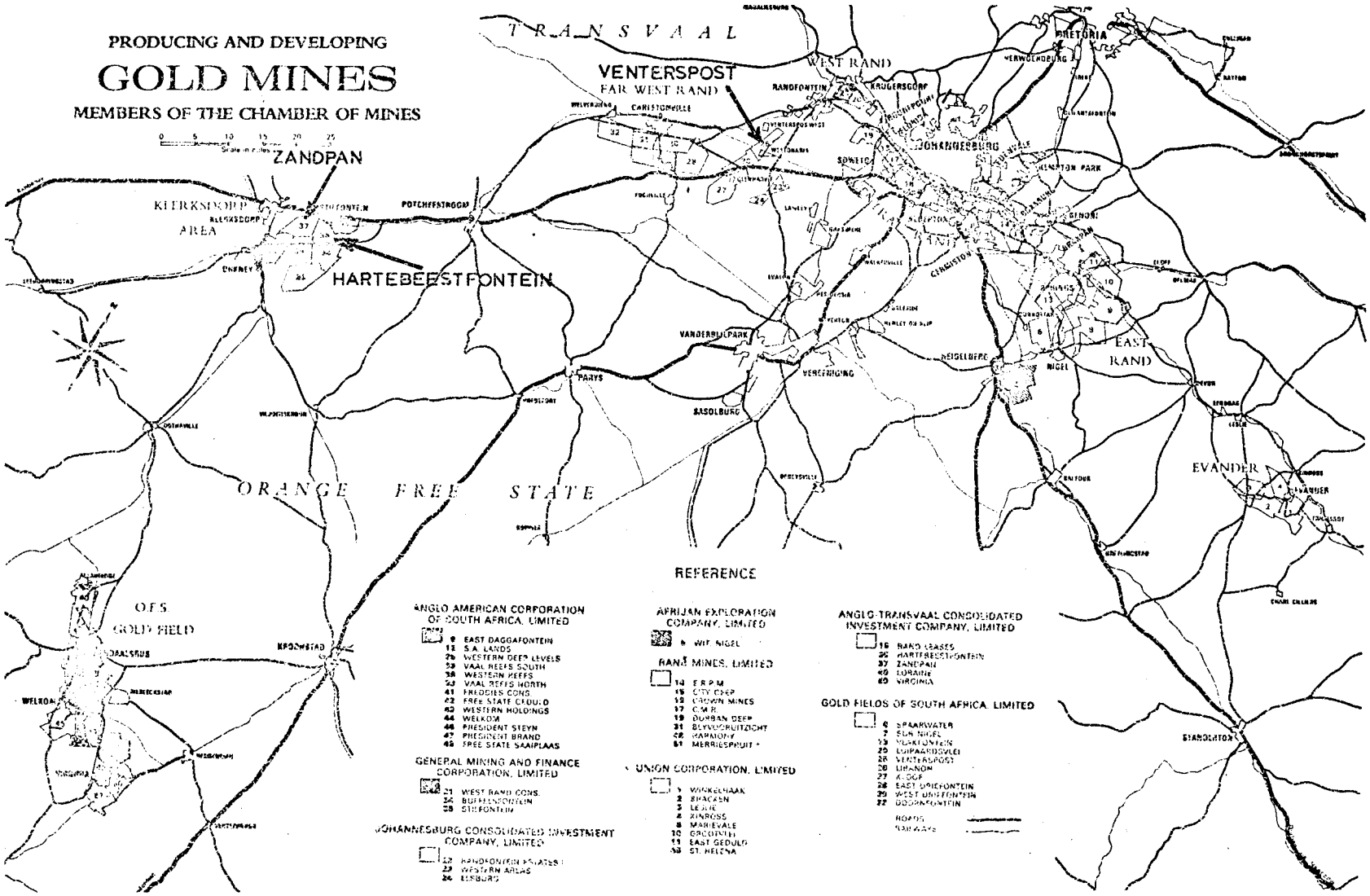


FIGURE 1 LOCATION MAP

1.4. Geological Setting.

1.4.1. The Witwatersrand System.

"The Witwatersrand System consists of a succession of arenaceous and argillaceous rocks deposited in a sedimentary basin which was set in a stable craton composed of some of the oldest rocks on the African continent. ..... Closely associated with the Witwatersrand System, temporally and structurally, are the Dominion Reef System and the Ventersdorp System. .... Their relationships suggest that the three Systems collectively constitute a major geological cycle. .... The Witwatersrand System is divided into an Upper Division and a Lower Division, which differ from each other lithologically and also with respect to their importance as gold carriers." (Brock and Pretorius, 1964, pp. 26 - 27).

The Lower Division of the Witwatersrand System consists mainly of shales and quartzites with some beds of conglomerate, whereas the Upper Division is composed mainly of quartzites and conglomerates. These conglomerates are referred to locally as banket. Most of the conglomerates contain gold but only a few are rich enough to be of economic importance, the productive beds being restricted to the Upper Division.

"The Lower Division is more widely distributed than the Upper, and there is no doubt that the original area of deposition of the former was of greater dimensions than that of the Upper Division. At present it is believed that the occurrence of rocks of the Upper Division is restricted to one main basin, referred to as the Rand basin ...., and a very much smaller basin, the Kinross basin, which lies about 40 miles east of the north-eastern extremity of the main basin. The long axis of the Rand basin is oriented north-east, the most south-westerly extremity occurring between Theunissen and Virginia in the Orange Free State, and the most north-easterly between Springs and Delmas in the Transvaal. The distance between these extremities is of the order of 180 miles. The maximum width of the Rand basin stretches from Krugersdorp in the north-west to a point between Greylingstad and Villiers in the south-east, this diameter being about 80 miles. The area thus underlain by the Rand basin amounts to approximately 15,000 square miles." (Brock and Pretorius, 1964, p. 27).

The genesis of the gold of the Witwatersrand has remained a matter of controversy ever since the gold was first discovered. In this regard there are now two major opposing theories, the "placer theory" and the "hydrothermal theory", with the "modified placer theory" being currently the most favoured.

According to the modified placer theory the gold was originally detrital, and the conditions of deposition that produced the extensive pebble beds of the Witwatersrand also caused the accumulation in these beds of rich concentrations of alluvial gold, uraninite, and platinoids. It is then postulated that at some subsequent period in geological history the conglomerates were subjected to dynamic metamorphism and metasomatism, and that this resulted in complicated changes being induced in the constituents of the conglomerates, more especially in the finer sandy material lodged between the more resistant pebbles. It is postulated that one of the changes occurring during this period was the recrystallization and/or solution of the original detrital gold and its re-precipitation almost, if not quite, in situ. The rival theory, the hydrothermal theory, is less generally supported than the modified placer theory. This theory maintains that the gold, uraninite and platinoids of the Witwatersrand were introduced into the conglomerates by post-sedimentary hydrothermal solutions. (Liebenberg, 1960, p. 836).

1.4.2. Vaal Reef.

The Vaal Reef is the most important auriferous conglomerate horizon mined at Hartebeestfontein and Zandpan. These two mines, together with three other gold-producing mines, are situated within an elliptical basin lying east and south of Klerksdorp some 100 miles south-west of Johannesburg (Figure 1).

Stratigraphically, the Vaal Reef is a member of the Main Bird Series of the Upper Division of the Witwatersrand System. The Main Bird Series is made up of the Bird Reef Stage, the Livingstone Reef Stage and the Main Reef Stage, and the Vaal Reef lies at the base of the MB4 Zone, the lowermost member of the Bird Reef Stage (Figure 2). Regionally, the Vaal Reef has been correlated with the Basal Reef, which occurs in the Orange Free State Goldfields, and with the Bird Reef of the West Rand.

The Vaal Reef is a small pebble, oligomictic, well-mineralized conglomerate, the thickness of which may vary from a few millimetres to nearly 2 metres. The pebbles are composed of quartz, quartzite and chert, and only very rarely exceed 40 mm in size. They are generally close-packed, and are in turn cemented together by finer interstitial quartz particles, phyllosilicates and sulphides. Thucholite ("carbon") is a common constituent and occurs either as "warty" granules up to 1 mm in diameter or as seams 2 to 3 mm thick, or, exceptionally, as wider seams some 25 mm thick.

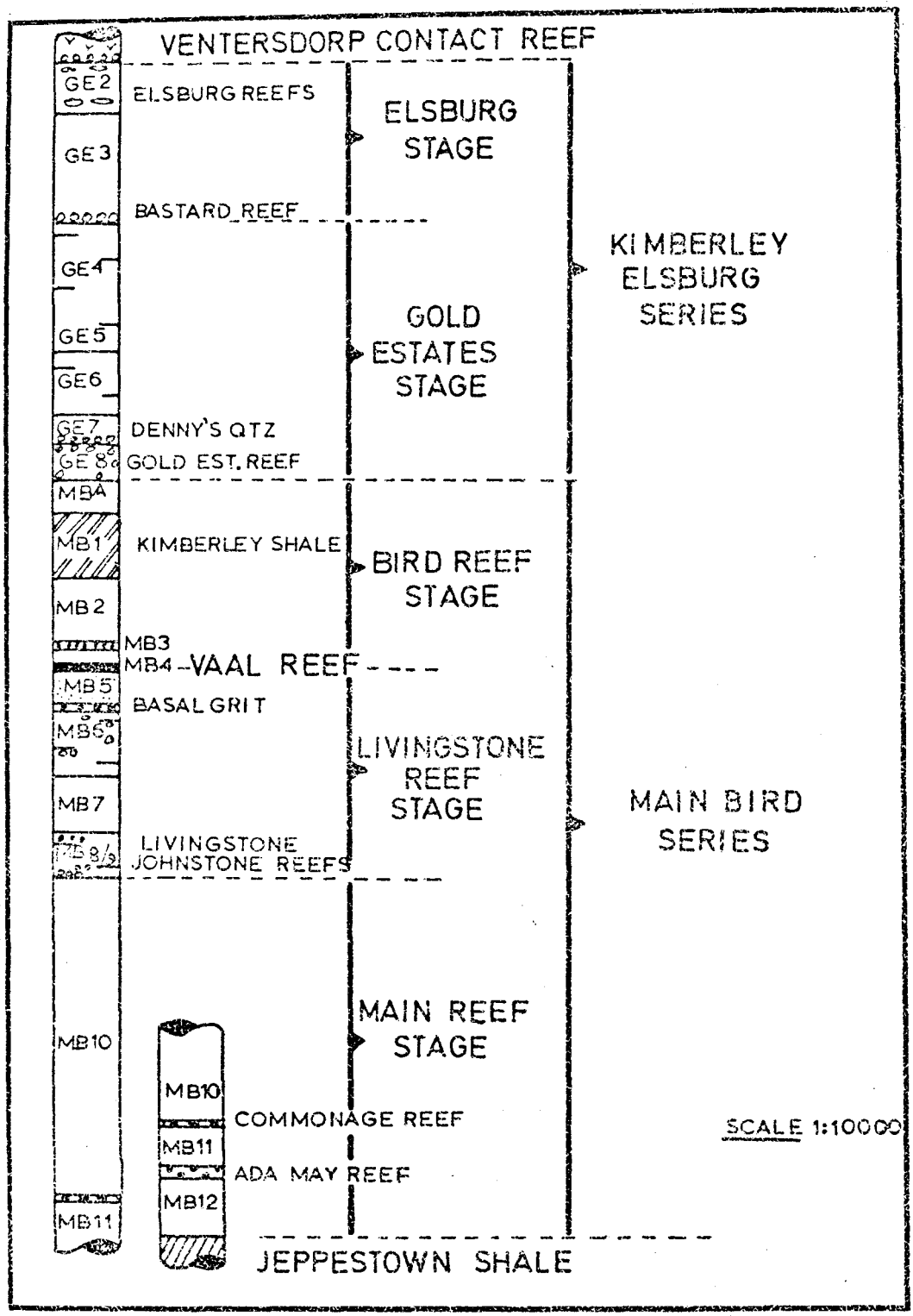


FIGURE 2 GENERALISED GEOLOGICAL SECTION THROUGH THE KLERKSDORP AREA (after Wilson et al, 1964)

The Vaal Reef at Hartebeestfontein and Zandpan is overlain by a siliceous orthoquartzite, which varies in colour from pale grey to white and which in turn serves to separate the Vaal Reef from the overlying Leader Reef. The MB5 Zone forms the immediate footwall of the Vaal Reef, and is composed of alternating argillaceous and silica-rich quartzites, which in turn are underlain by a pyrite-rich, small pebble, oligomictic conglomerate some 15 cm thick.

1.4.3. Ventersdorp Contact Reef.

The auriferous conglomerate known as the Ventersdorp Contact Reef (V.C.R.) may, according to de Kock (1964, p. 314) be considered to represent a reworked eluvial scree which accumulated on an old erosion surface of the Witwatersrand System and which owes its preservation to the outpouring of the overlying Ventersdorp Lavas. The term "Contact Reef" is merely a descriptive term adopted to indicate the position of the horizon at the stratigraphic contact of the Witwatersrand and Ventersdorp Systems (Figure 3).

The V.C.R. at Venterspost is characterized by a wide variation both in the size of the pebbles, which vary from 3 mm to 40 cm, and in the thickness of the bed, which varies from a single pebble layer to a thickness of over 3 metres. The pebbles are composed of a mixture of vein quartz, chert and shale fragments cemented by chloritic material which in turn contains embedded grains of pyrite and pyrrhotite. The pebbles are generally well-packed and fairly well sorted, except where the size of the pebbles exceeds 25 cm.

The "hanging wall" (the roof of the V.C.R.) is generally composed of tuffaceous material overlain in turn by bluish-green Ventersdorp Lava of andesitic composition. The "footwall" (the base of the V.C.R.) is composed of quartzites belonging to the Kimberley Series of the Upper Division of the Witwatersrand System (Figure 3).

1.5. Previous Work.

1.5.1. Vaal Reef.

The mineralogy of the Vaal Reef at Hartebeestfontein and Zandpan does not appear to have been extensively studied in the past. Liebenberg (1955, pp. 156 - 157) examined some samples from the Vaal Reef in the course of a study of gold and radioactive minerals in the Witwatersrand banket, and mentioned the occurrence of leucoxene accompanying unaltered detrital uraninite, secondary uraninite and thucholite in freshly-exposed conglomerate from the Vaal Reef at Ellaton,

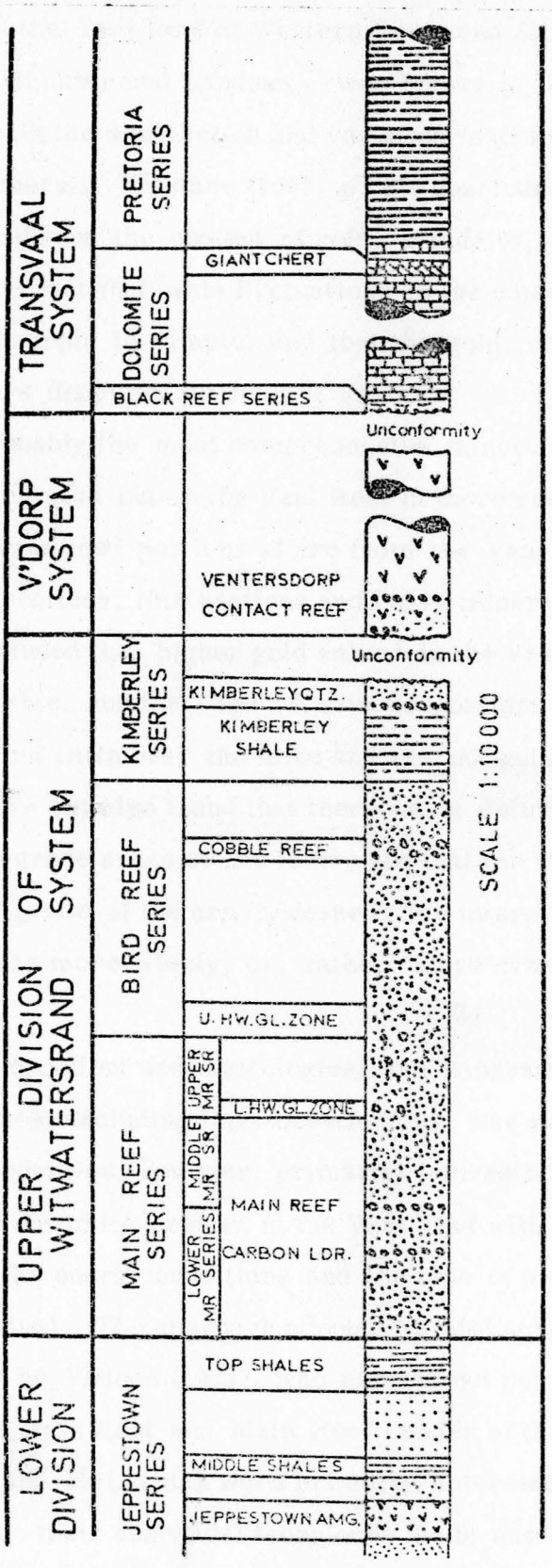


FIGURE 3 GENERALISED GEOLOGICAL SECTION OF THE WEST WITS LINE (after de Kock 1964)

Stilfontein, Hartebeestfontein and Buffelsfontein mines. Coetzee (1965, p. 61) examined ore from the Vaal Reef at Western Reefs and Stilfontein mines (which abut onto Hartebeestfontein and Zandpan -- see Figure 1), but this study was concerned primarily with the distribution and variation in grain size of gold, pyrite and other heavy minerals. Coetzee (1965, p. 87) concluded that a sympathetic relationship existed between the content of gold, uraninite, pyrite and other heavy minerals despite the fact that wide fluctuations in the content of these minerals might occur from sample to sample, and that the gold, uraninite, pyrite and other heavy minerals were deposited as detrital grains.

Probably the most comprehensive mineralogical and geological study to have been carried out on the Vaal Reef in more recent years is that by Jacob (1966), who examined portions of ore from the Vaal Reefs Gold Mine by means of polished sections, thin sections and heavy mineral concentrates. Jacob (1966, p. 110) concluded that higher gold values in the Vaal Reef were associated with larger pebble size, and that "the relative proportions of quartz, quartzite and chert pebbles vary but little over the mine and are not related to gold distribution". Jacob (1966, pp. 58 - 59) also found that there was a definite increase in the U_3O_8 : Au ratio in the low-grade areas of the mine, and that the U_3O_8 : Au ratio decreased as the payability of grade of the ore increased. He interpreted this as indicating that the uraninite was more widely, or, rather, more evenly, dispersed than the gold.

An excellent sedimentological and mineralogical study of the Vaal Reef at various mines, including Hartebeestfontein, was recently carried out by McLachlan (1968), who was, however, primarily interested in studies of the grain sizes of zircon and chromite present in the Vaal Reef with the aim of using the data as an indication of the energy conditions and the type of environment in which this material was deposited. The approach adopted by McLachlan was very similar to that originally used by Viljoen (1964), who carried out petrographic and mineralogical studies of the Main Reef and Main Reef Leader of the Main Bird Series. Since both Viljoen and McLachlan were primarily interested in the sizes of zircon and chromite in situ, their analytical techniques made use of thin sections, polished sections and large oil-covered polished rock slabs, which were examined by means of a binocular microscope.

From her studies, McLachlan (1968, pp. 93 - 96) concluded that:

(1) The pebbles and matrix of the Vaal Reef appeared to be unrelated. Most of the matrix sediment of the reef was transported in a north-easterly

direction, while pebbles were brought in from the north-west at Stilfontein and the northern half of Hartebeestfontein mine. Transport in the southern half of Hartebeestfontein mine was from the west and south-west.

(2) Gold and other heavy mineral constituents in the Vaal Reef appeared to be unrelated. Gold was generally concentrated in the lower portion of the reef, and although the gold might be associated with heavy minerals in this zone, it did not follow that concentrations of heavy minerals higher up in the reef were associated with gold.

(3) There was a distinct lack of correlation between pebble size and gold tenor.

(4) The large differences in size between matrix minerals and pebbles in the reef militated against the idea of pebbles and matrix having been in hydraulic equilibrium.

(5) The main current direction in the Vaal Reef depository was towards the east-northeast, with a north-easterly distributing current transporting much of the matrix sediment in the Klerksdorp Goldfield. This material was carried predominantly in suspension and deposited in a low-energy environment of the back-swamp type.

(6) The pebbles in the Vaal Reef may have been deposited under deltaic conditions, but in view of the narrowness of the pebble band (generally only 8-10 cm thick) it is not likely that long periods of time were spent at these higher energy levels. An influx of pebbles was taken to indicate an increase in energy, but low energies probably prevailed for the most part during the deposition of the Vaal Reef.

1.5.2. Ventersdorp Contact Reef.

The Ventersdorp Contact Reef at Venterspost mine has been examined mineralogically by Davies (1949) and by Liebenberg (1955). Liebenberg (1955, pp. 218 - 220) concluded that:

(1) The gold occurred as native gold and had a relatively uniform composition.

(2) Uraninite was an allogenic detrital mineral and also occurred as secondary uraninite, which Liebenberg regarded as being an authigenic component of the conglomerates.

(3) A sympathetic relationship existed between the gold and the uranium content of the banket, and the origin of the gold and uranium could best be explained in terms of the modified placer theory.

Von Rahden (1964) also carried out a detailed mineralogical examination of the V.C.R. at Venterspost and at the adjacent mine, Libanon. He used polished sections and thin sections to study the interrelation and paragenesis of the minerals, and carried out quantitative studies of heavy-mineral concentrates prepared from rock chippings taken across the entire width of the conglomerate band. Von Rahden (1964, p. 47) noted an apparent association between gold, chlorite and sericite, with areas rich in gold being associated with areas containing more phyllosilicates, but at the time he was unable to investigate this apparent association further. From parallel studies carried out on the Main Reef at Venterspost and Libanon, von Rahden (1964, p. 134) concluded that the origin of the gold in the V.C.R. could best be explained in terms of the modified placer theory. Furthermore, following detailed studies of zircons in the V.C.R. and Main Reef, he concluded that these zircons had a common origin, or alternatively, that the zircons at present in the V.C.R. were derived from the underlying Main Reef.

Knowles (1966, p. 157), who proposed a new geological approach as a standard technique for determining the pattern of gold distribution in a reef, applied his method to the V.C.R. at Western Deep Levels, Ltd. He fitted computed trend surfaces to the gold values and to the sedimentary properties of the V.C.R., and concluded that the deviations from the trend surfaces could be related to folding, and that folding was a major factor that controlled the deposition of the V.C.R. and its gold content.

1.5.3. Quantitative Studies.

Various workers, such as Simpson (1951, p. 131), Liebenberg (1955, p. 215), Malan (1959, p. 83) and Coetzee (1965, p. 87) have claimed that a "sympathetic relationship" exists between gold and uranium and heavy minerals in Witwatersrand conglomerates. These workers apparently intended the term "sympathetic relationship" to mean that, in the auriferous conglomerates, an increase in gold is associated with an increase in uranium and heavy minerals and vice versa. Simpson (1951, p. 131) bases his conclusions regarding the existence of a sympathetic relationship between the gold and uranium contents of the banket on results derived from more than 500,000 routine assays for gold and uranium, whereas Liebenberg's conclusions were based on critical examinations of polished sections. Malan (1959, Plate 2) attempted to illustrate the existence of a sympathetic relationship by means of histograms, while Coetzee (1965, pp. 68 - 69) plotted the total amount of heavy minerals (zircon, chromite and leucoxene) against the gold and uranium contents of the samples examined and found

that the relationships were almost linear (Coetzee, 1965, Figures 2 and 3).

Cousins (1956, p. 95), on the other hand, has stated that he had found "sympathetic ratios" between gold, silver, uranium and osmiridium in the gold-bearing conglomerates of the Witwatersrand System. The term "sympathetic ratio", which Cousins defined as the similarity in the distribution curves of two sets of values when they are plotted as cumulative logarithmic values on a probability scale, has been severely criticized by Hiemstra (1968, pp. 79 and 82). Hiemstra stated: "Such a similarity simply means that the dispersion of the logarithms of the two sets of values, which could for instance be expressed as standard deviations, is the same." Hiemstra stressed that a difference exists between the terms "sympathetic ratio" as used by Cousins and "sympathetic variation" as used by Simpson and others, and questioned the validity or usefulness of the term "sympathetic ratio" (Hiemstra, 1968, p. 81). Hiemstra also noted that most of the work on "sympathetic relationships" and "sympathetic ratios" had, in any case, been based to a large extent on the study of polished sections, a technique that is susceptible to subjective interpretation.

To date, no attempt appears to have been made to investigate whether the amounts of the phyllosilicates muscovite, pyrophyllite and chlorite present in the Witwatersrand banket are related in any way to gold, uranium, sulphide or heavy mineral values. This omission probably stems from the fact that suitable analytical methods for the quantitative determination of the phyllosilicates have hitherto been lacking. Viljoen (1964, p. 109) used a point-counting technique on a limited number of thin sections to obtain semi-quantitative data for phyllosilicate concentrations in the Main Bird Series, but these results are not considered to be reliable in view of the difficulty of obtaining representative samples of a coarse material in a microscope slide and in view of the difficulty of identifying intergrown fine-grained phyllosilicates such as muscovite and pyrophyllite. X-ray diffraction methods for the semiquantitative, or even quantitative, determination of 2- and 3-component mixtures have been described in the literature, but no published methods were found to be suitable for the quantitative analysis of a heterogeneous multi-component mixture such as the Witwatersrand banket. Accordingly, in order to complete the present investigation it was necessary to devise an X-ray diffraction method that would permit the phyllosilicates in the Witwatersrand banket to be determined quantitatively. This method is described in detail in Part III of this thesis.

1.6. Techniques Adopted in the Present Study.

From the earlier work quoted above, it became apparent that any conclusions regarding relationships between gold and other substances (such as uranium, the phyllosilicates and the sulphides) in the Witwatersrand banket would only be valid if objective techniques had been used in the investigation and if qualitative and subjective assessments had been avoided. It was clear that the whole rock would have to be examined as well as fragments such as polished sections, thin sections and heavy mineral concentrates. Existing methods of chemical and mineralogical analysis had to be carefully assessed, with techniques being modified where necessary, and new techniques of quantitative X-ray diffraction analysis had to be developed. In order to express the intensity of the relationships quantitatively and to judge whether the relationships were significant, the objective approach used by Hiemstra (1968) in his mineralogical and geochemical study of material from the Dominion Reef was adopted for the present investigation. Hiemstra used the product-moment correlation coefficient of the logarithms of the analytical values to evaluate the relationships, a procedure that permits the results to be tested for significance by standard statistical methods and so eliminates subjective judgments.

As a prelude to their quantitative determination, the phyllosilicates were examined in detail by infra-red spectrophotometry, X-ray diffraction, differential thermal analysis and thermogravimetric analysis. Crystallographic calculations of structures of muscovite, chlorite and pyrophyllite were performed on an IBM Model 360/50 digital computer, using existing programmes which had to be rewritten into Fortran IV in order to be compatible with this computer. The actual amounts of pyrophyllite, muscovite, chlorite and pyrite present in the samples were determined quantitatively by X-ray diffraction, use being made of specially-developed techniques which are described in Part III of this thesis.

Gold and silver in the samples were determined quantitatively by means of atomic absorption spectrophotometry, and uranium was determined by a standard chemical method. Fe, K, Ni, Ti, Zr and Cr were determined quantitatively by X-ray fluorescence with the use of a powdered whole rock technique and international rock standards SY-1, G-1, W-1 and NIM-D. The X-ray fluorescence technique used in the present study is outlined in Part III of this thesis, and all other techniques that had to be developed or modified for the purpose of the present study are also discussed in Part III.

Microscopic examination of polished and thin sections was used for the identification of the ore minerals and some of the non-opaque minerals.

The IBM Model 360/50 digital computer was extensively used for the calculation of the analytical results. It was also used for curve-fitting and for all the statistical manipulations required for the evaluation of the analytical results. The computer programmes used are listed in Part III of this thesis.

2. SAMPLING TECHNIQUES.

2.1. Collection of Bulk Samples from the Mines.

Oriented bulk samples were obtained from each of the selected mines as follows: five bulk samples were obtained from Hartebeestfontein, eight from Zandpan and eight from Venterspost. The samples were provided by the geological and sampling departments of the mines concerned from various accessible workings in each mine, and each sample weighed between 5 and 15 kg. The samples were taken with great care so that each consisted of a continuous piece of rock made up of a full cross-section of the conglomerate band itself (Vaal Reef at Hartebeestfontein and Zandpan, Ventersdorp Contact Reef at Venterspost) with adherent portions of the immediately overhanging and underlying rocks.

2.2. Subdivision of Individual Bulk Samples.

Since the bulk samples were to be subjected to detailed chemical and mineralogical analysis and to microscopic study, it was, of course, necessary to subdivide each bulk sample into a number of suitably-sized samples. Before this was done, however, each bulk sample was sawn in half and the gross features of the resulting flattened slabs of rock were recorded by means of macro-photographs. The distribution of the radioactive minerals in the bulk samples was then established by means of macro-autoradiographs, which were prepared by leaving the flattened slabs of rock in contact with medical X-ray film in light-tight boxes for 14 days. A complete cross-section of each bulk sample was then subdivided into a number of samples of approximately equal size, from which thin sections and serial polished sections were prepared for detailed microscopic examination, while an adjacent complete cross-section of the bulk sample was subdivided into samples for quantitative chemical and mineralogical analysis. In this latter case the bulk samples were subdivided on the basis of the distribution of radioactivity and of visible sulphide mineralization, being sawn into slabs of convenient size displaying either high radioactivity and/or visible sulphides or low radioactivity and/or low sulphide content, and accordingly these samples differed slightly from one another in size and shape. This method of subdivision was adopted in preparing the samples for quantitative analysis in order to facilitate the detection of any relationship between the distribution of sulphide minerals and/or radioactivity and the distribution of gold. Visible sulphide mineralization and radioactivity are both factors that can easily be detected at the rock face even by unskilled personnel, and it therefore seemed that these two factors were potentially very suitable

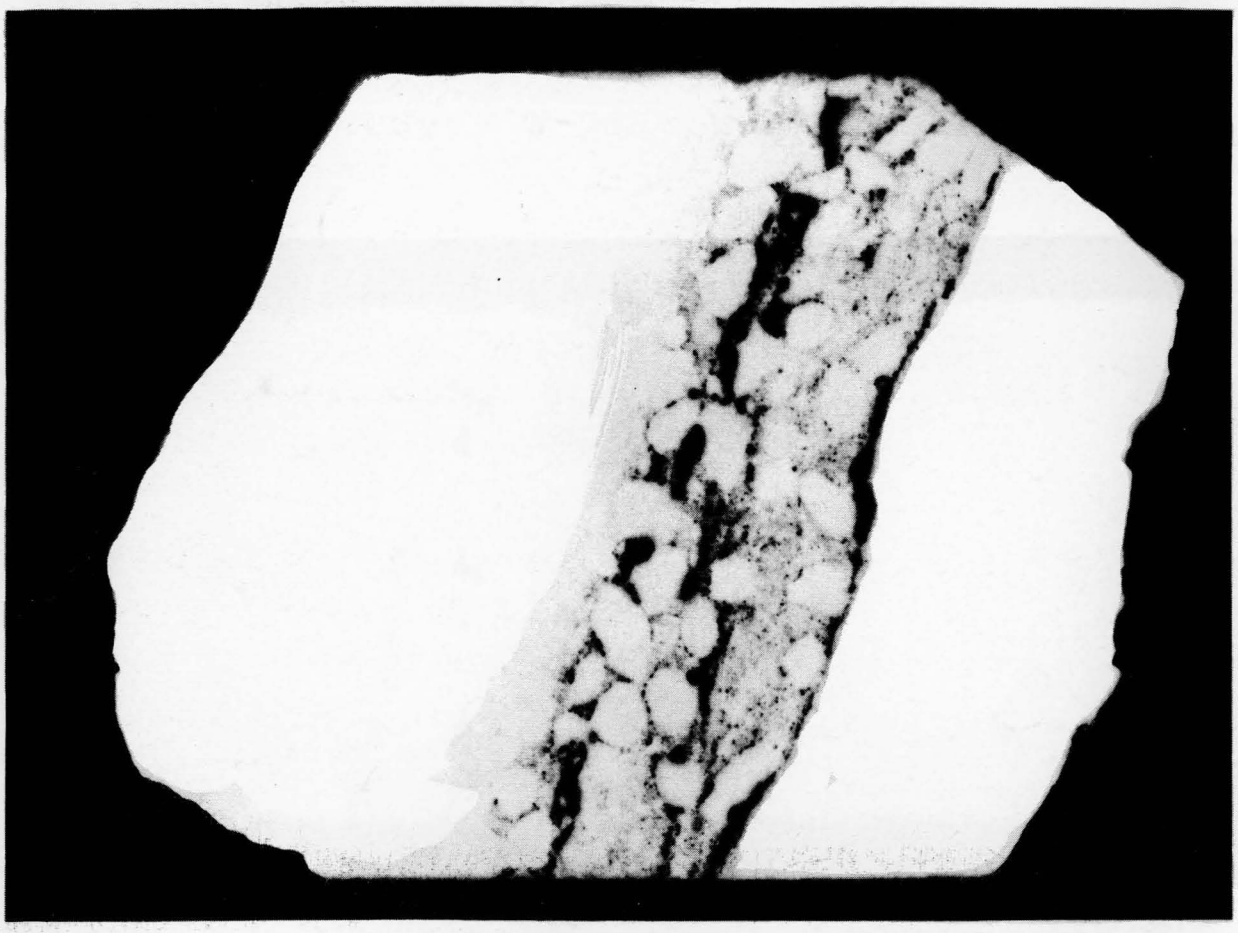
as indicators for positioning the rock-cutter, provided only, of course, that their distribution could be shown to bear a relationship to gold mineralization.

The manner in which the subdivision of the bulk samples was carried out is illustrated in the macro-photographs of three typical bulk samples shown in Figures 4, 5 and 6. These figures are described in detail in Section 3.1.

The five bulk samples from the Vaal Reef at Hartebeestfontein were subdivided into 43 samples for chemical and mineralogical analysis, while 61 polished sections were prepared. The eight bulk samples from the Vaal Reef at Zandpan were subdivided into 44 samples for chemical and mineralogical analysis, while 67 polished sections were prepared. The eight bulk samples from the Ventersdorp Contact Reef at Venterspost were subdivided into 56 samples for chemical and mineralogical analysis, while 73 polished sections were prepared.

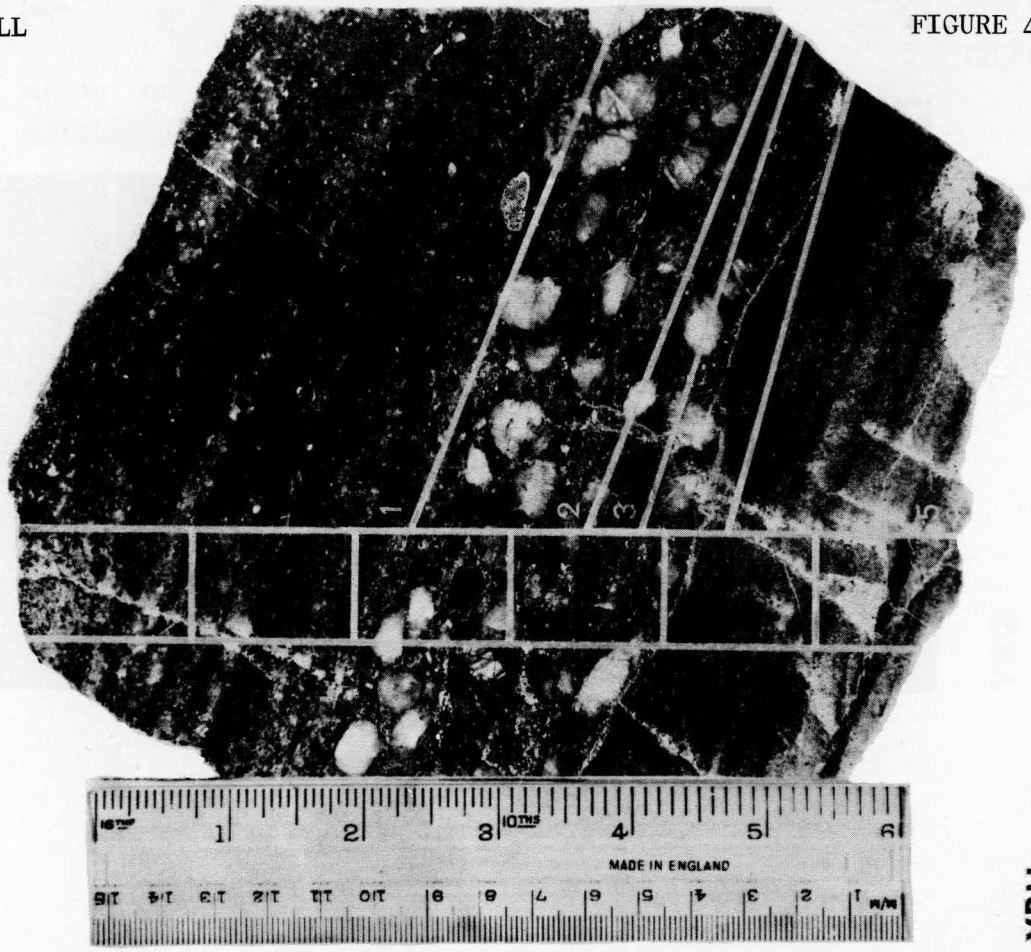
Details of the manner in which the samples were subsequently treated in preparation for chemical and mineralogical analysis are given in Part III of this thesis (Section 7).

MACRO-AUTORADIOGRAPH VAAL REEF ORE HARTEBEESTFONTEIN



HANGING WALL

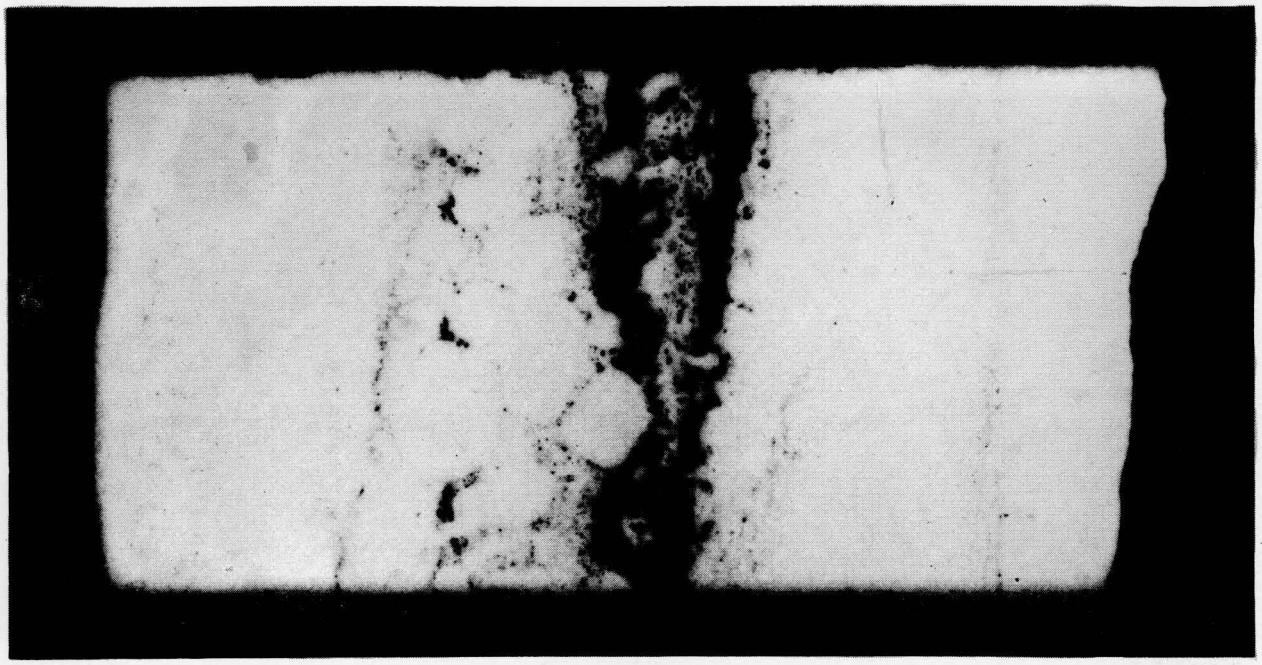
FIGURE 4



VRH

MACRO-PHOTOGRAPH VAAL REEF ORE HARTEBEESTFONTEIN

MACRO-AUTORADIOGRAPH VAAL REEF ORE ZANDPAN



HANGING WALL

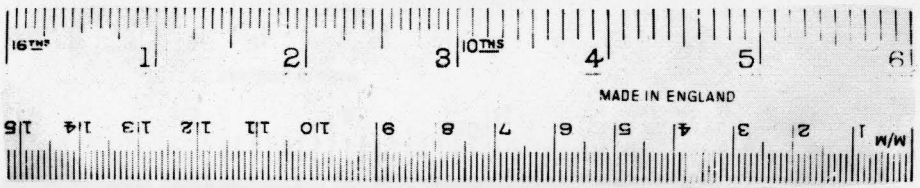
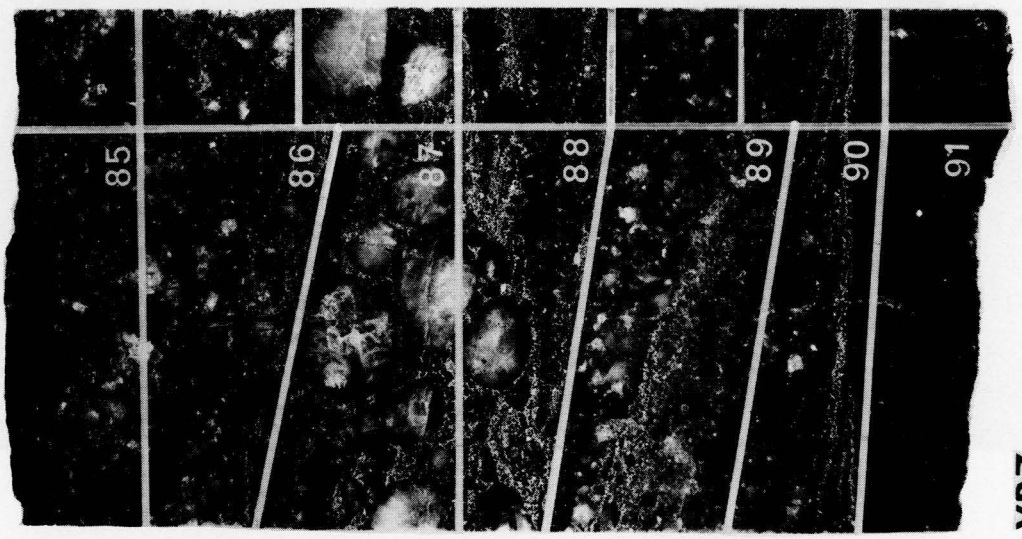
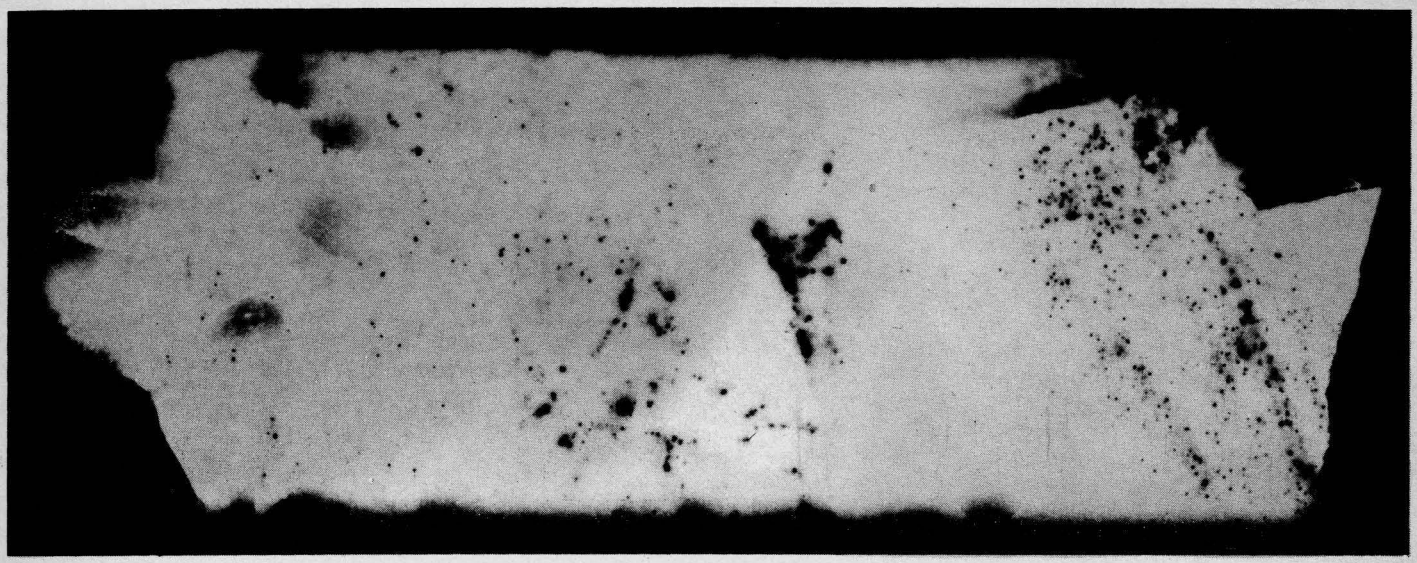


FIGURE 5



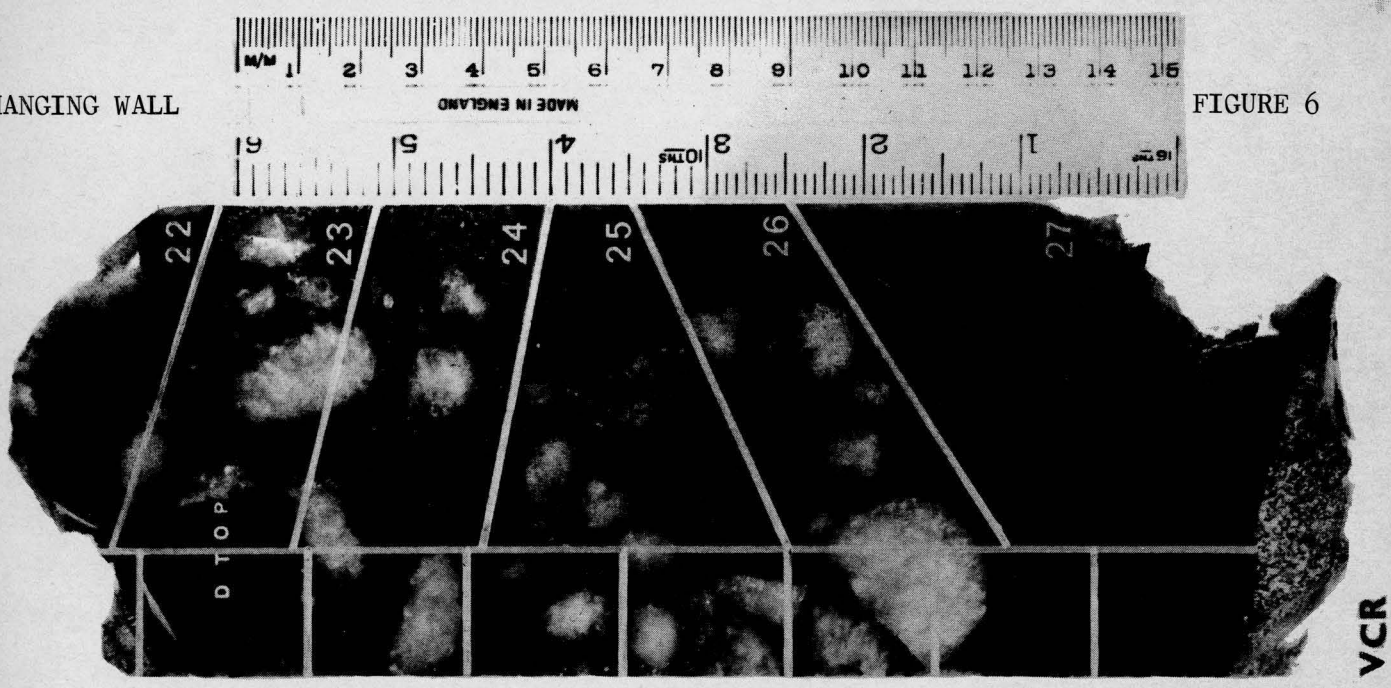
MACRO-PHOTOGRAPH VAAL REEF ORE ZANDPAN

MACRO-AUTORADIOGRAPH VENTERSDORP CONTACT REEF ORE VENTERSPOST



HANGING WALL

FIGURE 6



MACRO-PHOTOGRAPH VENTERSDORP CONTACT REEF ORE VENTERSPOST

3. OPTICAL STUDIES.

3.1. Macroscopic Studies.

The manner in which twenty-one oriented bulk samples (each consisting of a full cross-section of conglomerate band with adherent portions of the immediately overhanging and underlying rocks) were obtained from the Vaal Reef at Hartebeestfontein and Zandpan and from the Ventersdorp Contact Reef at Venterspost has been described in Section 2.1. As described in Section 2.2, the first step in the examination of these bulk samples involved sawing each bulk sample in half and recording the gross features of the resulting flattened slabs of rock with the aid of macro-photographs and macro-autoradiographs. In particular the distribution of visible sulphides and radioactivity across each bulk sample was noted, since, as explained in Section 2.2, it was considered possible that visible sulphide mineralization and radioactivity might well prove to fulfil best the requirements for indicators that could be used to position the rock-cutter.

In order to provide some indication of the general patterns of distribution of the visible sulphide minerals and radioactivity observed in the bulk samples, three typical bulk samples have been selected and their macro-photographs and accompanying macro-autoradiographs have been reproduced in Figures 4, 5 and 6. These bulk samples originated from, respectively, the Vaal Reef at Hartebeestfontein (labelled VRH), the Vaal Reef at Zandpan (VRZ) and the Ventersdorp Contact Reef at Venterspost (VCR). In all three cases the bulk sample has been photographed lying on its side, with the hanging wall on the left and the footwall on the right of the photograph. The visible sulphide minerals appear as fine white specks in the macro-photographs, while the distribution of the radioactive components can be judged from the black areas in the macro-autoradiographs. The markings on the macro-photographs indicate the manner in which the bulk samples were subdivided into samples for quantitative chemical and mineralogical analysis and for microscopic studies, the numbered samples being the ones taken for quantitative analysis while the unnumbered samples of approximately equal size were those from which thin sections and serial polished sections were prepared for microscopic examination. The samples for quantitative analysis differ slightly in size and shape because (as described in Section 2.2.) they were subdivided on the basis of visible sulphide mineralization and radioactivity.

In the bulk samples from the Vaal Reef at Hartebeestfontein and Zandpan shown in Figures 4 and 5, it can be seen that both pyrite and radioactive

minerals occur as fairly thin layers, from about one millimetre to a few centimetres thick, and that these pyrite- or uranium-rich layers are separated by layers in which the pyrite or uranium content is quite low. For example, if a cross-section of the bulk sample from the Vaal Reef at Hartebeestfontein shown in Figure 4 is examined in detail, the following features can be seen: the portion marked 1 (which is actually analytical sample VRH 1) contains fairly coarse cross-bedded quartzite above the conglomerate, and in this portion of the bulk sample no pyrite or radioactive minerals can be seen. Sample VRH 2 was taken in such a way that it included a layer of conglomerate 3 cm thick and fairly rich in pyrite, while reference to the autoradiograph shows that this sample contained two thin layers rich in uranium. These two layers of high radioactivity vary in thickness from 2 mm to 5 mm, one being parallel to the upper contact of the conglomerate while the other dips from the upper right-hand side towards the lower left-hand side. Sample VRH 3 represents a layer low in pyrite and uranium. Sample VRH 4 includes a pyrite- and uranium-rich band. Sample VRH 5 represents the footwall quartzite below the conglomerate band, with no evidence of the presence of pyrite or uranium.

A distribution pattern similar to that observed in the bulk samples from the Vaal Reef at Hartebeestfontein and Zandpan illustrated in Figures 4 and 5 (i.e. with pyrite and radioactive minerals occurring in fairly thin layers separated by layers with a low content of pyrite or uranium) was found to be the general rule in the 11 other bulk samples from the Vaal Reef. There was, however, a considerable variation from sample to sample as regards the location in the macro-autoradiographs of the narrow black bands representing areas rich in uranium-bearing minerals. In the macro-autoradiograph shown in Figure 4, for example, three distinct layers can be discerned and it is apparent that some of the highest concentrations of radioactive material do <u>not</u> occur along the footwall, while in Figure 5 the bulk of the radioactive material <u>does</u> occur on the footwall, although three or possibly four layers of uranium-rich material can be seen. In this regard, Liebenberg (1955, pp. 170 - 171), who examined conglomerate bands from many parts of the Witwatersrand System, has reported finding that the highest concentrations of uraninite mainly occurred at the lower portions of the conglomerate bands and frequently along their bedding planes, but that zones of uraninite concentration along any portion of an individual band of conglomerate were not unexpected.

In the case of the bulk samples from the Ventersdorp Contact Reef at Venterspost, the distribution pattern differed from that seen in the Vaal Reef samples in that, instead of the clearly-defined narrow layers of pyrite and radioactive minerals found in the samples from the Vaal Reef, both pyrite and uranium appeared to be more widely distributed, although small localized areas of high concentration were found to occur. For example, in the macro-autoradiograph of a Venterspost bulk sample shown in Figure 6 three broad areas of radioactive mineral enrichment are apparent, but take the form rather of clusters of grains than of distinct bands as in the Vaal Reef bulk samples. In this macro-autoradiograph it again appears as if the highest concentrations of radioactive material are not situated along the footwall.

3.2. Microscopic Studies.

After various macroscopic features of each of the twenty-one bulk samples from the Vaal Reef and Ventersdorp Contact Reef had been recorded with the aid of photographs and autoradiographs as described in Sections 2.2 and 3.1, each bulk sample was subdivided in the manner described in Section 2.2. This involved a complete cross-section of each bulk sample being subdivided into samples for quantitative analysis (the results of which are presented in Section 4 of this thesis) while an adjacent cross-section of each bulk sample was subdivided into a number of approximately equal-sized portions from which thin sections and polished sections were prepared for detailed microscopic examination. The results of this microscopic examination of samples from the Vaal Reef at Hartebeestfontein and Zandpan and from the Ventersdorp Contact Reef at Venterspost are discussed in Sections 3.2 and 3.3 of this thesis.

In Section 3.2, certain salient features of the mineralogy of the Vaal Reef and Ventersdorp Contact Reef revealed by the examination of the present suite of samples are discussed in the light of work carried out by earlier investigators. Previous mineralogical surveys of Vaal Reef and Ventersdorp Contact Reef material have been mentioned briefly in Sections 1.5.1. and 1.5.2. The most detailed mineralogical investigations of the Vaal Reef to have been carried out to date have been those by Jacob (1966) and McLachlan (1968), Jacob having undertaken a geological, petrographic and mineralogical study of the Vaal Reef at the Vaal Reefs gold mine while McLachlan was primarily interested in studying the grain-size relationships shown by zircon and chromite in the Vaal Reef of the Klerksdorp Goldfield. In addition, Liebenberg (1955) examined a

number of samples from the Vaal Reef in the course of a general survey of Witwatersrand gold- and uranium-bearing conglomerates. As regards the Ventersdorp Contact Reef, a detailed examination of its mineralogy and mode of deposition at the Venterspost and Libanon gold mines was carried out by von Rahden in 1964.

The main purpose behind the microscopic examination of the present suite of samples was not, however, to carry out another detailed mineralogical survey of the Vaal Reef and the Ventersdorp Contact Reef, but rather to provide information that could be used as a control in interpreting the results of the quantitative analyses of the present samples. During the course of the polished section studies, however, a careful record was kept of the numbers of grains of gold, uraninite, zircon and chromite present, and of the numbers of "uraninite ghosts" and the types of pyrite present. This was done in order to obtain some idea of the extent to which sympathetic relationships between minerals can be detected by strictly optical techniques, and the implications of the results obtained are discussed in Section 3.3. In a later part of the thesis (Section 5.2) these findings are compared with the results of the quantitative analyses.

When considering the results of the mineralogical examination of the present suite of samples, some idea of the concentrations of the minerals present in the Vaal Reef and Ventersdorp Contact Reef may be obtained from the results of the quantitative chemical, X-ray diffraction and X-ray fluorescence analyses carried out in the course of the present investigation and presented in Tables II, III, IV and V in Section 4.1 of this thesis. For convenience, however, a simplified version of Table V, listing only the mean values found for the major constituents of these horizons, is given here as Table I. In this Table the analytical values for zirconium and chromium have been recalculated in terms of the stoichiometric formulae for zircon and chromite.

3.2.1. Thin Section Studies.

Quartz and the phyllosilicates muscovite, pyrophyllite and chlorite constitute the suite of non-opaque minerals present in the samples taken from the Vaal Reef at Hartebeestfontein and Zandpan and from the Ventersdorp Contact Reef at Venterspost. The coarser "quartz fraction" occurring in both the Vaal Reef and the Ventersdorp Contact Reef was found to consist of pebbles of vein quartz, quartzite and chert, showing varying degrees of rounding. The interstices between the pebbles were invariably filled by an intimate mixture of mosaic-like fine quartz grains, thucholite and sulphide grains cemented by phyllosilicates. In all three

TABLE I.

MEAN ANALYTICAL VALUES FOR CERTAIN ELEMENTS AND MINERALS PRESENT IN SAMPLES FROM THE VAAL REEF AT HARTEBEESTFONTEIN AND ZANDPAN AND FROM THE VENTERSDORP CONTACT REEF AT VENTERSPOST

Au ppm	Ag ppm	U_3O_8 %	Pyrite %	Muscovite %	Pyrophyllite %	Chlorite %	"Quartz" %	Ti %	Zircon %	Chromite %
				HARTEBEESTFONTEIN - VAAL REEF						
50.1	7.6	0.087	6.6	4.4	0.1	0.8	88.3	0.092	0.08	0.20
				ZANDPAN - VAAL REEF						
39.9	3.3	0.093	14.0	7.0	2.5	0.9	75.8	0.185	0.09	0.17
				VENTERSPOST - VENTERSDORP CONTACT REEF						
43.8	4.9	0.029	3.2	3.0	0.2	4.9	88.9	0.106	0.18	0.15

mines muscovite and pyrophyllite were generally found to occur as intimately intergrown fine shreds and acicular flakes, the identity of which could not be established with any degree of certainty in thin section (see also Section 6.3.1). In the Ventersdorp Contact Reef samples, chlorite was often seen to replace the larger quartz pebbles and boulders along their peripheries and along cracks.

As may be judged from the macrophotographs of three typical bulk samples reproduced in Figures 4, 5 and 6, thin section studies can only be of limited value in the examination of coarse-grained material such as banket because of the difficulty of obtaining truly representative samples. Estimates of mineral concentrations based on thin section studies should therefore be regarded as being unreliable, and accordingly in the present study no such estimates were made. The relative amounts of minerals present in the samples examined are indicated in Table I.

The optical, chemical and mineralogical features of various phyllosilicates (including chlorite from the Ventersdorp Contact Reef at Venterspost and muscovite from the Vaal Reef at Hartebeestfontein) were studied in detail in the course of the present investigation, and the results of these studies are reported in Part II of this thesis.

3.2.2. Polished Section Studies.

3.2.2.1. Gold.

Examination of polished sections prepared from the Vaal Reef at Hartebeestfontein and Zandpan and from the Ventersdorp Contact Reef at Venterspost revealed that at all three mines the gold occurred in at least two generations. The older generation occurs in the form of small, generally rounded inclusions, totally enclosed within pyrite grains that show no evidence of healed cracks that could originally have permitted the entry of the gold. The second and younger generation of gold constitutes the major portion of the gold seen in polished sections. This younger gold occurs as stringer-like inclusions embedded in phyllosilicates, as anhedral growths replacing pyrrhotite, pyrite, chalcopyrite and uraninite, and occasionally as small euhedral crystals showing bright facets, embedded in phyllosilicates or occurring within cracks in the quartz grains. This second generation of gold has been described in considerable detail by Liebenberg (1960, p. 864), von Rahden (1964, pp. 48 - 49), Schidlowski (1965, p. 2 and 1968, p. 359) and Saager (1969, p. 95). These investigators have all supported the "modified placer theory" (see Section 1.4.1) and attributed the form shown by this second generation of gold to the effects of dynamic and localized metamorphism of the conglomerates, at

which time remobilization and recrystallization of the gold occurred. They postulated that it was during this period of remobilization of the gold that uraninite and sulphides were replaced by gold. The movement of the gold did not exceed perhaps a few millimetres, and was not sufficient to upset or affect the original sedimentary distribution pattern to any significant extent, so that this movement of the gold should not be compared with truly hydrothermal transportation.

A superficial examination of the current suite of polished sections (and of many other Witwatersrand ores, for example the Main Reef) might, in fact, suggest hydrothermal emplacement of the gold because of the lack of rounded grains of gold typical of placer deposits and because of certain apparently hydrothermal characteristics displayed by the gold (for example, the occurrence of some of the gold as anhedral growths). Supporters of the modified placer theory contend, however, that the shape of most gold grains at present found in various Witwatersrand horizons can be accounted for by the remobilization process envisaged by that theory. Among the evidence supporting the modified placer theory, Liebenberg (1955, p. 163) has reported locating a number of unquestionably detrital grains of gold in various ores from the Witwatersrand and von Rahden (1964, p. 32), who worked on ore from the Ventersdorp Contact Reef at Venterspost and Libanon, has reported finding a number of cornet-like grains of gold which he liberated from within pyrite grains by means of nitric acid. These liberated gold grains strongly resembled grains of undoubted detrital origin from Australia, and von Rahden concluded that the cornet-like particles owed their preservation to the shielding effect of the pyrite, which had prevented their remobilization.

Schidlowski (1968, p. 344), commenting on the apparent lack of sedimentary character shown by gold in Witwatersrand conglomerates from the Orange Free State Goldfield, suggested that the primary alluvial character of the gold had probably been obliterated by mechanical reshaping of the grains or an intermediate reshaping process followed by reprecipitation.

3.2.2.2. Uraninite.

Both in the Vaal Reef at Hartebeestfontein and Zandpan and in the Ventersdorp Contact Reef at Venterspost uraninite was found to occur in two forms, namely as primary unaltered grains and as secondary recrystallized grains and anhedral grains.

The primary uraninite in both the Vaal Reef and the Ventersdorp Contact Reef was often found to occur as discrete, subhedral, oval and severely

rounded grains set in the matrix. In the case of the Vaal Reef, however, the uraninite was more generally found to occur as clusters and aggregates intimately associated with thucholite. In those cases where the uraninite grains occurred embedded in thucholite, they appeared to have undergone very little alteration, as if the thucholite has acted as a protective medium. Radiogenically derived galena was commonly associated with the uraninite grains in the form of minute inclusions.

Uraninite was also found to occur in the form of stringers confined to the matrix, where it replaced genetically older sulphides and filled cracks in the quartz grains. Microscopic evidence suggested that this secondary uraninite was probably formed from original grains of uraninite by leaching and redeposition of the leached material. Electron microprobe electron backscatter pictures prepared in the course of the present study supported this theory, since they clearly showed that the stringers of uranium-rich material lead directly towards highly altered grains of uraninite.

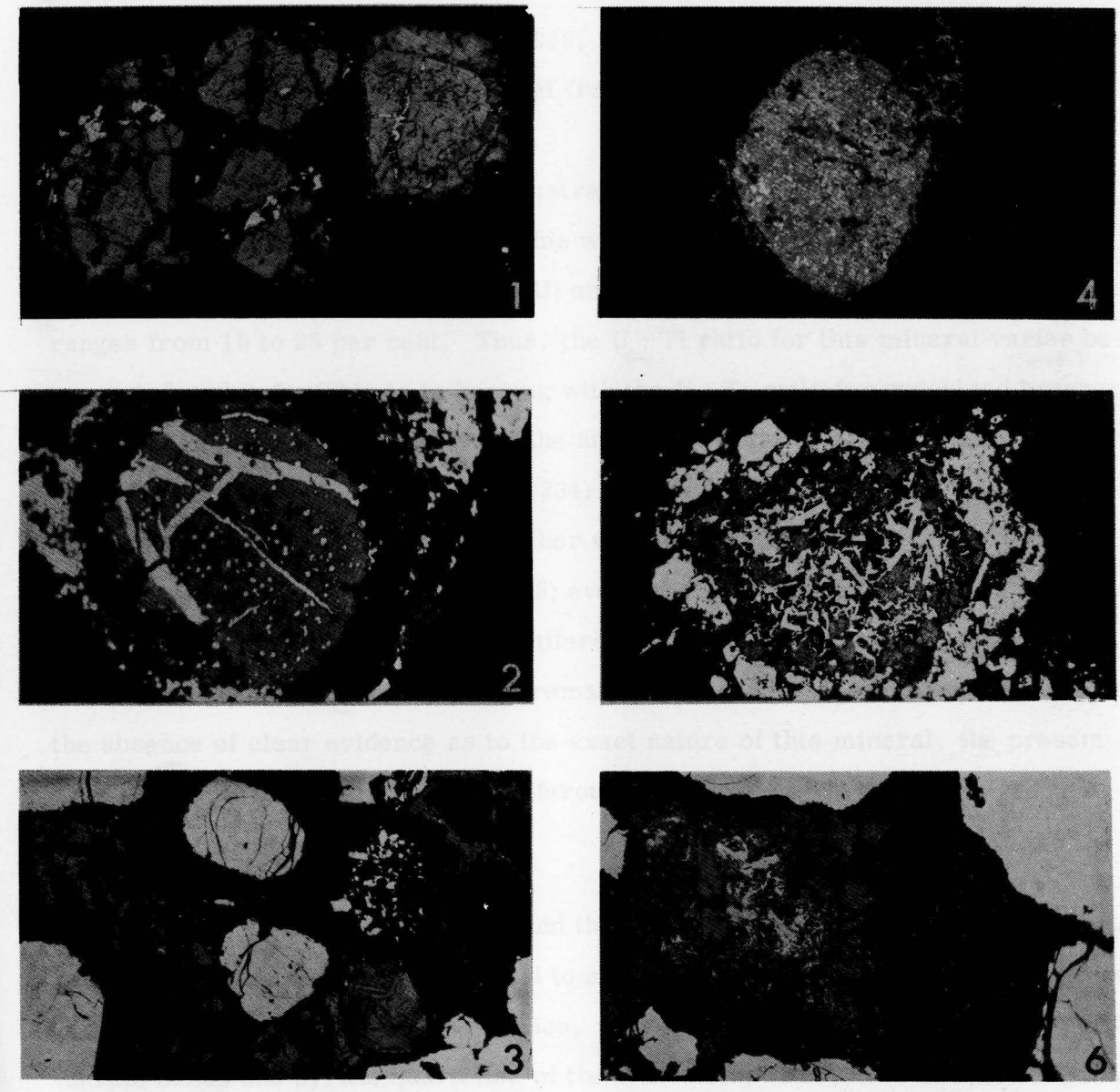
Photomicrographs 1 to 5 in Figure 7 show the typical forms and associations of uraninite, together with the various degrees of alteration that uraninite undergoes. The uraninite grains illustrated in these photomicrographs, and numerous other uraninite grains observed in the present suite of polished sections, are closely similar in form to those illustrated by Liebenberg (1955, Plates XVI, XX, XXII and XXIII), Koen (1961, Plates I and II) and Schidlowski (1966, Plates IX to XIII), to all of which uraninite grains these authors attributed a detrital origin.

3.2.2.3. The Alteration Products of Uraninite.

In the present suite of samples, the examination of uraninite grains under crossed nicols and oil immersion often revealed the presence of an off-white-coloured aureole of apparently amorphous material with a high refractive index surrounding the uraninite grain. This material has been referred to by Ramdohr (1958, pp. 26 - 27) as a "uraninite ghost".

When polished sections were left in prolonged contact with special nuclear track photographic plates sensitive to α particle radiation, the presence of weakly radioactive material was revealed. This material was similar in appearance to that illustrated in photomicrograph 6 in Figure 7. This material, which displayed orange to yellow internal reflections and was composed of a nest of fine felted needles, often contained a core consisting of fine laths of pyrrhotite and fine specks of galena. It was variously been referred to as "uraniferous leucoxene" by Liebenberg (1955, p. 157) and von Rahden (1964, pp. 92 - 96) and as "brannerite" by Ramdohr (1958,

1. Cluster of uraninite grains cemented by thucholite, showing inclusions of galena.
   Incident light, oil immersion , 90x. V.C.R. Venterspost.
2. Rounded grain of uraninite showing aureole, inclusions and infillings of galena.
   Incident light, oil immersion, 160x. Vaal Reef, Zandpan.
3. Cluster of shattered grains of uraninite cemented by thucholite. Note the secondary interstitial uraninite in the top right-hand corner. Rounded white grains are pyrite.
   Incident light, oil immersion, 135x. Vaal Reef, Zandpan.



4. Rounded grain of uraninite, riddled with inclusions of galena, showing alteration to wispy secondary uraninite on grain periphery.
   Incident light, oil immersion, 180x. Vaal Reef Hartebeestfontein.
5. Euhedral grain of uraninite with a core of euhedral pyrrhotite needles, surrounded by aureole of galena.
   Incident light, oil immersion, 275x. Vaal Reef, Zandpan.
6. Anhedral growth of uraniferous leucoxene with core of euhedral pyrrhotite needles. White grains are pyrite.
   Incident light, oil immersion, 275x. Vaal Reef, Hartebeestfontein.

FIGURE 7 - PHOTOMICROGRAPHS 1-6

pp. 26 - 27) and Schidlowski (1966, p. 311). Ramdohr and Schidlowski believe this material to be an authigenic component of the conglomerates and to have been formed from uraninite and rutile under pseudohydrothermal conditions by the reaction $UO_2 + 2TiO_2 \rightarrow UTi_2O_6$ as a result of localized metamorphism. Material similar to that found in the present suite of samples was extracted from the Ventersdorp Contact Reef by von Rahden in 1962 and sent to Professor Pabst of the University of California, who described this material as resembling brannerite from which uranium had been leached. Jacob (1966, p. 48) tentatively identified a mineral with a refractive index of 2.285 in material from the Vaal Reef at Vaal Reefs Mine as brannerite.

Von Rahden and Hiemstra (1967, p. 3) have shown, on the basis of electron microprobe analyses, that this weakly radioactive material contains approximately 15 per cent of uranium (U) and a variable amount of titanium (Ti), which ranges from 10 to 25 per cent. Thus, the U : Ti ratio for this mineral varies between 1.5 and 0.6. This is in keeping with the U : Ti ratio for undoubted brannerite, which varies between 1.7 and 0.5 if the analytical values for brannerite from various sources quoted by Frondel (1958, p. 334) are used.

Since, however, neither von Rahden and Hiemstra (1967), nor Schidlowski (1966) nor Ramdohr (1958) ever carried out heating experiments and X-ray diffraction studies on this uraniferous titanate to confirm its identity, the name to be assigned to this mineral remains a matter of personal preference. In the absence of clear evidence as to the exact nature of this mineral, the present investigator prefers the name "uraniferous leucoxene" to "brannerite".

3.2.2.4. Thucholite.

Both the Vaal Reef and the Ventersdorp Contact Reef contain a carbonaceous material, locally referred to as "carbon", which is actually a hydrocarbon-uraninite mixture. This substance, which has been observed in all the conglomerate bands and pyritic quartzites of the Witwatersrand System (Liebenberg, 1955, pp. 131 - 132), was first reported as a variety of thucholite by Liebenberg in 1948.

In the samples from the Ventersdorp Contact Reef the thucholite occurred as opaque blackish grains with very irregular outlines. Some of these grains gave the impression that they had been plastic or mobile in the past, as they were often found moulded in between and around grains of apparently older pyrite. Uraninite was generally present as an inclusion in the thucholite, but was sometimes totally absent. In the Vaal Reef, however, the thucholite occurred as "warty"

granules up to 1 mm in size, or as fine seams varying from 2 to 25 mm thick. This thucholite was invariably accompanied by included pieces of resorbed uraninite, whose cracks were often "healed" by small veinlets of thucholite.

Liebenberg (1955, p. 220) suggested that the thucholite was an authigenic component of the banket, and that it originated as a result of the irradiation of gaseous and/or liquid hydrocarbons by detrital uraninite.

In 1949 Sharpe postulated that the hydrocarbons in the Witwatersrand System possibly represented the remains of primitive forms of life, such as bacteria and algae. Ramdohr (1958, p. 48) mentioned the possibility that the carbonaceous material could have originated as the result of the activity of black mud bacteria. Von Rahden (1964, pp. 64 - 69) carried out mineralogical and chemical studies on thucholite separated from the Ventersdorp Contact Reef, the Carbon Leader, the Kimberley Reef and the Main Reef, and concluded that the varieties of thucholite extracted from these four horizons had very similar properties, and that a common mechanism had been responsible for their formation. These varieties could be classified as low- to medium-volatile bituminous coals on the basis of their chemical compositions. Von Rahden (1964, p. 72) supported the theory put forward by Sharpe in 1949 envisaging an algal origin for the thucholite in the Witwatersrand System. He postulated (von Rahden, 1964, pp. 79 - 80) that the carbonaceous matter might have adsorbed uranium from solution in the form of uranyl sulphate, and that this adsorbed uranium might then have been converted into uraninite as the degree of metamorphism of the horizon proceeded, while the carbonaceous material was converted into a less plastic form as a result of the loss of volatile matter. He drew attention to the fact that it had been found possible to synthesize uraninite at temperatures as low as 300°C using carbonaceous siliceous shale and a solution containing 1 g/litre of uranyl sulphate.

Snyman (1965, p. 225) independently examined and analysed thucholite from the Vaal Reef at Vaal Reefs gold mine, from the basal contact of the Vaal Reef at Hartebeestfontein and from the banded pyritic quartzite 20 feet below the Main Reef Leader at Daggafontein Mine. Snyman concluded that:

(1) Two structural types of thucholite could be distinguished, and these resembled algal structures from Carboniferous and Permian boghead coals and from Pleistocene lignite.

(2) The resemblance between thucholite and boghead coal is further borne out by the proximate and ultimate analyses and by the trace-element content.

(3) Despite the fact that thucholite contains higher amounts of gold and uranium and lesser amounts of molybdenum than any coal known so far, the thucholite from the Witwatersrand System actually represents a high rank boghead coal (Snyman, 1965, p. 235).

Snyman postulated (1965, p. 235) that, due to biological activity of algae or to the formation of organo-metallic complexes, uranium salts were precipitated from uranium-bearing solutions, and that bombardment of the sapropel by alpha particles led to pronounced dehydrogenation of the organic material and resulted in structural changes which were analogous to an increase in rank.

Schweigart and von Rahden (1964, p. 1147) also agreed with Sharpe's (1949) theory regarding the algal origin of the hydrocarbons in the Witwatersrand System, and further ascribed an algal origin to certain pyritic concretions in the Ventersdorp Contact Reef (see Section 3.2.2.5).

3.2.2.5. Pyrite.

In the Ventersdorp Contact Reef at Venterspost, pyrite is the major sulphide present. It was found to occur embedded in the chlorite matrix or as infillings in the quartz pebbles, and the pyrite grains varied in size from very small microscopic specks to rounded pebbles some 15 mm in diameter, which are referred to locally as "buckshot". The pyrite occurred in various forms : as pyritized banded ironstones, as skeletal growths of a "clear" compact nature or of a porous nature, as overgrowths on older pyrite and as fine stringers of juvenile or remobilized pyrite that often filled fine cracks in the quartz matrix. The abraded and rounded grains of pyrite probably represent the oldest generation, while the overgrowths are probably of intermediate age and the juvenile pyrite represents the youngest generation.

In the Vaal Reef at Hartebeestfontein and Zandpan the pyrite was found to occur in a manner very similar to that described for the Ventersdorp Contact Reef. In both horizons pyrite grains were often observed to contain inclusions of zircon, chromite, chalcopyrite and rutile, and fine grains of quartz, sphalerite and gold.

Von Rahden (1964, p. 45), who studied the Ventersdorp Contact Reef at Venterspost and Libanon mines, was able to show that the presence of coarse grains or pebbles of "buckshot" pyrite was not necessarily indicative of areas of above-average gold mineralization, as had previously been widely accepted.

Schweigart and von Rahden (1964, p. 1147) suggested that it was probable that some of the "radial pyrites" (pyrites displaying oolitic textures) occurring in the Ventersdorp Contact Reef had an algal origin.

The general characteristics of the pyrite in the Vaal Reef and Ventersdorp Contact Reef suggest that most of the pyrite grains have undergone considerable transportation, and that the overgrowth and juvenile pyrite present in these horizons probably resulted from the "pseudohydrothermal" metamorphism to which both horizons were subjected.

3.2.2.6. Rare Sulphides.

3.2.2.6.1. Pyrrhotite.

In the Vaal Reef at Hartebeestfontein and Zandpan only minor traces of pyrrhotite were found to occur, but this mineral was found to be widespread in the samples from the Ventersdorp Contact Reef.

Pyrrhotite occurred mainly as xenomorphic grains, or, more rarely, as subhedral grains showing hexagonal outline. Pyrrhotite was found to replace most of the earlier minerals such as pyrite and uraninite, and was in turn itself replaced by gold, chalcopyrite, galena and sphalerite. Inclusions of "flames" of pentlandite were also common.

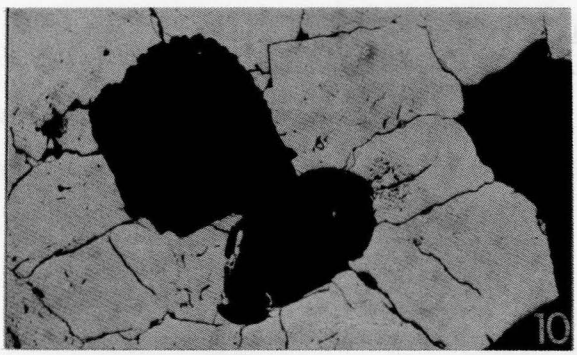
An interesting phenomenon noted in the suite of samples examined was the presence of monoclinic and hexagonal pyrrhotite co-existing within a single grain in close proximity (i.e., within a single microscope field) to the normal hexagonal variety of pyrrhotite. This is illustrated in photomicrograph 12 in Figure 8. According to recent research carried out by Arnold (1969. p. 418), the occurrence of natural monoclinic pyrrhotite co-existing in the same grain with natural hexagonal pyrrhotite can be taken as evidence of the heating of the deposit to a temperature above $304 \pm 6^{o}C$.

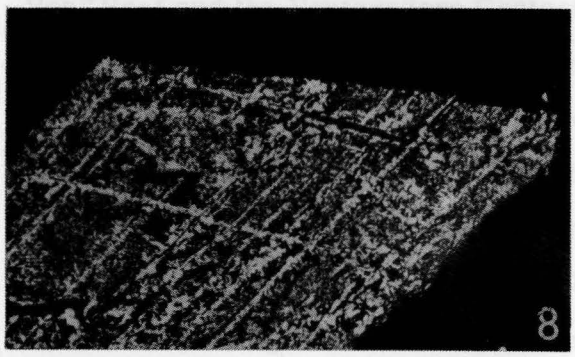
3.2.2.6.2. Cobaltian-gersdorffite and cobaltite.

In the Vaal Reef at Hartebeestfontein and Zandpan, the presence of sub-rounded grains of cobaltite and a cobalt-bearing variety of gersdorffite (whose identity was established by means of X-ray diffraction and electron microprobe analyses) appeared to be associated with above-average numbers of uraninite grains in polished section. Liebenberg (1955, p. 113) has also mentioned the presence of cobaltite and cobaltian gersdorffite in the Vaal Reef, but did not comment on any association of these minerals with uraninite. No evidence of any such quantitative re-

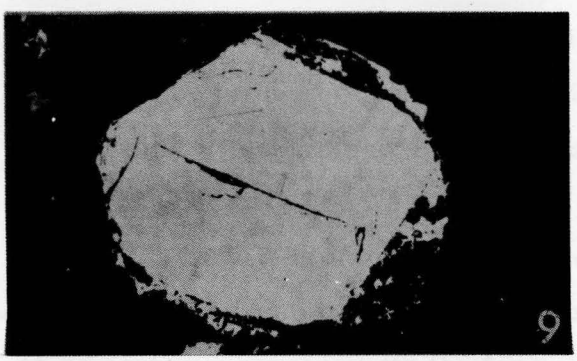
7. Anhedral grain of microcrystalline rutile with a whitish rim of leucoxene.
   Incident light, oil immersion, 90x. Vaal Reef, Hartebeestfontein.
8. Sphenoidal grain of fine rutile needles - probably relict titanite.
   Incident light, oil immersion, 115x. Vaal Reef, Hartebeestfontein.
9. Euhedral grain of cobalt-containing gersdorffite rimmed by galena.
   Incident light, oil immersion, 275x. Vaal Reef, Zandpan.













10. Grains of chromite and zircon included in, and replaced by pyrite.
    Incident light, oil immersion, 135x. Vaal Reef, Zandpan.
11. Grain of radioactive zircon within pyrite. Note the radiating cracks in the pyrite surrounding the zircon.
    Incident light, oil immersion, 125x. Vaal Reef, Zandpan.
12. Coexisting grains of monoclinic (dark) and hexagonal (light) pyrrhotite revealed after being etched with chromic acid.
    Incident light, oil immersion, 135x. V.C.R. Venterspost.

FIGURE 8 - PHOTOMICROGRAPHS 7-12

lationship between cobaltite, gersdorffite and uraninite could be found in the samples from the Ventersdorp Contact Reef.

In 1964 von Rahden (1964, p. 42) reported the presence of cobaltite grains being replaced by gold in samples from the Ventersdorp Contact Reef at Venterspost, but this phenomenon was not noticed in the current suite of samples from the Ventersdorp Contact Reef at Venterspost, or in the samples from the Vaal Reef.

3.2.2.6.3. Molybdenite.

In the samples from the Vaal Reef at Hartebeestfontein, a single grain of strongly anisotropic molybdenite embedded in quartz was positively identified by means of X-ray diffraction.

3.2.2.7. Titanium minerals.

Titanium-bearing minerals are ubiquitous components of both the Vaal Reef and the Ventersdorp Contact Reef. The members of this group of minerals encountered in the course of the present study included uraniferous leucoxene (which has already been discussed, see Section 3.2.2.3), rutile, anatase, leucoxene and relict structures of titaniferous magnetite and titanite. Rutile was found to occur in various associations: as fine euhedral needles within the phyllosilicates, as inclusions within pyrite or uraniferous leucoxene, or as fine criss-crossing euhedral needles imparting a bluish colour to quartz grains. Anatase was found to occur as bright blue octahedra encased within the chlorite in the Ventersdorp Contact Reef.

Ramdohr (1958, p. 40) has suggested that the euhedral and obviously authigenic needles of rutile owe their origin to the remobilization of leucoxene, which was formed from an original titaniferous mineral such as ilmenite or titaniferous magnetite.

It is interesting to note that, in the present suite of samples, the formation of "uraninite ghosts" or uraniferous leucoxene appeared in most cases to be contemporaneous with the formation of the fine needles of authigenic rutile.

3.2.2.8. Zircon.

The zircons found in the samples from the Ventersdorp Contact Reef differed somewhat in appearance from those in the Vaal Reef samples, the most conspicuous difference being the generally higher proportion of zoned zircon grains encountered in the Vaal Reef. In both horizons the zircons occurred within the quartz matrix or as inclusions within pyrite, and displayed varying degrees of

rounding typical of detrital grains (see photomicrographs 6, 10 and 11 in Figures 7 and 8).

The physical characteristics, overall sizes and length-breadth ratios (elongation ratios) of zircons present in various Witwatersrand conglomerates have been investigated by workers such as von Rahden (1964), Viljoen (1964), Bosch and Ortlepp (1966) and McLachlan (1968) in attempts to establish the source of the zircons and also to investigate their usefulness as possible indicators of areas of payable gold. Von Rahden (1964, p. 134) examined the zircons occurring in the Ventersdorp Contact Reef and underlying Main Reef at Libanon and Venterspost, and concluded that the zircons present in the Ventersdorp Contact Reef had probably been derived from the Main Reef. Viljoen in 1964 examined the mineragraphic and petrographic aspects of the Main Reef and Main Reef Leader of the Main Bird Series, and concluded that there was a definite correlation between the size of the heavy minerals (zircons whose median grain size was in excess of 200 microns) and the tenor of gold. Bosch and Ortlepp (1966, p. 122) then examined material from the Main Reef Leader at City Deep and from the Composite Reef at E.R.P.M., but failed to find any relationship between the median grain size of the zircons and gold assay values in individual samples. In addition, they deduced that there was no correlation between the median grain size of zircon and the payability of zones of ore within individual stopes. McLachlan (1968, p. 96), who carried out a comprehensive grain-size study of zircon and chromite in the Vaal Reef of the Klerksdorp Goldfield, could not find any clear relationship between gold values and the grain-size of the matrix minerals zircon and chromite.

3.2.2.9. Chromite.

Chromite was found to occur in the Vaal Reef and Ventersdorp Contact Reef as well-rounded or euhedral octahedra showing evidence of limited transportation. The grains were frequently, but by no means always, in close proximity to zircon grains. Photomicrograph 10 in Figure 8 shows grains of zircon and chromite encased in pyrite. There is little doubt concerning the detrital origin of the chromite (Liebenberg, 1960, p. 835).

3.3. Optical Studies -- Conclusions.

The results obtained in the present macro- and microscopic examination of samples from the Vaal Reef at Hartebeestfontein and Zandpan and from the Ventersdorp Contact Reef at Venterspost confirm the finding of Liebenberg (1955,

p. 111) and McLachlan (1968, p. 7) that the mineralogy of the Vaal Reef is basically the same as that of the Ventersdorp Contact Reef and other Witwatersrand auriferous conglomerates.

The following conclusions were arrived at on the basis of the optical studies carried out:

(1) Polished section studies of ore from the Vaal Reef at Hartebeestfontein and Zandpan failed to reveal any obvious mineralogical differences between these two mines.

(2) Collectively, the Vaal Reef samples appeared to contain a significantly higher proportion of pyrite, thucholite, uraninite, "uraninite ghosts", zircons and chromite than the Ventersdorp Contact Reef samples, while the pyrrhotite content of the Ventersdorp Contact Reef samples appeared to be considerably higher than that of the Vaal Reef samples. In addition, the chlorite content of the Ventersdorp Contact Reef is considerably higher than that of the Vaal Reef, and often reaches such a concentration that it imparts a dark green colour to the conglomerate.

(3) In polished sections from both the Vaal Reef and the Ventersdorp Contact Reef there was no visible relationship between the number of gold grains and the number of uraninite grains.

(4) There was also no apparent relationship between the number of gold grains and the number of zircon and/or chromite grains in polished sections from either the Vaal Reef or the Ventersdorp Contact Reef. Where a total of 50 or more zircon or chromite grains were found to occur in a single polished section, they were often found to be accompanied by an above-average number of uraninite grains and "uraninite ghosts". On the other hand, however, some polished sections that contained a total of 100 or more zircon and chromite grains were found to be totally devoid of gold, uraninite and the alteration products of uraninite.

(5) It was not possible to reach any conclusions regarding relationships between any of the heavy minerals and the phyllosilicates from polished section studies, because the phyllosilicates cannot be identified with any degree of certainty in polished section.

(6) In the Vaal Reef the uraninite was, on the whole, mainly associated with thucholite, whereas in the Ventersdorp Contact Reef uraninite grains were often found in polished sections totally devoid of thucholite. In the Vaal Reef the thucholite occurred in the form of fine seams as well as "warty" granules, but in the Ventersdorp Contact Reef only the granular type of thucholite was observed.

(7) The presence of cobaltite and cobaltian-gersdorffite appeared to be associated with above-average numbers of uraninite grains in polished sections from the Vaal Reef, but there was no evidence of any such association in the samples from the Ventersdorp Contact Reef.

(8) At all three mines there appeared to be a weak relationship between the number of zircon and chromite grains seen in polished section and the amount of rutile present.

(9) There was no apparent relationship between the occurrence of any particular type of pyrite (i.e., buckshot, euhedral, overgrowth etc.) and the presence of above-average numbers of uraninite, gold, zircon or chromite grains.

(10) Careful inspection of the serial polished sections failed to reveal any clear-cut trend regarding the spatial distribution of minerals such as zircon, chromite, gold and uraninite within an individual bulk sample, or, in other words, these minerals were not necessarily confined to the bottom or top of the conglomerate bed.

4. STATISTICAL EVALUATION OF RESULTS OF QUANTITATIVE ANALYSES.

4.1. Introduction.

In the search for possible indicators of areas rich in gold and/or uranium in Witwatersrand conglomerate bands, optical techniques could not be relied on to any great extent because they are, by their nature, subjective. Accordingly, the macroscopic and microscopic optical studies described in Section 3 of this thesis were only intended to provide a general indication of the spatial distribution of gold, uranium and other minerals in the 21 bulk samples of Witwatersrand conglomerate examined. When these studies had been completed, the next step in the investigation involved the quantitative determination of gold and uranium, and of other elements and minerals that might vary sympathetically with gold and uranium, in samples obtained by subdivision of the original bulk samples.

The manner in which the 21 original bulk samples from the Vaal Reef at Hartebeestfontein and Zandpan and from the Ventersdorp Contact Reef at Venterspost were subdivided into 143 samples for quantitative analysis has been described in Section 2. Using the analytical techniques described in Part III of this thesis, each of the 143 samples was analysed for 14 variables -- gold, silver, uranium, pyrite, muscovite, pyrophyllite, chlorite, quartz, iron, potassium, nickel, titanium, zirconium and chromium -- resulting in 2002 analytical values. These analytical values are listed in Tables II, III and IV. In these tables the samples originating from a single bulk sample are identified by a solid line on the right-hand side of each table. In each case the sample taken from the top of the bulk sample has the lowest number: for example, VRH 1 represents the hanging wall and VRH 5 the footwall of the first bulk sample from Hartebeestfontein, and similarly VRZ 85 and VRZ 91 represent, respectively, the hanging wall and the footwall of the fifth bulk sample from Zandpan. In Table V the mean values, standard deviations and coefficients of variation for all the variables are listed.

In order to evaluate these results without the subjectivity that appears to have plagued many Witwatersrand studies in the past, the approach advocated by Hiemstra (1968, p. 83) was adopted. Hiemstra defined a sympathetic variation between two elements (or between an element and a mineral, or between two minerals) as a significant positive correlation. Accordingly, use was made of the product-moment correlation coefficient to express the intensities of relationships, and, in order to judge objectively whether these relationships were signifi-

SAMPLE	Au ppm	Ag ppm	U_3O_8 %	PYRITE %	MUSC. %	PYROPH. %	CHLOR. %	QUARTZ %	Fe ppm	K ppm	Ni ppm	Ti ppm	Zr ppm	Cr ppm
VRH001 :	•80	•10	•0109	•1	17•2	•1	7•0	75•8	11231•	11051•	837•	1073•	133•	223•
VRH002 :	330•00	42•00	•5501	15•4	1•0	•1	5•4	78•2	38949•	1930•	5897•	1348•	479•	824•
VRH003 :	176•00	28•00	•2609	8•3	•1	•1	3•5	88•2	32356•	2424•	8521•	976•	410•	912•
VRH004 :	890•00	148•00	•7391	9•2	1•0	•1	5•8	84•0	26514•	2703•	5470•	826•	324•	7397•
VRH005 :	5•00	•50	•0123	•1	4•8	•1	4•8	90•4	12542•	4528•	1643•	489•	186•	321•
VRH006 :	•30	•44	•0083	•1	10•1	•1	•1	89•9	2188•	10706•	4304•	1120•	112•	482•
VRH007 :	6•35	1•05	•0476	7•4	4•8	•1	•1	87•8	18315•	4713•	5461•	1375•	438•	749•
VRH008 :	6•50	7•40	•0226	6•8	2•2	•1	•1	91•0	16474•	2371•	7627•	585•	257•	676•
VRH009 :	38•50	4•60	•0706	10•8	1•0	•1	•1	88•2	27304•	2426•	16264•	803•	389•	1008•
VRH010 :	1•80	•36	•0086	5•0	1•9	•1	•1	93•1	10159•	2431•	5215•	527•	503•	706•
VRH011 :	5•50	1•00	•2800	11•0	•1	•1	•1	89•0	36417•	1593•	24566•	1266•	1116•	1561•
VRH012 :	•55	•14	•0062	1•0	1•0	•1	•1	98•0	5016•	1699•	2122•	345•	316•	425•
VRH013 :	8•00	1•00	•0360	3•2	1•0	•1	•1	95•8	7990•	1589•	4418•	367•	247•	522•
VRH014 :	36•00	4•20	•0990	4•1	1•0	•1	•1	94•9	12169•	1504•	3637•	514•	315•	637•
VRH015 :	11•00	1•60	•0316	7•9	1•0	•1	•1	91•1	18814•	1170•	8946•	539•	362•	807•
VRH016 :	10•00	2•20	•0495	6•2	1•0	•1	•1	92•8	12457•	1787•	6462•	403•	254•	663•
VRH017 :	8•14	1•18	•0217	6•6	1•0	•1	•1	92•4	13672•	1795•	11763•	380•	218•	696•
VRH018 :	115•00	14•50	•0949	•1	1•7	•1	•1	98•3	1685•	2068•	1497•	208•	82•	192•
VRH019 :	56•00	6•80	•1538	1•0	8•7	•1	•1	90•3	5143•	7793•	2389•	819•	169•	282•
VRH020 :	2•70	•30	•0022	•1	31•9	•1	•1	68•1	2444•	13993•	794•	1267•	133•	259•
VRH021 :	2•55	•68	•0377	15•9	7•6	•1	1•6	74•9	28574•	4627•	7486•	1732•	427•	783•
VRH022 :	2•25	•48	•0109	5•0	3•1	•1	•1	91•9	13227•	2911•	4996•	620•	329•	668•
VRH023 :	1•65	•56	•0016	9•7	3•7	•1	•1	86•6	27668•	2554•	10045•	1218•	690•	1245•
VRH024 :	•75	•24	•0343	1•7	1•0	•1	•1	97•3	18706•	2729•	2836•	702•	452•	557•
VRH025 :	1•95	•50	•0143	1•7	•5	•1	•1	97•3	17893•	3762•	4489•	845•	539•	840•
VRH026 :	4•80	•88	•0381	10•2	4•2	•1	•1	85•6	27137•	2375•	11900•	878•	704•	1181•
VRH027 :	1•55	•32	•0126	2•7	2•4	•1	•1	94•9	6405•	2655•	2980•	366•	282•	459•
VRH029 :	8•80	1•42	•0553	8•1	3•1	•1	•1	88•8	19046•	2083•	6069•	588•	423•	670•
VRH030 :	•50	•12	•0082	1•0	29•8	•1	1•9	67•3	6264•	17133•	1406•	2889•	265•	384•
VRH031 :	•55	•12	•0163	•1	15•7	•1	•1	84•3	2979•	8936•	1403•	837•	142•	252•
VRH032 :	6•50	1•72	•0484	13•2	5•6	•1	•1	81•2	37496•	3974•	9943•	1819•	497•	920•
VRH033 :	2•75	•72	•0179	12•8	4•6	•1	•1	82•6	22010•	2661•	6896•	1106•	451•	750•
VRH034 :	12•00	2•46	•0921	17•5	5•7	•1	1•0	75•8	40038•	4090•	8772•	2834•	2652•	2103•
VRH035 :	9•55	1•86	•0846	13•5	•1	•1	•1	86•5	38012•	1964•	1621•	1308•	1083•	1556•
VRH036 :	3•15	•42	•0136	5•5	2•2	•1	•1	92•3	10842•	1961•	5211•	542•	420•	531•
VRH037 :	4•25	1•40	•0140	5•9	•1	•1	•1	94•1	78260•	1525•	7252•	1692•	872•	1753•
VRH038 :	6•85	1•84	•0472	22•3	•1	•1	•1	77•7	73733•	1367•	5606•	1355•	847•	1842•
VRH039 :	1•00	•20	•0076	5•6	1•0	•1	•1	93•4	14903•	1017•	7074•	579•	357•	785•
VRH040 :	4•50	•80	•0127	5•3	2•7	•1	•1	92•0	17173•	1830•	5343•	523•	288•	643•
VRH041 :	•50	•10	•0102	•1	1•5	•1	•1	98•5	2407•	2031•	3043•	341•	117•	332•
VRH042 :	•85	•16	•0111	2•9	1•5	•1	•1	95•6	5465•	1837•	4791•	269•	162•	519•
VRH043 :	34•00	4•60	•0840	8•3	1•0	•1	•1	90•7	18915•	1410•	6738•	422•	242•	757•
VRH044 :	336•00	41•60	•5722	9•3	1•0	•1	•1	89•7	22793•	1467•	7539•	685•	431•	825•

TABLE II

ANALYTICAL RESULTS FOR ELEMENTS AND MINERALS PRESENT IN THE VAAL REEF AT HARTEBEESTFONTEIN

SAMPLE	Au ppm	Ag ppm	U_3O_8 %	PYRITE %	MUSC. %	PYROPH. %	CHLOR. %	QUARTZ %	Fe ppm	K ppm	Ni ppm	Ti ppm	Zr ppm	Cr ppm
VRZ060 :	1•05	•14	•0091	•1	2•8	•1	•1	97•2	2841•	3000•	2222•	3388•	74•	322•
VRZ061 :	4•60	•56	•0295	16•3	4•9	•1	1•0	77•8	2897•	2677•	4332•	1333•	517•	1164•
VRZ062 :	160•00	12•80	•5489	23•9	15•3	•1	6•4	54•4	61505•	5762•	4108•	3235•	1246•	1698•
VRZ063 :	1•80	•30	•0040	•1	4•8	•1	1•0	94•2	3956•	5499•	1781•	700•	119•	278•
VRZ064 :	•40	•10	•0024	•1	9•1	•1	1•0	89•9	2456•	5471•	1622•	578•	118•	208•
VRZ065 :	•40	•10	•0017	2•8	2•8	1•9	•1	92•5	5888•	2628•	3418•	265•	79•	381•
VRZ066 :	4•05	•82	•0134	50•0	19•1	•1	•1	30•9	99004•	6231•	14335•	2543•	567•	1469•
VRZ067 :	4•75	1•06	•1028	43•5	1•0	•1	•1	55•5	109456•	4358•	17598•	2393•	654•	1501•
VRZ068 :	11•00	1•80	•0847	44•5	1•0	•1	•1	54•5	134552•	5093•	9015•	4951•	1607•	2044•
VRZ069 :	15•00	1•78	•1120	27•4	17•7	•1	•1	54•9	62291•	5825•	10454•	3059•	1142•	1309•
VRZ070 :	4•40	•46	•0124	•1	7•2	1•0	•1	91•8	3544•	4783•	1556•	510•	129•	306•
VRZ071 :	4•05	•60	•0033	•1	6•5	1•0	•1	92•5	2322•	5464•	1299•	574•	105•	218•
VRZ072 :	•30	•14	•0028	•1	5•0	•1	•1	95•0	2127•	4427•	1689•	501•	74•	194•
VRZ073 :	•50	•12	•0034	•1	3•8	•1	•1	96•2	2172•	3365•	1840•	285•	73•	211•
VRZ074 :	6•25	1•52	•0420	49•2	1•0	•1	•1	49•8	161227•	3474•	8247•	2670•	778•	1633•
VRZ075 :	10•00	2•60	•0349	51•5	1•0	•1	•1	47•5	230165•	4893•	6920•	4968•	928•	1793•
VRZ076 :	1•80	1•80	•0123	7•1	4•7	•1	•1	88•2	23097•	4829•	3760•	1658•	453•	524•
VRZ077 :	5•10	3•08	•1207	2•8	6•2	•1	•1	91•0	8127•	5462•	1776•	1123•	451•	520•
VRZ078 :	•65	•26	•0044	14•7	2•7	1•0	•1	81•6	10466•	3074•	2716•	916•	267•	532•
VRZ079 :	1•20	•25	•0116	4•3	5•3	2•4	•1	88•0	15382•	4621•	2753•	1631•	470•	675•
VRZ080 :	•55	•20	•0056	3•8	4•3	1•0	•1	90•9	8831•	3784•	2600•	1044•	317•	480•
VRZ081 :	6•90	1•00	•1021	12•9	6•3	•1	•1	80•8	44031•	3656•	5706•	2292•	872•	1158•
VRZ082 :	2•85	•66	•0342	11•2	5•0	1•0	•1	82•8	17938•	3734•	2589•	1040•	399•	568•
VRZ083 :	98•00	6•00	•1682	11•3	5•9	1•0	•1	81•8	30357•	4518•	3761•	1343•	644•	768•
VRZ084 :	•82	•18	•0039	•1	6•9	4•0	•1	89•1	1770•	5598•	1415•	600•	120•	205•
VRZ085 :	1•20	•58	•0147	10•3	8•8	8•2	1•0	71•7	32536•	7563•	2940•	3056•	912•	913•
VRZ086 :	•90	•42	•0169	7•9	5•6	4•2	1•0	81•3	17120•	3730•	2970•	1160•	343•	572•
VRZ087 :	6•05	•92	•0677	15•8	1•0	•1	1•0	82•2	41958•	2543•	7680•	1622•	620•	1132•
VRZ088 :	290•00	20•00	•3616	39•4	1•0	1•0	•1	58•6	105870•	3723•	15643•	3288•	999•	1800•
VRZ089 :	86•00	5•40	•1764	4•5	4•8	3•4	1•0	86•3	14635•	4116•	2804•	2589•	644•	454•
VRZ090 :	1•95	•32	•0088	3•4	6•6	4•4	1•0	84•6	11252•	5669•	2825•	3517•	519•	431•
VRZ091 :	1•40	•32	•0117	4•0	26•8	15•7	2•3	51•2	9677•	10308•	1956•	3645•	591•	444•
VRZ092 :	2•40	•46	•0105	13•5	3•8	1•0	2•2	79•5	21608•	3175•	4770•	1350•	480•	718•
VRZ093 :	2•50	•87	•0601	11•3	4•8	3•4	3•0	77•5	34683•	3190•	4963•	1321•	458•	744•
VRZ094 :	3•95	1•16	•0711	26•0	9•7	•1	5•0	59•3	67981•	3919•	11451•	3092•	1253•	1593•
VRZ095 :	1•75	•50	•0277	9•4	4•8	•1	1•0	84•8	29044•	3321•	4096•	1291•	683•	877•
VRZ096 :	113•00	9•60	•6035	14•0	7•2	4•2	3•8	70•8	38845•	3371•	3796•	2000•	857•	881•
VRZ097 :	14•00	1•60	•0316	2•7	6•5	11•4	•1	79•4	7981•	4717•	3249•	2652•	941•	558•
VRZ098 :	1•40	•28	•0115	•1	3•3	•1	•1	96•7	5823•	3851•	2040•	701•	158•	383•
VRZ099 :	680•00	44•00	•1826	17•6	16•3	13•9	4•8	47•4	30839•	6416•	4547•	2947•	585•	904•
VRZ100 :	32•00	4•80	•3323	27•2	1•0	1•0	•1	70•8	70741•	2267•	7655•	1920•	339•	1205•
VRZ101 :	43•00	3•20	•1879	7•6	4•6	19•1	•1	68•7	7177•	2236•	2660•	688•	158•	365•
VRZ102 :	125•00	13•00	•3998	23•2	1•0	1•0	•1	74•8	76109•	1674•	4470•	20•	345•	1052•
VRZ103 :	3•25	•54	•0268	•1	39•4	•1	•1	60•6	5205•	1249•	1588•	1004•	63•	222•

TABLE III

ANALYTICAL RESULTS FOR ELEMENTS AND MINERALS PRESENT IN THE VAAL REEF AT ZANDPAN

SAMPLE	Au ppm	Ag ppm	U_3O_8 %	PYRITE %	MUSC. %	PYROPH. %	CHLOR. %	QUARTZ %	Fe ppm	K ppm	Ni ppm	Ti ppm	Zr ppm	Cr ppm
VCR001 :	18•00	1•80	•0681	1•0	5•6	•1	3•5	89•9	45974•	1809•	8712•	453•	158•	1278•
VCR002 :	3•75	•38	•0219	1•0	1•0	•1	1•0	97•0	24224•	8893•	4531•	138•	70•	621•
VCR003 :	9•00	•70	•0469	•1	4•4	•1	•1	95•6	27294•	2650•	2804•	393•	148•	536•
VCR004 :	•85	•20	•0067	•1	1•0	•1	1•0	98•0	8199•	772•	2414•	83•	27•	259•
VCR005 :	9•00	•64	•0192	•1	2•8	•1	1•0	96•2	16626•	1109•	2227•	183•	75•	403•
VCR006 :	2•30	•28	•0218	•1	1•0	•1	2•0	97•0	9055•	367•	2708•	101•	38•	334•
VCR007 :	2•25	•24	•0057	•1	4•0	•1	9•2	86•8	36239•	6001•	2792•	780•	72•	478•
VCR008 :	1•30	•18	•0039	•1	10•9	•1	13•8	75•3	51344•	8468•	2343•	1954•	101•	565•
VCR009 :	•65	•16	•0030	•1	11•6	•1	12•3	76•1	41390•	9173•	2222•	1689•	116•	487•
VCR010 :	1•30	•24	•0115	•1	2•2	•1	1•0	96•8	9633•	1847•	4560•	544•	62•	619•
VCR011 :	16•00	1•20	•0249	•1	2•5	•1	1•0	96•5	22654•	1672•	4670•	265•	77•	553•
VCR012 :	6•00	•50	•0220	•1	3•7	•1	1•0	95•3	18987•	1711•	2501•	285•	78•	377•
VCR013 :	2•30	•32	•0220	•1	3•3	•1	•1	96•7	13503•	2390•	2640•	278•	78•	453•
VCR014 :	18•00	1•22	•0256	•1	3•8	•1	•1	96•2	19808•	2008•	2620•	282•	83•	398•
VCR015 :	4•40	•28	•0085	•1	1•0	•1	•1	99•0	6691•	492•	4426•	130•	41•	493•
VCR016 :	17•00	1•06	•0140	•1	•1	•1	1•0	99•0	11205•	469•	7363•	123•	38•	711•
VCR017 :	13•00	1•24	•0192	1•0	•1	•1	•1	99•0	3870•	164•	3171•	54•	17•	432•
VCR018 :	39•00	3•20	•0438	•1	•1	•1	2•1	97•9	12970•	572•	3627•	157•	59•	453•
VCR019 :	57•00	4•60	•0646	6•5	2•4	•1	6•1	85•0	25316•	1120•	1950•	267•	86•	308•
VCR020 :	1•85	•28	•0022	•1	3•5	•1	4•6	91•9	18175•	4178•	3363•	673•	69•	591•
VCR021 :	•60	•12	•0010	•1	5•7	•1	6•0	88•3	16051•	5139•	1805•	611•	78•	286•
VCR022 :	9•00	•92	•0036	5•9	1•0	•1	3•6	89•5	20224•	170•	8983•	96•	27•	933•
VCR023 :	92•00	9•00	•0152	18•2	•1	•1	6•8	75•0	75484•	103•	11731•	211•	39•	764•
VCR024 :	18•00	2•00	•0136	15•5	•1	•1	8•2	76•3	60726•	198•	3921•	337•	45•	506•
VCR025 :	91•00	8•40	•0420	26•4	•1	•1	11•8	61•8	122302•	393•	7001•	427•	67•	450•
VCR026 :	8•50	•94	•0196	5•0	2•5	•1	4•1	88•4	21242•	1130•	2423•	203•	91•	329•
VCR027 :	26•00	2•80	•0954	•1	1•7	•1	3•6	94•7	12469•	862•	2411•	192•	41•	364•
VCR029 :	•85	•10	•0060	•1	26•6	•1	23•2	50•2	55487•	350•	1959•	16728•	256•	5712•
VCR030 :	108•00	12•20	•0207	•1	8•9	•1	5•1	86•0	15022•	1151•	3463•	5968•	162•	2036•
VCR031 :	1•25	•16	•0018	•1	•1	•1	•1	100•0	1796•	838•	1558•	48•	14•	195•
VCR032 :	4•25	•42	•0040	4•6	1•0	•1	3•8	90•6	11493•	452•	1844•	285•	69•	291•
VCR033 :	•90	•20	•0029	2•8	•1	•1	1•8	95•4	11194•	476•	1880•	301•	56•	276•
VCR034 :	12•00	1•60	•0067	5•4	•1	•1	3•8	90•8	23881•	76•	4015•	128•	53•	347•
VCR035 :	1•90	•46	•0086	6•3	•1	•1	4•4	89•3	24121•	46•	2727•	181•	68•	466•
VCR036 :	45•00	4•60	•0729	•1	20•7	•1	5•0	74•3	17834•	15471•	2990•	9116•	526•	2975•
VCR037 :	21•00	2•00	•0301	•1	1•0	•1	1•0	98•0	7624•	1329•	5904•	4041•	121•	649•
VCR038 :	95•00	8•50	•0850	•1	1•0	•1	2•2	96•8	8903•	988•	2879•	292•	60•	288•
VCR039 :	168•00	14•40	•0821	•1	1•0	•1	2•6	96•4	9517•	589•	3570•	224•	96•	435•
VCR040 :	48•00	4•10	•0530	3•7	•1	•1	1•8	94•5	9740•	387•	3512•	121•	85•	453•
VCR041 :	94•00	8•00	•0927	•1	1•0	•1	2•5	96•5	10969•	316•	3534•	123•	61•	440•
VCR042 :	119•00	11•70	•1107	1•0	•1	•1	2•5	96•5	13288•	636•	3703•	186•	65•	458•
VCR043 :	28•00	2•50	•0452	1•0	•1	•1	1•0	98•0	10505•	348•	5174•	93•	43•	555•
VCR044 :	146•00	23•60	•0722	1•0	•1	•1	6•2	92•8	20831•	98•	4007•	325•	156•	705•
VCR045 :	180•00	24•80	•0596	•1	•1	•1	11•8	88•2	49218•	119•	3908•	481•	195•	838•
VCR046 :	84•00	11•60	•0380	•1	•1	1•1	12•9	86•1	50434•	69•	4234•	427•	105•	581•
VCR047 :	125•00	16•00	•0480	•1	•1	•1	12•2	87•8	48565•	296•	5428•	448•	131•	562•
VCR048 :	45•00	5•40	•0212	5•8	•1	•1	6•0	88•2	32604•	100•	4729•	246•	72•	529•
VCR049 :	340•00	38•00	•0232	8•7	•1	•1	8•9	82•4	45983•	65•	5279•	357•	94•	517•
VCR050 :	116•00	13•00	•0079	4•3	•1	•1	4•4	91•3	24119•	66•	2939•	134•	37•	292•
VCR051 :	176•00	21•60	•0167	6•8	•1	•1	4•6	88•6	24231•	56•	4320•	156•	70•	476•
VCR052 :	1•30	•26	•0168	•1	24•7	•1	19•3	56•0	59191•	17327•	1285•	5794•	758•	1738•
VCR053 :	3•30	•82	•0265	10•6	4•9	•1	7•5	77•0	38406•	3032•	2021•	1034•	526•	953•
VCR054 :	•70	•12	•0086	•1	•1	•1	•1	100•0	4603•	190•	6877•	62•	20•	676•
VCR055 :	•95	•30	•0001	1•0	1•0	•1	6•3	91•7	30497•	1606•	5337•	612•	63•	700•
VCR056 :	9•90	1•62	•0098	11•7	•1	•1	4•0	84•3	32192•	117•	7966•	128•	55•	824•
VCR057 :	12•00	1•80	•0069	20•6	•1	•1	5•9	73•5	61199•	268•	10125•	279•	80•	847•

TABLE IV

ANALYTICAL RESULTS FOR ELEMENTS AND MINERALS PRESENT IN THE VENTERSDORP CONTACT REEF AT VENTERSPOST

cant, standard statistical procedures were used to test the significance of the correlation coefficients obtained. For this purpose, the relationships between the 14 variables in the 143 samples were first examined by means of a matrix correlation programme (see Section 4.2.1) and subsequently by means of multivariate statistics, more generally referred to as factor analysis (see Section 4.2.2).

4.2. Statistical Concepts.

4.2.1. Product-moment correlation coefficient.

In the present study the intensity of the correlations between minerals and elements was expressed by means of the product-moment correlation coefficient, also known as the coefficient of linear correlation, which is denoted by the letter r. This is a measure of how much linear relationship exists between two variables x and y. It is calculated by the following formula (Hayslett, 1968, p. 133):

$$r = \frac{\Sigma (x - \bar{x})\ (y - \bar{y})}{\sqrt{[\Sigma (x - \bar{x})^2]\ [\Sigma (y - \bar{y})^2]}}$$

where $\bar{x}$ and $\bar{y}$ represent the arithmetric means of x and y.

The values of the sample correlation coefficients must always lie between the limits of +1 and -1. A value of r equal to -1 indicates a perfect linear relationship between the sample values of x and y, with the value of y decreasing as the value of x increases. A value of r equal to +1 also indicates a perfect linear relationship between the sample values, but one in which the value of y increases as x increases. If there is no linear relationship between sample values of x and y, then r will have a value of zero. Values of r above 0.7 or below -0.7 may be regarded as indicating a high degree of linear correlation. The selection of $r = 0.7$ as a convenient rule-of-thumb cut-off point in determining what may be regarded as a high degree of correlation is based on the quantity r^2, which is known as the "coefficient of determination". It can be shown (Richmond, 1964, p. 442) that r^2 can be interpreted as the percentage of the total variation in the y values that is associated with variation in the x values. Thus, where the correlation coefficient $r = 0.7$, $r^2 = 0.49$, and it can be said that 49% of the variation in y is associated with variation in x.

As pointed out by Hiemstra (1968, p. 82), it must be remembered that the value of the sample correlation coefficient r is only an estimate of the true population correlation coefficient ρ. The fact that r is calculated from only a limited number of samples drawn from the total population should not be overlooked.

The precision of the estimate of the correlation coefficient r is strictly dependent on the number of samples examined. The confidence interval of ρ may easily be evaluated (95% confidence interval in the present case) by means of the Fisher-z value (Hayslett, 1968, p. 167). Use was made of tables published by Fisher and Yates (1957, p. 59) to judge the degree of significance of the estimate of the correlation coefficient. A level of significance of 0.1% indicates that, if the variables are in fact completely unrelated ($\rho = 0$), the chances are less than 1 in 1000 that an estimate r of the correlation coefficient will be as high as the value actually obtained. Similarly, levels of significance of 1%, 5% and 10% indicate that the chances are, respectively, 1 in 100, 1 in 20 and 1 in 10 that such high r values will be obtained if ρ is actually 0. Where the chances of obtaining such high r values even when ρ is 0 are better than 1 in 10, these r values are indicated in the correlation matrix by the letters "n.s.". It should, however, be pointed out that the use of this symbol (implying "non-significance") does not mean that no correlation exists, but merely that the number of samples examined was insufficient to establish whether a relationship in fact exists or not.

In the present study, to investigate the relationship between each of the 14 variables in the 143 samples analysed, estimates of the correlation coefficient "r" were obtained by the use of a matrix correlation coefficient programme originally written by Mr. D. Hawkins of the Department of Statistics of the University of the Witwatersrand, but rewritten to be compatible with the IBM Model 360/50 digital computer. This programme is set out as programme No. 3 in Section 9 (in Part III of this thesis).

4.2.2. Factor Analysis. .

Any investigator attempting to gain a clear picture of the concentration and mineralization processes that have resulted in the formation of the Vaal Reef and Ventersdorp Contact Reef is faced with the problem that upwards of thirty minerals are known to occur in these conglomerate bands in major or minor quantities, and that the same elements are often associated with two or more minerals. In fact, the minerals present in these conglomerate bands may be compared to a stream sediment, and, as pointed out by Garrett and Nichol (1969, pp. 245 - 246), "The active stream sediment is nature's approximation of a composite sample of the rock and soil upstream from the sampling point." The interpretation of the minor element contents of stream sediments must take into account the fact that the data are frequently related to a number of geochemical populations, each of

which represents a discrete geological or geochemical feature in the environment. Where such complex interrelated multi-element or mineral data have to be interpreted, the estimation of correlation coefficients may only reveal the more obvious relationships while subtle though significant relationships may remain undetected.

In the present study, in an attempt to overcome this problem, the technique of factor analysis (a branch of multivariate statistics) was adopted. The whole concept of factor analysis as a method for finding common underlying factors in many interdependent variables was introduced by Spearman (1904) as a tool in the field of psychometric research. Although other workers have used the technique, the most significant application of the technique in the geological sciences has been the heavy mineral provenance study carried out by Imbrie and van Andel (1964, pp. 1131 - 1155). Their work demonstrated the existence of apparently simple relations in complex data corresponding to zones of littoral transport. More recently, Garrett and Nichol (1969) have used factor analysis as an aid in the interpretation of regional geochemical stream sediment data in Sierra Leone, and Saager and Esselaar (1969, p. 445) have examined Co, Ni, Cu, Zn, Pb, Ag, Au and U_3O_8 in ore from the Basal Reef by factor analysis and expressed their findings in terms of three factors supporting the modified placer theory.

The prime aim of factor analysis is an attempt to simplify the interpretation of a complex set of variables (14 variables in the case of the present study) by expressing the total variance of the set in as few "factors", or theoretical variables, as possible. Either the relationships between variables (R-mode of analysis) or between samples (Q-mode of analysis) may be examined. In the present study, however, only the relationships between variables (R-mode) were examined.

According to Saager and Esselaar (1969, pp. 447 - 448): "Factor analysis assumes that each variable x_i can be expressed in the form

$$x_i = a_{i1}f_1 + a_{i2}f_2 + \ldots\ldots\ldots\ldots + a_{im}f_m + a_iu_i$$

where the f_j are common factors and the a_{ij} indicates the relative importance of the common factor f_j. A common factor is a factor that is present in each variable, while u_i is a factor that is unique to the particular variable in question."

Since the readings are arranged so that the variance of each variable is unity, the sum of squares of the coefficients of the common factors indicates to what extent the common factors account for the variance of that variable, and this is known as the "communality". All the factors might account for one hundred

per cent of the variation in the data, but the common factors might account for only ninety per cent of the variation. The first factor is chosen to account for as much of the variance as possible, and each succeeding factor is then chosen so that it also accounts for as much of the variance as possible and is uncorrelated with all preceeding factors.

There are various techniques for relating each variable to the statistically independent hypothetical factors, but the method described by Harman (1960) is the one most used. This results in what is known as an "initial factor matrix", which may be visualised geometrically as providing an orthogonal coordinate scheme in which the hypothetical factors are the reference axes and the variables are vectors in the space of dimension determined by the number of axes. These reference axes are rotated so that they correspond as closely as possible to any definite grouping of the observed variables, resulting in the "rotated factor matrix" in which it is usually possible to identify each of the hypothetical factors with one or more of the observed variables.

In the case of the present investigation, factor analysis was carried out with the aid of the IBM Model 360/50 digital computer, using the programme designated as subroutine package (360-A-CM-03) in the IBM catalogue. This programme, however, was first rewritten by Mr. P.A. Esselaar, statistician in the Economic Geology Research Unit of the University of the Witwatersrand, to permit the taking of logarithms of the concentrations of the data used (see Section 4.3). In the programme used, the proportion of the overall data variability contained in each factor is expressed by the magnitude of the eigenvalues, which are derived by standard techniques of matrix algebra. The choice of the number of factors to be used is somewhat subjective, but in the present case, since there were unities in the diagonal of the correlation matrix, only factors associated with eigenvalues greater than unity were used in accordance with a suggestion made by Harman (1967, p. 420).

The validity of the factors should, of course, be checked by other independent observations where possible, and in the present study polished section analysis was used as a control.

Whilst it is realized that processes are rarely mutually exclusive in nature, so that a certain amount of correlation must be introduced into the factor model thereby making the axes no longer mutually perpendicular, it was not possible to use the Promax oblique rotation technique (Hurley and Cattell, 1962, pp. 258 - 262) in the present investigation, as no relevant programme was available for the

IBM Model 360/50 digital computer at the time. In any case, it is felt that this procedure would in all probability not have produced any factors significantly different from those obtained by the use of orthogonal axes.

4.3. Logarithmic Transformation of Data.

Cousins (1956, p. 96) has stated that if any ore body is sampled for a particular mineral, it will be found that the value distribution of a large number of such samples will follow a log-normal frequency distribution curve, irrespective of whether the origin of the mineralization is hydrothermal, chemical, magmatic or placer. Hiemstra (1968, p. 82), who examined material from the Dominion Reef, agreed with Cousins' views as far as gold, pyrite and uranium were concerned, and added that it was highly probable that the value distributions of the minor components of the Dominion Reef were also lognormal. Hiemstra accordingly handled his data on a logarithmic scale. Garrett and Nichol (1969, pp. 246 - 251), who determined 15 elements quantitatively in stream sediments in Sierra Leone, also found that their data were lognormally distributed and could best be interpreted with the aid of a logarithmic transformation of the original analytical data. Krige (1960, pp. 231 - 232), on the other hand, found that in some of the 31 mines he examined (on the East, Central and West Rand, at Klerksdorp and in the Orange Free State) gold, uranium and pyrite departed from the lognormal model. Krige pointed out that this departure, although not applicable to all mines, tended to give a positive bias to grade estimates.

In view of Krige's findings, and in the absence of prior information on any of the three mines examined in the present study, all the analytical data obtained in the present investigation were examined by means of a computer programme REGLOG written by Mr. C.J. van Tonder of the National Institute for Metallurgy. This programme showed that in the majority of cases far higher correlation coefficients could be obtained when the results were first logarithmically transformed than when the correlation coefficients were calculated directly from the original analytical data. Accordingly, a lognormal distribution was assumed and all the results were logarithmically transformed before statistical parameters were computed.

4.4. Results of Statistical Treatment of Analytical Data.

As has already been mentioned (see Section 4.1), the original analytical results of the quantitative chemical, X-ray diffraction and X-ray fluorescence analyses carried out on the 143 samples from the Vaal Reef at Hartebeestfontein and Zandpan and from the Ventersdorp Contact Reef at Venterspost are set out in

Tables II, III and IV. Table V lists the mean values, standard deviations and coefficients of variation for these variables.

These results were then logarithmically transformed (see Section 4.3) and subjected to the statistical procedures outlined in Section 4.2. The resulting 14 by 14 correlation matrices, one for each of the three mines examined, are shown in Tables VI, VII and VIII, while the rotated factor loadings for all three mines are shown in Table IX.

4.5. Discussion of Results.

4.5.1. Means, standard deviations and coefficients of variation for the three mines examined.

Inspection of the coefficients of variation shown in Table V reveals the wide dispersion in the values obtained for certain elements (for example Au and Ag in the Vaal Reef), while other elements (such as Zr and Ti in the Vaal Reef) show a much smaller dispersion. This merely indicates that, at Hartebeestfontein and Zandpan, sample estimates of the population means of Zr and Ti are likely to approximate more closely to the true population means of these elements than the sample estimates of the population means for Au and Ag do to their true population means.

4.5.2. Correlation studies.

When attempting to interpret the significance of correlations revealed by the correlation coefficient matrix or by the factor analysis programme, the following two points mentioned by Hiemstra (1968, p. 83) should be borne in mind:

(1) Those elements that occur in the same host mineral can be expected to show a high degree of correlation.

(2) Elements introduced simultaneously into the ore by the same mechanism can be expected to have significant correlations.

Elements possessing similar geochemical properties will often occur in the same mineral species and partake in the same processes of concentration. Thus, two or even more causes may contribute to a high correlation in some cases.

The interpretation of the results of the matrix correlation coefficient programme and the factor analysis programme is made much simpler if the particular elements involved in significant correlations and associations can rather

TABLE V

MEANS, STANDARD DEVIATIONS AND COEFFICIENTS OF VARIATION OF Au, Ag, U_3O_8, PYRITE, MUSCOVITE, PYROPHYLLITE, CHLORITE, QUARTZ, Fe, K, Ni, Ti, Zr & Cr IN SAMPLES FROM HARTEBEESTFONTEIN, ZANDPAN AND VENTERSPOST.

	Au ppm	Ag ppm	U_3O_8 %	PYRITE %	MUSC. %	PYROPH. %	CHLOR. %	QUARTZ %	Fe %	K %	Ni %	Ti %	Zr %	Cr %
							HARTEBEESTFONTEIN - VAAL REEF							
$\bar{x}$	50.1	7.6	0.087	6.6	4.4	0.1	0.8	88.3	2.004	0.366	0.608	0.092	0.045	0.092
s	149.2	23.7	0.159	5.4	6.9	-	1.7	7.7	1.649	0.352	0.435	0.060	0.042	0.109
V	2.98	3.11	1.83	0.82	1.57	-	2.16	0.09	0.83	0.97	0.72	0.65	0.94	1.18
							ZANDPAN - VAAL REEF							
$\bar{x}$	39.9	3.3	0.093	14.0	7.0	2.5	0.9	75.8	3.808	0.430	0.476	0.185	0.053	0.081
s	111.9	7.4	0.143	15.1	7.2	4.4	1.5	16.6	4.823	0.161	0.387	0.123	0.037	0.052
V	2.80	4.45	1.54	1.08	1.03	1.76	1.66	0.22	1.26	3.75	0.81	0.66	0.71	0.64
							VENTERSPOST - VENTERSDORP CONTACT REEF							
$\bar{x}$	43.8	4.9	0.029	3.2	3.0	0.2	4.9	88.9	2.688	0.198	0.406	0.106	0.107	0.071
s	64.5	7.6	0.028	5.6	5.6	0.1	4.9	10.8	2.161	0.351	0.222	0.267	0.129	0.081
V	1.47	1.55	0.97	1.75	1.86	0.72	1.0	1.22	0.80	1.78	5.46	2.52	1.21	1.14

SYMBOLS: $\bar{x}$ = mean, s = standard deviation, V = coefficient of variation ($s/\bar{x}$)

MUSC. = Muscovite, PYROPH. = Pyrophyllite, CHLOR. = Chlorite.

TABLE VI

CORRELATION MATRIX FOR HARTEBEESTFONTEIN - VAAL REEF

	Au	Ag	U_3O_8	PYRITE	MUSC.	PYROPH.	CHLOR.	QUARTZ	Fe	K	Ni	Ti	Zr	Cr
Au	1.00	0.96 0.1%	0.86 0.1%	0.42 1.0%	-0.44 1.0%	-0.00 N.S.	0.29 5.0%	-0.01 N.S.	0.37 2.0%	-0.33 5.0%	0.28 5.0%	-0.02 N.S.	0.15 N.S.	0.41 1.0%
Ag		1.00	0.85 0.1%	0.47 1.0%	-0.46 1.0%	-0.00 N.S.	0.26 10.0%	0.00 N.S.	0.40 1.0%	-0.32 5.0%	0.36 2.0%	0.04 N.S.	0.18 N.S.	0.49 0.1%
U_3O_8			1.00	0.44 1.0%	-0.52 0.1%	0.00 N.S.	0.29 5.0%	-0.00 N.S.	0.41 1.0%	-0.29 5.0%	0.33 5.0%	0.09 N.S.	0.26 10.0%	0.43 1.0%
PYRITE				1.00	-0.62 0.1%	-0.00 N.S.	-0.09 N.S.	-0.04 N.S.	0.86 0.1%	-0.60 0.1%	0.81 0.1%	0.27 1.0%	0.81 0.1%	0.80 0.1%
MUSCOVITE					1.00	0.00 N.S.	0.20 N.S.	-0.56 0.1%	-0.65 0.1%	0.94 0.1%	-0.53 0.1%	0.19 N.S.	-0.56 0.1%	-0.66 0.1%
PYROPHYLLITE						1.00	0.00 N.S.	0.01 N.S.	0.01 N.S.	0.01 N.S.	0.01 N.S.	0.01 N.S.	0.00 N.S.	0.00 N.S.
CHLORITE							1.00	-0.52 0.1%	0.19 N.S.	0.35 2.0%	-0.20 N.S.	0.36 2.0%	-0.01 N.S.	0.12 N.S.
QUARTZ								1.00	-0.18 N.S.	-0.60 0.1%	0.19 N.S.	-0.76 0.1%	-0.16 N.S.	-0.09 N.S.
Fe									1.00	-0.41 1.0%	0.62 0.1%	0.49 0.1%	0.83 1.1%	0.78 0.1%
K										1.00	-0.56 0.1%	0.48 0.1%	-0.33 5.0%	-0.41 1.0%
Ni											1.00	0.10 N.S.	0.55 0.1%	0.66 0.1%
Ti												1.00	0.55 0.1%	0.39 1.0%
Zr													1.00	0.75 0.1%
Cr														1.00

KEY

Ag

Au

0.96: Estimated correlation coefficient r

0.1%: Level of significance

Confidence limits at 95% probability for 43 pairs

ρ	LOWER	UPPER
0.3	0.010	0.532
0.4	0.125	0.619
0.5	0.245	0.690
0.6	0.286	0.758
0.7	0.513	0.806
0.8	0.664	0.884
0.9	0.825	0.944

TABLE VII

CORRELATION MATRIX FOR ZANDPAN - VAAL REEF

	Au	Ag	U_3O_8	PYRITE	MUSC.	PYROPH.	CHLOR.	QUARTZ	Fe	K	Ni	Ti	Zr	Cr
Au	1.00	0.97 0.1%	0.88 0.1%	0.50 0.1%	-0.15 N.S.	0.24 N.S.	0.22 N.S.	-0.44 1.0%	0.53 0.1%	-0.07 N.S.	0.42 1.0%	0.19 N.S.	0.51 0.1%	0.53 0.1%
Ag		1.00	0.91 0.1%	0.60 0.1%	-0.22 N.S.	0.20 N.S.	0.23 N.S.	-0.48 0.1%	0.63 0.1%	-0.03 N.S.	0.48 0.1%	0.22 N.S.	0.60 0.1%	0.61 0.1%
U_3O_8			1.00	0.64 0.1%	-0.28 1.0%	0.09 N.S.	0.24 N.S.	-0.43 1.0%	0.66 0.1%	-0.19 N.S.	0.55 0.1%	0.26 10.0%	0.64 0.1%	0.67 0.1%
PYRITE				1.00	-0.52 0.1%	0.09 N.S.	0.23 N.S.	-0.62 0.1%	0.87 0.1%	-0.01 N.S.	0.82 0.1%	0.41 1.0%	0.85 0.1%	0.91 0.1%
MUSCOVITE					1.00	0.42 1.0%	0.73 0.1%	-0.22 N.S.	-0.64 0.1%	0.64 0.1%	-0.70 0.1%	0.23 N.S.	-0.18 N.S.	-0.61 0.1%
PYROPHYLLITE						1.00	0.37 2.0%	0.07 N.S.	-0.14 N.S.	0.16 N.S.	-0.27 10.0%	-0.02 N.S.	0.05 N.S.	-0.20 N.S.
CHLORITE							1.00	-0.16 N.S.	0.12 N.S.	0.27 10.0%	0.06 N.S.	0.33 5.0%	0.41 1.0%	0.21 N.S.
QUARTZ								1.00	-0.69 0.1%	-0.20 N.S.	-0.67 0.1%	-0.48 0.1%	-0.54 0.1%	-0.66 0.1%
Fe									1.00	0.01 N.S.	0.86 0.1%	0.43 1.0%	0.80 0.1%	0.92 0.1%
K										1.00	-0.06 N.S.	0.44 1.0%	0.30 5.0%	0.02 N.S.
Ni											1.00	0.43 1.0%	0.70 0.1%	0.89 0.1%
Ti												1.00	0.61 0.1%	0.48 0.1%
Zr													1.00	0.87 0.1%
Cr														1.00

KEY

Ag

Au

0.97: Estimated correlation coefficient r

0.1%: Level of significance

Confidence limits at 95% probability for 44 pairs

ρ	LOWER	UPPER
0.4	0.119	0.629
0.5	0.236	0.688
0.6	0.371	0.760
0.7	0.508	0.824
0.8	0.658	0.886
0.9	0.824	0.945

TABLE VIII

CORRELATION MATRIX FOR VENTERSPOST - VENTERSDORP CONTACT REEF

	Au	Ag	U_3O_8	PYRITE	MUSC.	PYROPH.	CHLOR.	QUARTZ	Fe	K	Ni	Ti	Zr	Cr
Au	1.00	0.98 0.1%	0.70 0.1%	0.27 10.0%	-0.48 0.1%	0.14 N.S.	0.23 10.0%	0.08 N.S.	0.19 N.S.	-0.47 0.1%	0.38 1.0%	-0.11 N.S.	0.10 N.S.	0.02 N.S.
Ag		1.00	0.64 0.1%	0.32 1.0%	-0.51 0.1%	0.17 N.S.	0.34 1.0%	0.04 N.S.	0.24 10.0%	-0.50 0.1%	0.38 1.0%	-0.08 N.S.	0.15 N.S.	0.03 N.S.
U_3O_8			1.00	-0.07 N.S.	-0.11 N.S.	0.09 N.S.	-0.05 N.S.	0.09 N.S.	0.02 N.S.	-0.12 N.S.	0.10 N.S.	-0.05 N.S.	0.27 5.0%	0.08 N.S.
PYRITE				1.00	-0.58 0.1%	-0.12 N.S.	0.37 1.0%	-0.25 10.0%	0.41 1.0%	-0.53 0.1%	0.37 1.0%	-0.28 5.0%	-0.12 N.S.	-0.08 N.S.
MUSCOVITE					1.00	-0.16 N.S.	0.09 N.S.	-0.33 2.0%	0.11 N.S.	0.90 0.1%	-0.53 0.1%	0.72 0.1%	0.59 0.1%	0.41 1.0%
PYROPHYLLITE						1.00	0.17 N.S.	-0.02 N.S.	0.16 N.S.	-0.20 N.S.	0.05 N.S.	0.03 N.S.	0.06 N.S.	0.01 N.S.
CHLORITE							1.00	-0.73 0.1%	0.82 0.1%	-0.08 N.S.	0.03 N.S.	0.56 0.1%	0.55 0.1%	0.38 1.0%
QUARTZ								1.00	-0.70 0.1%	-0.12 N.S.	0.08 N.S.	-0.66 0.1%	-0.56 0.1%	-0.62 0.1%
Fe									1.00	-0.02 N.S.	0.23 10.0%	0.44 0.1%	0.52 0.1%	0.40 1.0%
K										1.00	-0.42 0.1%	0.49 0.1%	0.41 1.0%	0.15 N.S.
Ni											1.00	-0.24 10.0%	-0.24 10.0%	0.23 10.0%
Ti												1.00	0.80 0.1%	0.69 0.1%
Zr													1.00	0.62 0.1%
Cr														1.00

KEY

Ag

Au

0.98: Estimated correlation coefficient r

0.1%: Level of significance

Confidence limits at 95% probability for 56 pairs

ρ	LOWER	UPPER
0.3	0.040	0.521
0.4	0.155	0.660
0.5	0.273	0.672
0.6	0.400	0.745
0.7	0.536	0.814
0.8	0.680	0.878
0.9	0.834	0.940

TABLE IX

ROTATED FACTOR LOADINGS (R MODE) FOR ELEMENTS AND MINERALS FROM HARTEBEESTFONTEIN, ZANDPAN AND VENTERSPOST

	HARTEBEESTFONTEIN				ZANDPAN				VENTERSPOST				
VARIABLE	factor 1	factor 2	factor 3	commun-ality	factor 1	factor 2	factor 3	commun-ality	factor 1	factor 2	factor 3	factor 4	commun-ality
Au	0.17	0.04	-0.95	0.94	0.34	0.00	0.88	0.89	-0.06	-0.35	-0.90	0.09	0.94
Ag	0.23	0.03	-0.93	0.92	0.43	-0.00	0.85	0.91	-0.13	-0.39	-0.86	0.14	0.93
U_3O_8	0.26	0.00	-0.88	0.84	0.49	-0.10	0.80	0.89	0.03	0.11	-0.90	-0.02	0.82
Pyrite	0.89	0.09	-0.22	0.84	0.84	-0.05	0.35	0.83	-0.24	-0.81	0.05	-0.13	0.73
Muscovite	-0.55	-0.53	0.30	0.67	-0.28	0.75	0.00	0.64	-0.35	0.81	0.20	-0.20	0.85
Pyroph.	0.00	0.00	0.00	0.00	-0.29	0.40	0.48	0.47	-0.07	0.02	-0.11	0.92	0.87
Chlorite	-0.09	-0.64	-0.43	0.59	0.11	0.61	0.26	0.44	-0.80	-0.21	-0.03	0.24	0.74
Quartz	-0.08	0.92	0.00	0.85	-0.73	-0.22	-0.16	0.60	0.89	0.02	-0.16	0.01	0.81
Fe	0.90	-0.14	-0.23	0.88	0.90	-0.13	0.29	0.91	-0.84	-0.26	-0.04	0.12	0.79
K	-0.49	-0.77	0.23	0.88	0.19	0.74	-0.25	0.65	-0.16	0.79	0.23	-0.25	0.77
Ni	0.76	0.27	-0.14	0.67	0.91	-0.21	0.13	0.88	-0.05	-0.62	-0.26	-0.18	0.49
Ti	0.46	-0.83	0.07	0.90	0.64	0.50	-0.09	0.67	-0.78	0.51	-0.00	-0.04	0.87
Zr	0.92	-0.14	0.02	0.87	0.84	0.25	0.30	0.85	-0.75	0.45	-0.28	-0.02	0.85
Cr	0.84	-0.05	-0.29	0.80	0.93	-0.10	0.26	0.95	-0.71	0.18	-0.13	-0.23	0.61

Pyroph. = Pyrophyllite

be expressed in terms of minerals. In the case of the present study, the elements analysed for can be allocated to specific host minerals with a high degree of certainty on the basis of the information provided by the microscopic studies reported in Section 3 of this thesis. The specific elements and their host minerals are listed below:

Gold and Silver

In the Witwatersrand banket, gold and silver occur alloyed with each other.

Uranium

The presence of uranium in the samples is accounted for by the presence of uraninite and its alteration products. Minor amounts of uranium are associated with other minerals, such as uraniferous leucoxene and radioactive zircon, but these are of lesser importance.

Zirconium

Zirconium occurs exclusively in zircon.

Chromium

Chromium occurs in the mineral chromite.

Titanium

Titanium is distributed between the secondary minerals leucoxene, uraniferous leucoxene and rutile, thought to be largely the alteration products of original detrital ilmenite. It also occurs to a very much lesser extent in pyrite.

Potassium

The presence of potassium is accounted for by the potassium-bearing mica, muscovite.

Iron

Iron is distributed between pyrite and chlorite.

Nickel

Nickel occurs in the pyrite lattice. Nickel also occurs in pyrrhotite, but in the samples from the Vaal Reef the very minor amounts of pyrrhotite shown to be present by ore microscopy (see Section 3) would probably not account for much of the total nickel content. In the Ventersdorp Contact Reef, however, pyrrhotite (although not specifically analysed for) is often present in an amount equal to that of pyrite.

4.5.2.1. Correlation Coefficient Matrix.

Inspection of Tables VI, VII and VIII, showing the correlation coefficients calculated by means of the matrix correlation coefficient programme for the elements and minerals in the Vaal Reef at Hartebeestfontein and Zandpan and in the Ventersdorp Contact Reef at Venterspost, reveals the following:

(1) The correlation coefficient for gold and silver is very high at all three mines, being 0.96 at Hartebeestfontein, 0.97 at Zandpan and 0.98 at Venterspost. This is to be expected in view of the fact (mentioned in Section 4.5.2) that most of the silver occurs alloyed with the gold, and that the silver content of the gold, transformed to a logarithmic value, will therefore vary between narrow limits.

(2) Gold and uranium also show a very high degree of correlation, the correlation coefficients at Hartebeestfontein, Zandpan and Venterspost being 0.86, 0.88 and 0.70 respectively.

(3) No other strong correlations between gold and any other mineral or element, or between uranium and any other mineral or element, are revealed in Tables VI, VII and VIII.

(4) At Zandpan there is a low degree of correlation between gold and pyrite ($r = 0.50$) and between uranium and pyrite ($r = 0.64$). No such correlations are apparent at Hartebeestfontein or Venterspost.

(5) At Zandpan a low degree of correlation was found to exist between gold and zirconium and chromium (which are present in the detrital minerals zircon and chromite respectively), and between uranium and zirconium and chromium. The relevant correlation coefficients were: gold-zirconium 0.51, gold-chromium 0.53, uranium-zirconium 0.64 and uranium-chromium 0.67. There was no evidence of the existence of such correlations at Hartebeestfontein or Venterspost.

(6) At Hartebeestfontein and Zandpan pyrite shows a high degree of correlation with both zirconium and chromium (correlation coefficient greater than 0.8 in all cases), but at Venterspost there is no evidence of the existence of such a correlation.

(7) At Venterspost titanium (which is distributed between rutile, leucoxene and uraniferous leucoxene) shows a high degree of correlation with zirconium ($r = 0.80$) and with chromium ($r = 0.69$). At Hartebeestfontein and Zandpan titanium shows a low degree of correlation with zirconium ($r = 0.55$ and 0.61 respectively) but not with chromium ($r = 0.39$ and 0.48 respectively).

(8) Except at Hartebeestfontein, there is no evidence of any correlation between either gold or uranium and any of the three phyllosilicates muscovite, pyro-

phyllite and chlorite. At Hartebeestfontein there is a low degree of negative correlation between uranium and muscovite (r= -0.52).

(9) Muscovite displays a low degree of negative correlation with pyrite at all three mines (r =-0.62 at Hartebeestfontein, -0.52 at Zandpan and -0.58 at Venterspost).

(10) Muscovite displays a low degree of negative correlation with both zirconium and chromium at Hartebeestfontein (r = -0.56 and -0.66 respectively) and with chromium at Zandpan (r = -0.61). At Venterspost, however, muscovite is weakly but positively correlated with zirconium (r = 0.59), while chlorite and zirconium also display a low degree of positive correlation at Venterspost (r = 0.55).

(11) At Venterspost only, there is a high degree of positive correlation between muscovite and titanium (r = 0.72), while there is a low degree of positive correlation between chlorite and titanium (r = 0.56).

(12) At Zandpan only, there is a high degree of positive correlation between muscovite and chlorite (r = 0.73), but there is no evidence of this relationship at Hartebeestfontein or Venterspost.

(13) Chromium and zirconium are strongly correlated with one another in the Vaal Reef (r = 0.75 at Hartebeestfontein and 0.87 at Zandpan), but this relationship is somewhat weaker in the Ventersdorp Contact Reef (r = 0.62 at Venterspost).

(14) At Hartebeestfontein quartz is negatively correlated to a high degree with titanium (present in rutile, leucoxene and uraniferous leucoxene), the correlation coefficient being -0.76. Quartz also displays a low degree of negative correlation with muscovite (r= -0.56) and chlorite (r= -0.52). At Zandpan quartz displays a low degree of negative correlation with pyrite (r= -0.62), zirconium (r = -0.54) and chromium (r = -0.66). At Venterspost quartz displays a high degree of negative correlation with chlorite (r = -0.73) and a low degree of negative correlation with titanium, zirconium and chromium (r= -0.66, -0.56 and -0.62 respectively).

4.5.2.2. Factor analysis.

The rotated factor loadings for the Vaal Reef at Hartebeestfontein and Zandpan and for the Ventersdorp Contact Reef at Venterspost are set out in Table IX.

In the case of Hartebeestfontein, three factors accounting for approximately 76 per cent of the total variation in the data have been extracted from the correlation matrix, in the case of Zandpan three factors again accounting for approxi-

mately 76 per cent of the total variation have been extracted, and in the case of Venterspost four factors accounting for approximately 79 per cent of the total variation have been extracted. The system has then been rotated so that the three (or four) independent factor axes correspond with groupings present in the data. The grouped variables that correspond most closely to any particular factor axis may then be obtained by inspection of each column of the rotated factor matrix (Table IX), noting the variables corresponding to values of the coefficients of the common factors above 0.7. Thus it can be seen that (for example) Factor 1 at Hartebeestfontein may be represented by Zr, Fe, pyrite, Cr and Ni.

The column headed "communality" in Table IX indicates what proportion of the variability of any particular variable has been explained by the three or four factors listed. The communality is obtained by summing the squares of the values in each row. To give an example, the communality of 0.87 for Zr at Hartebeestfontein is obtained by summing $(0.92)^2 + (-0.14)^2 + (0.02)^2$. The closer the communality approaches unity, the less is the proportion of the variability of a particular variable left unexplained by the factors shown in the table.

The variables corresponding most closely to the rotated factors are shown, for each mine, in Table X.

TABLE X

ELEMENTS AND MINERALS CORRESPONDING MOST CLOSELY TO ROTATED FACTOR AXES AT HARTEBEESTFONTEIN, ZANDPAN AND VENTERSPOST

HARTEBEESTFONTEIN

Factor 1: Zr, Fe, pyrite, Cr, Ni

Factor 2: Quartz, Ti, K

Factor 3: Au, Ag, U_3O_8

ZANDPAN

Factor 1: Cr, Ni, Fe, pyrite, Zr, quartz

Factor 2: Muscovite, K, Chlorite

Factor 3: Au, Ag, U_3O_8

VENTERSPOST

Factor 1: Quartz, Fe, chlorite, Ti, Cr, Zr

Factor 2: Pyrite, muscovite, K, Ni

Factor 3: Au, Ag, U_3O_8

Factor 4: Pyrophyllite

The results shown in Table X can be expressed in terms of mineral relationships if the elements analysed for are allocated to their host minerals in the manner indicated in Section 4.5.2. These results are set out in Table XI.

TABLE XI

RESULTS OF FACTOR ANALYSIS ON SAMPLES FROM HARTEBEESTFONTEIN, ZANDPAN AND VENTERSPOST EXPRESSED IN TERMS OF MINERAL ASSOCIATIONS

HARTEBEESTFONTEIN

Factor 1: Zircon, pyrite, chromite

Factor 2: Quartz, muscovite, rutile/leucoxene

Factor 3: Gold, uraninite

ZANDPAN

Factor 1: Chromite, pyrite, zircon, quartz

Factor 2: Muscovite, chlorite

Factor 3: Gold, uraninite

VENTERSPOST

Factor 1: Quartz, chlorite, rutile/leucoxene, chromite, zircon

Factor 2: Pyrite, muscovite

Factor 3: Gold, uraninite

Factor 4: Pyrophyllite

From these results it can be said that factor analysis of ore from Hartebeestfontein, Zandpan and Venterspost reveals the existence of the following generalized trends and mineral associations:

(1) Gold and uraninite are sympathetically related to each other in all three mines, and display no relationship to any other minerals.

(2) A second distinct association of minerals, namely the association of chromite with zircon, is also present in all three mines, but this appears to be unrelated to the gold-uraninite association. At Hartebeestfontein and Zandpan pyrite is strongly sympathetically related to the chromite-zircon association, but at Venterspost there does not appear to be any clear relationship between pyrite and the chromite-zircon association.

(3) The phyllosilicates do not appear to be related to gold and uraninite

or to chromite and zircon. At Zandpan muscovite and chlorite show a significant positive correlation with one another, while muscovite and pyrite appear to be antipathetically related to one another at Venterspost.

(4) Pyrophyllite at Venterspost appears to have been formed completely independently of the remainder of the minerals present in the horizon (see also Section 6.3.1).

(5) Quartz is antipathetically related to rutile/leucoxene at Hartebeestfontein, to pyrite, zircon and chromite at Zandpan and to chlorite, zircon, chromite and rutile/leucoxene at Venterspost.

(6) The relationships revealed by factor analysis are somewhat different at Venterspost from those at the other two mines. Inspection of factor 1 at Venterspost indicates that quartz is antipathetically associated with the remainder of the minerals listed in factor 1. Pyrite in factor 2 is antipathetically related to muscovite in factor 2, and, as mentioned earlier, does not appear to be related to chromite and zircon, as in the other two mines. In factor 1, chlorite is sympathetically related to rutile/leucoxene, zircon and chromite. In addition, at Venterspost pyrophyllite emerges as a fourth factor and appears to be unrelated to the rest of the minerals.

4.5.2.3. Summary of results of correlation studies.

The results of all the correlation studies (the matrix correlation coefficient programme and factor analysis) may be summarized as follows:

(1) At all three mines, Hartebeestfontein, Zandpan and Venterspost, gold and uraninite are associated with one another in factor 3 and show a strong positive correlation with one another ($r = 0.86$ at Hartebeestfontein, 0.88 at Zandpan and 0.70 at Venterspost). On the basis of these results, it can be said that in these three mines radioactivity should be a very good indicator of the spatial distribution of gold, and that gold content could even be predicted from uranium content (and vice versa) with a fair degree of accuracy.

(2) Neither gold nor uraninite ever appear in the same factor as pyrite, although at Zandpan there is a low degree of correlation between gold and pyrite ($r = 0.50$) and between uranium and pyrite ($r = 0.64$). Thus it can be said that pyrite mineralization would not be suitable as a guide to the positioning of the rock-cutter during mining operations for gold and uranium, although it would appear that, at Zandpan only, pyrite content could possibly be used (in the absence of any other criteria) as a very crude indicator of the distribution of gold and uranium. At Hartebeestfontein and Venterspost, however, judging by the present results, pyrite

would be totally unsuitable as an indicator of gold and uranium distribution.

(3) Neither gold nor uraninite ever appear in the same factor as any of the three phyllosilicates (muscovite, pyrophyllite and chlorite), although at Hartebeestfontein there is a very low degree of negative correlation between uranium and muscovite ($r = -0.52$). The factor analysis results indicate further that pyrophyllite at Venterspost appears to have been formed completely independently of the remainder of the minerals present in the horizon. Thus it can be said that the phyllosilicates would appear to be totally unsuitable as indicators of gold and uranium mineralization.

(4) It is interesting to note that gold and uraninite never appear in the same factor as zircon and chromite at any of the three mines. A low degree of positive correlation was, however, observed at Zandpan between gold and zircon, uraninite and zircon, gold and chromite and uraninite and chromite (r being 0.51, 0.64, 0.53 and 0.67 respectively), but there was no evidence of any such relationships at Hartebeestfontein and Venterspost.

(5) The positive correlation between the detrital minerals, zircon and chromite, which was observed at all three mines, is confirmed by the factor analysis results.

(6) In the Vaal Reef at Hartebeestfontein and Zandpan pyrite shows a high degree of positive correlation with both zircon and chromite. This is confirmed by the factor analysis results, which show that at these two mines pyrite, zircon and chromite are associated with one another in the same factor. In the case of the Ventersdorp Contact Reef at Venterspost there is no evidence of any correlation between pyrite and either zircon or chromite, and the factor analysis results indicate that pyrite occurs in a different factor from zircon and chromite.

(7) Titanium (mainly rutile) shows a high degree of positive correlation with both zircon and chromite in the Ventersdorp Contact Reef at Venterspost, a relationship which is confirmed by the factor analysis results. At Hartebeestfontein and Zandpan there is no evidence of any such relationship in the factor analysis results, although at both these mines a low degree of positive correlation between titanium and zircon was observed.

(8) Muscovite displays a low degree of negative correlation with pyrite at all three mines ($r = -0.62$ at Hartebeestfontein, -0.52 at Zandpan and -0.58 at Venterspost), but, as far as the factor analysis results are concerned, this relationship between pyrite and muscovite is only apparent at Venterspost, where the two minerals are antipathetically associated in factor 2.

(9) At Zandpan there is a strong positive correlation between chlorite and muscovite ($r = 0.73$). This is confirmed by the factor analysis results, which associate chlorite and muscovite at Zandpan in factor 2.

(10) Despite the fact that there is a high degree of positive correlation between muscovite and titanium at Venterspost ($r = 0.72$), there is no evidence of this relationship in the factor analysis results, where muscovite and titanium appear in different factors.

5. DISCUSSION OF RESULTS AND CONCLUSIONS.

5.1. Introduction.

"The ultimate objective of all exploration within the Witwatersrand Basin is the location of concentrations of gold which can be exploited economically. . . . . It cannot be disputed that such operations are most effectively carried out, and that the consequent predictions attain their maximum level of confidence, when the data considered are quantitative rather than qualitative. Geology, as the foundation stone of any philosophy of exploration, must, therefore, evolve towards a quantitative basis if the future of the Witwatersrand gold mining industry is dependent on the discovery of new sources of ore." (Pretorius, 1966, p. 225).

Pretorius' call for the adoption of a more quantitative approach in Witwatersrand exploration is as valid today as it was in 1966, and should be borne in mind whether the problem is one of delimiting an area containing sufficient gold and/or uranium to warrant the commencement of mining operations, or of looking for additional deposits of gold in new pay-shoots within mines, or of extracting gold and uranium economically from an area where mining operations are in progress. It is especially relevant to the investigation described in the present thesis, where the problem requiring solution was one of determining whether areas rich in gold and/or uranium within an orebody could be delimited on site, so that the rich ore could be selectively removed by means of the rock-cutter. The solution of a problem of this nature obviously requires knowledge, on a quantitative basis, of the relationships between minerals in the gold-bearing conglomerate bands. A number of investigators have, in fact, studied inter-mineral relationships in the Witwatersrand banket in the past, but the approach adopted has usually depended on conventional mineralogical techniques, which can at best only yield semi-quantitative results and which necessarily involve subjective interpretations of observations. In the case of the present study it was clearly preferable to adopt a geochemical approach, involving the collection of quantitative analytical data and the use of statistical procedures to assess the data in a more objective way. Since, as Saager and Esselaar (1969, p. 445) have pointed out, the geochemical investigation of the Witwatersrand banket is still in its infancy, the present study may be regarded as a pilot study of the geochemistry of the Vaal Reef and the Ventersdorp Contact Reef as well as being a pilot study of the feasibility of carrying out on-site delimitation of areas rich in gold and uranium.

Although the approach adopted in the present study was primarily geochemical, conventional mineralogical techniques were also used to provide information that would serve as a control for the statistical analysis. Before discussing the results of the present investigation of samples from the Vaal Reef and Ventersdorp Contact Reef in the light of the work of earlier investigators and of the requirements of the rock-cutter, it is interesting to compare the relationships between minerals revealed by the geochemical study with those indicated by the mineralogical study.

5.2. Comparison of Results of Mineralogical and Geochemical Studies.

On comparing the results of the mineralogical studies reported in Section 3 of this thesis with the results of the geochemical studies reported in Section 4, the following points emerge:

(1) The correlation studies provided clear evidence of the existence of a significant positive correlation (a "sympathetic relationship" as defined by Hiemstra, 1968, p. 83) between gold and uraninite in the samples from the Vaal Reef at Hartebeestfontein and Zandpan and from the Ventersdorp Contact Reef at Venterspost. On the basis of the number of gold and uraninite grains seen in polished section, however, there was no indication that this sympathetic relationship existed.

(2) Similarly, the correlation studies provided clear evidence of a sympathetic relationship between pyrite, zircon and chromite in the Vaal Reef, whereas polished section studies failed to indicate that such a relationship existed. In the samples from the Ventersdorp Contact Reef at Venterspost, however, both polished section and correlation studies indicated that there was no relationship between pyrite and either zircon or chromite.

(3) The optical studies gave no indication of the existence of a sympathetic relationship between pyrite and gold or between pyrite and uraninite. In the samples from Hartebeestfontein and Venterspost the correlation studies confirmed that there was no such relationship. At Zandpan, however, a low degree of positive correlation between pyrite and gold and between pyrite and uraninite was found, but these relationships were not confirmed by factor analysis.

(4) There was no relationship between the number of gold grains and the number of zircon and chromite grains seen in polished section. Correlation studies confirmed the absence of any relationship between gold and zircon and chromite at Hartebeestfontein and Venterspost, although at Zandpan a low degree of positive correlation was found between these minerals. Again, this relationship at Zandpan

was not confirmed by factor analysis.

(5) The optical studies indicated that where 50 or more zircon or chromite grains occurred in a single polished section, they seemed to be accompanied by an above-average number of uraninite grains and "uraninite ghosts". The relationship that, from this observation, might have been inferred to exist between uraninite, zircon and chromite was, however, not confirmed by the correlation studies, although, at Zandpan only, a low degree of correlation was found between uraninite and zircon and chromite. Once more, this relationship at Zandpan was not confirmed by factor analysis.

(6) As far as the phyllosilicates muscovite, pyrophyllite and chlorite are concerned, polished section studies were unable to provide any indication of their relationships with other minerals because of the difficulty of identifying the phyllosilicates in polished section. The correlation studies indicated that there was no relationship between the phyllosilicates and either gold or uraninite at any of the three mines examined.

(7) Polished section studies indicated that at all three mines there might be a weak relationship between the number of zircon and chromite grains seen and the amount of rutile present. Correlation studies confirmed that a sympathetic relationship between these minerals did, in fact, exist in the samples from the Ventersdorp Contact Reef at Venterspost. In the case of the Vaal Reef samples, however, the correlation studies indicated that there was only a low degree of positive correlation between rutile and zircon and that there was no evidence of a correlation between rutile and chromite.

From all these results, it is clear that any conclusions regarding relationships between minerals based purely on optical (mineralogical) studies of the type described in Section 3 should always be treated with considerable reserve.

5.3. Relationships between Minerals in the Vaal Reef and Ventersdorp Contact Reef.

In considering the relationships between minerals revealed by the present, primarily geochemical, study of samples from the Vaal Reef at Hartebeestfontein and Zandpan and from the Ventersdorp Contact Reef at Venterspost, it is interesting to compare the findings of the present study with some of the conclusions arrived at by other investigators of Witwatersrand samples.

5.3.1. Gold and uranium.

The results of the statistical analyses reported in Section 4 of this thesis show quite clearly that there was a strong sympathetic relationship between gold and uranium in the samples from all three mines. Although the association between gold and uranium was very strong in the Ventersdorp Contact Reef samples ($r = +0.70$), the correlation coefficients were even higher in the Vaal Reef samples (Hartebeestfontein $r = +0.86$, Zandpan $r = +0.88$). This difference may possibly be related to the fact that the uranium-bearing minerals were found to be more patchily distributed in the bulk samples from the Ventersdorp Contact Reef than in those from the Vaal Reef, where clearly-defined narrow layers of radioactive minerals and pyrite were seen (see Section 3.1). It is also interesting to note that the relationship between gold and uranium was maintained at a very high level in the Zandpan samples despite the fact that some of the samples originated from the low and unpay areas that occur in the Vaal Reef at Zandpan.

A sympathetic relationship between gold and uranium in samples from the Witwatersrand System has also been reported by other investigators. Simpson (1951, p. 131), reporting on half a million samples drawn from the whole of the Witwatersrand System that had been assayed for gold and uranium, found that a sympathetic relationship existed between the gold and the uranium. Liebenberg (1955, p. 215), after carrying out a mineralogical survey of various Witwatersrand ores (including samples from the Ventersdorp Contact Reef and Vaal Reef), commented in the following words on the association that he had observed between gold and uranium: "This relationship is quite close in some areas, but in others becomes more erratic. In all cases the more persistent element is U, and this is subjected to fluctuations in content which tend to take place sympathetically with variations in Au content." Jacob (1966, p. 2), who examined Vaal Reef ore from the Vaal Reefs gold mine and carried out assays for gold and uranium, stated: "There is a definite uranium-gold relationship in the Vaal Reef. With increase in grade the amount of U_3O_8 increases but the U_3O_8 : Au ratio decreases."

It is interesting to note that Hiemstra (1968, p. 67), who worked on a limited number of samples from a small-pebble conglomerate occurring near the base of the Dominion Reefs System at the Dominion Reefs Mine, Klerksdorp Area, only found a low degree of positive correlation between gold and uranium ($r = +0.55$ at the 10% level).

5.3.2. Pyrite, gold and uranium.

In the samples from the Vaal Reef at Zandpan, a low degree of positive correlation between pyrite and gold and between pyrite and uranium was found, but this weak relationship was not confirmed by factor analysis. In the samples from the Vaal Reef at Hartebeestfontein and from the Ventersdorp Contact Reef at Venterspost no relationship could be detected between pyrite and either gold or uranium.

Various other investigators have discussed the question of whether a relationship exists between the occurrence of pyrite and the occurrence of gold in the Witwatersrand. Coetzee (1965, p. 87) examined ore from various Witwatersrand horizons (including the Ventersdorp Contact Reef at Western Deep Levels and Western Reefs mines, and the Vaal Reef at Western Reefs and Stilfontein) in the form of heavy mineral concentrates, polished sections and thin sections. He concluded that a sympathetic relationship existed between the content of gold, uraninite, pyrite and other heavy minerals in each conglomerate band, although wide fluctuations might occur from sample to sample. Winter (1964, p. 436) examined ore from the Elsburg Stage near Loraine gold mine in the Orange Free State. He studied the relationship between gold and pyrite and concluded: "The concentration of buckshot pyrite in a gold-bearing reef is an indicator of high gold content. However, some conglomerates contain much pyrite but little gold." A similar conclusion was reached by Davies (1949, p. 89), who stated: "In the V.C.R., the presence of coarse grains and pebbles of 'buckshot' pyrite is generally indicative of high gold values. In addition, polished sections of V.C.R. ore have shown that 'buckshot' is usually accompanied by coarser grains of gold." Von Rahden (1964, p. 45) examined this purported relationship between "buckshot" or nodular pyrite and gold in samples from the Ventersdorp Contact Reef at Venterspost and Libanon mines. He established that whilst gold often accompanied the nodular pyrite, it did not occur as inclusions within the pyrite nodules themselves. This observation differed from the findings of Liebenberg (1955, p. 161), who reported the presence of minute roundish and irregular inclusions of gold in buckshot pyrite from the Vaal Reef at Buffelsfontein.

From these findings it can be conceded that the presence of "buckshot" or nodular pyrite (which generally occurs intermingled with other types of pyrite in the ore) may possibly, in a particular mine, be of limited local use as an indicator of areas of high gold content. Whether this relationship between buckshot

pyrite and gold is, in fact, valid on a quantitative basis has not been established, and the results of the present investigation can shed no light on this question since the amount of buckshot pyrite (as opposed to total pyrite) relative to gold could not be determined. What can, however, be concluded with a high degree of confidence from the results of the present study is that the occurrence of high, visible, concentrations of pyrite in a conglomerate band can not be regarded as a reliable indicator of the location of areas rich in gold or uranium.

5.3.3. Zircon, chromite and other heavy minerals.

In the present suite of samples from the Vaal Reef at Hartebeestfontein and from the Ventersdorp Contact Reef at Venterspost , no relationship could be found between gold and uranium content and the concentrations of zircon, chromite and the titanium minerals (rutile, leucoxene and uraniferous leucoxene). In the samples from the Vaal Reef at Zandpan, however, a low degree of positive correlation was found between gold and zirconium and chromium, and between uranium and zirconium and chromium, but the existence of these relationships was not confirmed by factor analysis.

The results of the present study indicate that the relationships between the heavy minerals zircon, chromite, pyrite and the titanium minerals are not the same in the Vaal Reef as in the Ventersdorp Contact Reef. In the Vaal Reef samples there was a strong correlation between pyrite and zirconium or chromium concentration, whereas in the Ventersdorp Contact Reef samples there was no evidence of any association at all between pyrite, zirconium and chromium. In the Ventersdorp Contact Reef samples, however, a strong correlation emerged between the concentrations of titanium, zirconium and chromium, while this relationship was only very poorly developed in the Vaal Reef samples.

As regards the interrelationships between gold, uranium and the heavy minerals, the conclusions arrived at by other investigators are not in complete agreement. Koen (1961, p. 44), after examining a suite of Witwatersrand samples that included ore from the Vaal Reef at Vaal Reefs mine, stated: "It has been shown repeatedly that the general distribution pattern of uraninite in the Rand banket coincides closely with that of the heavy minerals present in this formation. .....The uraninite distribution is, however, inclined to be patchy -- a feature not generally shared by the other detrital heavy constituents." Coetzee (1965, p. 87) examined samples from a number of Witwatersrand horizons, including the Vaal Reef at Western Reefs and Stilfontein and the Ventersdorp Contact Reef at

Western Deep Levels and Western Reefs, and reported that he had found a sympathetic relationship between the content of gold, uraninite, pyrite, chromite, zircon and leucoxene. McLachlan (1968, pp. 93-94), on the other hand, stated: "Gold and other heavy mineral constituents in the Vaal Reef are thought to be unrelated, for the following reasons. Gold is generally concentrated in the lower portion of the reef, and, although it may be associated with heavy minerals in this zone, it does not follow that concentrations of heavy minerals higher up in the reef are associated with gold."

If the results of the present study are compared with the earlier work summarized above, it can be seen that the findings of the present study do not support Coetzee's (1965) conclusions regarding the existence of a sympathetic relationship between gold and pyrite and the heavy minerals, and between uranium and pyrite and the heavy minerals. The results of the present study partially support McLachlan's (1968, pp. 93 - 94) conclusions, inasmuch as they also indicate that gold (and uranium) is apparently unrelated to the heavy minerals. On the other hand, however, inspection of Tables II, III and IV (which list the actual analytical values obtained for gold in each sample of the present suite, while indicating the position from which each sample originated relative to the top and bottom of the conglomerate band) clearly shows that in the present suite of samples the gold was not preferentially concentrated in the footwall area, as suggested by McLachlan. In addition, in view of the strong sympathetic relationship between gold and uranium revealed by the present study, it is possible to obtain some idea of the probable distribution of gold across a conglomerate band by examining the distribution of areas of high radioactivity in macro-autoradiographs of the conglomerate band. The distribution of the radioactivity in macro-autoradiographs of three bulk samples typical of the present suite (Figures 4, 5 and 6) provides a further, visible, indication that, in the present suite of samples, the gold was not preferentially concentrated in the footwall area.

In 1964, following a study of the Main Reef and Main Reef Leader of the Main Bird Series, Viljoen reported that he had found that payable areas contained zircons having a median grain-size greater than 200 microns, while areas containing low or erratic gold values were characterized by zircons having a median grain-size smaller than 200 microns. He concluded that, on a regional scale, there was a relationship between the gold tenor of the ore and the size of the heavy mineral components, basing this conclusion on the assumption that, during the deposition of the Witwatersrand conglomerates, gold particles were deposited together with grains of heavy mineral components under conditions of hydraulic equilibrium. This con-

clusion has, however, been the subject of a certain amount of controversy. Bosch and Ortlepp (1966, p. 131) examined the median grain-sizes of the zircons and the gold content in samples from the Main Reef Leader at City Deep and from the Composite Reef at E.R.P.M., and concluded that the use of zircon grain-size analysis as an indication of payability could not be applied on the scale of individual stopes or development ends and was apparently only applicable to the detection of regional trends, which may not be noticeable within the boundaries of a single mining property. They added, however: "No correlation between zircon grain-size and the payability of a reef has even been suggested by the present investigation." McLachlan (1968, p. 94) examined the relationship between zircon and chromite grain-size and gold tenor in the Vaal Reef of the Klerksdorp Goldfield, and concluded: "No apparent relationship exists between the gold distribution map and the trend-surfaces of grain-size in the goldfield." In the case of the present investigation, the grain-sizes of the heavy minerals were not measured, since grain-size analysis was considered to be far too time-consuming a procedure to be of any practical use in carrying out on-site delimitation of areas rich in gold and/or uranium for the benefit of the rock-cutter. Since only concentrations of elements and minerals were determined, the results of the present study can, unfortunately, shed no light on the validity of Viljoen's conclusions.

5.3.4. Phyllosilicates.

On the basis of polished section studies of samples from the Ventersdorp Contact Reef at Venterspost and Libanon mines, von Rahden suggested (1964, p. 47) that there might be an association between gold and the phyllosilicates. The results of the present geochemical study, however, give no indication of the existence of a sympathetic relationship between either gold or uranium and any of the three phyllosilicates muscovite, pyrophyllite and chlorite in either the Vaal Reef or the Ventersdorp Contact Reef. In fact, muscovite was found to display a low degree of negative correlation with uranium in the samples from the Vaal Reef at Hartebeestfontein.

5.4. Conclusions.

As was stated in Section 1, the primary aim of the present study was to investigate the feasibility of carrying out rapid on-site delimitation of areas of high gold and uranium content in Witwatersrand conglomerate bands. The conclusions arrived at in this regard may be summarized as follows:

(1) Examination of macro-autoradiographs prepared from the current suite of bulk samples from the Vaal Reef at Hartebeestfontein and Zandpan and from

the Ventersdorp Contact Reef at Venterspost revealed that a major portion of the uranium-bearing minerals appeared to be restricted to narrow bands within the individual bulk samples of conglomerate (see Section 3.1). This was true of both the Vaal Reef and the Ventersdorp Contact Reef samples, although in the case of the Ventersdorp Contact Reef samples the distribution of the uranium-bearing minerals appeared to be slightly more haphazard than in the samples from the Vaal Reef. The fact that a major portion of the uranium-bearing minerals occurred in narrow bands would, in theory, permit the removal of a large proportion of the uranium-bearing minerals present by the cutting-out of only a small proportion of the total conglomerate band, thus fulfilling the first requirement for the successful operation of the rock-cutter.

(2) As can also be seen from the macro-autoradiographs, the location of the narrow black bands representing areas rich in uranium-bearing minerals varied considerably from sample to sample, obviously being governed by the sedimentological conditions prevailing at the time of deposition of the horizon. The position of these areas of enrichment was not necessarily restricted to the footwall of the conglomerate band, which has, in mining circles, often been presumed to be the case.

(3) The results of the statistical analyses described in Section 4 show quite clearly that, in the samples examined, a strong sympathetic relation existed between gold and uranium. Consequently, radioactivity (which can easily be detected at the rock face by appropriate radiation monitors) would, in the mines and horizons examined in the present study, be suitable as an indicator of those places where simultaneous removal of gold and uranium could be made. Because of this relationship, conclusions (1) and (2) regarding the location of the uranium-bearing minerals within the conglomerate bands also apply to the location of the gold.

(4) In the samples from the Vaal Reef at Zandpan, the distribution of pyrite within the conglomerate was found to have a weak relation to the distribution of gold and uranium. In the Ventersdorp Contact Reef, and in the Vaal Reef at Hartebeestfontein, no relation between pyrite and gold or uranium was detected. The intensity of pyrite mineralization is, therefore, <u>not</u> a reliable guide to the spatial distribution of gold and uranium in the present suite of samples.

(5) The correlation studies did not reveal the existence of any relationship between the distribution of gold and uranium and the distribution of the three phyllosilicates chlorite, muscovite and pyrophyllite. This indicates that the green colour imparted to the Ventersdorp Contact Reef by chlorite <u>cannot</u> be used as a

guide to the positioning of the rock-cutter for the extraction of gold and uranium.

(6) In the samples from the Vaal Reef at Zandpan, the distribution of both zirconium and chromium was found to have a weak relation to the distribution of gold and uranium, but no such relation could be detected in the samples from the Vaal Reef at Hartebeestfontein or from the Ventersdorp Contact Reef at Venterspost. This is taken to indicate that the distribution of zircon and chromite would not be suitable as an indicator of the spatial distribution of gold and uranium in the present suite of samples.

(7) In view of conclusion (3), it is apparent that in the Vaal Reef at Hartebeestfontein and Zandpan and in the Ventersdorp Contact Reef at Venterspost rapid on-site delimitation of areas of high gold and uranium content would be feasible, with radioactivity being used as the indicator for positioning the rock-cutter. The present investigation was only intended to be a pilot study, however, and before any final conclusions can be reached as to whether this technique will be generally feasible in Witwatersrand conglomerates, a detailed investigation of gold-uranium relationships in a wide range of other mines and horizons will be necessary.

PART II

PHYLLOSILICATE MINERALOGY.

6. PHYLLOSILICATE MINERALOGY.

6.1. Introduction.

In the present thesis, the term "phyllosilicates" is used to designate as a whole the lattice-layer silicates chlorite, pyrophyllite, muscovite and chloritoid.

In the course of the present survey, thin section studies were carried out on portions of ore from the Vaal Reef at Hartebeestfontein and Zandpan and from the Ventersdorp Contact Reef at Venterspost, and in these samples it was found that the banket was composed in the main of pebbles of vein quartz cemented by a fine mosaic consisting of an intimate mixture of finer quartz grains and phyllosilicates, which together constituted the matrix material of the conglomerate (see Part I of this thesis, Section 3.2.1). In the case of the Vaal Reef, McLachlan (1968, pp. 95 & 97) has assembled evidence indicating that the matrix material was deposited under a low energy backswamp type of environment while the pebbles were deposited under deltaic conditions.

Quantitative analyses (reported in detail in Part I, Section 4) indicated that the average quartz content of the samples examined in the present study varied between 75 and 85 per cent, while total phyllosilicates varied between 5 and 10 per cent, sulphides varied between 3 and 15 per cent, and minor amounts of accessory minerals, such as gold, uraninite, chromite and zircon, made up the remainder of the mineral assemblage of the samples. Thus the phyllosilicates as a group constituted a major part of the non-quartz mineral assemblage, although the individual phyllosilicates were often only present in trace amounts.

Despite the fact that the phyllosilicates occur widely distributed throughout the shales, quartzites and auriferous conglomerates (also referred to as "banket") of the Witwatersrand System, comparatively few detailed mineralogical studies appear to have been carried out on Witwatersrand System phyllosilicates. The lack of detailed mineralogical information regarding this group of minerals may probably be attributed to two factors. Firstly, characterization of the phyllosilicates, whether by chemical analysis or by instrumental methods, is hampered by the often low concentrations of the individual phyllosilicates, their fine particle size and the fact that they often occur intergrown with one another, so that the separation of sufficient material for analysis is a tedious process. Secondly, the mining companies are generally only concerned with the extraction of the economic components of the auriferous conglomerates (for example, gold,

uranium and pyrite), and consequently they regard the phyllosilicates as being unimportant, unless they happen to form a "marker" or distinctive horizon such as the Black Bar (a chloritoid-rich shale that immediately underlies the Main Reef Leader in certain localities in the Central Rand).

Some of the earliest and most comprehensive studies of Witwatersrand phyllosilicates were carried out by Frankel, who reported the results of these studies in 1939, 1944 and 1949. In 1939 Frankel (p. 15) described the occurrence of a green chromiferous muscovite in the Hospital Hill quartzites, where it occurred interstitially dispersed between fine quartz grains, cementing them to one another. In the same paper, Frankel (1939, p. 17) proposed a source for the chromium that was present in the chromiferous muscovite. In 1944 Frankel (p. 172) reported that the "sericite" in the Rand Banket gave X-ray patterns consistent with those of the muscovite type. He presented chemical analyses for material obtained from a quartz vein at the C.M.R. Mine, material from the hanging wall of the Main Reef at Simmer and Jack Mine and for the chromiferous muscovite from the Hospital Hill quartzites. He further reported (Frankel, 1944, p. 172) the presence of pyrophyllite "in association with quartz veins from practically all Reef Mines". He mentioned (pp. 172-173) the replacement of a dolerite dyke at the C.M.R. Mine by pyrophyllite, and reported the results of a chemical analysis of pyrophyllite from the E.R.P.M. Mine, where it occurred associated with kyanite. Frankel also (1964, p. 173) presented a chemical analysis for a bottle-green chlorite occurring as nests of small platy crystals in a quartz vein from Knights Deep Mine, and reported the presence of a chlorite similar to penninite in certain greenish quartzites at the C.M.R. Mine. In addition, Frankel presented chemical analyses of pale olive brown crystals obtained from a vein "infilling" at Crown Mines and from the Black Bar, showing that this mineral was chloritoid. In 1949 Frankel (p. 582), on analysing a number of specimens obtained from various sources, confirmed Whiteside's (1941, pp. 121 - 126) original identification of dickite as a component of gold-bearing rocks of the Witwatersrand System. Frankel (1949, p. 582) claimed that dickite was a fairly widespread component in rocks belonging to the Main Bird Series, and presented chemical analyses and lists of the optical and physical properties of dickite occurring within vugs in quartz at Rand Leases Mine, Langlaagte Estates, the C.M.R. Mine and Daggafontein Mine. Only at the C.M.R. Mine, however, was the dickite associated with conglomeritic material. Frankel attributed a hydrothermal origin to all the dickite examined by him.

The work reported by Fuller (1958, pp. 42 - 44) appears to have been the next detailed investigation to be carried out on Witwatersrand phyllosilicates. Fuller examined pyrophyllite, which he found to be a widespread component of the quartzites of the Upper Division of the Witwatersrand System and to be particularly characteristic of the Main Bird Series. Fuller also mentioned (1958, p. 21) the occurrence of brunsvigite in a specimen of shale from the Jeppestown Series on the East Rand, about 60 feet below the Main Reef horizon, and of diabantite in a specimen from the Kimberley shale on the farm Withok in the East Rand area (Fuller, 1958, p. 41).

Von Rahden (1964, p. 100) reported the presence of two chlorites, ripidolite and brunsvigite, in ore obtained from the Ventersdorp Contact Reef at Venterspost, where they were found to occur as interstitial matrix material between the quartz pebbles of the auriferous conglomerate. Von Rahden ascribed a secondary origin to these two chlorites, considering them to have been derived from the alteration of volcanic ash exuded prior to the outpouring of the Ventersdorp Lavas.

From this brief survey of previous work on the phyllosilicates of the Witwatersrand System, it can be seen that very few investigations have in fact been carried out on phyllosilicates occurring specifically in auriferous conglomerates, as opposed to those occurring in the shales and quartzites of the Witwatersrand System. Where work has been done on auriferous conglomerate phyllosilicates, these phyllosilicates have generally been found to occur in a manner similar to that described for the phyllosilicates examined in the present study, i.e., as interstitially dispersed material that helps to cement the other components of the banket. For the most part a secondary origin has been ascribed to the phyllosilicates in the auriferous conglomerates, although Viljoen (1964, p. 35) has postulated a hydrothermal origin for the minor amounts of chlorite in the Pebbleless Bastard Reef at the Rose Deep Mine, and a hydrothermal origin was also postulated by Frankel for the pyrophyllite associated with a dolerite dyke at the C.M.R. Mine (Frankel, 1944, p. 172).

In view of the lack of data concerning the chemical composition and the structural and physical properties of phyllosilicates occurring specifically within the auriferous conglomerates (banket) of the Witwatersrand System, the results of the examination of various phyllosilicates from the Witwatersrand banket are reported in detail in subsequent paragraphs. When these examinations of various banket phyllosilicates were carried out during the course of the present study, an

attempt was made to assemble more detailed structural information on these phyllosilicates than has hitherto been available. In addition, an attempt was made to review and assess critically the various classification systems that have been proposed in the past for subdividing the phyllosilicates into species and varieties, and to assess the usefulness of the analytical techniques that are generally employed in arriving at these classifications.

6.2. Chlorite.

6.2.1. Chlorite in Witwatersrand conglomerates.

The presence of chlorites in various Witwatersrand auriferous conglomerates has been commented on by numerous investigators, but to date very little detailed mineralogical work appears to have been carried out on Witwatersrand chlorites. The reason for this state of affairs probably stems to a large extent from the difficulty of identifying the members of the chlorite group of minerals with any certainty when (as is often the case) only optical techniques are available to the investigator. Where thin section analyses have been carried out, the identity of the chlorite has often been dismissed with comments similar to those of Viljoen (1964, p. 32): "No attempt was made to identify individual members of the chlorite family in this investigation - - - - the material studied apparently belongs to the orthochlorite group - - - - of this group, the variety penninite occurs most commonly as judged by its characteristic anomalous Berlin Blue interference colour."

Various authors have, however, attempted to identify chlorites occurring in Witwatersrand conglomerates. Fuller (1958, pp. 21 & 41), using only X-ray methods, has characterized brunsvigite in material from the Jeppestown Series on the East Rand about 60 feet below the Main Reef horizon, and diabantite from a specimen of Kimberley Shale, which separates the Main Bird and Kimberley - Elsburg quartzites and is the only thick argillaceous formation in the Upper Division of the Witwatersrand System. Von Rahden (1964, p. 100), solely on the basis of optical measurements, has reported the presence of ripidolite and brunsvigite in material from the Ventersdorp Contact Reef at Venterspost. Jacob (1966, p. 17) has, on the basis of optical measurements, reported the presence of prochlorite and penninite in Vaal Reef ore at Vaal Reefs Mine. Jacob further mentions the presence of minor amounts of chloritoid in samples examined by him.

At various times, authors have speculated on the possibility of

there being a quantitative relationship between the amount of chlorite present in Witwatersrand conglomerates and the amount of gold present. This question has been discussed in Part I of this thesis.

6.2.2. Chlorite in the Ventersdorp Contact Reef and Vaal Reef.

The examination of thin sections prepared in the course of the present investigation from pieces of banket from the Ventersdorp Contact Reef at Venterspost and from the Vaal Reef at Hartebeestfontein and Zandpan indicated that the chlorite occurred in an identical manner in all three mines. The chlorite, which is considered to be an authigenic component of both the Ventersdorp Contact Reef and the Vaal Reef, characteristically occurred as interstitial material confined to the areas between the vein-quartz pebbles of the banket. In these samples it was invariably intergrown with minute grains of quartz, muscovite or pyrophyllite. Preliminary optical measurements carried out on thin sections of ore suggested that the composition of the chlorite was identical in the samples from all three mines.

Since so few attempts to identify members of the chlorite group of minerals occurring in Witwatersrand deposits seem to have been made, and since the chlorite in the Ventersdorp Contact Reef often reaches concentrations high enough to impart a dark greenish colouration to the rock, it was decided to attempt to extract sufficient pure chlorite from the Ventersdorp Contact Reef samples to permit the structure and composition of this chlorite to be established as fully as possible. The characterization of this chlorite was, however, a far from simple task. In the first place, examination of the literature revealed that a variety of different analytical techniques and systems of classification have been proposed at various times for the purpose of differentiating between members of the chlorite group. In an attempt to arrive at as accurate an identification of the Ventersdorp Contact Reef chlorite as possible, it was decided that several different analytical techniques and systems of classification would have to be applied and the results compared. To assist in the interpretation of the results, however, it further became necessary to compare the results with those obtained when the same techniques were applied to two other high-purity chlorites derived from non-Witwatersrand sources. The results obtained from this comparison of various systems of classification of the chlorite group of minerals are discussed at length in subsequent sections, together with the final conclusions reached as to the identity of the chlorite present in the samples taken from the Ventersdorp Contact Reef at Venterspost.

6.2.3. The identification of minerals of the chlorite group.

6.2.3.1. The structure of chlorite.

Chlorites are a group of hydrous silicates whose structure permits extensive isomorphous substitution, and hence the chlorites show an extremely wide range of chemical composition. Ideally, the structure of chlorite as proposed by Pauling (1930, p. 578) may be thought of as consisting of alternating series of brucite-like layers and mica layers. Due to the replacement of Si by Al in the four-fold position, the mica layer becomes negatively charged. This negative charge is balanced by a corresponding number of Al atoms replacing divalent ions in the six-fold position in the brucite-like layer.

Chemical analyses of chlorites are generally recalculated in terms of cation numbers per 10 cations. They then correspond to a structural formula (based on the assumption that all 6 six-fold and all 4 four-fold coordination positions are filled) which has the form given below (Albee, 1962, p. 855):

$$[(Fe^{2+}, Mn, Fe^{3+}, Mg)_{6-a}(Cr, Al)_a]^{VI} \quad [(Al_b Si_{4-b})]^{IV} O_{x18} H_{x(8-Fe^{3+})}$$

(Coordination numbers are given by Roman superscripts and charges by Arabic superscripts).

6.2.3.2. Proposed systems of classification of chlorites -- a review.

As mentioned in the preceding section, the chlorites show a extremely wide range of chemical composition. Various investigators have attempted to subdivide these large mineralogical units into logical and significant mineral varieties, and some of these systems are reviewed below.

6.2.3.2.1. Optical methods.

Various subdivisions based on a study of the optical properties of chlorites have been made by Albee (1962, p. 864), Winchell (1936, pp. 642 - 651) and Hey (1954, pp. 277 - 292). The validity and applicability of Hey's optical system is examined for the Ventersdorp Contact Reef chlorite, and for two other chlorites, in the light of results obtained by other systems of classification, in Section 6.2.3.5.4.

6.2.3.2.2. Chemical composition as a basis for the classification of chlorites.

Hey (1954, pp. 277 - 292), on the basis of the chemical compositions of the chlorites, divided the chlorites into two series, an "unoxidized normal"

and an "oxidized" series. An arbitrary figure of 4% Fe_2O_3 was taken as the dividing line between "unoxidized" and "oxidized" chlorites. Further subdivision within the "unoxidized" series was based on the number of Si atoms in the half cell and the Fe:(Fe+Mg) ratio. Hey's scheme has been criticized by Foster (1962, p. 17) on the grounds that it leaves the great majority of ferrous chlorites undifferentiated, but provides several categories for the classification of the small minority of chlorites that contain less than 4% Fe_2O_3.

Foster (1962, pp. 17 - 21) classified the iron-magnesium chlorites into nine varieties, on the basis of the two principal types of ionic replacement (i.e. replacement of Mg by Fe^{2+} and also of tetrahedral and octahedral Al by Si and Mg). Phillips (1964, p. 1116) has pointed out, however, that Foster's classification does not take chlorites rich in manganese, chromium or nickel into account, and that it ignores the presence of ferric iron, making only the provision that the designation "ferrian" can be applied to those chlorites containing considerable amounts of Fe_2O_3.

Phillips (1964, p. 1116) suggested that, in order to define any chlorite completely, it is necessary to consider the kinds of cations in tetrahedral (four-fold) co-ordination and their relative abundance, the kinds of cations in octahedral co-ordination and their relative abundance, the relative number of O^{--} and OH^{-} anions, and the structural type. The scheme proposed by Phillips (1964) is probably the soundest scheme proposed to date for the classification of the chlorites, as it attempts to reconcile chemical data with structural data.

The results obtained when the three systems of subdivision of the chlorites suggested by Hey, Foster and Phillips (together with the purely optical system proposed by Hey) were used to identify the Ventersdorp Contact Reef chlorite, and two other chlorites, are compared and discussed in Section 6.2.3.5.4.

6.2.3.3. Analytical techniques used as aids in the characterization of chlorites.

6.2.3.3.1. X-ray diffraction as an aid in the classification of the chlorites.

X-ray diffraction analysis, involving precise measurement of the lattice dimensions and X-ray diffraction intensities, can be used to assist in the determination of the structural formulae of chlorites. This technique is discussed in detail in Section 6.2.3.5.1., and its usefulness assessed in the light of the results obtained from the X-ray diffraction analysis of the Ventersdorp Contact Reef chlorite and two non-Witwatersrand chlorites.

In addition, the structure factors of the chlorites can be calculated and used to obtain additional information concerning the location of various ions in the chlorite structure, but these calculations are involved and tedious and were felt to be beyond the scope of the present investigation.

Bailey and Brown (1962, p. 819) and Brown and Bailey (1963, p. 42) have shown, on the basis of detailed X-ray diffraction studies carried out on single crystals, that it is possible to make further subdivisions into various polytypes within the chlorites. This subdivision is based on differences in stacking sequences, distortions from geometrically ideal structures and order-disorder relationships within the chlorite lattice. In the present study the lack of a suitable integrating single crystal camera precluded any rigorous determination of the polytypes of chlorite present in the Ventersdorp Contact Reef.

6.2.3.3.2. Infra-red spectroscopy as an aid to the classification of the chlorites.

In recent years, numerous investigators, notably Tuddenham and Lyon (1959, pp. 377 - 380), Stubican and Roy (1961, pp. 42 - 46), Hayashi and Oinuma (1965, p. 476), Oinuma and Hayashi (1966, pp. 8 - 10) and Hayashi and Oinuma (1967, p. 1209), have examined the chlorites by means of infra-red spectroscopy. These investigators have been able to relate, nearly quantitatively, shifts in vibration frequency in infra-red spectra to variations and redistributions of various ions in the chlorite structure.

In Section 6.2.3.5.2, the usefulness of the technique of infra-red spectroscopy in the characterization of the chlorites is discussed with reference to the infra-red absorption spectra obtained from the Ventersdorp Contact Reef chlorite and from two non-Witwatersrand chlorites.

6.2.3.3.3. Differential thermal analysis and thermogravimetric analysis as aids to the classification of the chlorites.

Differential thermal analysis (D.T.A.) and thermogravimetric analysis (T.G.A.) are two techniques that are extensively used for the study of phyllosilicates in the ceramics industry. Martin (1955, pp. 118 - 121) has ably reviewed all pertinent data relating to investigations using D.T.A. and T.G.A. prior to 1955. Phillips (1963, p. 404) has carried out a considerably more detailed and objective assessment of the suitability and usefulness of D.T.A. for the identification of chlorites. He concluded that D.T.A. alone appeared to be inadequate as a tool for distinguishing between the many chlorite varieties. The

technique could, however, be used to distinguish the 7 Angstrom septechlorite structure from the normal 14 Angstrom structure.

The reaction products formed during the heating of iron-rich chlorites have been examined by Shirozu (1962, p. 109) by means of X-ray diffraction, whilst Hayashi and Oinuma (1963, p. 134) have used both infra-red spectroscopy and X-ray diffraction for the examination of the reaction products formed on heating chlorites.

In Section 6.2.3.5.3., the D.T.A. and T.G.A. spectra of the Ventersdorp Contact Reef chlorite and two non-Witwatersrand chlorites are discussed, together with the X-ray diffraction and infra-red data obtained from the products that resulted when the three chlorites were heated.

6.2.3.3.4. Electron microscopy and electron diffraction as aids to the study of the chlorites.

Zvyagin (1967) used electron diffraction in an attempt to obtain more detailed structural information about chlorites and the micaceous minerals than could normally be obtained by X-ray diffraction. This technique has not been widely used, however, possibly because of the specialized methods of sample preparation that this technique calls for, and possibly also in view of the fact that changes in the structure of the sample may be induced by the high vacuum conditions required for analysis and by the heating effect of the electron beam passing through the sample.

Beutelspacher and van der Marel (1968) have used electron micrographs to illustrate morphological features of the phyllosilicates. The usefulness of electron micrographs for the identification of chlorites seems, however, to be limited.

6.2.3.4. The characterization of chlorite from the Ventersdorp Contact Reef at Venterspost, and of two other chlorites.

As was mentioned in Section 6.2.2, the characterization of the chlorite occurring in samples from the Ventersdorp Contact Reef at Venterspost was carried out with the aid of as many as possible of the analytical techniques that have been discussed above. This was done in order to arrive at as accurate an identification of the Ventersdorp Contact Reef chlorite as possible, and also in order to assess the usefulness of the different analytical methods and systems of classification that have been suggested for the characterization of the chlorites.

To assist in the interpretation of the results obtained for the Ventersdorp Contact Reef chlorite, it was found necessary to characterize two other chlorites in exactly the same way. These two non-Witwatersrand chlorites were obtained from Ward's Natural Science Establishment, Rochester, New York: one of these was a magnesium-rich chlorite labelled "prochlorite, Chester, Vermont", and the other was an iron-rich chlorite marked "thuringite, New Mexico".

The results of these analyses are described in subsequent sections.

6.2.3.4.1. Optical studies.

Earlier optical studies carried out by von Rahden (1964, pp. 99 - 100) on the Ventersdorp Contact Reef at Venterspost indicated that two varieties of chlorite were present. These were identified as ripidolite and brunsvigite using Hey's (1954, pp. 277 - 292) system of classification.

A new suite of samples from the Ventersdorp Contact Reef at Venterspost was obtained for the present investigation, and in this suite only one variety of chlorite could be detected. Optical examination of this chlorite, and of the two U.S.A. chlorites, was limited to the determination of the optic sign and intermediate refractive index β of the three chlorites. These constants, which were determined at $24^{o}C$ using monochromatic sodium light (λ = 589 m μ) and conventional oil immersion techniques, are listed in Table XII, together with the classification of the three chlorites that was deduced from these constants according to Hey's (1954, pp. 277 - 292) system.

TABLE XII

OPTICAL CONSTANTS DETERMINED ON CHLORITES FROM VERMONT, VENTERSPOST AND NEW MEXICO

	VERMONT	VENTERSPOST	NEW MEXICO
Optic sign	Biaxial (+)	Biaxial (-)	Biaxial (-)
Intermediate refractive index (β) (all values $\pm$ 0.002)	1.589	1.629	1.647
Classification of chlorite (Hey's optical system)	clinochlore	brunsvigite	brunsvigite

From the foregoing Table, it can be seen that the use of a system of chlorite classification that is based purely on optical determinations (Hey, 1954, pp. 277 - 292) results in the two non-Witwatersrand chlorites being identified in a

manner that does not agree with the identification proposed for these chlorites by the suppliers, Messrs. Ward's Natural Science Establishment. The validity of Hey's optical system of classification of the chlorites is discussed further in Sections 6.2.3.5.4. and 6.2.3.5.5.

6.2.3.4.2. Sample preparation for X-ray diffraction, and other, studies on chlorites.

The conglomerate sample from the Ventersdorp Contact Reef at Venterspost had, as received, a dark green colour due to the presence of large amounts of chlorite. A chlorite concentrate was prepared from this sample by grinding the conglomerate under acetone to avoid structural rearrangement (Shirozu, 1963, pp. 3 - 8), and then carrying out repeated centrifugation with heavy liquids. This procedure removed the bulk of the quartz that was originally associated with the chlorite, and yielded a concentrate consisting of 85% chlorite and 15% quartz, as determined by X-ray diffraction. The quartz remaining in the concentrate was present as fine intergrown particles and could not be removed. The particles in the concentrate had a median grain size of 15 microns.

The two non-Witwatersrand chlorites were comminuted and treated throughout the study in a manner identical to that in which the Venterspost chlorite was treated.

6.2.3.4.3. X-ray diffraction studies on the three chlorites.

The three chlorites were examined by the X-ray diffraction method described in Part III (Section 8.6) of this thesis. An end-loading technique was used throughout this study. Integrated intensities were obtained by means of a Disc Integrator. The lattice constants and indices were calculated and allocated using two computer programmes that were specially adapted from previously existing programmes. These programmes are listed in Part III (Section 9) of this thesis.

The lattice constants determined for the three chlorites are set out in Table XIII.

The indices, intensities and interplanar spacings determined by X-ray diffraction analysis are set out in Table XIV.

TABLE XIII

LATTICE CONSTANTS OF CHLORITES FROM VERMONT, VENTERSPOST AND NEW MEXICO

	VERMONT	VENTERSPOST	NEW MEXICO
a_o Å	5.339 ± .001	5.363 ± .001	5.380 ± .001
b_o Å	9.250 ± .002	9.291 ± .001	9.317 ± .002
c_o Å	14.316 ± .002	14.257 ± .002	14.241 ± .003
Volume Å^3	701.5	704.6	708.3
β	97° 06' ± 2'	97° 16' ± 2'	97° 06' ± 2'
Space Group	C2/m	C2/m	C2/m

TABLE XIV

X-RAY DIFFRACTION POWDER DATA FOR CHLORITES FROM VERMONT, VENTERSPOST AND NEW MEXICO

VERMONT						VENTERSPOST						NEW MEXICO					
'd' Å observed	'd' Å calculated	I/I_1	h	k	l	'd' Å observed	'd' Å calculated	I/I_1	h	k	l	'd' Å observed	'd' Å calculated	I/I_1	h	k	l
14.243	14.201	100	0	0	1	14.180	14.137	84	0	0	1	14.152	14.130	32	0	0	1
7.127	7.103	82	0	0	2	7.088	7.075	100	0	0	2	7.063	7.063	100	0	0	2
4.741	4.735	43	0	0	3	4.718	4.713	32	0	0	3	4.706	4.711	36	0	0	3
4.619	4.624	12	0	2	0	4.638	4.645	17	0	2	0	3.531	3.534	63	0	0	4
3.555	3.552	51	0	0	4	4.619	4.616	17	1	1	0	2.824	2.826	16	0	0	5
2.841	2.814	16	0	0	5	3.537	3.535	70	0	0	4	2.684	2.684	4	1	3	0
2.675	2.675	2	1	1	4	2.829	2.829	22	0	0	5	2.684	2.684	4	2	0	-1
2.592	2.590	15	1	3	1	2.668	2.670	12	1	1	4	2.669	2.670	6	2	0	0
2.446	2.445	16	1	3	2	2.599	2.599	30	1	3	1	2.605	2.605	15	2	0	-2
2.386	2.386	13	1	3	-3	2.556	2.556	30	2	0	1	2.458	2.457	17	2	0	-3
2.264	2.263	9	1	3	3	2.454	2.453	5	2	0	-3	2.396	2.398	27	1	3	-3
2.007	2.008	19	2	0	4	2.393	2.393	28	1	3	-3	2.268	2.269	7	2	0	-4
2.007	2.007	19	1	3	-5	2.393	2.392	28	2	0	2	2.019	2.019	4	0	0	7
1.8849	1.8848	2	2	0	-6	2.266	2.266	20	1	3	3	2.009	2.010	16	1	3	-5
1.8267	1.8271	5	1	3	-6	2.084	2.083	2	0	4	3	1.8882	1.8887	7	1	3	5
1.6653	1.6649	5	1	3	-7	2.071	2.071	5	1	3	4	1.8845	1.8852	7	2	0	-6
1.5681	1.5684	16	1	3	7	2.007	2.007	39	2	0	4	1.6903	1.6901	2	2	4	-3
1.5410	1.5412	24	3	3	-1	1.8859	1.8860	21	2	0	-6	1.6709	1.6704	4	1	5	-3
1.5063	1.5065	8	0	6	2	1.7415	1.7415	2	3	1	0	1.6639	1.6639	2	1	3	-7
1.5063	1.5064	8	3	3	1	1.6891	1.6897	3	1	2	7	1.5527	1.5528	4	0	6	0
1.4200	1.4206	5	0	0	10	1.5666	1.5661	24	2	0	-8	1.5508	1.5499	5	1	5	4
1.4142	1.4141	6	0	6	4	1.5485	1.5484	5	0	6	0	1.5480	1.5485	5	2	4	-5
1.3970	1.3973	21	2	0	8	1.5267	1.5263	3	2	5	-1	1.5215	1.5216	4	1	5	-5
1.3970	1.3966	21	1	3	-9	1.5131	1.5126	17	0	6	2	1.5158	1.5162	7	3	3	-3
1.3251	1.3247	5	3	1	6	1.4142	1.4142	8	0	0	10	1.4227	1.4228	4	3	3	3
						1.3937	1.3932	20	2	0	8	1.4123	1.4120	6	3	1	5
						1.3803	1.3804	7	2	4	-7						
						1.3303	1.3303	6	2	6	-2						

6.2.3.4.4. Infra-red spectroscopy studies on the three chlorites.

The absorption spectra obtained for the three chlorites using the alkali halide disc method (which is described in detail in Part III of this thesis) are shown in Figure 9, and the peak positions and bond assignments are listed in Table XV.

TABLE XV

INFRA-RED VIBRATION FREQUENCIES AND BOND ASSIGNMENTS FOR CHLORITES FROM VERMONT, VENTERSPOST AND NEW MEXICO

VERMONT		VENTERSPOST		NEW MEXICO	
ν cm^{-1}	bond assignment	ν cm^{-1}	bond assignment	ν cm^{-1}	bond assignment
3675	OH in mica layer				
		3637	OH	3629	OH
3568	OH in brucite layer	3548	OH in brucite layer	3548	OH in brucite layer
3415	HOH interlayer	3414	HOH interlayer	3415	HOH interlayer
		1171	?		
1075	Si-O stretch				
1040	Si-O	1071	Si-O		
1014	Si-O stretch	980	Si-O stretch	981	Si-O stretch
960	Si-O-Si				
818	Si-O-Al	791	Si-O-Al?		
757	Si-O	775	Si-O	753	Si-O
663	Si-O	644	Si-O	665	Si-O
				630	Si-O
535	$Si-O-Al^{VI}$	535	$Si-O-Al^{VI}$	535	$Si-O-Al^{VI}$
458	$Si-O-Mg^{VI}$	456	$Si-O-Mg^{VI}$	450	$Si-O-Mg^{VI}$
435	Si-O	432	Si-O	429	Si-O

6.2.3.4.5. Chemical analyses of the three chlorites.

The results of the chemical analyses carried out on the chlorites from Vermont, Venterspost and New Mexico are set out in Table XVI.

6.2.3.4.6. Structural formulae of the three chlorites.

The structural formulae of the chlorites from Vermont, Venterspost and New Mexico have been calculated in accordance with the scheme outlined by

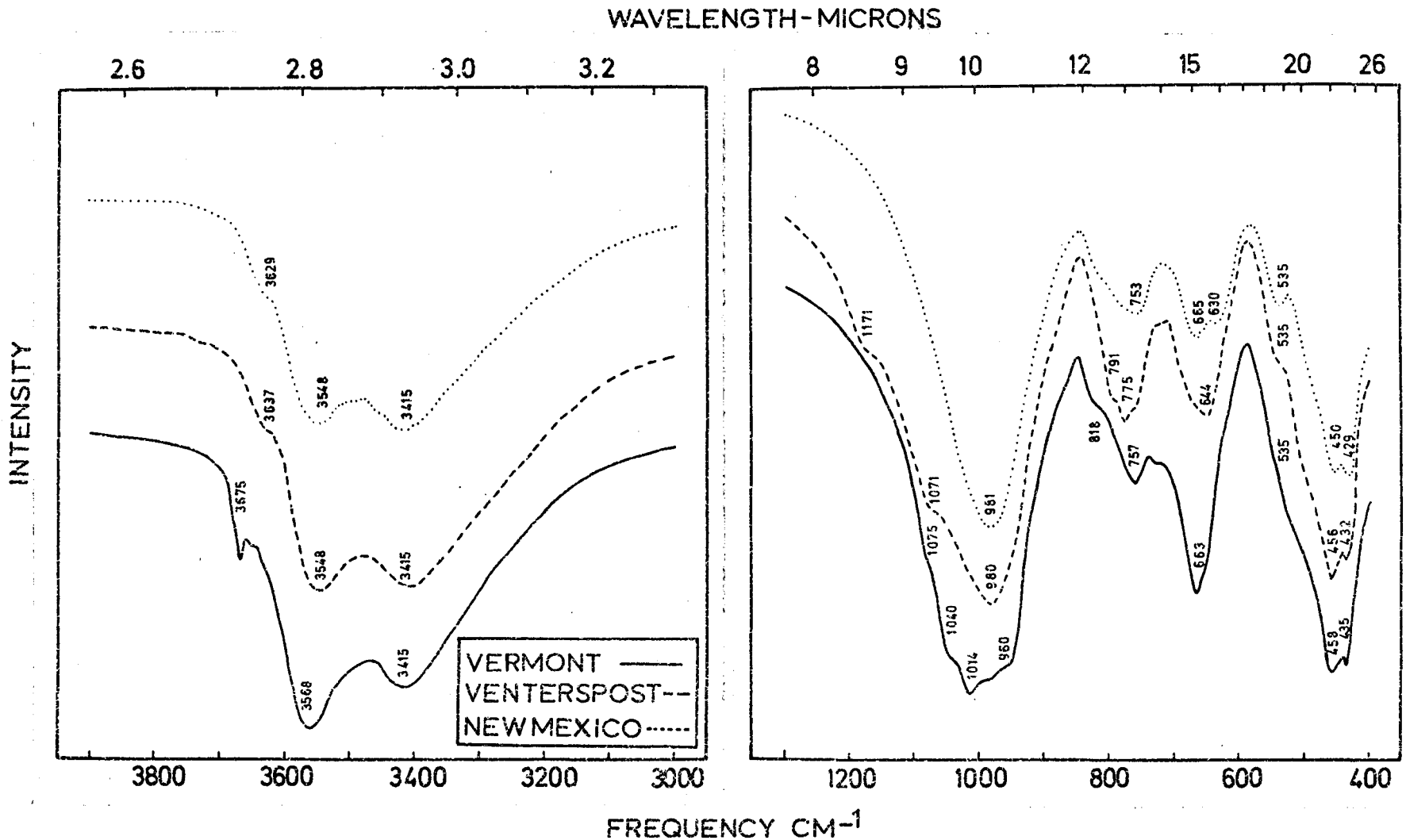


FIGURE 9 INFRARED ABSORPTION SPECTRA OF THREE CHLORITES

TABLE XVI

CHEMICAL ANALYSES OF CHLORITES FROM VERMONT, VENTERSPOST AND NEW MEXICO

	VERMONT per cent	VENTERSPOST** per cent	NEW MEXICO per cent
SiO_2	30.22	27.46	24.01
TiO_2	0.12	0.71	0.65
Al_2O_3	18.80	20.02	20.90
Fe_2O_3	1.40	2.53	4.87
FeO	7.62	22.16	29.47
MnO	0.07	0.78	0.72
MgO	28.20	14.37	8.00
CaO	0.10	0.06	0.05
Na_2O	1.30	0.44	0.30
K_2O	0.35	0.14	0.15
H_2O^+	12.27	11.18	11.14
H_2O^-	0.53	0.13	0.29
Total	100.98	99.98	100.55

** indicates recalculated analysis. Original sample contained 15 per cent of SiO_2.

TABLE XVII

STRUCTURAL FORMULAE OF CHLORITES FROM VERMONT, VENTERSPOST AND NEW MEXICO

Vermont:

$$[(Al_{1.12}Fe^{3+}_{0.11}Fe^{2+}_{0.62}Mg_{4.10})(Si_{2.95}Al_{1.05})O_{10.04}(OH)_{7.96}]$$

Venterspost:

$$[(Al_{1.37}Fe^{3+}_{0.21}Fe^{2+}_{1.96}Mg_{2.27}Mn_{0.01})(Si_{2.88}Al_{1.12})O_{10.20}(OH)_{7.80}]$$

New Mexico:

$$[(Al_{1.36}Fe^{3+}_{0.41}Fe^{2+}_{2.72}Mg_{1.32}Mn_{0.01})(Si_{2.64}Al_{1.36})O_{9.85}(OH)_{8.15}]$$

Foster (1962, p. 3) and are presented in Table XVII. The structural formulae are based on the recalculation of the chemical analyses (Table XVI) into cation numbers per 10 cations.

The alkalis CaO, Na_2O and K_2O have not been included in the calculations of the structural formulae. Foster (1962, p. 2) considers that cations as large as Na^+, K^+ and Ca^{2+} are probably interlayed, or represent an admixture of mica, associated carbonates or silicates, rather than forming part of the chlorite structure proper.

6.2.3.4.7. Differential thermal analysis and thermogravimetric analysis of the three chlorites.

The differential thermal (D.T.A.) and thermogravimetric (T.G.A.) analyses of the three chlorites were carried out using apparatus developed and built at the National Institute for Metallurgy. This apparatus permits simultaneous D.T.A. and T.G.A. determinations to be carried out on samples weighing as little as 1 gram, in any chosen atmosphere. The conditions used throughout all runs are set out in Table XVIII.

The results of the three runs, which were carried out under identical conditions on three consecutive days, are shown in Figures 10, 11 and 12. After being heated to $1000^{o}C$, the maximum temperature attainable with the apparatus, the samples were cooled in a stream of high purity nitrogen (to forestall oxidation of the ferrous iron) and then transferred to a desiccator flushed with high purity nitrogen prior to further analysis.

TABLE XVIII

INSTRUMENTAL SETTINGS USED FOR D.T.A. AND T.G.A. ANALYSIS OF CHLORITES FROM VERMONT, VENTERSPOST AND NEW MEXICO

Atmosphere:	High purity nitrogen
Heating rate:	$7.2^{o}C$ / minute
Thermocouples:	Chromel/alumel
Sample weight:	1 gram
Sample particle size:	Less than 25 microns median grain size
Reference sample:	α alumina
T.G.A. calibration:	0.2 gram equivalent to 10 inches
D.T.A. calibration:	10 microvolts

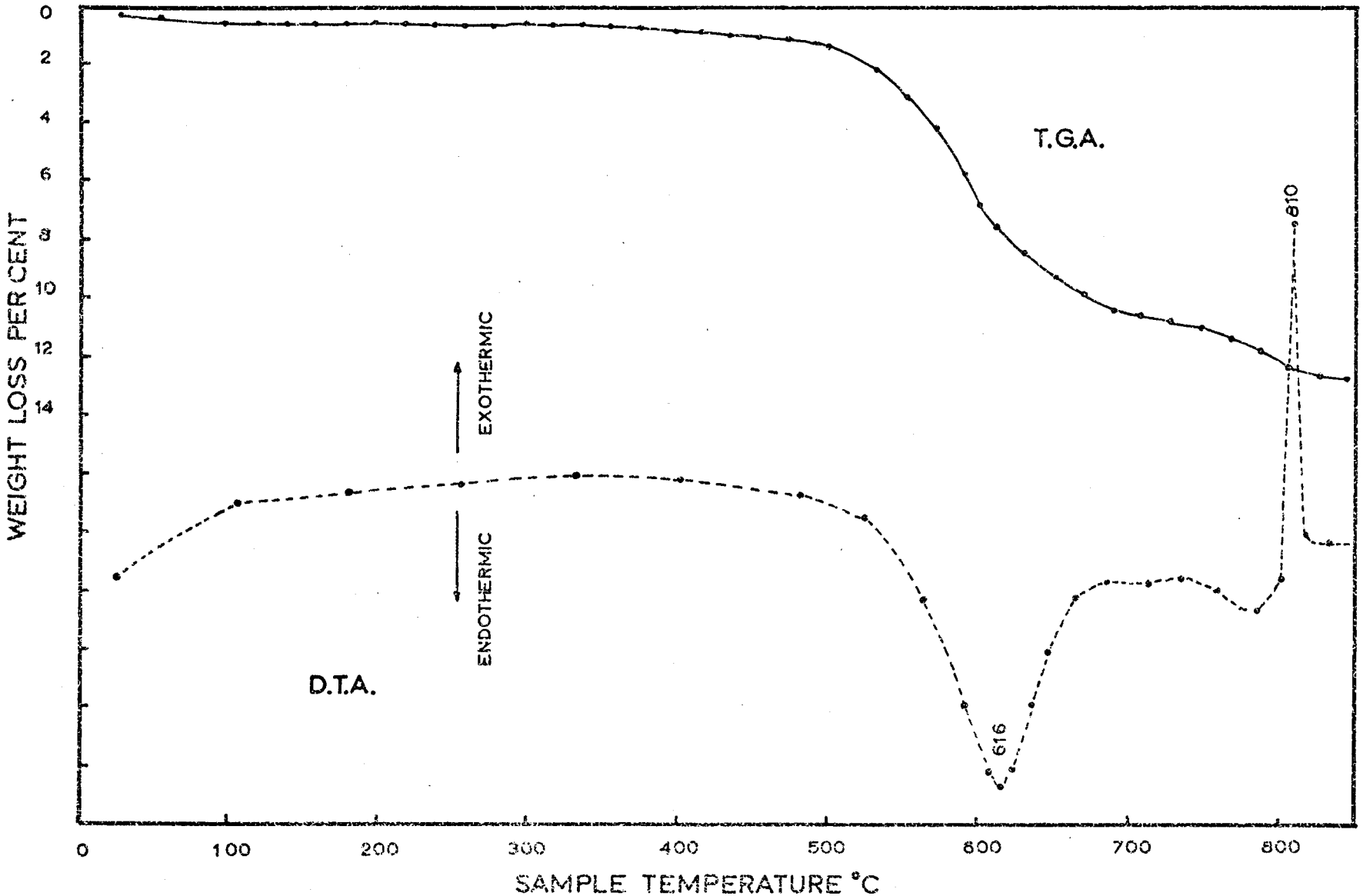


FIGURE 10 D.T.A. AND T.G.A. CURVES FOR CHLORITE FROM VERMONT

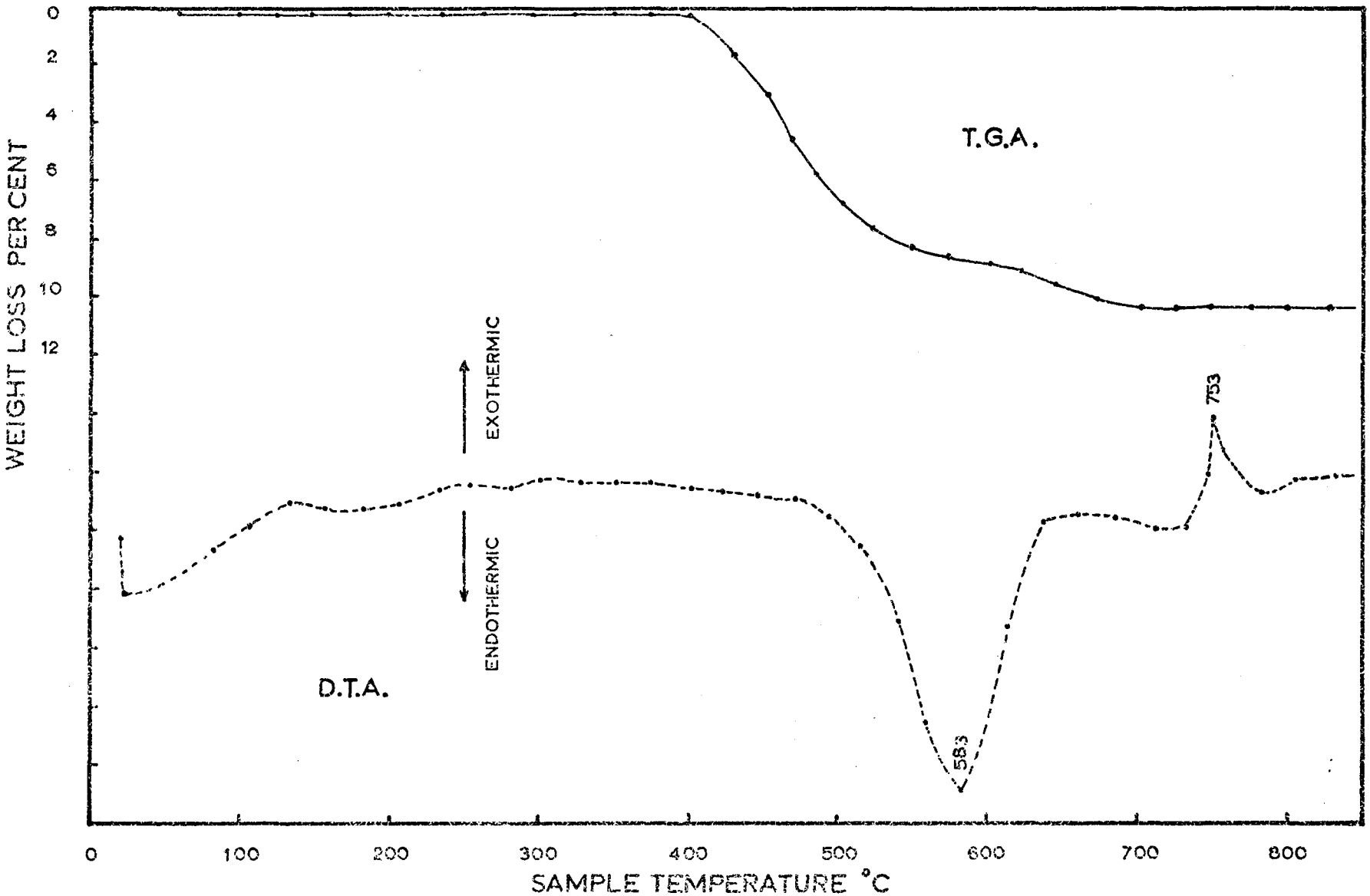


FIGURE 11 D.T.A. AND T.G.A. CURVES FOR CHLORITE FROM VENTERSPOST

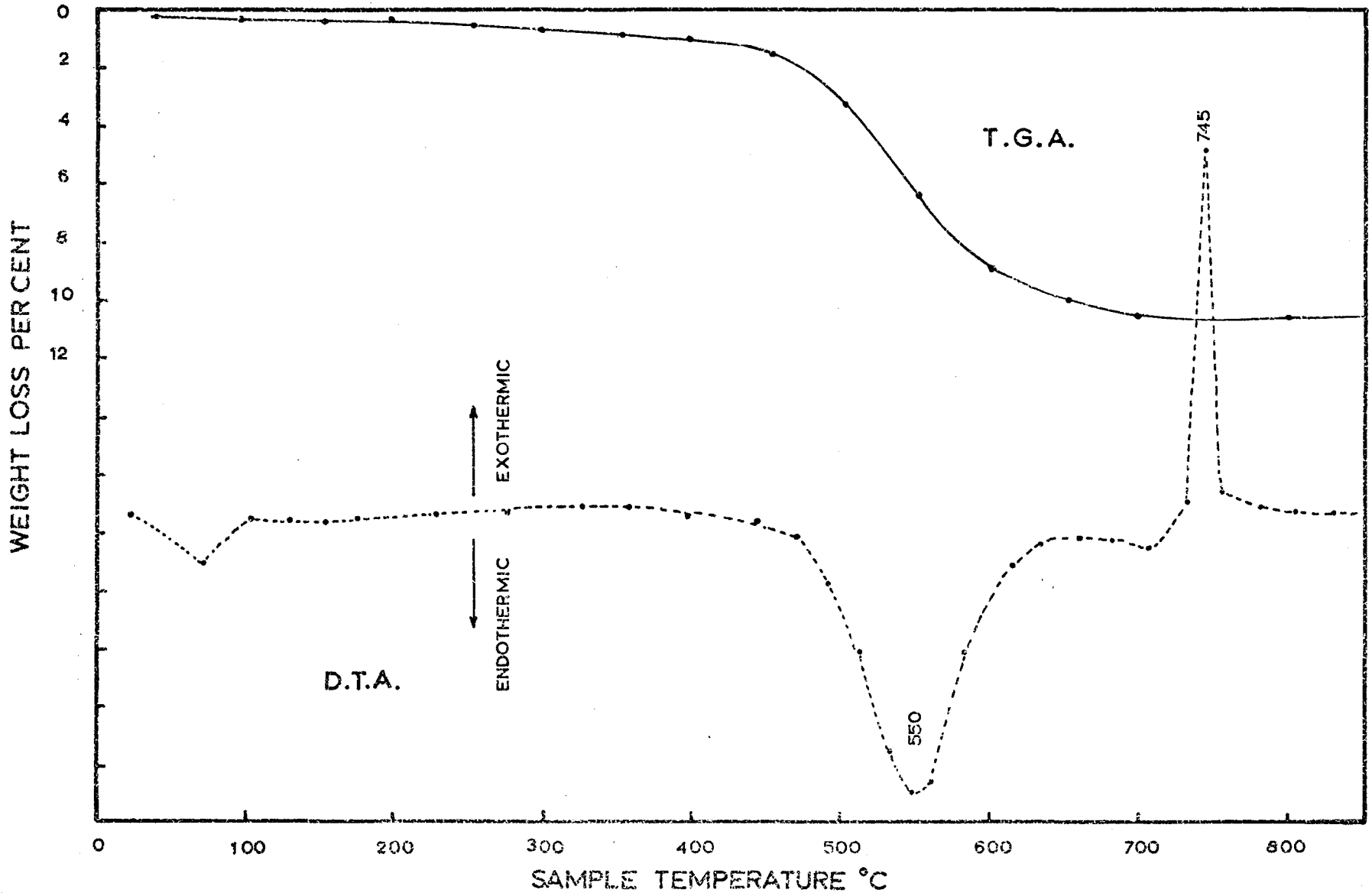


FIGURE 12 T.G.A. AND D.T.A. CURVES FOR CHLORITE FROM NEW MEXICO

6.2.3.4.8. Subsequent heat treatment of the chlorites from Vermont, Venterspost and New Mexico.

Following examination of the three D.T.A. curves obtained for the three chlorites (Figures 10, 11 and 12), it was decided to heat fresh samples of each of the three chlorites to 670°C, 820°C and 1000°C ± 5°C at a rate of 7°C per minute in a stream of high purity nitrogen, in the hope that examination of the phases formed at these temperatures would permit each of the chlorites to be uniquely characterized. The temperature 670°C was chosen because the D.T.A. curves indicated that in all three chlorites the endothermic reaction had occurred before this temperature had been reached. Similarly, 820°C was chosen because the D.T.A. curves indicated that the exothermic reaction had occurred before the temperature 820°C had been reached.

The temperature was held constant for 1 hour at each of the three temperatures in order to allow any phases that might be forming to stabilize.

The products obtained on heating the three chlorites to 670°C, 820°C and 1000°C were examined by X-ray diffraction using an 11 cm Debye Scherrer powder camera. They were also examined by infra-red spectroscopy. On inspection of the results of these analyses, however, it was found that the majority of the phases formed could not be identified by means of the A.S.T.M. X-ray diffraction index, and similarly that it was not possible, from the infra-red spectra, to make bond assignments with any degree of certainty.

The results obtained by means of this technique are discussed further in Section 6.2.3.5.3.

6.2.3.5. Discussion of results of analyses carried out on the three chlorites from Vermont, Venterspost and New Mexico.

6.2.3.5.1. X-ray diffraction.

The application of X-ray diffraction analysis to the differentiation of chlorite species most generally involves the use of the b parameter and the basal plane spacing d(00 ℓ) in calculations of the structural formulae of the chlorites. This procedure calls for a high degree of precision in the measurement of the positions and intensities of the X-ray reflections. The b_o parameter is then used to calculate the number of ferrous ions in the chlorite structure in accordance with one of the various equations that have been proposed in the past in an attempt to relate these two variables. Three of these equations are listed below:

$b = 9.202 + 0.028$ Fe (total) $+ 0.047\ Mn^{++}$ . . . . Hey (1954, p. 286)

$b = 9.210 + 0.037\ (Fe^{++}, Mn)$ . . . . . Shirozu (1958, p. 209)

$b = 9.23 + 0.03 Fe^{++}$ ($\pm$ 0.03 Å) . . . . . Radoslovich (1962, p. 623)

These equations are all based on the assumption that the octahedral cations are equally distributed between the talc and brucite layers in the formula:

$$(Mg_{6-x-y} Fe^{2+}_{y} Al_{x}) (Si_{4-x} Al_{x}) O_{10} (OH)_{8}$$

where y is the number of ferrous ions in octahedral coordination and x is the number of aluminium ions in tetrahedral co-ordination.

The b_o and c_o parameters of the three chlorites examined in the present study have been listed in Table XIII (Section 6.2.3.4.3). The y numbers (the number of ferrous ions in octahedral co-ordination) of these three chlorites were calculated from their b_o dimensions by means of each of the three equations listed above, and these y numbers were then compared with one another and with the structural formulae of the three chlorites calculated from chemical data (these structural formulae have been set out in Table XVII, Section 6.2.3.4.6).

Assessing the equations proposed by Hey, Shirozu and Radoslovich in the manner described above leads to the following conclusions:

(1) The equations proposed by Hey and Shirozu do not appear to be suited to the analysis of magnesium-rich chlorite (Vermont chlorite) since they grossly overestimate the y number of the Vermont chlorite. (y number: from structural formula 0.62; Hey 1.72; Shirozu 1.08)

(2) The equation proposed by Shirozu yields y numbers fairly close to the values derived from the structural formulae in the case of the Venterspost and New Mexico chlorites, which are richer in iron than the Vermont chlorite.
(Venterspost, y number: from structural formula 1.96; Shirozu 1.92
New Mexico, y number: from structural formula 2.72; Shirozu 2.89)

(3) Hey's equation appears to be inferior to that proposed by Shirozu.
(Vermont, y number: from struct. formula 0.62; Hey 1.72; Shirozu 1.08
Venterspost, y no.: from struct. formula 1.96; Hey 1.33; Shirozu 1.92
New Mexico, y no.: from struct. formula 2.72; Hey 1.31; Shirozu 2.89)

(4) Radoslovich's equation may probably be regarded as the one producing the most consistent results. It produced far better results than those produced by the equations of Hey or Shirozu in the case of the Vermont chlorite (from structural formula 0.62; Radoslovich 0.67; Hey 1.72; Shirozu 1.08). In the case of the other two chlorites, Radoslovich's equation produced y numbers of 2.26 for the Venterspost

chlorite and 2.90 for the New Mexico chlorite, values that are reasonably close to the structural formula values and to those yielded by Shirozu's equation.

As regards the x number (defined as the number of aluminium ions in tetrahedral co-ordination in the formula:

$(Mg_{6-x-y}Fe^{2+}_{y}Al_{x})(Si_{4-x}Al_{x})O_{10}(OH)_{8}$), this cannot be determined satisfactorily by optical means. A number of workers have, however, shown that the basal spacing of chlorites tends to decrease with increasing Al content, and Hey (1954, p. 286) has suggested the relation:

$$d_{(001)} = 14.385 - 0.23x - 0.05Fe^{3+} + 0.05Mn$$

while Brindley (1961, p. 269) has proposed the following equation:

$$d_{(001)} = 14.55 - 0.29x$$

The equations proposed by Hey (1954, p. 286) and Brindley (1961, p. 269) were used to calculate the x numbers of the three chlorites examined in the present study from the X-ray data listed in Table XIII (Section 6.2.3.4.3). The structural formulae (Table XVII, Section 6.2.3.4.6) derived from chemical analyses of these three chlorites were then used to assess the equations proposed by Hey and Brindley. It was found that :

(1) The equation proposed by Hey tends to underestimate the x number grossly. The x values derived from the structural formulae are 1.09 for Vermont chlorite, 1.25 for Venterspost chlorite and 1.36 for New Mexico chlorite, but Hey's equation yields 0.30, 0.56 and 0.63 respectively.

(2) The equation proposed by Brindley underestimates the x number to a far lesser extent. Brindley's equation yielded x values of 0.81 for Vermont chlorite, 1.01 for Venterspost chlorite and 1.07 for New Mexico chlorite.

The substitution of Al^{3+}, or any other trivalent ion, for Si^{4+} gives the tedrahedral layers a negative charge equivalent to the amount of R^{3+} proxying for Si^{4+}. In order to retain structural balance, the octahedral layers must have a corresponding positive charge, and consequently must contain at least as many R^{3+} ions as the tetrahedral layers. Thus, in theory at least, the Al in the octahedral layer should be equivalent to the Al present in the tetrahedral layer. Foster (1962, p. 7) has pointed out, however, that in most of the structural formulae calculated from chemical analyses of chlorite the octahedral Al is either greater or less than the tetrahedral Al. For example, in the case of the samples examined in the course of the present study, the structural formulae (Table XVII, Section 6.2.3.4.6) show

that octahedral Al predominates over tetrahedral Al in the chlorites from Vermont and Venterspost, but that in the iron-rich chlorite from New Mexico the aluminium is equally distributed between the octahedral and the tetrahedral layers.

Albee (1962, p. 867) has attempted to demonstrate the relationship between the basal spacing d(001) and $(Al^{IV} + Al^{VI}) + Cr$ (expressed as atoms per 10 cations) for iron-containing chlorites. Unfortunately, however, the regression equation for this relationship given in Albee's text, p. 867 (i.e., $y=-7.117x + 103.346$) is obviously incorrect when compared with the regression line shown in his Figure 5, and accordingly a new regression equation was calculated as an approximation to the line shown in Albee's Figure 5. This new regression equation is as follows:

$$y = -0.1405x + 14.5185$$

where x refers to total aluminium and chromium ions present $(Al^{IV} + Al^{VI}) + Cr$ and y refers to the basal spacing d(001).

The d(001) basal spacings that were measured for the Vermont, Venterspost and New Mexico chlorites (Table XIII, Section 6.2.3.4.3) were substituted in the recalculated Albee regression equation and the corresponding values for $(Al^{IV} + Al^{VI}) + Cr$ alculated. The values obtained for total aluminium and chromium in this way were 1.44, 1.86 and 1.98 for, respectively, Vermont, Venterspost and New Mexico chlorite, whereas when total aluminium and chromium was calculated from the chemical analyses of these three chlorites, values of 2.17, 2.49 and 2.72 were obtained. Thus, the recalculated Albee regression equation tends to underestimate the total aluminium and chromium content of the three chlorites examined in the present study by an average of 29%.

On the same axes (i.e., basal spacing d(001) vs. $(Al^{IV} + Al^{VI}) + Cr$ expressed as atoms per 10 cations), Albee in his Figure 5 (Albee, 1962, p. 867) also plotted some values obtained for magnesium-rich chlorites synthesized by Nelson and Roy (1958, p. 707). It is interesting to note that when the results obtained from the three chlorites examined in the present study are plotted in Albee's Figure 5, the three points correspond much more closely to the line plotted by Albee for Nelson and Roy's synthetic magnesium-rich chlorites than to the line determined by Albee for naturally-occurring chlorites. Albee's Figure 5 is reproduced in the present thesis as Figure 13, with the results obtained for the three chlorites examined in the present study being plotted on the same axes. It was found that when the "Nelson and Roy line" was used to read off the total aluminium and chromium content of these three chlorites from their d(001) basal spacings, the values obtained were 1.78, 2.80 and 3.20 for the Vermont, Venterspost and New

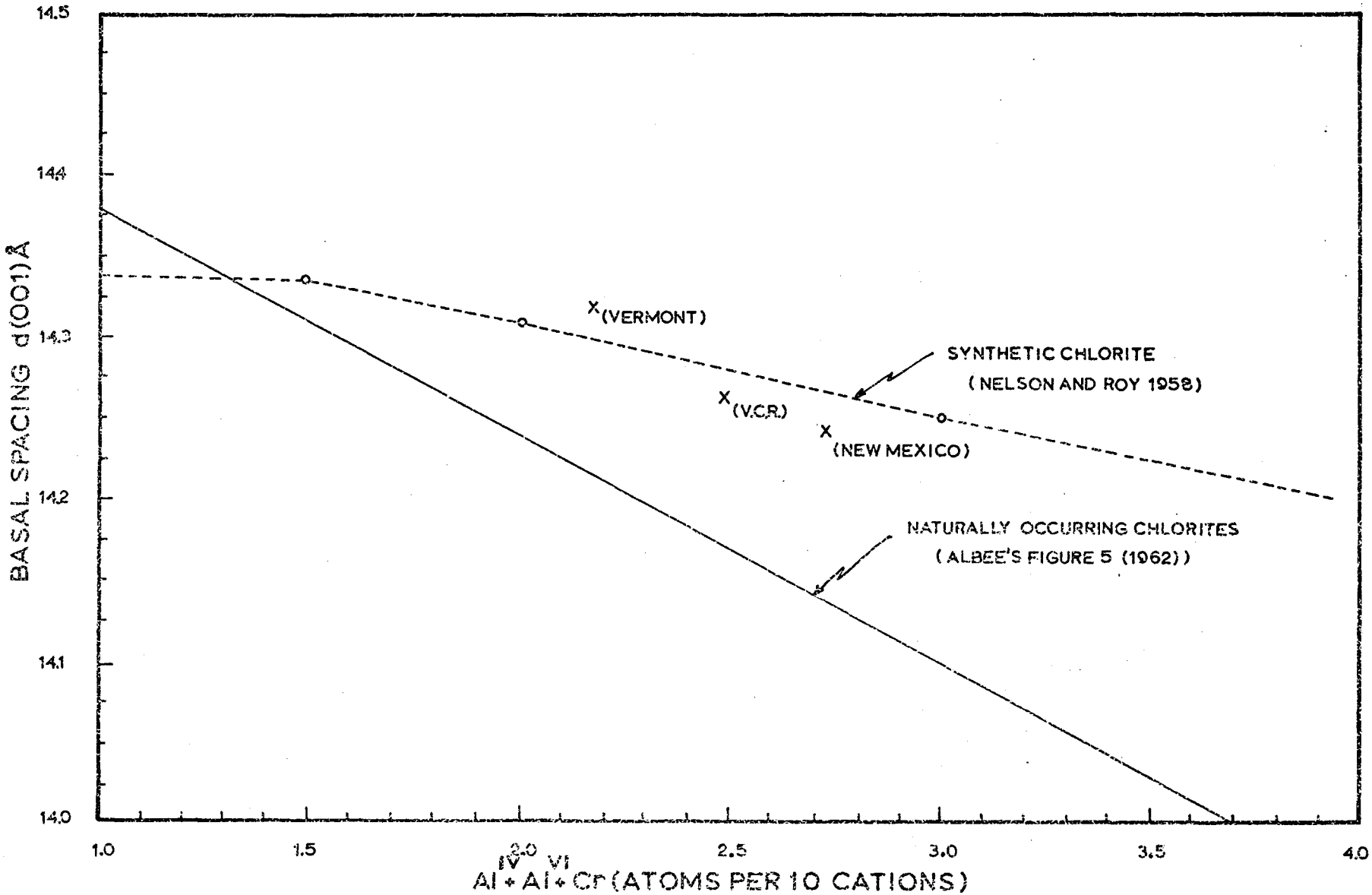


FIGURE 13 RELATIONSHIP BETWEEN BASAL SPACING d(001) AND Al CONTENT OF CHLORITE

Mexico chlorites respectively. Thus, the "Nelson and Roy line" underestimates the total aluminium and chromium content of the Vermont chlorite by 18 per cent relative to the results obtained by chemical analysis, while in the case of the iron-richer chlorites from Venterspost and New Mexico it overestimates the total aluminium and chromium by 11 and 15 per cent respectively.

When assessing the usefulness of X-ray diffraction techniques in the differentiation of chlorite species, the conclusion that must be drawn from the foregoing comparisons between structural formulae derived from chemical analyses and data derivable from the b_o and c_o parameters obtained from X-ray diffraction analyses is that the calculation of exact structural formulae for chlorites from X-ray diffraction data does not appear to be possible. X-ray diffraction data can, however, give rise to a reasonable estimate of the composition of chlorites.

Even when detailed and involved structure factor calculations have been carried out, the agreement between chlorite structural formulae derived from X-ray diffraction data and those calculated from chemical analyses still does not appear to be good. Brindley and Gillery (1956, p. 181) derived the following structural formula for a chlorite on the basis of structure factor calculations:

$$Mg_{4.4}Fe^{2+}_{0.5}Al_{1.1}(Si_{2.9}Al_{1.1})O_{10}(OH)_8$$

From chemical analyses, the structural formula of this chlorite was found to be:

$$Mg_{4.29}Fe^{2+}_{0.14}Al_{1.52}(Si_{3.06}Al_{0.94})O_{10.46}(OH)_{7.54}$$

Although Brindley and Gillery claimed that the agreement between these two structural formulae was very good as regards the tetrahedral Al and the Mg (but less good as regards the Fe^{2+} and the Al in octahedral coordination), calculation shows that the differences between the two structural formulae were in fact as follows:

(1) tetrahedral Al was overestimated by 17% by the X-ray method

(2) octahedral Mg was overestimated by 2.6% by the X-ray method

(3) octahedral Fe^{2+} was overestimated by 257% by the X-ray method

(4) octahedral Al was underestimated by 28% by the X-ray method.

6.2.3.5.2. Infra-red spectroscopy.

The infra-red absorption spectra obtained for the three chlorites examined in the present survey have been shown in Figure 9, and the vibration frequencies and their relevant bond assignments have been set out in Table XV (Section 6.2.3.4.4). Inspection of these results, together with those obtained for the lattice constants by means of X-ray diffraction (Table XIII, Section 6.2.3.4.3) and the

structural formulae calculated from chemical analyses (Table XVII, Section 6.2.3.4.6), permits the following generalizations to be made:

(1) Hayashi and Oinuma (1965, pp. 477-482) have claimed that variations in the position of the strong Si-O absorption band located at approximately 1000 cm^{-1} may be used to estimate the amount of tetrahedral aluminium present in the chlorite structure. This is not supported by the results of the present investigation, in which the Al^{IV} content (as shown in the structural formulae) increased from 1.05 for Vermont chlorite through 1.12 for Venterspost chlorite to 1.36 for New Mexico chlorite, while the Si-O stretch bond frequency for these three chlorites was, respectively, 1014, 980 and 981 cm^{-1}.

(2) Although Hayashi and Oinuma (1965, p. 480) claim that variations in absorption band frequencies in the 540-560 cm^{-1} range may be correlated with aluminium in octahedral coordination, the position of this band stayed essentially constant at 535 cm^{-1} for the three chlorites examined in the present study, despite the fact that the structural formulae of these chlorites indicate that the content of octahedral aluminium varied from 1.12 for Vermont chlorite to 1.37 for Venterspost chlorite, while the New Mexico chlorite had an octahedral aluminium content of 1.36. It would therefore seem that this absorption band is not to be relied on as an indicator of the amount of octahedrally coordinated aluminium.

(3) Furthermore, Hayashi and Oinuma (1965, p. 482) claim that a correlation exists between the Si-O-Al^{VI} absorption peak position and the b_o parameter. This correlation was not apparent in the three chlorites examined, since the b_o parameter changed from 9.250 Å for Vermont chlorite through 9.291 for Venterspost chlorite to 9.317 Å for New Mexico chlorite, while the Si-O-Al^{VI} vibration frequency remained constant at 535 cm^{-1} for all three chlorites.

(4) In the three chlorites examined, the position of the absorption band tentatively assigned to Si-O-Mg^{VI} appears to show a decrease in the wavenumber (from 458 cm^{-1} for Vermont chlorite through 456 cm^{-1} for Venterspost chlorite to 450 cm^{-1} for New Mexico chlorite) as iron increases in the chlorite lattice and magnesium decreases.

(5) Inspection of Figure 9, showing the absorption spectra of the three chlorites examined in the present study, fails to reveal the presence of quartz in the spectrum of the chlorite from Venterspost, which is known to contain 15 per cent of quartz as an impurity. The sensitivity of infra-red methods as regards the detection of impurities in chlorites may therefore be considered to be poor.

6.2.3.5.3. Differential thermal and thermogravimetric analyses (D.T.A. and T.G.A.).

Examination of Figures 10, 11 and 12, showing the combined D.T.A. and T.G.A. spectra of the three chlorites examined in the present study, permits the following generalizations to be made:

(1) In the magnesium-rich chlorite from Vermont, both the endothermic and exothermic peaks are situated at considerably higher temperatures (616 and 810°C respectively) than in the other two chlorites. The endothermic and exothermic peaks are, respectively, situated at 583 and 753°C for the Venterspost chlorite and at 530 and 745°C for the New Mexico chlorite. Since the structural formulae derived from chemical analyses show that the magnesium content is highest in the Vermont chlorite and lowest in the New Mexico chlorite, there is thus a crude direct relationship between the Mg content of the chlorites and the position of the endothermic and exothermic peaks.

(2) The three chlorites show a crude inverse relationship between iron content (which is lowest in the Vermont chlorite and highest in the New Mexico chlorite) and the position of their endothermic and exothermic peaks.

(3) Endothermic peaks below 200°C are due to adsorbed water.

(4) The endothermic peaks located between 550°C and 616°C represent loss of OH from the brucite layer of the chlorite (Martin, 1955, p. 119).

(5) The exothermic peaks located between 745°C and 810°C represent a breakdown in the structure and a loss of OH from the talc layer of the chlorite (Martin, 1955, p. 119).

(6) Martin (1955, p. 137) concluded that, for a given particle size, the position of the major endothermic peak could be used to differentiate iron-rich chlorites. This is borne out by the present results, in view of the crude inverse relationship that was found to exist between iron content and the position of the major endothermic peak.

(7) On heating three samples of each of the the three chlorites to 670°C, 820°C and 1000°C respectively and examining the resulting products by X-ray diffraction and infra-red spectroscopy, the following conclusions could be reached:

(a) Considerable structural disordering was found to occur at 670°C. This was indicated by the diffuse nature of the X-ray diffraction lines and the broadness of the infra-red peaks produced by the phases formed at this temperature.

(b) A progressive increase of ordering within the lattices of the phases being formed at 820°C and 1000°C was indicated by the sharpening of the X-ray diffraction lines and infra-red absorption bands.

(c) Only in the case of the magnesium-rich chlorite from Vermont could the reaction products of thermal treatment be identified by X-ray diffraction (they were forsterite and a magnesium spinel).

(d) X-ray and infra-red examination of the reaction products formed on heating chlorites of various compositions appear to be of very limited value in characterizing the original unheated chlorites.

From the present investigation into the applicability of D.T.A. and T.G.A. techniques to the study of chlorites, it must be concluded that these two techniques are of little use for the varietal classification of chlorites. This finding confirms previous observations made by Phillips (1963, p. 404) and Martin (1955, p. 144). Phillips, as has been mentioned earlier, concluded that D.T.A. alone appeared to be inadequate as a tool for distinguishing the many chlorite varieties, although the technique could be used to distinguish the 7 Å septechlorite structure from the normal 14 Å structure. Martin (1955, pp. 140 - 141) considered that the inherent disadvantage of all D.T.A. techniques is that, depending on particle size distribution and the type of instrument used, D.T.A. thermograms may often be so different that they cannot be compared with published data, which seriously limits the usefulness of the technique.

6.2.3.5.4. The varietal classification of the three chlorites examined.

In Section 6.2.3.2, four of the various systems of chlorite classification that have been proposed for the purpose of subdividing the chlorites into logical and significant mineral varieties were briefly reviewed. In view of the difficulty of deciding which of these systems should be used to identify the variety of chlorite occurring in the Ventersdorp Contact Reef at Venterspost, it was found necessary to assess the four systems by comparing the varietal names that each of them would assign to the V.C.R. chlorite, and to two other high-purity chlorites, on the basis of the results obtained from extensive analyses of these three chlorites.

The four systems of chlorite classification that were used are listed below:

System No. 1: This system was proposed by Hey (1954, p. 277), and requires optical data, such as intermediate refractive index β, optic sign and birefringence.

System No. 2: This system was also proposed by Hey (1954, pp. 277 - 292), and depends on the chemical compositions of the chlorites. 4% Fe_2O_3 is arbitrarily taken as the dividing line between "unoxidized normal" and "oxidized" chlorites, and the "unoxidized" series (i.e. those chlorites with Fe_2O_3 content below 4 per cent) is then subdivided into 11 species and 4 varieties depending on the number of Si atoms in the half cell and the Fe:(Fe + Mg) ratio. The chlorites in the "oxidized" series (i.e. those chlorites with Fe_2O_3 content higher than 4 per cent) are subdivided into three species based only on Si content, with only one of these species, thuringite, being subdivided into varieties with respect to the Fe:(Fe + Mg) ratio.

System No. 3: This system was proposed by Foster (1962, p. 20)[17]. It is based on the two principal types of ionic replacement which characterize the chlorites, i.e., the replacement of tetrahedral and octahedral Al by Si and Mg, and the replacement of Mg by Fe^{2+}. The classification scheme based on these two replacement series divides the chlorites into nine species which are strictly defined on the basis of Si content and the ratio of Fe^{2+} to R^{2+}.

System No. 4: This system was proposed by Phillips (1964, p. 1116). It is based on consideration of the kinds of cations in tetrahedral coordination and their relative abundance, the kinds of cations in octahedral coordination and their relative abundance, the relative number of O^{--} and OH^{-} anions and the structural type.

The varietal names assigned to the three chlorites examined by each of the four systems of chlorite classification are summarized in Table XIX.

Inspection of Table XIX reveals the confused situation that exists at present regarding the varietal classification of the chlorites, as it can be seen that the different systems may often give directly contradictory results. It was originally hoped that the situation might be clarified by the examination of two high-purity chlorites from Vermont and New Mexico, since these had already been classified as prochlorite and thuringite respectively by the suppliers (Messrs. Ward's Scientific Establishment, Rochester, New York). The results of this examination shown in Table XIX, however, made it seem doubtful that the Vermont chlorite could have been correctly classified by the suppliers, and it thus became impossible to use these two chlorites as "standards" in the evaluation of the four systems of classification.

TABLE XIX

VARIETAL NAMES ALLOCATED BY DIFFERENT CLASSIFICATION SYSTEMS TO THEE CHLORITES FROM VERMONT, VENTERSPOST AND NEW MEXICO

Chlorite Source	System No. 1 (Hey, optical)	System No. 2 (Hey)	System No. 3 (Foster)	System No. 4 (Phillips)
Vermont	clinochore	clinochlore	clinochlore	clinochlore
Venterspost	brunsvigite?	pycnochlorite	brunsvigite?	pycnochlorite
New Mexico	brunsvigite	thuringite*	thuringite	aphrosiderite

* Name allocated on the basis that Fe_2O_3 content is greater than 4%.

The varietal classification that was finally adopted for the three chlorites is discussed below:

Vermont chlorite: All four systems of classification agree in identifying this chlorite as clinochlore. This chlorite is therefore not prochlorite, as originally suggested by the suppliers, Messrs. Ward's Scientific Establishment.

New Mexico chlorite: Two systems of classification, systems 2 and 3 (respectively, Hey's chemical system of classification and Foster's system), identify this chlorite as thuringite, which was also the identification suggested by Messrs. Ward's Scientific Establishment. Phillips' system (system 4) classifies this chlorite as aphrosiderite, a variation of ripidolite. If only optical data is used (system 1, Hey), without knowledge of the Fe_2O_3 content, this chlorite would be identified as brunsvigite, but this identification falls away when the Fe_2O_3 content, which is greater than 4 per cent, is taken into account. The weight of evidence therefore suggests that this chlorite is in fact thuringite, as claimed by the suppliers.

Venterspost (Ventersdorp Contact Reef) chlorite: Systems 2 and 4 (Hey's chemical system and Phillips' system) identify this chlorite as pycnochlorite, while systems 1 and 3 (Hey's optical system and Foster's system) identify this chlorite as brunsvigite?. The allocation of the name "brunsvigite" is considered to be suspect for the following reasons:

(a) Using system 1 (Hey, 1954, p. 277): Chlorites with a β refractive index of 1.629 and a birefringence of the order of 0.002 (as, for example, the Venterspost chlorite) fall virtually on the line dividing ripidolite and brunsvigite in Hey's system of classification. An additional complication has been pointed out by Albee (1962, p. 864), that is, that an optical sign change occurs in chlorites at $\beta = 1.630$. In view of these considerations, it is felt that Hey's system (system 1) cannot be applied with any degree of certainty in the case of this chlorite, so that the identification "brunsvigite" is suspect.

(b) Using system 3 (Foster, 1962, p. 21): Although the structural formula of this chlorite (calculated from chemical data) corresponds best to the compositional area allocated by Foster to brunsvigite, the $Fe^{2+} : R^{2+}$ ratio calculated for this chlorite was 0.86. Since this lies outside the limits of 0.25-0.75 assigned to brunsvigite by Foster, the identification of this chlorite as brunsvigite is again suspect.

It can thus be seen that, in the case of the Venterspost chlorite, it is not possible to arrive at an unequivocal identification of the chlorite when either sytem 1 or system 3 is used. The evidence thus indicates that the Venterspost (Ventersdorp Contact Reef) chlorite should be identified as pycnochlorite, as suggested by systems 2 and 4, and not as brunsvigite.

6.2.3.5.5. The characterization of chlorites -- conclusions.

The main reason for the confusion at present surrounding the varietal classification of the chlorites is that the classification systems that have been proposed by various authors at different times all impose arbitrary, and not necessarily similar, subdivisions on the chlorites. In the absence of a definitive ruling from some international body (such as the International Mineralogical Association Commission on New Minerals and Mineral Names), it is not really possible to select any one of the proposed classification systems as being more "correct" than any other one, and the decision as to which classification system should be adopted can only be based on the personal preference of the individual investigator.

All that can be concluded from the comparison of four chlorite classification systems carried out in the course of the present study is that it appears that the classification system proposed by Phillips (1964, p. 1116) is among the sounder schemes proposed to date, as it attempts to reconcile chemical data with structural data. It also appears that the use of optical data alone, without a knowledge of the chemical composition of the chlorite, may lead to an erroneous result. In fact, Hey's scheme (system 1), although based primarily on optical measurements, does really require some chemical data for its operation.

As regards the analytical techniques necessary for the varietal classification of chlorites, the results of the present investigation indicate that infrared spectroscopy and differential thermal analysis, in their current state of development, do not appear to make any significant contribution to the characterization of 14 Å chlorites. It seems therefore that chemical analysis, a limited amount of X-ray diffraction work and the optical determination of the intermediate

refractive index (β) are all the techniques necessary for the characterization of varieties of chlorite.

6.3. Pyrophyllite.

6.3.1. Occurrence and genesis of pyrophyllite in the Witwatersrand.

During the course of this study, the presence of minor amounts of pyrophyllite in samples of Ventersdorp Contact Reef ore from Venterspost, and of Vaal Reef ore from Hartebeestfontein and Zandpan, was detected by means of X-ray diffraction analysis (see Part I of this thesis). On examination of thin sections prepared from this suite of samples, the pyrophyllite was found to occur intergrown with muscovite as interstitial material between the quartz pebbles.

Little detailed mineralogical or X-ray work appears to have been carried out on pyrophyllite occurring in Witwatersrand horizons. Liebenberg (1955, p. 112), when describing the mineralogy of Witwatersrand conglomerates, reported that "in some areas pyrophyllite is the main micaceous silicate in the matrix, e.g. at Blyvooruitzicht (Carbon Leader) where it is accompanied by only a small proportion of sericite and muscovite". He did not, however, discuss the occurrence of pyrophyllite in detail. Fuller (1958, pp. 42 - 44) was the first to record pyrophyllite as a component of the matrix of the quartzites of the Upper Division of the Witwatersrand System. He found that pyrophyllite was widespread in the Upper Division of the System, and that it was particularly characteristic of the Main Bird Series. Viljoen (1964, pp. 30 & 109), who studied the conglomerates of the Main Bird Series, mentioned that the material that he identified as pyrophyllite invariably occurred intermixed with sericite as interstitial material between quartz grains and pebbles. Viljoen added that he found pyrophyllite to be microscopically indistinguishable from sericite when these two minerals were intergrown.

The genesis of pyrophyllite has been most extensively studied in commercial pyrophyllite deposits, where the host rocks are usually original lava flows, breccias and tuffs of acid composition. The principal reactions involved in the formation of pyrophyllite are, according to Stuckey (1925, p. 449): (1) silicification, accompanied by a decrease in alkalis and alumina, and (2) the hydrolysis of alkali feldspar with the production of sericite and/or pyrophyllite. In massive pyrophyllite deposits, pyrophyllitisation usually appears to have occurred under conditions of intermediate temperature and pressure, aided by hydrothermal solutions that are in part juvenile. Fuller (1958, p. 43) has summarized the process as follows: "Field and laboratory evidence suggests therefore that pyrophyllite is

commonly produced by the hydrothermal alteration of fine-grained quartzo-feldspathic rocks at moderate depth and at temperatures in the vicinity of 400°C and that its formation is accompanied by breakdown of feldspars, silicification, and leaching of alkalis. The fact that the mineral does not occur in the zone of weathering indicates that elevated temperatures are required regardless of the chemical conditions obtaining." Recent laboratory studies of the stability of pyrophyllite (Kerrick, 1968, p. 205) have shown that the probable upper stability limit of pyrophyllite is below $455 \pm 7^{\circ}C$ at 3.8 to 3.9 kilobars and below $447 \pm 7^{\circ}C$ at 1.7 to 1.8 kilobars.

As regards the genesis of pyrophyllite occurring in the Upper Division of the Witwatersrand System, the only mechanism suggested to date has been that proposed by Fuller (1958, p. 44). He postulated that this pyrophyllite was only formed in rocks that were subject to local increase in temperature and at the time were sufficiently permeable to permit the passage of hydrothermal solutions. This hydrothermal activity was accompanied by changes in the gross composition of the rocks involved, particularly the removal of alkalis and the redistribution of silica. In the case of the present suite of samples, no better mechanism can be suggested for the genesis of the pyrophyllite occurring in the Vaal Reef at Hartebeestfontein and Zandpan than that proposed by Fuller. The pyrophyllite in the Ventersdorp Contact Reef at Venterspost, however, was found to occur in a very sporadic fashion, and this probably represents localized hydrothermal alteration of pumiceous ash exuded prior to the outpouring of the Ventersdorp Lavas.

6.3.2. Characterization of pyrophyllites from Loraine and Gestoptefontein.

6.3.2.1. Introduction.

The quantitative relationship between pyrophyllite and the other minerals in the samples from the Vaal Reef at Hartebeestfontein and Zandpan and from the Ventersdorp Contact Reef at Venterspost has been commented on in Part I of this thesis. Before the amount of pyrophyllite occurring in these samples could be quantitatively estimated, however, it was necessary to find a suitable source of pyrophillite for use as an X-ray diffraction standard. Gibbs (1967, p. 80) has pointed out that the best way to overcome the problems of variability of composition and crystallinity of clay minerals when carrying out quantitative X-ray diffraction analysis is to extract the individual clays from the samples themselves and then to use these separated clays as the standards for the series of samples. In the case of the present suite of samples, however, the pyrophyllite was found to be present in very small amounts (generally less than 2 per cent), and this pre-

cluded the extraction of sufficient pyrophyllite to permit its complete characterization as an X-ray diffraction standard by chemical analysis and detailed X-ray diffraction analysis. An alternative source (preferably still a Witwatersrand ore) from which pyrophyllite could be extracted in a quantity sufficient to permit its detailed study and characterization was thus required.

At the time when the need for a pyrophyllite standard became apparent, the author became involved in the investigation of metallurgical extraction problems that were being encountered in the filtration of the "pregnant" gold-cyanide complex solutions at the Loraine Gold Mine. Here the "B" Reef, the basal conglomerate of the Kimberley Stage of the Kimberley-Elsburg Series, is mined, and X-ray diffraction studies revealed that the "B" Reef at this mine contained large amounts of pyrophyllite and lesser amounts of intercalated muscovite. Since the settling characteristics of phyllosilicates (and in particular of pyrophyllite) in the gold extraction plant were only poorly understood, it was considered important to carry out a detailed structural and chemical analysis of the pyrophyllite occurring in the "B" Reef, as this was suspected of being the mineral species responsible for the poor gold recovery. At the same time it was realized that an investigation of the Loraine pyrophyllite would make available a well-characterized pyrophyllite that would probably be suitable for use as a standard in investigating pyrophyllite from other Witwatersrand horizons. A pyrophyllite concentrate with a purity of 90% was obtained from ground portions of the "B" Reef at Loraine by beneficiation in a flotation cell using a frothing agent, and this pyrophyllite was then carefully characterized. This investigation appears to be the first detailed infra-red, X-ray diffraction and chemical study to be carried out on pyrophyllite occurring in Witwatersrand conglomerates, and the results of this study are therefore reported at length in subsequent sections.

Pyrophyllite from a non-Witwatersrand source (Gestoptefontein near Ottosdal in the Western Transvaal) was also at one time considered as a possible standard for quantitative X-ray diffraction analysis, and was subjected to the same investigations as the Loraine pyrophyllite. This Gestoptefontein pyrophyllite, which is commonly referred to as "Wonderstone", occurs in massive amounts in a relatively pure form (approximately 89% pyrophyllite), and has the advantage that it can be utilized as a standard simply by crushing the ore without having to resort to involved metallurgical procedures. Its suitability as a standard for Witwatersrand pyrophyllites was questionable, however, as the work of Net et al. (1937, p. 15) indicated that its genesis was very different from the genesis postulated by Fuller

(1958, p. 44) for Witwatersrand pyrophyllite. (Net et al. attributed a secondary origin to the Gestoptefontein pyrophyllite, and believed that it represented the end product of the alteration of volcanic ash). The analytical results obtained for the Gestoptefontein pyrophyllite were therefore compared with those obtained for the Loraine pyrophyllite in order to see whether the differences between the two pyrophyllites were such that they would rule out the possibility of using the Gestoptefontein pyrophyllite as an X-ray standard for quantitative determinations of Witwatersrand pyrophyllite.

6.3.2.2. Chemical analyses.

The results of the chemical analyses of the pyrophyllites from Loraine and Gestoptefontein are set out in Table XX. These chemical analyses have been recalculated to allow for the presence of various impurities which were initially identified by optical and X-ray methods.

TABLE XX

CHEMICAL ANALYSES OF PYROPHYLLITE FROM GESTOPTEFONTEIN AND LORAINE GOLD MINE

	GESTOPTEFONTEIN per cent	LORAINE GOLD MINE per cent
SiO_2	60.00	65.00
Al_2O_3	33.00	29.10
CaO	0.07	---
MgO	0.11	---
Na_2O	0.17	0.04
K_2O	0.30	0.15
H_2O	6.42	5.51
	99.87	99.90

Impurities	per cent	Impurities	per cent
rutile	1	muscovite	1
hematite	0.7	quartz	7
muscovite	2	rutile	0.4
kaolinite	2	pyrite	0.2
		hematite	0.3

6.3.2.3. Structure and structural formulae of pyrophyllite from Gestoptefontein and Loraine Gold Mine.

The structure of pyrophyllite may be visualized as consisting of a sheet of octahedrally coordinated Al ions sandwiched between two sheets of linked SiO_4 tetrahedra, resulting in the so-called 2:1 type of layer structure. In the pyrophyllite structure, each composite layer (consisting of two SiO_4 sheets and an octahedrally coordinated Al layer) is neutral, and the successive layers are held together only by weak van der Waals forces. If, however, substitution by Al^{3+} takes place for Si^{4+} in the tetrahedral layer, or other cations such as Mg^{2+} substitute for Al^{3+} in the octahedral layer, then this substitution results in a negative charge being developed on the composite layer, which is in turn compensated for by the introduction of other cations lying between the layers.

The structural formulae of the two pyrophyllites, based on the chemical analyses (recalculated to allow for the presence of impurities), are given in Table XXI.

TABLE XXI

STRUCTURAL FORMULAE OF PYROPHYLLITE FROM GESTOPTEFONTEIN AND LORAINE GOLD MINE

Gestoptefontein:

$(Al_{3.72}\ Ca_{0.01}\ Mg_{0.01}\ Na_{0.06}\ K_{0.06})\ (Si_{7.36}\ Al_{0.64})\ O_{20}\ (OH)_4$

Loraine:

$(Al_{3.94}\ Na_{0.04}\ K_{0.03})\ (Si_{7.80}\ Al_{0.20})\ O_{20}\ (OH)_4$

6.3.2.4. X-ray diffraction.

Both samples of pyrophyllite were examined by X-ray diffraction, using the technique outlined in Part III. The lattice constants are given in Table XXII, and the interplanar spacings and indices in Table XXIII (see pages 94 and 95).

6.3.2.5. Infra-red spectroscopy.

Both samples of pyrophyllite were analysed by means of infra-red spectroscopy. The method used is described in Part III of this thesis. The results of the infra-red analyses are set out in Table XXIV (see page 96), and the infra-red absorption spectrum for the Loraine pyrophyllite is shown in Figure 14.

TABLE XXII

LATTICE CONSTANTS FOR TWO PYROPHYLLITE SAMPLES FROM GESTOPTEFONTEIN AND LORAINE GOLD MINE

	GESTOPTEFONTEIN	LORAINE GOLD MINE
a_o	5.150 ± 0.002 Å	5.164 ± 0.001 Å
b_o	8.945 ± 0.003 Å	8.937 ± 0.001 Å
c_o	18.682 ± 0.011 Å	18.671 ± 0.002 Å
β	$99^o\ 55' \pm 4'$	$99^o\ 47' \pm 4'$
Volume	847.8 $Å^3$	849.2 $Å^3$
Space group	C2/c	C2/c

6.3.2.6. Discussion of results.

The infra-red vibration frequencies for the Si-O bands in the two pyrophyllites from Gestoptefontein (G) and Loraine Gold Mine (L) can be seen from Table XXIV (Section 6.3.2.5) to lie at 1113 and 1119 cm^{-1} respectively. Both of these bands are Si-O stretching vibrations. The shift from 1119 (L) to 1113 (G) cm^{-1} is interpreted as indicating the effect of substitution by Al^{3+} for Si^{4+} in the tetrahedral position of the structure. The two absorption bands located at 944 (G) and 948 (L) cm^{-1} are thought to be due to H-O--Al^{3+} vibrations. Here the hydroxyl group (O-H bending mode) has Al as its nearest neighbour in the pyrophyllite structure. The shift in (O-H) vibration frequency from 948 (L) to 944 (G) cm^{-1} is interpreted as being due to a change in aluminium content in the octahedral layer, and the shift in the Si-O-Al^{VI} vibration band from 535 (L) to 530 (G) cm^{-1} is likewise interpreted as reflecting a change in aluminium content in the octahedral layer.

These interpretations of the infra-red spectra appear to be in accord with the X-ray diffraction data shown in Table XXII, and with the structural formulae listed in Table XXI. The pyrophyllite from Loraine Gold Mine has much smaller b_o and c_o dimensions than that from Gestoptefontein. The Gestoptefontein pyrophyllite shows more extensive interlayer substitution by Ca and Mg, and much greater substitution by Al^{3+} for Si^{4+} in the tetrahedral position of the structure, than does the Loraine pyrophyllite, and this has led to changes in the lattice dimensions.

Inspection of Table XXIII clearly shows the wide differences between the Loraine and Gestoptefontein pyrophyllite as regards the integrated intensity of

TABLE XXIII

X-RAY DIFFRACTION POWDER DATA FOR PYROPHYLLITE FROM GESTOPTEFONTEIN AND LORAINE GOLD MINE

GESTOPTEFONTEIN				LORAINE GOLD MINE			
'd' Å observed	'd' Å calculated	I/I_1	h k l	'd' Å observed	'd' Å calculated	I/I_1	h k l
9.215	9.205	100	0 0 2	9.205	9.192	43	0 0 2
4.600	4.601	32	0 0 4	4.597	4.600	23	0 0 4
4.445	4.445	55	1 1 -1	4.448	4.451	42	1 1 -1
4.412	4.412	30	1 1 0	4.423	4.423	42	1 1 0
3.065	3.067	73	0 0 6	3.065	3.065	100	0 0 6
2.971	2.970	5	1 1 4	2.571	2.571	8	1 3 0
2.569	2.571	5	1 3 0	2.534	2.533	14	1 3 -2
2.535	2.536	47	2 0 0	2.422	2.422	24	1 1 -7
2.219	2.220	5	0 4 1	2.332	2.333	1	1 3 -4
2.152	2.153	26	2 2 1	2.299	2.301	1	0 0 8
2.079	2.076	17	2 0 4	2.236	2.235	1	0 4 0
2.079	2.076	17	2 2 2	2.236	2.235	1	2 2 -1
2.061	2.061	8	1 3 -6	2.167	2.167	4	1 3 4
1.8398	1.8403	11	0 0 1	2.098	2.099	1	0 4 3
1.6897	1.6890	5	1 5 -1	2.081	2.082	6	2 0 4
1.6851	1.6850	5	2 4 -2	2.058	2.059	7	1 3 -6
1.6851	1.6857	5	3 1 -2	2.006	2.006	1	2 0 -7
1.6609	1.6615	15	3 1 0	1.8925	1.8925	2	1 3 6
1.6434	1.6429	15	1 5 2	1.8395	1.8400	5	0 0 10
1.4925	1.4921	27	1 1 11	1.6893	1.6891	4	2 4 -1
1.4893	1.4875	5	3 3 -2	1.6879	1.6879	9	1 5 -1
1.4813	1.4815	5	3 3 -3	1.6475	1.6471	9	1 1 -11
1.4718	1.4716	5	0 6 2	1.5294	1.5299	1	2 2 -10
1.4704	1.4709	5	3 3 0	1.5136	1.5140	1	1 5 -6
1.3835	1.3835	5	3 0 6	1.4936	1.4933	6	1 1 11
				1.4901	1.4897	6	0 6 0
				1.4901	1.4903	6	3 3 -2
				1.3696	1.3696	7	1 3 -12
				1.3136	1.3139	1	1 1 -14
				1.2941	1.2937	1	1 1 13
				1.2389	1.2390	5	1 7 -1

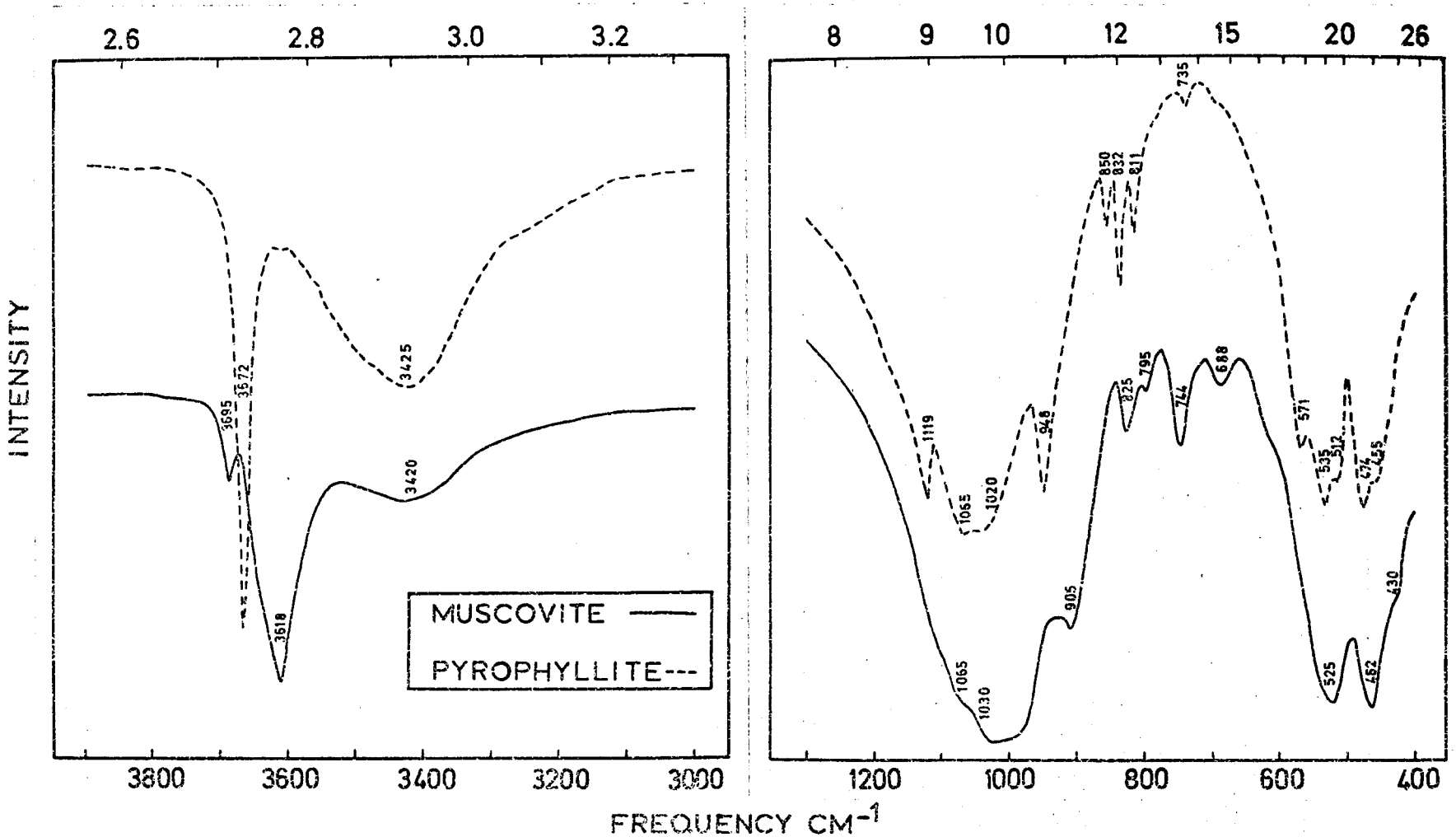


FIGURE 14 INFRARED ABSORPTION SPECTRA OF MUSCOVITE AND PYROPHYLLITE

TABLE XXIV

INFRA-RED VIBRATION FREQUENCIES AND BOND ASSIGNMENTS FOR TWO SAMPLES OF PYROPHYLLITE FROM GESTOPTEFONTEIN AND LORAINE GOLD MINE

GESTOPTEFONTEIN		LORAINE GOLD MINE	
ν cm^{-1}	Bond assignments	ν cm^{-1}	Bond assignments
3670	OH stretch	3672	OH stretch
3617	OH stretch		
3425	HOH	3425	HOH
2370	?		
		1875	(quartz)
1620	HOH	1625	HOH
1113	Si-O	1119	Si-O
1050	Si-O-Si stretch	1065	Si-O-Si stretch
		1020	Si-O-Si
944	H-O--Al	948	H-O--Al
848	Si-O-(Al)	850	Si-O-(Al)
830	Si-O-Al	832	Si-O-Al
808	Al-O	811	Al-O
735	Si-O-Al	735	Si-O-Al
695	Si-O		
566	?	571	?
530	Si-O-Al^{VI}	535	Si-O-Al^{VI}
508	Si-O?	512	Si-O?
474	Si-O	474	Si-O
455	Si-O		

the basal reflection. For example, the integrated intensity of the (002) basal reflection of the Gestoptefontein pyrophyllite was 100, whereas that of the Loraine pyrophyllite was only 43. It is therefore apparent that if the (002) basal reflection were to be used for quantitative X-ray diffraction analyses, widely different results would be obtained depending on which pyrophyllite was selected as the standard. In view of Gibbs' (1967, p. 80) recommendations concerning the desirability of using a standard as similar as possible to the unknown, the Gestoptefontein pyrophyllite, with a genesis very different from that of the Witwatersrand pyrophyllites, had clearly to be rejected in favour of the Loraine pyrophyllite.

Pyrophyllite extracted from the "B" Reef at the Loraine Gold Mine was accordingly used as the standard for quantitative X-ray diffraction determinations of the pyrophyllite in the present suite of samples, since pyrophyllite of a sufficient degree of purity was not obtainable from either the Vaal Reef or Ventersdorp Contact Reef.

6.4. Muscovite.

6.4.1. Introduction.

In the course of the present survey, the examination of samples of auriferous conglomerate taken from the Vaal Reef at Hartebeestfontein and Zandpan and from the Ventersdorp Contact Reef at Venterspost revealed the presence of muscovite, which was positively identified as such with the aid of X-ray diffraction analysis and infra-red spectroscopy (see Part I of this thesis). Examination of thin sections prepared from these samples revealed that the muscovite occurred as interstitially dispersed acicular grains intimately intergrown with other phyllosilicates such as chlorite and pyrophyllite, all these phyllosilicates being intermixed with fine mosaic-like quartz grains and sulphides to form the matrix material of the conglomerate. This matrix material helps to cement the larger quartz pebbles and boulders in the conglomerate.

The presence of a micaceous mineral occurring interstitially in the auriferous conglomerates, and also in the shales and quartzites, of the Witwatersrand System has previously been reported by numerous authors. (The term "mica" is used in the present thesis to refer to the group of minerals that includes muscovite, phlogopite, lepidolite, paragonite, biotite, glauconite and zinnwaldite, and also the brittle micas margarite, clintonite and xanthophyllite.) This mica mineral has often been referred to simply as "sericite", but, as Yoder and Eugster (1955, p. 255) have pointed out, the term "sericite" is a field term that can be used to describe any fine-grained white mica. Since the white micas include both muscovite and paragonite, it becomes apparent that the name "sericite" is not specific enough to permit the particular mica occurring in the Witwatersrand horizons to be properly characterized. In 1944 Frankel commented (p. 171): "Frequently the identity of the dominant silicate in the Rand banket is questioned, although the presence of alkalis in analyses of the total rock suggests that it is a mica. Professor Young, and other writers, have shown from microscopical studies that the mineral is a sericite." Frankel then proceeded to carry out X-ray diffraction analyses of silicates collected from mines along the Reef, and concluded (1944, p. 171): "In all

cases the patterns were of the muscovite type and unit cell dimensions varied slightly."

One of the few investigators of Witwatersrand material who has, to date, been explicit concerning the exact nature of the Witwatersrand "sericite" has been Fuller (1958, p. 35). When examining quartzites of the Upper Division of the Witwatersrand System, Fuller stated: "The dominant mineral in the matrix of these quartzites is sericite, or, more explicitly, common 2M muscovite." Other investigators of samples from Witwatersrand horizons have been less explicit, however. Von Rahden (1964, p. 101), Viljoen (1964, p. 30) and Jacob (1966, p. 11) all reported the presence of sericite or sericitic material in the Witwatersrand conglomerates examined by them, but did not specify whether the material was in fact muscovite.

In view of the confusion surrounding the identity of the micaceous mineral commonly found in the auriferous conglomerates, shales and quartzites of the Witwatersrand System, the nomenclature that has been used in classifying certain micaceous minerals closely related to muscovite (i.e., muscovite, sericite, hydromuscovite and illite) is briefly reviewed in subsequent paragraphs, and some of the differences between the structures and properties of these micas are discussed. This review is followed by a description of the characterization of the muscovite found in samples from the Vaal Reef at Hartebeestfontein, which was carried out by investigating this mineral in detail with the aid of several different analytical techniques and comparing the results with those obtained when samples of muscovite, hydromuscovite and illite from non-Witwatersrand sources were subjected to the same analytical techniques.

6.4.2. A review of the structure and nomenclature of the muscovites.

Muscovite, sericite, hydromuscovite and illite are all members of the mica group of minerals. Deer, Howie and Zussman (1966, p. 193) have described the micas as follows: "The mica minerals as a whole show considerable variation in chemical and physical properties, but all are characterized by a platy morphology and perfect basal cleavage which is a consequence of their layered atomic structure. ..... The basic structural feature of mica is a composite sheet in which a layer of octahedrally coordinated cations is sandwiched between two identical layers of linked $(Si,Al)O_4$ tetrahedra."

6.4.2.1. Muscovite.

Muscovite is one of the most common micas, and occurs in a wide variety of geological environments. The structure of a muscovite was first established by Jackson and West for a 2-layer monoclinic muscovite in 1930 (p. 211) and 1933 (p. 160), and subsequently refined in 1939 by Hendriks and Jefferson (1939, p. 729). In muscovite, one quarter of the tetrahedral sites are occupied by Al and three quarters by Si, with the twelve-fold coordinated positions between composite layers being fully occupied by potassium ions. The succession of atomic layers in muscovite is as follows:

$$\left\{\begin{array}{l} 6O^{-} \\ 3Si^{4+} + Al^{3+} \end{array}\right. \qquad \text{Tetrahedral layer}$$

$$\left\{\begin{array}{l} 4O^{-} + 2(OH, F)^{-} \\ 4Al^{3+} \\ 4O^{-} + 2(OH, F)^{-} \end{array}\right. \qquad \text{Octahedral layer}$$

$$\left\{\begin{array}{l} 3Si^{4+} + Al^{3+} \\ 6O^{-} \end{array}\right. \qquad \text{Tetrahedral layer}$$

$$2K^{+}$$

$$6O^{-}$$

$$3Si^{4+} + Al^{3+} \qquad \text{(Foster, 1956, p. 58)}$$

Smith and Yoder (1956, p. 210), from a consideration of possible rearrangement positions of the tetrahedral layers relative to each other, were able to predict that six simple polymorphs should be observed. For muscovite only the 1M, $2M_1$ and, less commonly, 3T polymorphs have been found. The $2M_2$ polymorph has also been observed, but only in lepidolite, whereas the 2O and 6H polymorphs have yet to be found in nature.

In addition to the three structurally ordered 1M, $2M_1$ and 3T polymorphs of muscovite, the presence of a structurally disordered one layer monoclinic 1Md polymorph has also been reported (Yoder and Eugster, 1955, p. 225).

It is fortunate that differentiation between the various polymorphs is possible by means of X-ray diffraction. The characteristic X-ray diffraction re-

flections attributable to each of these polymorphs were listed by Smith and Yoder (1956, p. 230) and are summarized in Table XXV.

TABLE XXV

CHARACTERISTIC X-RAY REFLECTIONS (INTERPLANAR SPACINGS) FOR THE RECOGNITION OF 1Md, 1M AND $2M_1$ POLYMORPHS OF MUSCOVITE

POLYMORPH	INTERPLANAR SPACING Å
1Md	4.48, 3.33, 2.58
1M	4.48, 3.66, 3.33, 3.07, 2.58
$2M_1$	4.48, 4.29, 3.89, 3.74, 3.54, 3.33, 3.21, 3.01, 2.87, 2.80, 2.58

As may be seen from inspection of Table XXV, it would be difficult to identify the presence of the 1Md polymorph in the presence of the 1M and $2M_1$ polymorphs, because of the existence of coincident reflections. The two unique reflections of the 1M muscovite, namely those at 3.66 and 3.07 Å, would, if both were present (Velde, 1965, p. 440), be sufficient to establish the presence of the 1M form in a mixture of both 1M and $2M_1$ polymorphs.

The extremely detailed work carried out by Yoder and Eugster (1955, pp. 245 - 246), who studied the stability relations and polymorphs of synthetically-prepared muscovite with a chemical composition of $K\,Al_2\,(Si_3\,Al)\,O_{10}\,(OH)_2$, has often been used to predict the stability and behaviour of naturally-occurring muscovite polymorphs. From this study Yoder and Eugster found that at 15000 p.s.i. water pressure at temperatures below 200°C a metastable form designated as the 1Md polymorph made its appearance, and that as the temperature was increased, ordering of the structure occurred. The next phase to form was found to be the 1M polymorph, followed in turn by the $2M_1$ polymorph. Yoder and Eugster found that they could not reverse the sequence 1Md → 1M → $2M_1$. Yoder and Eugster (1955, pp. 246 & 254) and Smith and Yoder (1956, p. 223) accordingly accepted that an irreversible reaction of this type probably occurred during the progressive metamorphism that sediments might experience in nature.

Studies carried out by Weaver (1958, p. 856) have, however, indicated that a $2M_1$ 10 Å polymorph of muscovite will weather to a mineral with an expandable lattice and 1Md disordered structure. The original $2M_1$ structure may, however, be reconstituted by simply replacing the potassium lost during weathering.

Velde (1965, pp. 436 & 443) is of the opinion that the only stable mica polymorph in nature is the $2M_1$ form, but he conceded that at low and moderate temperatures the metastable 1Md and 1M polymorphs probably preceded its formation.

The claim made by Mackenzie and Milne (1953, p. 178) that dry grinding of muscovite would induce a transformation from the $2M_1$ polymorph to the 1M form has been repudiated by Yoder and Eugster (1955, p. 259),

so that this mechanism should not be invoked to explain polymorphic transformations in muscovite.

6.4.2.2. Sericite.

As was pointed out by Yoder and Eugster (1955, p. 255), the term "sericite" is a field term used to describe any fine-grained white mica. Consequently, it includes, but does not differentiate between, paragonite (the sodium-rich mica) and muscovite (the potassium-rich mica). Materials called sericite and having the general muscovite composition have been shown by Heinrich and Levinson (1955, p. 983) to exhibit the same polymorphs as muscovite. The major distinction that can be drawn between muscovite proper and the micas that may be described as sericite lies in the field of chemical composition. Since muscovite is included in the sericite micas, it is apparent that these micas are not necessarily chemically different from muscovite, but non-muscovite sericites often have high SiO_2, MgO and H_2O contents and low K_2O contents.

Heinrich and Levinson (1955, p. 983) have shown that the phengites (muscovites in which the Si:Al ratio exceeds 3:1, and in which an increase in Si is accompanied by substitution of Mg or Fe^{2+} for Al in octahedral sites) also exhibit the 1M, 2M and 3T polymorphs shown by muscovite, and may also be included under the general heading of sericites.

Since, therefore, the general term "sericite" gives no clear indication regarding the composition of the mineral or the polymorph present, the continued use of this term to describe the micas present in the auriferous conglomerates, shales and quartzites of the Witwatersrand System is to be deprecated.

6.4.2.3. Hydro(us)-muscovites.

Subdivision within the muscovites on the basis of differences in K_2O and H_2O contents and on the basis of the Si:Al ratio has resulted in the establishment of two rather ill-defined species, namely the hydro(us) muscovites and the illites. Although these two materials are sometimes considered to be synony-

mous with one another (Levinson, 1955, p. 48), this view is not shared by all workers in the field of clay mineralogy. Accordingly, for the sake of clarity, the hydro(us) muscovites and illites are here considered under separate headings.

Brown and Norrish (1952, pp. 929 - 931) have stated: "Hydrous micas differ from normal micas in that they contain less potassium and more water." The high water and low potassium content of the hydrous micas is thought to be due to the partial replacement of the interlayer K^+ ions by oxonium ions $(H_3O)^+$.

Heystek (1955, p. 338) is one of the workers in the field of clay mineralogy who believes that a distinction exists between hydromuscovite and illite. He classified material collected at the upper contact of Ongeluk Lava with Pretoria Series shale in Lynnwood Township as hydromuscovite in view of the similarity of its chemical analyses and X-ray diffraction values to those reported by Brammall, Leech and Bannister (1937, p. 516) for hydromuscovite from Ogofau, Wales, and then subjected this material to differential thermal analysis and in addition determined its ion exchange capacity. On comparing the data with those reported for Fithian illite by Grim, Bray and Bradley (1937, p. 823), Heystek found that the hydromuscovite had an apparently better degree of crystallinity, a higher K_2O content and lower H_2O content, and an ion exchange capacity (of 2.5 m.e./100 g dried material) that was considerably lower than the values of 20-40 m.e./100 g dried material usually reported for illites.

From his study of hydrothermally altered rocks in Japan, Kodama (1962, p. 89) concluded that the presence of the 1M and $2M_1$ polymorphs of hydromuscovite was dependent on their chemical composition. In general, those hydromuscovites with a $2M_1$ structure had a higher total alkali content than the 1M variety. Kodama further concluded that the development of a particular polymorph of muscovite might be influenced not only by the chemical potential of the water, but also by the amount of potasium in the environment.

6.4.2.4. Illites.

The term "illite", which was coined by Grim, Bray and Bradley in 1937 as a general term to describe a mica-like clay mineral from Illinois, has given rise to confusion ever since it was introduced. The confusion has, in fact, been such that the committee of the International Mineralogical Association, meeting in 1965, could reach no unanimity as to whether this material constituted a valid group separate from the micas or whether it ought to be included along with the interstratified minerals (Brindley, 1965, p. 30).

Deer, Howie and Zussman (1966, p. 260) define illites as clay minerals structurally related to micas, most of them being dioctahedral, like muscovite, but containing more silica and less potassium than muscovite proper. They add that most of the illites have fewer inter-layer cations than muscovite, so that forces between layers are weaker and there is considerably less regularity of stacking, and thus the most common polymorph for illites has a disordered one-layered monoclinic cell (1Md). Velde and Hower (1963, pp. 1239 & 1253), however, define an illite as a mineral found in sediments and having a primarily dioctahedral-type structure with less than 10 per cent of interlayered expandable layers. Yoder and Eugster (1955, p. 254) expressed the opinion that the use of the term "illite" should be restricted to the field. In addition, they felt that proof still had to be obtained that materials called illite were not in fact all mixed-layer structures.

X-ray diffractometer traces of material usually described as illite show a tailing or broadening of the 10 Å reflection towards the low angle side of the peak. Factors which could cause such a phenomenon are either strain within the lattice or extremely fine particle size. In the case of the potassium-depleted and silica-enriched muscovites (i.e., illite as defined by Deer, Howie and Zussman, 1966, p. 260) the regularity of stacking in the structure is far less than in the case of muscovite, as was mentioned above, and this irregularity of stacking could lead to X-ray line broadening.

Lapham and Jaron (1964, p. 276) concluded that line broadening in illite appeared to be primarily the result of structural strain within the mica, rather than the result of a decrease in grain size.

Possibly the best attempt to explain the actual structure of illite is that which was made by Gaudette, Grim and Metzger (1966, p. 1655). These authors, on the basis of cesium absorption experiments, concluded that the structure and X-ray behavior of illites could be visualized in terms of a "rind and core". The structure of illite was considered to consist of a structurally coherent silicate core which, although somewhat deficient in interlayer potassium ions, nevertheless still produced a 10 Å diffraction peak. This coherent core was then regarded as being surrounded by a more "incoherent" rind, which served as a locus for sorption and cation exchange, and was the area from which the physical properties for a particular 10 Å mineral were derived. The contact between core and rind was visualized as being gradational. The rind was considered to differ from the core

in containing even less potassium, possibly as a result of replacement by H_2O or other ions, and in having a slightly larger and somewhat irregular "c" dimension, but was regarded as possessing a skeletal framework reminiscent of the more coherent portion of the grain. A well-crystallized 10 Å material would have a greater core to rind ratio, with a consequent improvement in the diffraction characteristics and lower cation exchange capacity.

Levinson (1955, p. 49) has shown that although illite may occur as the 1Md, 2M and 3T polymorphs, these polymorphs do not appear to be related to any evident geological, environmental or chemical variations. He further mentioned that he had noted the presence of the 2M and 1Md polymorphs in illites from Fithian, Illinois, and that while the 3T and 1M polymorphs had been found only in non-sedimentary environments, specifically in decomposed granites, the 2M and 1Md polymorphs appeared to be restricted purely to sedimentary environments.

Heystek (1955, p. 341) examined a micaceous mineral from the clay at Gollel, Swaziland, by X-ray diffraction, chemical analysis and differential thermal analysis, and also determined the ion exchange capacity of the mica. He found that the X-ray diffraction data compared very well with those published for the Fithian illite by Grim, Bray and Bradley (1937, p. 823), and that the chemical composition, differential thermal analysis curve and ion exchange capacity (20.7 m.e./100 g of material dried at 110°C) of the Gollel mica were all consistent with the accepted values for illite obtained by other workers. A further check carried out by Heystek involved subjecting the mineral to mild thermal or chemical treatment. When this was done, the basal 10 Å reflection showed no significant change, supporting the classification of the Gollel clay mica mineral as an illite.

6.4.2.5. Properties of the muscovite minerals -- a summary.

The similarities and differences in the properties of muscovite, hydromuscovite and illite may be summarized as follows:

(1) Muscovite, hydromuscovite and illite all show the same polymorphs, namely the 1Md, 1M and $2M_1$ polymorphs.

(2) When the minerals are arranged according to their ion exchange capacity, the order is: illite > hydromuscovite > muscovite.

(3) When differential thermal analysis curves are compared, it is found that muscovite has a single endothermic peak at 900°C, whereas typical hydromuscovite shows a single endothermic peak at 720°C and illite has three endothermic peaks at 150°C, 560°C and 950°C and an exothermic peak at 990°C (Heystek, 1955, pp. 339-341).

(4) When the minerals are arranged according to their K_2O content, the order is: muscovite > hydromuscovite > illite.

(5) When the minerals are arranged according to their H_2O content, the order is: illite > hydromuscovite > muscovite.

(6) The degree of perfection of crystallinity may be judged from the X-ray diffraction patterns, with the more perfectly crystalline minerals having more sharply defined and more abundant X-ray diffraction peaks. When the minerals are arranged according to the perfection of their crystallinity judged from the X-ray diffraction patterns, the order is: muscovite > hydromuscovite > illite.

6.4.3. Experimental studies on muscovites, hydromuscovite and illite.

As was mentioned earlier, thin section studies on the present suite of samples from the Vaal Reef at Hartebeestfontein and Zandpan and from the Ventersdorp Contact Reef at Venterspost revealed the presence of muscovite occurring as interstitially dispersed acicular grains in the matrix of the auriferous conglomerate. In one sample from the Vaal Reef at Hartebeestfontein sufficient muscovite was present to permit its characterization by means of infra-red and X-ray diffraction techniques, although unfortunately this muscovite was not present in a suitable quantity or degree of purity to permit chemical analysis to be carried out on it. In view of the paucity of information regarding micas occurring in Witwatersrand horizons, however, it was decided that the Hartebeestfontein muscovite should be investigated in as much detail as possible. At the same time it was decided that several non-Witwatersrand micas should be subjected to the same analytical procedures for control purposes and in order to evaluate in practice the applicability of infra-red and X-ray diffraction techniques to the study of micas.

The non-Witwatersrand micas examined consisted of the following: muscovite from a pegmatite from Selati, Transvaal; muscovite from the Noumas pegmatite in Namqualand; hydromuscovite from the Lynnwood Township, Pretoria; and illite from Gollel, Swaziland. (The hydromuscovite and illite were portions of the samples originally analysed and characterized by Heystek in 1955.) The techniques used in the investigation were: X-ray diffraction analysis, infra-red spectroscopy and chemical analysis. The fine-grained nature of the micas and their overlapping optical properties precluded the use of optical techniques in the present study.

New chemical analyses are presented for the two muscovites derived from the two pegmatites, and the chemical analyses for illite and hydromuscovite

originally reported by Heystek in 1955 have been recalculated to allow for minor impurities which were not reported or allowed for by Heystek but which were detected when the samples were re-examined in the course of the present study. Similarly, the hydromuscovite and illite were reanalysed by means of X-ray diffraction and infra-red spectroscopy during the course of the present study, and the results of these revised analyses, not Heystek's original data, were used when making the comparison with the results obtained for the three muscovites.

6.4.3.1. X-ray diffraction studies on muscovites, hydromuscovite and illite.

The three muscovites, hydromuscovite and illite were examined by the X-ray diffraction method described in Part III of this thesis, and the lattice constants and indices were calculated and allocated using the computer programmes which are also listed in Part III.

The lattice constants obtained for the various micas are set out in Table XXVI, while the integrated intensities and interplanar spacings are listed in Tables XXVII and XXVIII. The X-ray results are discussed in Section 6.4.3.5.

TABLE XXVI

LATTICE CONSTANTS OF MUSCOVITES FROM HARTEBEESTFONTEIN, SELATI AND NOUMAS, HYDROMUSCOVITE FROM LYNNWOOD AND ILLITE FROM SWAZILAND

	HARTEBEEST.	SELATI	NOUMAS	LYNNWOOD	SWAZILAND
a Å	5.192 ± 0.002	5.198 ± 0.002	5.204 ± 0.002	5.192 ± 0.001	5.207 ± 0.002
b Å	9.019 ± 0.002	9.034 ± 0.002	9.049 ± 0.002	9.002 ± 0.002	9.005 ± 0.002
c Å	20.112 ± 0.006	20.077 ± 0.003	20.087 ± 0.002	20.077 ± 0.002	20.315 ± 0.008
β	$95^{\circ}45' \pm 3'$	$95^{\circ}46' \pm 2'$	$95^{\circ}46' \pm 2'$	$95^{\circ}46' \pm 3'$	$95^{\circ}53' \pm 3'$
vol.	936.9 Å^3	938.0 Å^3	941.1 Å^3	933.7 Å^3	947.5 Å^3
space group	C2/c	C2/c	C2/c	C2/c	C2/c
structure type	$2M_1$	$2M_1$	$2M_1$	$2M_1$	$2M_1$

6.4.3.2. Infra-red spectroscopy studies on muscovites, hydromuscovite and illite.

The analytical techniques adopted for the infra-red analyses carried out on the three muscovites, hydromuscovite and illite are described in detail in Part III of this thesis.

TABLE XXVII

X-RAY DIFFRACTION POWDER DATA FOR MUSCOVITE FROM HARTEBEESTFONTEIN, HYDROMUSCOVITE FROM LYNNWOOD AND ILLITE FROM SWAZILAND

HARTEBEESTFONTEIN						LYNNWOOD						SWAZILAND					
'd' Å observed	'd' Å calculated	I/I_1	h	k	l	'd' Å observed	'd' Å calculated	I/I_1	h	k	l	'd' Å observed	'd' Å calculated	I/I_1	h	k	l
10.040	9.995	100	0	0	2	10.040	9.995	100	0	0	2	10.040	10.111	100	0	0	2
4.995	4.998	24	0	0	4	5.112	5.108	28	0	0	4	5.035	4.992	20	0	0	4
4.458	4.453	23	1	1	-1	4.453	4.455	69	1	1	-1	4.480	4.489	31	1	1	0
4.103	4.107	8	0	2	2	4.392	4.388	5	0	2	1	3.897	3.899	5	1	1	-3
3.880	3.877	13	1	1	-3	3.814	3.814	23	1	1	-3	3.510	3.531	11	1	1	-4
3.734	3.732	14	0	2	3	3.726	3.729	27	0	2	3	3.005	3.007	1	0	2	5
3.490	3.490	19	1	1	-4	3.580	3.578	5	1	1	3	2.880	2.879	6	1	1	5
3.202	3.200	17	1	1	4	3.486	3.488	27	1	1	-4	2.601	2.603	1	2	0	-1
2.992	2.991	17	0	2	5	3.197	3.199	37	1	1	4	2.596	2.597	1	1	3	0
2.861	2.861	13	1	1	5	3.121	3.119	5	1	1	-5	2.590	2.590	1	2	0	0
2.791	2.793	11	1	1	-6	2.987	2.988	38	0	2	5	2.584	2.586	1	1	1	6
2.583	2.585	12	2	0	0	2.860	2.861	29	1	1	5	2.574	2.573	34	2	0	-2
2.559	2.558	22	1	3	1	2.855	2.854	29	0	0	7	2.447	2.449	1	2	0	2
2.499	2.499	7	0	0	8	2.788	2.791	17	1	1	-6	2.409	2.407	7	2	0	-4
1.9993	1.9999	14	1	3	6	2.584	2.583	5	2	0	0	2.384	2.383	1	1	3	3
1.9993	1.9993	14	0	0	10	2.556	2.557	63	1	3	1	2.009	2.009	1	0	2	9
1.4977	1.4975	14	0	6	1	2.499	2.498	12	0	0	8	2.009	2.007	1	1	3	6
1.4977	1.4984	14	3	3	-1	2.460	2.460	5	1	3	-3	1.6995	1.6998	1	1	5	-1
						2.393	2.393	5	2	0	-4	1.6995	1.6990	1	2	4	0
						2.277	2.276	5	2	0	-5	1.6851	1.6938	1	0	0	12
						2.237	2.237	5	0	4	1	1.6163	1.6163	1	2	0	9
						1.9981	1.9985	5	1	3	6	1.5029	1.5024	15	3	3	-1
						1.7293	1.7303	7	1	3	9	1.5005	1.5007	15	0	6	0
						1.6955	1.6955	8	3	1	-2						
						1.6502	1.6500	5	2	2	-9						
						1.5244	1.5242	8	1	3	-11						
						1.4968	1.4961	42	0	6	1						
						1.4945	1.4943	42	1	5	6						

TABLE XXVIII

X-RAY DIFFRACTION POWDER DATA FOR MUSCOVITE FROM SELATI AND NOUMAS

SELATI						NOUMAS					
'd' Å observed	'd' Å calculated	I/I_1	h	k	l	'd' Å observed	'd' Å calculated	I/I_1	h	k	l
9.995	9.990	100	0	0	2	10.016	9.983	100	0	0	2
4.987	4.994	21	0	0	4	4.997	4.991	18	0	0	4
4.480	4.489	27	1	1	0	4.494	4.488	38	1	1	0
4.308	4.300	8	1	1	1	3.498	3.493	29	1	1	-4
4.116	4.116	7	0	2	2	3.351	3.351	90	0	2	4
3.969	3.968	12	1	1	2	3.330	3.329	90	0	0	6
3.889	3.882	12	1	1	-3	3.125	3.125	10	1	1	-5
3.739	3.739	14	0	2	3	2.996	2.994	33	0	2	5
3.497	3.493	21	1	1	-4	2.795	2.793	20	1	1	-6
3.327	3.329	71	0	0	6	2.572	2.569	44	1	1	6
3.205	3.202	24	1	1	4	2.510	2.509	6	1	1	-7
3.126	3.123	24	1	1	-5	2.495	2.497	7	2	0	-3
2.993	2.993	23	0	2	5	2.468	2.468	8	1	3	-3
2.865	2.862	17	1	1	5	2.396	2.398	25	2	0	-4
2.793	2.793	13	1	1	-6	2.387	2.385	25	1	3	3
2.603	2.603	2	1	3	0	2.131	2.133	20	1	3	5
2.571	2.569	46	1	1	6	2.060	2.059	9	0	4	4
2.512	2.510	9	1	1	-7	1.9976	1.9968	23	0	0	10
2.496	2.497	9	2	0	-3	1.9754	1.9736	10	1	3	-7
2.465	2.466	6	1	3	-3	1.9509	1.9497	8	2	0	6
2.395	2.397	16	2	0	-4	1.7363	1.7365	9	1	1	-11
2.385	2.384	16	1	3	3	1.6628	1.6635	12	2	0	-10
2.258	2.259	2	0	4	0	1.6480	1.6483	19	1	3	9
2.151	2.149	8	2	0	-6	1.6330	1.6342	5	1	1	11
2.141	2.139	8	0	4	3	1.6060	1.6063	7	2	0	9
2.076	2.078	10	2	0	5	1.5625	1.5624	7	2	3	7
2.062	2.062	10	1	1	-9	1.5582	1.5581	7	3	1	4
1.9959	1.9908	22	0	0	10	1.5582	1.5578	7	2	4	-6
1.9737	1.9730	6	1	3	-7	1.5251	1.5258	12	1	3	-11
1.7329	1.7325	5	1	3	-9	1.5065	1.5069	29	0	6	0
1.6645	1.6645	2	0	0	12	1.5065	1.5060	5	2	4	-7
1.6488	1.6479	2	1	2	-11	1.4539	1.4543	5	0	2	13
1.6039	1.6038	6	2	4	-5	1.3535	1.3531	5	1	3	-13
1.5258	1.5260	4	1	3	-11	1.2823	1.2829	5	2	6	2
1.5056	1.5059	4	0	6	0	1.2767	1.2767	5	1	5	10
1.5051	1.5055	22	2	4	-7	1.2088	1.2089	5	3	0	-13
1.3399	1.3400	2	0	4	12						
1.3057	1.3060	2	2	0	-14						
1.3042	1.3044	2	3	1	-11						
1.2913	1.2915	2	2	2	-13						

The results obtained when the five micas were analysed by infra-red spectroscopy are set out in Table XXIX, and discussed in Section 6.4.3.5.

TABLE XXIX

INFRA-RED VIBRATION FREQUENCIES AND BOND ASSIGNMENTS FOR MUSCOVITES FROM HARTEBEESTFONTEIN, SELATI & NOUMAS, HYDROMUSCOVITE FROM LYNNWOOD AND ILLITE FROM SWAZILAND

HARTEBEEST		SELATI		NOUMAS		LYNNWOOD		SWAZILAND	
ν cm^{-1}	bond	ν cm^{-1}	bond	ν cm^{-1}	bond	ν cm^{-1}	bond	ν cm^{-1}	bond
						3667	O-H		
						3662	O-H		
3644	O-H					3638	O-H		
3625	O-H stretch	3618	O-H stretch	3621	O-H stretch	3621	O-H stretch	3621	O-H stretch
3425	H-O-H	3420	H-O-H	3420	H-O-H	3427	H-O-H	3420	H-O-H
1619	H-O-H	1621	H-O-H	1620	H-O-H	1625	H-O-H	1618	H-O-H
								1412	?
						1115	Si-O-Si	1115	Si-O-Si
1060	Si-O	1060	Si-O	1065	Si-O			1085	Si-O
1020	Si-O	1030	Si-O	1020	Si-O	1020	Si-O	1025	Si-O
990	Si-O	985	Si-O	980	Si-O				
940	O-H--Al	925	O-H--Al	925	O-H--Al	940	O-H--Al	920	O-H--Al
827	Si-O	821	Si-O	821	Si-O	826	Si-O	820	Si-O
794	O-H libration	790	O-H libration	795	O-H libration	797	O-H libration	788	O-H libration
751	Si-O-Al	742	Si-O-Al	741	Si-O-Al	748	Si-O-Al	742	Si-O-Al
690	O-H	683	O-H	680	O-H	690	O-H	680	O-H
530	Si-O-Al^{VI}	520	Si-O-Al^{VI}	523	Si-O-Al^{VI}	528	Si-O-Al^{VI}	520	Si-O-Al^{VI}
470	Si-O	468	Si-O	468	Si-O	473	Si-O	465	Si-O

The infra-red spectrum obtained for the muscovite from Selati is shown in Figure 14 (see Section 6.3.2.5).

6.4.3.3. Chemical analyses of muscovites, hydromuscovite and illite.

As has been mentioned earlier, the muscovite in the Vaal Reef at Hartebeestfontein was unfortunately not present in a suitable quantity or degree of purity to permit chemical analyses to be carried out on it. Chemical analyses

were, however, carried out on the two muscovites obtained from pegmatites from Selati and Noumas. The results of these analyses are set out in Table XXX, which also shows the chemical compositions of hydromuscovite and illite. In the case of these last two minerals, the compositions listed are based on chemical analyses originally carried out by Heystek (1955, pp. 338 & 341) but recalculated to allow for previously unreported impurities that were detected by X-ray diffraction analysis during the course of the present study. The results of all these chemical analyses are discussed, in relation to the results obtained by X-ray diffraction analysis and infra-red spectroscopy, in Section 6.4.3.5.

TABLE XXX

CHEMICAL ANALYSES OF TWO MUSCOVITES FROM SELATI AND NOUMAS, HYDROMUSCOVITE FROM LYNNWOOD AND ILLITE FROM SWAZILAND

	SELATI	NOUMAS	LYNNWOOD*	SWAZILAND**
	per cent	per cent	per cent	per cent
SiO_2	47.96	44.63	42.80	50.60
Al_2O_3	31.45	37.25	38.70	33.70
Fe_2O_3	2.76	0.25	1.04	1.24
FeO	N.D.	1.01	N.D.	N.D.
TiO_2	0.26	0.12	1.63	0.89
CaO	0.02	0.02	0.33	0.18
MgO	1.05	0.02	0.67	N.D.
K_2O	10.14	9.60	8.76	5.63
Na_2O	1.14	0.63	1.26	0.19
Li_2O	0.22	0.36	N.D.	N.D.
P_2O_5	0.03	N.D.	N.D.	N.D.
MnO	0.11	0.18	N.D.	N.D.
H_2O	4.27	5.13	5.17	7.95
F	0.57	N.D.	N.D.	N.D.
Total	99.98	99.20	100.36	100.38

N.D. = not determined.

* = recalculated to allow for presence of 3% pyrophyllite and 5% quartz.

** = recalculated to allow for presence of 5% quartz.

6.4.3.4. Structural formulae for two muscovites, hydromuscovite and illite.

The structural formulae for the two muscovites from Selati and Noumas, for the hydromuscovite from Lynnwood and for the illite from Swaziland were calculated from the chemical analyses of these minerals in accordance with the method outlined by Deer, Howie and Zussman (1966, pp. 515 - 518). These calculations were based on the assumption that O = 20 and (OH + F) = 4.

TABLE XXXI

STRUCTURAL FORMULAE FOR TWO MUSCOVITES, HYDROMUSCOVITE AND ILLITE

1. Muscovite, Selati (pegmatite), Transvaal:

$(K_{1.62}Na_{0.29}Li_{0.12})(Al_{3.28}Fe^{3+}_{0.28}Ti_{0.03}Mg_{0.21}Mn_{0.01})(Al_{1.64}Si_{6.36})O_{20}(OH, F)_4$

2. Muscovite, Noumas (pegmatite), Namaqualand:

$(K_{1.61}Na_{0.16}Li_{0.19})(Al_{3.61}Fe^{3+}_{0.25}Fe^{2+}_{0.14}Ti_{0.01}Mn_{0.02})(Al_{2.15}Si_{5.85})O_{20}(OH, F)_4$

3. Hydromuscovite, Lynnwood (shale), Pretoria:

$(K_{1.48}Na_{0.32}Ca_{0.05})(Al_{2.22}Fe^{3+}_{0.10}Ti_{0.02}Mg_{0.13})(Al_{2.32}Si_{5.68})O_{20}(OH, F)_4$

4. Illite, Gollel (clay), Swaziland:

$(K_{0.89}Na_{0.05}Ca_{0.02})(Al_{1.94}Fe^{3+}_{0.12}Ti_{0.08})(Al_{1.74}Si_{6.26})O_{20}(OH, F)_4$

6.4.3.5. Discussion of results.

6.4.3.5.1. X-ray diffraction.

Examination of Tables XXVI, XXVII and XXVIII, in which the lattice parameters and X-ray data for the three muscovites, hydromuscovite and illite are set out, permits the drawing of the following conclusions:

(1) No linear relationship appears to exist between either the a_o or b_o dimensions of the micas examined and their K_2O content (or, in fact, their total alkali content).

(2) Comparison of Tables XXVII and XXVIII (Section 6.4.3.1), in which the interplanar spacings of the five micas are listed, with Table XXV (Section 6.4.2.1), which shows the characteristic interplanar spacings by which muscovite polymorphs may be recognized, indicates that all the muscovites, the hydromuscovite and the illite examined in the course of the present study could be satisfactorily indexed as having the $2M_1$ structure. In view of the absence of

the 3.66 and 3.07 Å diffraction peaks from the diffraction traces of the five micas examined, there is no possibility that any 1M polymorph was present in these micas.

(3) For all five micas, the X-ray reflections could be satisfactorily indexed using the C2/c space group, to which muscovite has commonly been assigned in the past (Radoslovich, 1960, p. 919).

(4) The volumes of the unit cells of the five micas (listed in Table XXVI, Section 6.4.3.1) could not be related to the chemical compositions of these micas.

(5) The β angle value obtained for the illite from Gollel was slightly higher than that for the muscovites or the hydromuscovite. This is consistent with a greater degree of structural disordering in the lattice of this mica than in the lattices of the other micas.

(6) The X-ray diffraction powder data listed in Tables XXVII and XXVIII reveals that the pegmatitic micas yielded the most diffraction peaks, followed in turn by the hydromuscovite and the illite. The apparently small number of peaks recorded for the muscovite from Hartebeestfontein is a consequence of its low degree of purity (i.e., contamination by minerals such as quartz), which resulted in peaks being present which were coincident with the muscovite peaks. From the original X-ray diffraction traces, it could be seen that the three muscovites yielded sharp well-formed symmetrical peaks, whereas those of the hydromuscovite and illite were less symmetrical. This falling-off in sharpness and symmetry of the peaks is a consequence of smaller particle size and greater structural disorder in the hydromuscovite and illite. Thus the findings of the present study confirm the observations made by Heystek (1955, p. 341): "When comparing the d-values of the illite with those of hydromuscovite, it is quite noticeable that the hkl reflections of the former are weak or absent as a result of its poorer crystallinity. In turn, this hydromuscovite has a lower perfection of crystallinity than a muscovite mica."

6.4.3.5.2. Infra-red spectroscopy.

Examination of the data shown in Table XXIX (Section 6.4.3.2) permits the following deductions to be made concerning the infra-red behaviour of the micas:

(1) Despite the wide differences in the Al_2O_3 and SiO_2 contents of the micas which were revealed by chemical analysis (Table XXX) and reflected in the structural formulae (Table XXXI), there was no evidence of any linear relationship

between the position of the O-H--Al or Si-O-Al^{VI} absorption bands of the micas and their Al_2O_3 or SiO_2 contents. Thus, it would not be possible to make use of differences in the infra-red vibration frequencies of these bonds to differentiate between muscovite, illite and hydromuscovite.

(2) The three muscovites, the hydromuscovite and the illite were indexed as having the $2M_1$ structure on the basis of their interplanar spacings as determined by X-ray diffraction analysis (see Section 6.4.3.5.1). The infra-red spectra of these minerals showed only a single absorption band located between 827 and 820 cm^{-1}, with no suggestion of any band located at 804 cm^{-1}. This is in agreement with the published spectra for 2M muscovite presented by Stubican and Roy (1961, p. 48), but directly contradicts the data presented by Oinuma and Hayashi (1965, p. 1219), who stated that 2M type illite showed doublets at 804 cm^{-1} and 824 cm^{-1}, while the 1M type illite had only one broad absorption band at 822 cm^{-1}.

In addition, the spectra published by Stubican and Roy (1961, p. 48) for 3T and 1M polymorphs show the existence of two absorption bands in the spectral region 850 - 800 cm^{-1}, which again directly contradicts the data of Oinuma and Hayashi (1965, p. 1218).

(3) In Saksena's view (1964, p. 1725), the occurrence in muscovite of infra-red vibration frequencies located at 3667, 3662 and 3638 cm^{-1} indicates lack of perfect crystallinity within the lattice, or some distortion within the structure. It is interesting to note that these vibration frequencies were <u>not</u> found in the infra-red spectrum of the illite examined in the present study, although, on the basis of the X-ray diffraction results, the illite has been regarded as being the most poorly crystalline of the five micas examined, but that these vibration frequencies <u>were</u> present in the infra-red spectrum of the hydromuscovite from Lynnwood.

6.4.3.5.3. Chemical composition of the micas.

The results of the chemical analyses of the muscovites from Selati and Noumas and of the hydromuscovite from Lynnwood and the illite from Swaziland have been listed in Table XXX (Section 6.4.3.3). Inspection of this table permits the following observations to be made:

(1) As one progresses from muscovite through to hydromuscovite and illite the decrease in K_2O content, or even in (K_2O + Na_2O + Li_2O) content, is quite apparent.

(2) In the case of the illite, the significantly lower K_2O content is counter-balanced by a significantly higher H_2O content. The H_2O is probably

present as H_3O^+ ions in the manner suggested by Brown and Norrish (1952, pp. 929 - 931).

6.4.3.5.4. The usefulness and limitations of X-ray diffraction analysis and infra-red spectroscopy in the study of the micas.

On comparing the results obtained for the micas examined by means of X-ray diffraction analysis, infra-red spectroscopy and chemical analysis, the following conclusions were reached:

(1) X-ray diffraction analysis was found to be a far more sensitive tool than infra-red spectroscopy for the identification of polymorphs of muscovite. The results of the present study indicated, however, that infra-red analysis may assist in determining the type of polymorph present (in conjunction with X-ray diffraction analysis) if the infra-red spectra obtained are compared with the spectra for muscovite polymorphs published by Stubican and Roy (1961, p. 48), which were found to be preferable for use as standards to the data published by Oinuma and Hayashi (1965, p. 1219). On this basis, the presence of a single infra-red absorption band located between 800 and 827 cm^{-1} is diagnostic of the presence of only the $2M_1$ polymorph, while if <u>two</u> absorption bands are found to occur between 800 and 827 cm^{-1} it is likely that 1M or 3T polymorphs are present. It is apparent, however, that infra-red spectroscopy <u>alone</u> would not be suited to the identification of mixtures consisting of either 1M and 2M, or 2M and 3T, polymorphs, as the absorption spectra are coincident and only the 1M and 3T polymorphs would be recognized while the presence of the 2M polymorph would be concealed.

(2) The results of the present study indicate that infra-red spectroscopy cannot differentiate between muscovite, hydromuscovite and illite, and furthermore, in the case of muscovite, hydromuscovite and illite, infra-red spectroscopy cannot be used to predict chemical composition.

(3) It was found that the chemical composition of the micas studied could not be predicted directly from measurements of the lattice constants of the micas.

6.4.3.6. The nature of the mica present in samples from the Vaal Reef at Hartebeestfontein and Zandpan and from the Ventersdorp Contact Reef at Venterspost.

Summarizing the results of the characterization of the mica found in a sample from the Vaal Reef at Hartebeestfontein, it may be concluded that this mica was a $2M_1$ polymorph of muscovite belonging to the C2/c space group and having the following lattice dimensions:

a_o = 5.192 ± 0.002 Å

b_o = 9.019 ± 0.002 Å

c_o = 20.112 ± 0.006 Å

β = 95° 45' ± 3'

Volume = 936.9 Å^3

Apart from this sample from the Vaal Reef at Hartebeestfontein where mica was present in sufficient quantity to permit it to be characterized, mica was detected as being present in the majority of the 142 other samples (from the Vaal Reef at Hartebeestfontein and Zandpan and from the Ventersdorp Contact Reef at Venterspost) that were examined quantitatively in the course of the present study. Unfortunately, however, the average mica content in these samples was only about 5%, which was too low to permit detailed structural analyses to be carried out. Although the micas in these samples could thus not be identified with certainty, examination of all the X-ray spectra revealed no evidence of the presence of 1M polymorphs (as judged by the fact that the 3.66 and 3.07 Å peaks were absent from all the spectra), and accordingly the micas in these samples could tentatively be classified as $2M_1$ polymorphs. Since they showed the same X-ray diffraction patterns as were shown by the characterized muscovite from Hartebeestfontein, it seems likely that the micas in these samples were also $2M_1$ polymorphs of muscovite.

Weaver (1956, p. 159) has postulated that the great majority of clay minerals in sedimentary rocks are detrital in origin, and that they reflect the character of their source material and are only slightly modified in their depositional environments. If Weaver's suppositions are in fact correct, then, in theory at least, it should be possible to trace the source and depositional history of the muscovite present in the Witwatersrand conglomerates and sediments. In the case of the present suite of samples, however, no such deductions can be made, in view of the fact that no evidence could be found that any muscovite polymorph other than the $2M_1$ polymorph was present in these samples. This makes it impossible to decide whether this muscovite originated in the $2M_1$ form or whether it was introduced as a 1M variety and subsequently modified to the $2M_1$ variety in situ.

PART III

ANALYTICAL TECHNIQUES AND COMPUTER PROGRAMMES.

7. PREPARATION OF SAMPLES FOR QUANTITATIVE ANALYSIS.

7.1. Introduction.

Part I of this thesis describes an investigation into the relationship between the occurrence of gold, uranium and other minerals in certain Witwatersrand horizons. This investigation required that quantitative analyses for 14 components should be carried out on samples collected from Witwatersrand conglomerate beds. The manner in which 21 bulk samples obtained from the Vaal Reef at Hartebeestfontein and Zandpan and from the Ventersdorp Contact Reef at Venterspost were subdivided into smaller samples for analysis has been described in Section 2.2 and illustrated in Figures 4, 5 and 6. The number of analytical samples resulting from the subdivision was as follows:

The 5 bulk samples from the Vaal Reef at Hartebeestfontein were subdivided into 43 samples for analysis.

The 8 bulk samples from the Vaal Reef at Zandpan were subdivided into 44 samples for analysis.

The 8 bulk samples from the Ventersdorp Contact Reef at Venterspost were subdivided into 56 samples for analysis.

Thus, subdivision of the twenty-one original bulk samples resulted in the production of 143 analytical samples, each of which was analysed quantitatively for 14 components by means of the chemical, atomic absorption, X-ray fluorescence and X-ray diffraction techniques described in Section 8 of this thesis.

7.2. Sample Preparation.

In any investigation that involves the analysis of a relatively large number of samples by a number of different analytical techniques, sample preparation should be rigidly standardized and sample handling should be reduced to a minimum to prevent sample contamination. In the case of the present study, it was desirable that, after comminution, the particle size distribution of each of the 143 samples should be such that it would be suitable for <u>all</u> the analytical techniques involved (i.e., chemical, atomic absorption, X-ray fluorescence and X-ray diffraction techniques) without further comminution or handling being necessary. The particle size distributions required for X-ray fluorescence and X-ray diffraction analysis are more fully discussed in Sections 8.4 and 8.5, but, in brief, both these techniques require that the median grain size (at the 50% probability level) should be of the order of 15-20 microns. Accordingly, in order to ensure that the median grain size of the 143 samples would conform to these requirements, grinding tests were carried out in the following manner:

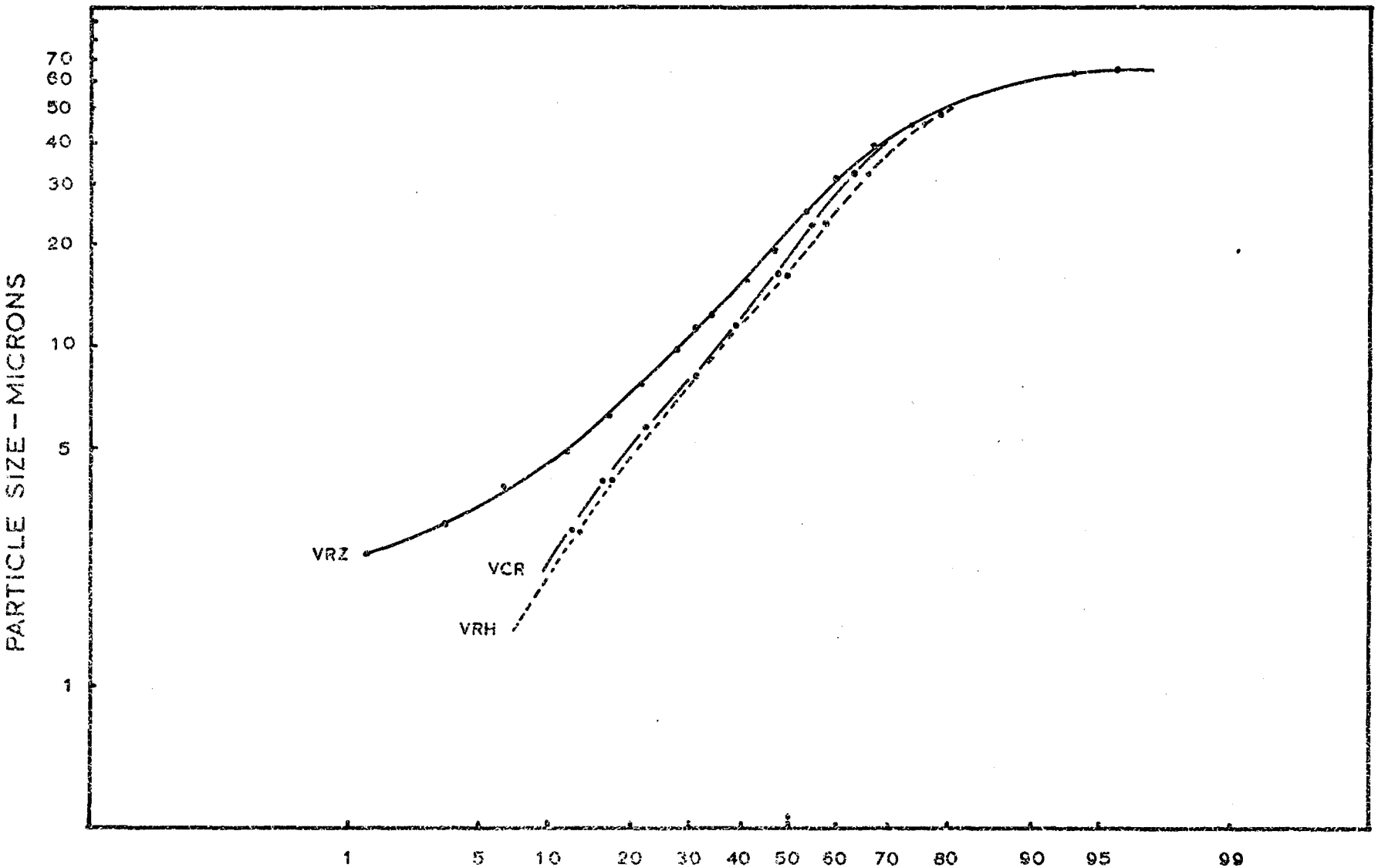


FIGURE 15 CUMULATIVE WEIGHT - PERCENT PROBABILITY

Three composite samples (one from each of the three mines involved) were prepared from fragments of either Vaal Reef or Ventersdorp Contact Reef ore and were crushed to less than $\frac{1}{2}$ inch mesh size. From each of these composites, nine 100-gram portions were successively weighed into a Siebtechnik grinder and ground for periods ranging from 10 to 120 seconds. The median grain sizes of these portions were then determined by sieving through a set of standard Tyler mesh sieves, while the finer powders were infra-sized by means of a Sartorius sedimentation balance.

The results of these grinding tests are shown in Figure 15. It was found that a grinding time of 90 seconds in the Siebtechnik grinder produced samples whose median grain sizes lay between 16 and 22 microns, and accordingly a grinding time of 90 seconds was adopted for all of the 143 rock samples that were to be analysed.

Repeated treatment of each sample with a bar magnet was found to be sufficient to remove all "tramp iron" formed in the samples as a result of the grinding process.

8. ANALYTICAL TECHNIQUES USED IN THE PRESENT STUDY.

8.1. Introduction.

The main analytical techniques used in the course of the present study were : chemical analysis, atomic absorption spectrophotometry, X-ray fluorescence, X-ray diffraction and infra-red spectroscopy.

In subsequent paragraphs some of the uses and limitations of these techniques are reviewed and the reasons underlying the choice of certain specific techniques are discussed. Where it was found necessary, for the purposes of the present study, to develop new techniques or to modify existing techniques, the procedure finally adopted is described in detail.

8.2. Chemical Analysis.

Chemical analyses were used to determine the chemical composition of the phyllosilicates investigated (see Part II of this thesis) and to determine the concentration of uranium in the 143 Witwatersrand samples that were analysed quantitatively (see Part I). Conventional methods involving the dissolution and spectrophotometric determination of uranium were chosen in preference to radiometric methods of determination of uranium in the interests of speed and accuracy.

8.3. Atomic Absorption Spectrophotometry.

Conventional fire assay methods for the determination of gold and silver could not be used in the present study because they called for more sample (30 grams, equal to 1 assay ton) than was generally available. Instead, an atomic absorption method developed by Oliver and others (1968) at the National Institute for Metallurgy was used for the quantitative determination of Au and Ag in the 143 Witwatersrand samples, since this method required only 2.5 grams of sample.

As has been pointed out by Beevers (1967, p. 428), who used a method similar to the one adopted in the present study, atomic absorption spectrophotometry offers a rapid means of analysis whose results compare well with those obtained by conventional fire assay methods.

8.4. Quantitative X-ray Fluorescence Analysis.

In the present study, the whole rock pressed briquette method of X-ray fluorescence analysis was used for the quantitative determination of Fe, K, Ni, Ti, Zr and Cr in the 143 samples from the Vaal Reef at Zandpan and Hartebeestfontein and from the Ventersdorp Contact Reef at Venterspost.

8.4.1. Sample preparation for X-ray fluorescence analysis.

As was mentioned in Section 7.2, the grinding technique that had been adopted for all the samples gave rise to a median grain size of 16 to 22 microns when it was tested on the composite samples prepared from Venterspost, Hartebeestfontein and Zandpan. This is much smaller than the 400 mesh Tyler screen size (30 microns) generally used in X-ray fluorescence analysis (Volborth, 1963, pp. 7-8), and is therefore quite suitable for powdered whole rock analysis.

Volborth (1965, p. 1) has pointed out that one of the most difficult problems associated with the analysis of rocks, minerals and ores is the detection of impurities introduced by grinding, irrespective of the manner of comminution used. In the present investigation all the samples were treated identically in an attempt to ensure that any impurities that might be introduced during the grinding processes would be more or less constant for all samples.

8.4.1.1. Reasons for choice of pressed powder briquette technique for X-ray fluorescence analysis.

Matrix effects, especially effects resulting from variations in particle size, can cause major problems when powdered materials are analysed by means of X-ray fluorescence. The only certain way in which particle size effects can be eliminated completely is by the use of a solution or fusion method. The use of a fusion method may introduce other problems, however, since the fusion method dilutes the sample, thereby lowering the concentration of the elements in the analytical sample, and, in addition, fusion may result in the loss of some of the more volatile elements, such as potassium. Since particle size effects may, at least, be minimized by high-pressure pelleting at 30 tons per sq. inch (Baines, 1966, pp. 118-120), it was decided to adopt this latter "pressed powder" method in the present study in preference to the fusion method.

8.4.1.2. Preparation of pressed powder briquettes.

Four grams of the ground sample were transferred to an agate mortar, to which 6 drops of a 3 per cent weight-for-volume solution of Mowiol (water-soluble plastic) in deionized water were added. The sample was then thoroughly blended with the Mowiol solution. The Mowiol was added to prevent shearing when the pellet was pressed in a hydraulic press to a pressure of 30 tons per sq. inch for 60 seconds. The backing material used to hold the pressed disc was one made of an intimate mixture of equal weights of Bakelite powder and boric acid that had

previously been blended for 60 seconds in a Siebtechnik mill.

8.4.2. Matrix effects.

In quantitative X-ray fluorescence spectrometry, any mixture may be regarded as consisting of two components, i.e., the element being analysed for and the remainder of the elements, referred to as the "matrix".

The accuracy of the X-ray fluorescence method of analysis of rocks (or any other material) depends on the precision and the reliability with which the intensities of the different characteristic X-ray radiations in the spectrometer can be measured, and on how accurately these measurements can be related to the concentrations of the different elements present. There are three principal causes of error in X-ray fluorescence analysis:

(1) Instability in the spectrograph and its ancillary equipment, including drift and fluctuations. This factor may be reduced to an insignificant level by operating the spectrograph under optimum conditions and by comparing each unknown against a control standard.

(2) Heterogeneity within the sample, caused by segregation of certain components in the matrix, and by surface effects such as particle size variations. In the present study, the effects resulting from heterogeneity have been minimized as far as possible by fine grinding (see Section 8.4.1) followed by the pressing of the powders into briquettes under high pressure, as recommended by Baines (1966, pp. 118-120)(see Section 8.4.1.1).

(3) Absorption and enhancement effects related to the chemical nature of the sample. According to Reynolds (1963, p. 1133), the effects of enhancement may usually be disregarded in the analysis of trace elements (elements present below the 1 per cent level), and in any case these corrections are negligible, difficult to make and generally ignored in practice. The effects of absorption on the emitted radiation are, however, very important and cannot be overlooked. Accurate analyses are not possible unless some correction is made for variations in the mass absorption coefficients of the samples.

8.4.2.1. Mass absorption coefficient.

If the matrix is constant in composition, then a linear relation is found to hold between the concentration of a given trace element (ppm Z) and the intensity of the radiation (I_{ZK_α}) from a member of the characteristic spectrum of that element. For very thick specimens (such as were used in the present study) the relation may be expressed as follows (Reynolds, 1963, p. 1133):

$$\text{ppm Z} = \frac{\mu^*_\lambda}{k} \cdot I_{ZK_\alpha} \quad \text{Equation 1}$$

In the above equation the value of k is determined by (1) the efficiency and design of the spectrometer, and (2) the basic relations that govern the generation of the particular spectral line involved (ZK_α). The value of k is constant for all measurements made with the same spectrometer, provided it is perfectly adjusted. The factor μ^*_λ is termed the mass absorption coefficient at wavelength λ and is a simple function of the composition of the sample and the radiation utilized in the analysis (ZK_α).

In the suite of samples examined in the present study, the composition of the matrix was not constant but varied between wide limits. In view of the fact that, in silicate rocks, for any particular wavelength shorter than Co K_α, the mass absorption coefficients can differ by approximately a factor of two as the matrix composition changes, it was apparent that the mass absorption coefficient of each sample would have to be determined accurately before it would be possible to carry out meaningful quantitative X-ray fluorescence analyses on these samples.

There are four possible ways of arriving at a correction for variations in the mass absorption of the sample:

(1) The background intensity of the matrix is inversely proportional to the mass absorption coefficient, and may give an indication of the latter. The intensity of the background is, however, not entirely independent of the wavelength used, and hence this method should possibly only be applied to the analysis of the heavier elements.

(2) If the major element composition of the sample is known fairly accurately, then the mass absorption coefficient of the sample can be calculated according to the formula:

$$\mu^*_{\text{sample}} = W_A \cdot \mu^*_A + W_B \cdot \mu^*_B + \ldots\ldots\ldots + W_N \cdot \mu^*_N \quad \text{Equation 2}$$

where W_A = weight fraction of element A (and $W_A + W_B + \ldots\ldots + W_N = 1$)

and μ^*_A = mass absorption coefficient of element A at the wavelength under consideration.

This method has two inherent disadvantages: firstly, the major element composition of the sample must be known fairly accurately, and secondly, the accuracy of the answer is dependent on, and limited by, the accuracy of published values for the mass absorption coefficients of the elements concerned.

(3) The method advocated by Reynolds (1963, p. 1136) may be used. This method utilizes the fact that the intensity of the Compton scattered portion of

the characteristic radiation from an X-ray tube is inversely and closely related to the mass absorption coefficient of the sample. Here again, however, the method has some limitations. The range of elements that can be studied is limited in the long wave direction by the absorption edge of iron, while the short wave limit is controlled by the capability of the equipment to excite and measure the K_α spectra of the heavier elements (Reynolds, 1963, p. 1142).

(4) Direct measurement of the mass absorption coefficient of a sample is probably the best method of arriving at a correction for variations in the absorption of the sample. This procedure offers the added advantage that, when a portion of the sample has also had to be analysed by means of X-ray diffraction, the mass absorption coefficient results obtained by direct measurement by means of X-ray fluorescence may, if certain precautions are observed, also be used to correct for the matrix effects encountered in X-ray diffraction (see Section 8.5.5.3).

8.4.2.2. Development of a method for the determination of the mass absorption coefficient of a sample by direct measurement.

A technique devised by Norrish and Taylor (1962, p. 101) was used as the basis for the method of mass absorption measurement employed in the present study. In outline, the method involves positioning a pressed disc of the material whose mass absorption is to be measured in front of the detector (scintillation counter) and measuring the incident radiation that falls onto the detector with and without the pressed disc in position. The mass absorption coefficient of the sample can then be calculated from the following equation (equation 3), which is based on the elementary absorption theory that all X-rays are absorbed to some extent in passing through matter.

$$\mu^* = \frac{1}{\rho x} \cdot \ln \frac{I_o}{I} \quad \text{Equation 3}$$

(rewritten from Baines, 1966, p. 118)

where ρx is the mass per cm^2 of the sample (x being the sample thickness and ρ the sample density)

μ^* is the mass absorption coefficient

I_o is the intensity of the incident radiation

I is the attenuated intensity of the transmitted radiation after having passed through the sample

$\ln N$ is $2.303 \log_{10} N$

When measuring mass absorption coefficients, the spectrometer is set up to give high intensity radiation (I_o) at the desired wavelength, normally the wavelength of the analytical line of the element that is being analysed for. If, for example, Fe radiation is required, then a disc of pure iron with the spectrometer adjusted to the setting for Fe K_α would be a suitable source. In fact, since iron is the heaviest major element encountered in most rocks, a single measurement of the mass absorption coefficient at the wavelength of Fe K_α could be made, since this would be satisfactory for the determination of all elements on the short wavelength side of the iron absorption edge, i.e., nickel and those elements above nickel in the periodic table. In this wavelength region, the ratio $\frac{\mu * \text{unknown}}{\mu * \text{standard}}$ remains constant (Reynolds, 1967, p. 1499).

In the present investigation, since it was not practical to determine the mass absorption coefficients at the wavelengths of each of the analytical lines used (since six elements, Fe, K, Ni, Ti, Zr and Cr, were being analysed for), a compromise had to be adopted, and it was decided that the mass absorption coefficients of all the samples should be measured at the wavelength of Cu K_α. Copper radiation (Cu K_α) was chosen in preference to iron radiation (Fe K_α) because X-ray diffraction analyses using copper radiation had been carried out on the same 143 samples as were being investigated by X-ray fluorescence, and only if the mass absorption coefficients were measured at the wavelength of Cu K_α would it be possible to apply these matrix absorption corrections directly to the X-ray diffraction analyses as well as to the X-ray fluorescence analyses. Leroux, Lennox and Kay (1953, p. 741) and Reynolds (1967, p. 1499) have shown that even when the mass absorption coefficients of substances have been determined at wavelengths different from those of the analytical lines in question, the ratio between the values obtained at the wavelength of the analytical line and the values obtained at another wavelength remains a constant. Hence, although the absolute values of the quantitative results obtained in the present study for elements of lower atomic number than copper may possibly be subject to minor error, this will in no way invalidate the results when correlations and comparisons are made between samples.

In the present study, it was found to be impossible to press discs for mass absorption coefficient measurements that would be selfsupporting without the addition of some binding material, even when pressures of 60 tons per sq. inch were used. The binding material selected was powdered cellulose, which was added to the sample in the proportion of 0.0600 grams of cellulose to 0.1400 grams of sample. This was thoroughly mixed in an agate mortar and pressed in

a die at 60 tons per sq. inch to yield self-supporting discs suitable for measurement. All discs were reweighed to 4 significant places of decimals after the intensity measurements had been carried out. All measurements were made on duplicate pellets, and the average value obtained for the mass absorption coefficient was used in making matrix corrections.

The addition of any diluent with a low absorption (such as cellulose) does, however, mean that the measured absorption coefficient must be corrected for the amount of diluent added. The following experiment was carried out in order to determine the amount of correction that would be necessary to compensate for the binding material:

Mass absorption coefficients were measured on five discs consisting of pure cellulose, five discs consisting only of finely powdered Brazilian quartz (with a median grain size of 15.4 microns) and five discs consisting of a mixture of 0.1400 grams of quartz and 0.0600 grams of cellulose. The values obtained were as follows:

cellulose	$\mu^* = 7.36$
quartz	$\mu^* = 35.01$
cellulose-quartz mixture	$\mu^* = 26.31$

On calculating the mass absorption coefficient for the cellulose-quartz mixture with the aid of Equation 2 (using the measured absorption coefficients for pure cellulose and pure quartz and the weight fractions of each component present in the mixture) a value of 26.72 was obtained. When this calculated mass absorption coefficient was compared with the measured mass absorption coefficient of the mixture (26.31), the absolute error was found to be only 1.52 per cent.

From the results of this experiment, it was calculated that the correction factor that would have to be applied to all measured mass absorption coefficients to compensate for the presence of the cellulose binder would be 26.31/35.01, or 0.751. In order to check on the constancy and applicability of this observation, two samples whose mass absorption coefficients were expected to be vastly different (in view of differences in pyrite content observed in the original ore) were chosen from the suite of 143 samples awaiting analysis, and their mass absorption coefficients were measured with and without binder. The results were as follows:

Sample 473

Without cellulose binder	$\mu^* = 37.86$
With binder	$\mu^* = 28.39$
Factor (28.39/37.86)	$= 0.750$

Sample 476

Without cellulose binder	μ^*	= 62.57
With binder	μ^*	= 47.00
Factor (47.00/62.57)		= 0.751

Other considerations that had to be borne in mind when determining the mass absorption coefficient were:

(1) Grain size. According to von Engelhardt (1955, p. 437), the maximum grain size of the particles should not exceed that which can be calculated from the equation:

$$d_{max} = \frac{100}{\mu} \quad \ldots\ldots\ldots \text{Equation 4}$$

where d_{max} is the grain size measured in microns
and μ is the measured linear absorption coefficient. ($\mu = \mu^* . \rho$).

Weiskirchner (1960, p. 258), who measured mass absorption coefficients on carefully-sized fractions of powdered quartz, found that the maximum value for the mass absorption coefficient of quartz (34.85) was obtained when grains in the range of 2-4 microns were measured. These results are in accordance with the predictions of equation 4. Weiskirchner (1960, p. 265) also examined the effect of using particle size distributions different from those recommended by von Engelhardt in equation 4. Although theoretically the presence of grains of a size larger than the recommended size should yield values for the mass absorption coefficients smaller than the expected values, Weiskirchner found that some as yet unexplained factor compensated in full for the effect of variations in grain size in the region 2-30 microns. This factor seemed to be dependent on the mass absorption coefficient of the sample, so that the amount of compensation appeared to be a function of the mass absorption coefficient, with more compensation occurring in samples with a higher mass absorption coefficient.

(2) Quality of the discs. It is essential that the pressed discs should be fashioned in such a manner that parallel-sided discs are formed: any tendency towards a wedge shape in the discs leads to incorrect values. This problem was, in fact, encountered in the course of the present study, and accordingly, in order to overcome it, the discs were rotated through 360 degrees in arcs of 90 degrees during the process of measurement. This produced a total of 8 measurements on the two discs prepared from each sample, the mean of all 8 values being taken as the mass absorption coefficient.

(3) Monochromatic radiation. Ideally, it is necessary to carry out all mass absorption measurements using monochromatic radiation. The radiation pro-

duced by the X-ray tube does, however, contain a fair proportion of harmonic radiation with a wavelength of $\lambda/2$. One way in which the amount of radiation of the harmonically-related type can be minimized is by using pulse height discrimination with the scintillation counter. Since, however, this requires the use of extremely narrow window settings, which may result in undesirable variations in the recorded intensities, a more satisfactory method of reducing harmonic radiation is to lower the excitation potential, i.e. the voltage applied to the X-ray tube. This results in less radiation with a wavelength of $\lambda/2$ being generated.

8.4.2.3. Verification of analytical procedure for determination of mass absorption coefficient.

In order to check on the correctness of all the instrumental conditions and analytical procedures used in the measurement of the mass absorption coefficient by means of X-ray fluorescence, a series of mixtures containing varying amounts of carefully-sized calcite (found to have a median grain size of 3 microns when the sizes were checked on a Sartorius sedimentation balance) and cellulose were prepared and their mass absorption coefficients were measured using the method that had been adopted for the present study. The values obtained were then plotted against the concentration of calcite in the mixtures, and a straight line was fitted to the points by a least squares method. On extrapolation of this line, a value of 67.00 was obtained for the mass absorption coefficient of pure calcite. This is in excellent agreement with the value of 67.75 reported by Weiskirchner (1960, p. 258) for calcite with a grain size distribution of 2-4 microns.

Using the same technique, the mass absorption coefficient for quartz with a median grain size of 15.4 microns was found to be 34.99, while for discs composed only of pure quartz powder a value of 35.01 was obtained. Once more, these values are in excellent agreement with the value of 36.1 reported for quartz by Norrish and Taylor (1962, p. 102), the value of 34.9 obtained by Alexander and Klug (1948, p. 887), and with the theoretical value of 35.00 obtained by calculation from the published mass absorption coefficients of the elements. Norrish and Taylor (1962, p. 102) have commented that the deviations between calculated and experimentally-derived absorption coefficients are generally less than the uncertainty in the published absorption coefficients of the elements.

After the analytical procedure for the determination of mass absorption coefficients had been verified as described above, a computer programme was drawn up to assist in calculating the mass absorption coefficients of any

powdered material. This programme (NIMMNHMU, programme 6 listed in Section 9) takes into consideration the correction factor of 0.750 that had to be applied for cellulose binder in the disc (see Section 8.4.2.2) and the dead time of the scintillation counter used in the present study (see Section 8.4.4.1.4).

8.4.3. Methods of quantitative X-ray fluorescence analysis.

Quantitative X-ray fluorescence analysis attempts to deduce the concentration of an element present in a sample from the intensity of the radiation produced by a member of the characteristic spectrum of that element. A standard of known concentration is required to provide radiation of a reference intensity with which the intensity of the analytical line of the element being analysed for can be compared. Two methods of quantitative X-ray fluorescence analysis are in use, an internal standard method and a method involving an external standard.

8.4.3.1. The internal standard method.

Use of the internal standard method obviates the need for measuring the mass absorption coefficient but produces other problems in its wake. Essentially the method involves the addition to the sample of a known amount of an element whose line and absorption edge are near those of the element that is being analysed for. Since the intensity of radiation produced by the added element undergoes the same absorption and enhancement as the analytical line, the ratio of the concentration of the added element to that of the analytical element is related to the ratio of their intensities by a constant factor. Although the method is well established and is capable of yielding excellent results, it has some serious disadvantages in the circumstances of the present study. Firstly, the element used as the internal standard should be within two or three atomic numbers of, and should have the same concentration level as, the analytical element. It was impossible to comply with this requirement in the case of the present study, where six elements of widely varying concentration were to be analysed for. Secondly, the use of the internal standard method carries with it the possibility of introducing errors because of the necessity for increased handling of the sample, with the consequent danger of contamination, and because of the difficulty of ensuring that the internal standard is adequately mixed with the sample. Thirdly, the internal standard method is most satisfactorily applied to the analysis of the heavier elements in low and moderate concentration where only one or two elements are to be determined. Fourthly, the addition of elements to a sample dilutes the sample and thereby lowers the concentration of the elements that are to be analysed for. All these considerations mili-

tated against the use of the internal standard method in the present investigation.

8.4.3.2. The external standard method -- international rock standards.

Since it had been decided that the use of any method that required the addition of other elements to the sample, whether as internal standards or as fluxing agents to overcome matrix effects, would be undesirable in the present study, it was decided to adopt the method of comparison employing external standards.

A number of well-analysed rock samples, such as Diabase W-1 (Fleischer, 1965, pp. 1263-1283) and Syenite SY-1 (Webber, 1965, pp. 229-248), with their currently-accepted analyses, were available for use as standards. Dunite NIM-D, a sample of dunite that has been prepared by the National Institute for Metallurgy as a future international rock standard, was also used in this study. The elemental contents of the three standard rock powders (W-1, SY-1 and NIM-D), which were used in the determination of the six elements Fe, Ti, Zr, K, Cr and Ni in the 143 samples from Hartebeestfontein, Zandpan and Venterspost, are listed in Table XXXII.

TABLE XXXII

ELEMENTAL CONTENTS OF THREE ROCK POWDERS USED AS STANDARDS FOR THE DETERMINATION OF Fe, Ti, Zr, K, Cr AND Ni BY X-RAY FLUORESCENCE

ELEMENT	ROCK STANDARD	CONCENTRATION PPM.
Fe	W-1	72523
Ti	W-1	6400
Zr	SY-1	2920
K	SY-1	27000
Cr	NIM-D	2750
Ni	NIM-D	2200

8.4.4. Method of quantitative X-ray fluorescence analysis adopted in the present study.

In the present study, the whole rock pressed briquette method of X-ray fluorescence analysis, using international rock standards as external standards, was adopted for the quantitative determination of the six elements Fe, Ti, Zr, K, Cr and Ni in the 143 samples from the Vaal Reef at Hartebeestfontein and Zandpan and from the Ventersdorp Contact Reef at Venterspost. The method of preparation

of the pressed powder briquettes has been outlined in Section 8.4.1.2. The Philips instrument used in the present study had four sample holders, three of the holders being used for samples while the standard (one of the international rock powders described in Section 8.4.3.2) was placed in the fourth sample holder. In each analytical run, measurements of peak and background intensity were made on the three samples, followed in turn by peak and background measurements on the standard, made under the same conditions as were used for the samples.

The instrumental conditions and counting times used are discussed below.

8.4.4.1. Instrumental variables in X-ray fluorescence analysis.

The conditions used in the analysis of the samples are listed in Table XXXIII. In selecting these conditons, the following factors were taken into consideration:

8.4.4.1.1. X-ray tube target.

In order to achieve maximum sensitivity, the target chosen was, in each case, the one providing the best excitation of the specific element that was to be analysed for. Other factors that were also borne in mind when choosing the target were:

(a) the presence of impurities in the target material that might result in blank corrections having to be made;

(b) the possibility of interference to the analytical line by the characteristic radiation from the target itself.

8.4.4.1.2. Analysing crystals.

The analysing crystals used were chosen by, where possible, comparing one crystal with another in order to see which one would give the highest intensity coupled with the maximum amount of dispersion to prevent line interference. In the present study, the presence of extra reflections in the LiF (220) crystal, caused by the existence of sets of planes slightly tilted with respect to the main reflecting plane, was not found to produce any interference.

8.4.4.1.3. Choice of counter.

A scintillation counter was used for the determination of the heavier elements, while a flow counter was used for the lighter elements.

TABLE XXXIII

X-RAY FLUORESCENCE SPECTROMETRY

INSTRUMENTAL CONDITIONS USED FOR THE DETERMINATION OF Fe, Zr, Ni, Cr, Ti AND K IN PRESSED WHOLE ROCK POWDER BRIQUETTES

ELEMENT	CRYSTAL	COLLIMATOR	X-RAY TARGET	COUNTER*	PATH
Fe K_α	LiF (220)	fine	W	S.C.	air
Zr K_α	LiF (220)	fine	W	S.C.	air
Ni K_α	LiF (220)	coarse	W	S.C.	air
Cr K_α	LiF (220)	coarse	W	F.C.	vacuum
Ti K_α	LiF (100)	coarse	Cr	F.C.	vacuum
K K_α	P.E.T.	coarse	Cr	F.C.	vacuum

* S.C. = scintillation counter
F.C. = flow counter

8.4.4.1.4. Counting losses.

As can be seen from Table XXXIII, it was necessary to make use of the scintillation counter for the determination of some of the elements. The counting rates associated with some of these elements were high enough to cause overloading of the detector and counting circuitry, and consequently, to correct for this, the so-called "dead time" of the counter had to be determined. This was measured by means of the well-known "foil technique" (Cullity, 1956, pp. 197 - 198), the value obtained for the Philips instrument used in the present study being 0.2440×10^{-6} seconds. This factor was applied in all work requiring the use of the scintillation counter.

It was not found necessary to determine the "dead time" of the flow counter, as in this case the counting rates were never sufficiently high (greater than 10,000 counts per second) to cause overloading of the counter and its associated circuitry.

8.4.4.1.5. Counting times.

For each sample or standard, counts were accumulated for 10 seconds on peak and 10 seconds on background, the whole procedure being repeated 10 times. The means of all the values obtained were used to calculate the concentrations of the elements in the samples. These counting times, coupled with the

number of counts recorded, were found to give adequate counting statistics. The relative probable error was found to be less than 1 per cent when calculated according to the formulae given by Mirkin (1964, p. 76).

(Relative probable error $\mu_p = \frac{0.675}{\sqrt{n}}$ where n is the number of pulses)

8.4.4.2. Calculation of results of quantitative X-ray fluorescence analysis.

The results of the analyses were calculated according to the fomula proposed by Reynolds (1967, p. 1500), which is shown below (Equation 5).

For any particular element, say chromium:

$$\text{ppm } Cr^u = \frac{I_{(CrK_\alpha)}{}^u \cdot \mu^{*u}}{I_{(CrK_\alpha)}{}^s \cdot \mu^{*s}} \cdot \text{ppm } Cr^s \quad \text{Equation 5}$$

where

I is the measured nett intensity = (peak intensity - background)

μ^{*u} is the mass absorption coefficient of the unknown powder sample

μ^{*s} is the mass absorption coefficient of the powdered rock standard

Cr^u is the chromium content of the rock sample

Cr^s is the chromium content of the rock standard.

This formula was incorporated into two computer programmes, Nos. 4 and 5 (see Section 9), into which were fed the mass absorption coefficients and the peak and background intensities.

8.4.4.3. Check on the self-consistency of the method of X-ray fluorescence analysis used in the present study.

Checks on the self-consistency of the method were carried out using the following samples: Tonalite T-1 (Ingamells and Suhr, 1963, p. 902), Syenite SY-1 (Webber, 1965, pp. 229-248), Diabase W-1 (Fleischer, 1965, pp. 1263 - 1283), Granites GA, GH, Basalt BR (Roubault, de la Roche and Govindaraju, 1966, pp. 107 - 121) and Dunite NIM-D (unpublished analytical results, National Institute for Metallurgy).

The method used was as follows: Each of the samples in turn was used as an "unknown" and analysed for the particular element required using one of the other samples as a "standard". It was found that the results obtained were close to the published values when samples T-1, W-1, SY-1 and NIM-D were used, and that there was good self-consistency between these samples. For example, a value of 105 ppm (instead of the published value of 100 ppm) was found for zirconium

in W-1 when SY-1 was used as a "standard". On the other hand, poor results, often differing by as much as 50% from the published values, were obtained when the French standards GA, GH and BR were used, but these wide discrepancies may possibly be attributed to the fact that in most cases a total of only 3 published analyses, often with widely different analytical results, was available for these samples. The grain size distribution in the French samples may be another factor responsible for the observed discrepancies, but this was not investigated in the present study.

On the basis of this investigation, it was decided that the results obtainable by the method of quantitative X-ray fluorescence analysis adopted for the present study were satisfactory.

Volborth (1963, p. 64) carried out similar work on pressed rock powders of wide modal and chemical compositions, and was able to conclude that the X-ray fluorescence method of analysis could be used satisfactorily to determine the major, and some of the minor, components of the rock. Volborth's method also involved the use of finely-ground pressed rock powders without the use of binders, and the use of International Rock Standards Granite G-1 and Diabase W-1. He summarized the main advantages of this technique as being simplicity, sensitivity, speed, precision and accuracy, coupled with the fact that no weighing, diluting or fluxing operations had to be performed on the samples and that no additions of any kind had to be made to the samples.

8.5. Quantitative X-ray Diffraction Analysis.

8.5.1. Introduction.

In the present study, X-ray diffraction analysis was used for the quantitative determination of pyrite, the three phyllosilicates muscovite, pyrophyllite and chlorite, and "quartz" (which was determined by difference) in the 143 samples from the Vaal Reef at Zandpan and Hartebeestfontein and from the Ventersdorp Contact Reef at Venterspost (see Part I of this thesis).

The quantitative X-ray diffraction analysis of a heterogeneous multicomponent mixture (the Witwatersrand banket) in itself presented problems of considerable complexity, which were rendered more complex by the fact that quantitative determination of phyllosilicates in the presence of other minerals was also involved. Among the difficulties that are encountered when quantitative X-ray diffraction powder analysis is carried out on phyllosilicates are the following:

(1) Since most of the phyllosilicates display a less perfect degree of crystallization than other minerals, and have an extremely fine-grained nature, the X-ray reflections produced by phyllosilicates are generally broader and of

lower intensity than the reflections produced by other minerals, and measurable reflections are few.

(2) Strutural imperfections and rearrangements in the phyllosilicate lattice result in reflections with variable and often diffuse peaks, whose exact positions may be difficult to determine in view of their being asymmetrically broadened.

(3) The inherent platy morphology of the phyllosilicates is a factor that causes preferred orientation, often to an unpredictable degree, during sample preparation.

In view of these difficulties, special precautions had to be exercised in the present study at all stages of sample preparation, diffractometer recording and interpretation of results. The techniques adopted are described and discussed in subsequent paragraphs.

8.5.2. Fundamental concepts and techniques in quantitative X-ray diffraction analysis.

8.5.2.1. Choice of radiation.

Selection of the radiation to be used in an investigation is governed to a very large degree by the type of material that is to be examined, as well as by the availability of suitable X-ray tubes. In cases where the material that is to be examined has a high iron content (i.e., over 20%), the use of an X-ray tube with an iron or chromium target would normally be favoured. For analyses of silicate materials, however, despite the fact that they may contain moderate amounts of iron, the use of an X-ray tube with a copper target is preferred in view of its better dispersion at the low angle settings of the goniometer. Since silicate materials predominated in the present suite of samples, an X-ray tube with a copper target was selected for use in the present investigation.

8.5.2.2. Detection limit.

Examination of a diffractometer chart raises the question of how large a "peak" must be before it can be regarded as being a valid reflection. As a rough guide, Zussman (1967, p. 280) stated that a "peak" that is three times as big as the standard deviation of the background is likely to represent a reflection. De Vries (1966, p. 5), on the other hand, defined the lower level of detectability as that concentration which permits one to distinguish the peak from the background, but which is not necessarily a region where practical analysis can still be performed. This latter concept of the detection limit is the one that has been adopted

for the purposes of the present study.

8.5.2.3. Peak position.

Chayes and MacKenzie (1957, p. 534) investigated the random errors inherent in the determination of the peak locations and the distances between peaks in X-ray powder diffractometer patterns. They concluded that the major part of the error in determining the position of a peak was apparently associated with operations contingent upon setting up the specimen and getting the instrument in motion (operations such as, for example, the synchronization of the chart recorder with the instrument). Chayes and MacKenzie took the position of the peak as being a point midway between the edges of the peak at two-thirds of the peak height, both coordinates being judged by eye. Differences between chart and standard of the order of 0.0156^{o} at 50^{o} 2θ were attributed mainly to operator error. Chayes and MacKenzie suggested that internal standards should be used whenever close decisions have to be made.

Zussman (1967, p. 280) concurred with Chayes and MacKenzie that the position of a peak on a diffractometer chart is best measured at the centre at about two-thirds of the peak height, and not at the apex of the peak. He added that the centre of an unresolved α_1, α_2 doublet can be used as 2θ for a weighted mean wavelength $\lambda = \frac{1}{3}(2\lambda_{\alpha_1} + \lambda_{\alpha_2})$. The instrument must be set up and calibrated accurately with a standard specimen, and whatever measuring procedure is adopted for the standard's peaks should also be used for the peaks from other specimens.

8.5.2.4. The measurement of intensity.

As Zussman (1967, p. 284) has pointed out, various techniques may be used in the measurement of intensities. The intensity at a given Bragg angle can be measured by counting for a fixed time, or by timing a fixed count with a stationary goniometer. A similar result can be obtained, but with far less accuracy, by measuring the deflection of the recorder pen. In all these cases, the background measurements must also be made and subtracted. More generally, however, use is made of the scanning goniometer and the reflection profile as traced by the recorder. Zussman stated that the correct procedure is to obtain the integrated intensity by measurement of the area under the peak, but added that often the peak height can be assumed to be proportional to the area, with the consequence that in these cases only the peak height needs to be measured. Zussman stressed, however, that in those cases where, as a result of variations in the degree of crystal-

linity of the substance, changes in peak shape occur, measurement of the area under the peak becomes mandatory.

Norrish and Taylor (1962, pp. 102 - 103) stated that the most accurate method of measuring diffraction intensities is to take a large number of counts at the required angle, since, if sufficient counts are accumulated, the accuracy obtainable is limited only by the output stability (usually of the order of 1 per cent) of the X-ray generator used. If no other lines lie near the line being measured, and if the background in this region is flat, then no problem should be encountered with the measurement of the height of the peak above background. Where complex mixtures are being examined, however, Norrish and Taylor state that some integration method is to be preferred. During the analysis of rocks, for example, the background obtained invariably tends to be a sloping one, so that averaging the background on either side of the line does not necessarily give an accurate estimate of the line background, particularly if other lines lie near the one being measured.

8.5.2.5. Techniques used in integration.

In cases where materials yield broad, low and "hashy" X-ray reflections, the measurement of the X-ray intensities presents a most difficult problem. Reflections of this sort are often produced by poorly crystalline materials or severely strained crystallites (such as many of the phyllosilicates). Maximum peak intensity is almost useless for the quantitative estimation of such materials, and in these cases the areas under the peaks must be integrated.

The most commonly used methods for computing the area under a diffraction peak are: triangulation, planimetry, the calculation of height times width at half height, cut and weigh techniques, and the use of a Disc Integrator. The merits of the various methods are reviewed below.

8.5.2.5.1. Triangulation.

In this case a triangle is constructed by drawing tangents to the slopes of the peak. The base is taken as the intersection of the two tangents with the baseline. The height is measured from the base to the point where the tangents intersect. The area is then calculated from the formula: area = $\frac{1}{2}$ base x height.

The accuracy and precision of this method are dependent on the skill employed in the construction of the triangle, and on the shape of the peak itself. Even when the peak shape is Gaussian, however, only 97 per cent of the area under the peak is accounted for when this technique is used.

8.5.2.5.2. Planimetry.

The precision obtainable by means of the planimeter is governed by the design of the instrument and by the skill of the operator. Higher precision can be obtained by tracing each peak several times and taking a mean value, but this procedure is very time-consuming.

8.5.2.5.3. Height times width at half peak height.

Since normal peaks approximate a triangle, the area under the peak can be approximated by multiplying the peak height by the width of the peak at half height. The normal peak base is not used in this calculation because large deviations may be caused by tailing or absorption.

Symmetrical peaks can be measured with reasonable accuracy by this technique, although narrow peaks set limits to the precision and accuracy obtainable. Poor results are obtained when this technique is used to measure the area under asymmetrical peaks.

8.5.2.5.4. Cut and weigh.

In this case the areas under peaks are compared by cutting out the diffraction peaks and weighing the paper on an analytical balance. The accuracy of the method depends on the care used in the cutting-out, and on the constancy of thickness and moisture content of the chart paper. A major disadvantage of this technique is that recorded spectra are destroyed, but this problem may be avoided by photocopying the peak in question and using this cut-out for integration purposes.

8.5.2.5.5. Disc Integrator.

Of all the integration techniques, the one that has been found to be the best is based on the use of an attachment called the Disc Integrator. This is coupled to the normal recorder so that integration is performed simultaneously with the recording of the diffractogram. The use of the Disc Integrator permits allowances to be made for peak broadening, asymmetry and sloping backgrounds. Anderson (1964, p. 33) has investigated the precision of the results obtainable when the Disc Integrator is used. He reported that when samples containing varying amounts of bayerite were analysed, the mean coefficient of variation of measurments made with the Disc Integrator was 0.83 per cent, while when the technique of measuring peak heights was used the coefficient of variation was 1.69 per cent. Similarly, he found that the measurement of a sample containing 70 per cent (repeated analyses) of poorly crystalline pseudeboehmite with a "hashy" peak resulted in a coefficient of

variation of 1.1 per cent when the Disc Integrator was used, while when a compensating polar planimeter was employed the coefficient of variation was 3.6 per cent.

In view of the fact that the use of the Disc Integrator enables rapid permanent records, complete with integrated intensities, to be made at the time of analysis, and, in addition, permits allowance to be made for sloping backgrounds, the Disc Integrator technique was selected for use in the present study. Comparisons can be made between the integrated intensities obtained by means of the Disc Integrator in the present survey and the peak-height-to-background measurements quoted in the A.S.T.M. Powder Data File if the graph of peak height vs. integrated area given by Swanson, Morris, Stinchfield and Evans (1962, pp. 2-3) is used. (The integration results plotted by Swanson et al. were obtained by use of the planimeter and cut-and-weigh techniques).

8.5.2.6. The choice of divergence slits.

The size of divergence slit that should be used in a particular investigation is another factor that must be considered before commencing X-ray diffraction analysis. Leroux and Mahmud (1959, p. 337) and Schoen (1962, p. 1390) have examined the focussing arrangements of the X-ray goniometer that delineate the geometric shape of the volume fraction of the sample being irradiated. Leroux and Mahmud reported that the departures of actual observed analytical results from the theoretical results expected could in each case be correlated with the volume fraction of the sample irradiated, as the width of the X-ray beam was changed. Leroux and Mahmud found that the best results were obtained when 1 degree divergence slits were used with copper radiation, and concluded that, for quantitative analysis where the resolution of the peak line was not a problem, the use of the maximum permissible divergence slit opening was to be recommended.

Bearing these recommendations in mind, the following conditions were selected for use in the present investigation: the largest possible divergence slit opening, which would permit the greatest possible amount of the sample to be irradiated, was chosen. This meant that a divergence slit of 1 degree was used between 2 and 73 degrees 2θ for all measurements made with Cu K_α radiation, while at goniometer readings above 73 degrees 2θ a 4 degree divergence slit was used. A scatter slit of 0.1° and a receiving slit of 1° were used throughout the study to ensure maximum peak resolution.

8.5.3. Factors affecting the intensity of reflections in X-ray diffraction analysis.

Many factors affect the intensity of the reflections obtained when substances are irradiated by an X-ray beam. Some of these factors, which must be taken into account in quantitative X-ray diffraction analysis, are reviewed in subsequent paragraphs.

8.5.3.1. Intensity and sample particle size.

"The question of the effect of grain or particle size on the relative intensities of X-ray reflections from powders consisting of a mixture of two or more substances is of fundamental importance in several different connections. It arises, for example, when mixtures of known composition are used for the purpose of making accurate comparison of the intensities reflected by the individual components. The question is equally important in connection with the converse problem of determining the composition of a mixture from the reflected X-ray intensities." (Brindley, 1945, p. 347). The theoretical calculation of the intensity of X-ray reflection by crystalline powders is usually based on the assumption that the intensity reflected by any small volume element dV of the powder is proportional to dV, provided that there is only negligible absorption within the volume element. The total reflected intensity may then be obtained by integration over the volume of the powder specimen, making due allowance for absorption and for the random orientation of the crystallites. If the particles of a mixture are sufficiently fine, the reflected intensities from different components may be regarded as being equally influenced by the mean macroscopic absorption of the mixture, but with coarser particles this equalization of absorption may not occur.

Klug and Alexander (1954, p. 292) have statistically examined the relationship between peak intensity, reproducibility and crystallite size. From an examination of four quartz-powder fractions containing crystallites with mean dimensions of, respectively, 5-50 microns, 15-50 microns, 5-15 microns and less than 5 microns, Klug and Alexander found that the reproducibility of the intensity measurements was considerably better in the case of the finer fractions (i.e., those with mean dimensions less than 15 microns) than in the case of the coarser fractions. The reproducibility of peak heights for quartz is dependent on the random orientation of the crystallites, and this is most easily achieved in powders with a small particle size. Klug and Alexander also found that the average observed intensity of the finer fractions was greater than that of the coarser fractions. This

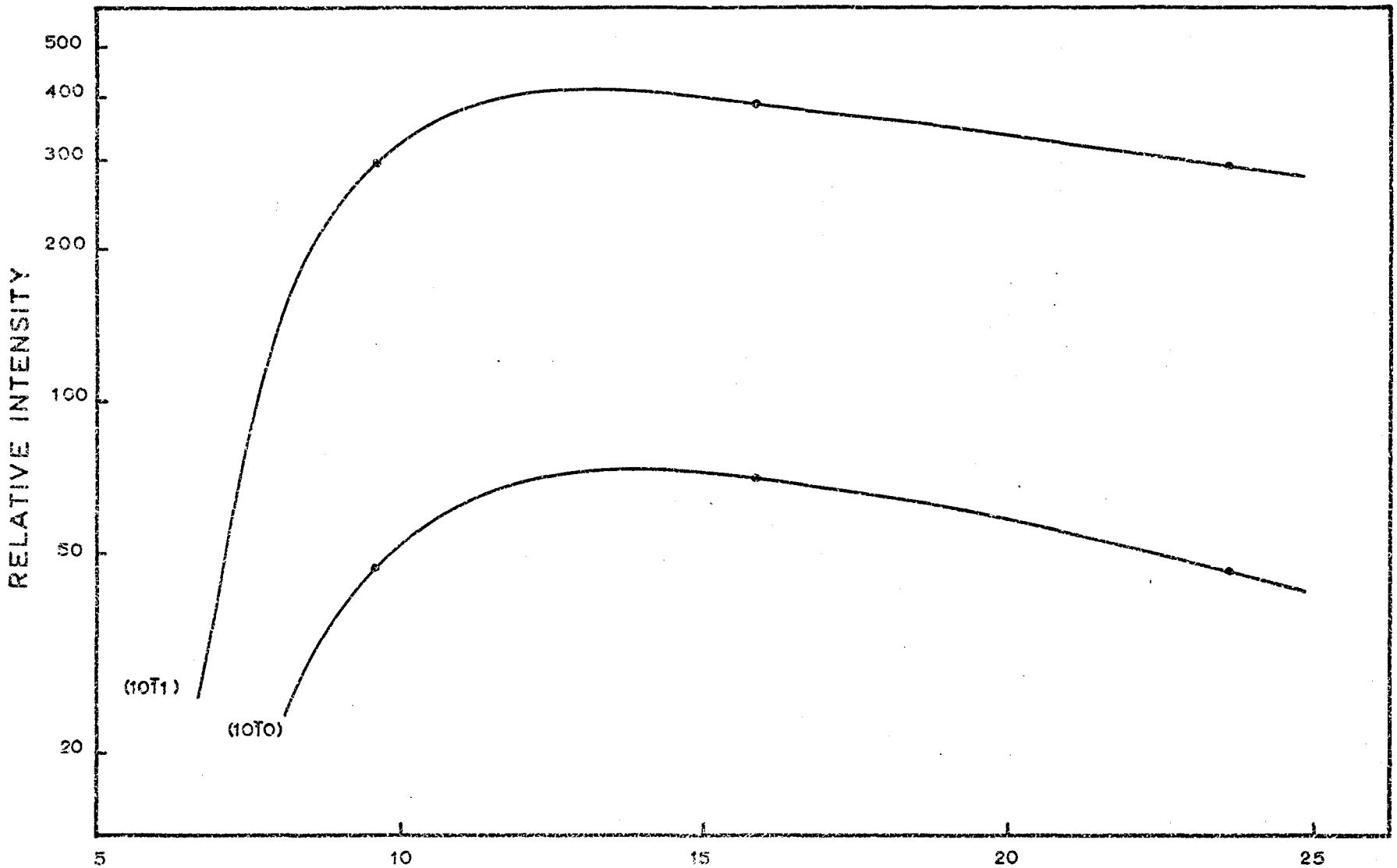


FIGURE 16 MEDIAN GRAIN SIZE OF QUARTZ PARTICLES – MICRONS

could be attributed to a reduction in extinction in samples made up of very small crystallites, since small particle size reduces extinction and microabsorption effects to a negligible level so that near-maximum peak intensity results. When, however, the average particle size of quartz is reduced to below 2 microns the X-ray peak intensity decreases, probably as a result of the formation on the particle surfaces of a thin "amorphous" material that is developed during grinding and contributes to X-ray absorption (Tatlock, 1966, p. 5). Weiskirchner (1960, p. 265), who studied the X-ray intensities of quartz and calcite powders, reported a similar effect.

In the course of the present investigation, the relative intensities for the quartz $(10\bar{1}1)$ and $(10\bar{1}0)$ peaks were examined in relation to the median grain size, which was determined on a Sartorius sedimentation balance. The results are plotted in Figure 16. It can be seen that, for both quartz peaks, the maximum intensity occurred with particles whose median grain size was 13.6 microns.

It would seem that where the crystallites have a grain size larger than 30-40 microns, a reduction in the intensities due to extinction can be expected. According to Tatlock (1966, p. 6), experimental work on sized fractions of pure minerals indicates that sample powders should have a maximum crystallite size of 40 microns and a minimum size greater than 2 microns if both optimum reproducibility and near-maximum intensity are to be obtained in quantitative X-ray diffraction analysis. Tatlock unfortunately did not specify this optimum particle size distribution in terms of median grain size, although a particle size distribution is more meaningful expressed as median grain size than as a size range. The results obtained for quartz in the present investigation (reported in the previous Section) indicate, however, that a median grain size in the region of 15 microns (13.6 microns for pure quartz) is probably close to the optimum. It is obvious that samples should conform to the optimum median grain size if possible, but when a whole rock powder is to be analysed, it must be remembered that the use of any separation technique (such as sedimentation) to extract from the sample a fraction that conforms to the optimum median grain size is likely to render the sample unrepresentative. The quantitative analysis of a multicomponent mixture requires that the sample as a whole should be analysed, not just any particular size fraction of that sample, and hence it is necessary to employ a grinding technique that will produce, from the original complete sample, a powder whose median grain size approximates to the optimum.

Mirkin (1964, p. 78) has pointed out that the mean error for samples

with the same mass absorption coefficient but different grain size distributions can vary from 4 per cent for grains with a median grain size of 15 microns to 15 per cent for particles with a median grain size of 40 microns. For particles with a median grain size lying between 5 and 10 microns, Mirkin found that the error was between 1 and 2 per cent for samples with a mass absorption coefficient of 50 $cm^2 g^{-1}$.

The maximum permissible crystallite size at which micro-absorption effects are still negligible will depend on the difference between the component and the matrix as regards their absorption of the radiation being used. (The matrix is defined as the components other than the component being analysed for, so that the analytical component and the matrix together constitute the sample as a whole.) As was mentioned in Section 8.4.2.2, von Engelhardt (1955, pp. 436 - 437) has proposed the following equation, relating grain size to the linear absorption of the substance, as a guide to the optimum grain size distribution:

$$d_{max} = \frac{100}{\mu} \quad \text{(in microns)} \quad . \quad . \quad . \quad \text{Equation 4}$$

where d_{max} is the maximum particle size of the substance in microns and μ is the linear absorption coefficient of the substance ($\mu = \mu^* \rho$).

Particles with a median grain size in accordance with equation 4 will show the minimum micro-absorption effects.

Alexander, Klug and Kummer (1948, p. 742) have calculated that if an error of 1 per cent in the intensity measurements can be tolerated, then in the case of silicates whose mass absorption coefficients lie in the range between 20 and 100 the maximum permissible grain size would be of the order of 5 microns.

8.5.3.2. Intensity and the effect of background.

It is important to remember that the total intensity and the background intensity should be known with approximately the same degree of absolute error, as decreasing the absolute error in only one of the two quantities will not improve the overall accuracy but will only improve the precision of the difference, i.e., the net intensity.

For good quantitative results to be obtained, it is necessary to remember that the peak-to-background ratio of the most intense line of the powder pattern of a substance determines the minimum detectable amount of that substance in the mixture. Any decrease in the peak-to-background ratio will, therefore, be markedly detrimental to the accuracy of the determination. Buerger and Kennedy

(1958, pp. 756 - 757) have rightly pointed out that, when a small amount of material is supported in an X-ray path, the background noise from the mounting media includes random reflections that may be indistinguishable from low intensity peaks of the diffraction pattern. Provided that the specimens are large enough to be packed or pelleted or are of quasi-infinite thickness the background noise contributed by the holder or support is usually masked. This is one of the reasons why an adequate sample thickness is necessary.

8.5.3.3. Intensity and sample thickness.

In order to achieve maximum diffracted intensity, the thickness of the sample must exceed a certain minimum given by the equation published by Alexander and Klug (1948, p. 886):

$$t \geq \frac{3.2}{\mu} \cdot \frac{\rho}{\rho'} \cdot \sin\theta \quad \text{Equation 6}$$

where t is the thickness of the sample

μ is the mean linear absorption coefficient of the solid material composing the powder

ρ is the density of the solid uncrushed material

ρ' is the density of the sample powder including interstices

θ is the Bragg reflection angle.

This relationship between thickness and absorption should be noted, as the absorption of the material will determine the thickness of sample required. For example, the mass absorption coefficient (which is obtained by dividing linear absorption coefficient by density) of magnesium chlorites is lower than that of iron chlorites, and therefore magnesium chlorite samples should be thicker than iron chlorite samples. Schoen (1962, p. 1388), using Cu K_α radiation, found that a minimum thickness of 0.09 mm satisfies equation 6 for a magnesium chlorite up to a 2θ angle of 18.8°. If one iron atom was substituted for magnesium, however, Schoen found that the minimum thickness decreased to 0.046 mm, while a pure iron chlorite only required a sample thickness of 0.016 mm.

Zussman (1967, p. 280), in discussing the effect of absorption errors that occur in diffractometry, mentioned that the higher the absorption coefficient of the sample was, the lower the error was likely to be. This effect was also noted by Weiskirchner (1960, p. 265). The practical way in which to minimize absorption errors is to keep samples as thin as possible, while taking care that the minimum thickness specified by equation 6 is exceeded.

Williams (1959, p. 1842) used gum tragacanth as a diluent in order to minimize absorption effects in quantitative work. Normally Williams used a sample depth of only 0.005 mm, but for many materials this thickness proved to be too small, necessitating the use of a greater sample depth and dilution of the sample by gum tragacanth to yield final samples with mass absorption coefficients of about 20 $cm^2 g^{-1}$.

8.5.3.4. Sample holders and their effect on intensity measurements.

Various designs and types of sample holders have been proposed in the past, and a great deal of discussion has taken place regarding the relative efficiencies and advantages of different sample holders.

Sample holders may be broadly classified into two types, rotary sample holders and stationary sample holders.

8.5.3.4.1. Rotary sample holders.

The basic concept underlying the use of a device with the sample holder rotating in its own plane is that, relative to a stationary holder, a rotary device permits more crystallites to contribute to the reflections and offers a better chance that all orientations will be equally represented. In other words, the use of a rotary device has, in theory, the following advantages: firstly, it helps to average out inhomogeneities, since a larger surface area than that of the conventional Philips holder is presented to the X-ray beam, and different parts of the specimen are covered during the rotation; secondly, since the X-ray beam is not parallel but slightly divergent, crystallites that are not accurately parallel to the surface may be able to reflect at some position during the rotation.

The use of a rotating sample holder for the study of samples containing material likely to adopt a preferred orientation during packing into the sample holder (such as the phyllosilicates) has been advocated by some workers and equally loudly decried by others. According to Mirkin (1964, p. 78) the mean relative error in the measurement of peak intensity for a sample with a median grain size of 15 microns and a mass absorption coefficient of 50 decreases from the 4.00 per cent obtained when a stationary mount is used to 0.27 per cent when the sample is rotated. This represents a very worthwhile improvement in the accuracy of the measured intensity of the peak. Williams (1959, p. 1842) advocated the use of a rotating sample holder constructed from copper (see also Section 8.5.4). On the other hand, Schmalz (1958) is quoted by Tatlock (1966, p. 34) as having found that no better reproducibility could be obtained when the rotating

sample holder was used than was obtained when samples were mounted in a stationary holder.

A rotating sample device was initially tried out in the course of the present investigation, but was discarded for the following reasons:

(1) The construction of the sample holder provided was such that preferred orientation could not be avoided during the loading of the sample.

(2) A modification suggested by Byström-Asklund (1966, p. 1233) to overcome this drawback was considered, but the mechanical problems associated with the use of the rotating sample device, and the fact that small divergence slits would have had to be used to produce full irradiation of the sample, militated against the use of the rotary sample holder.

(3) The mechanical construction of the rotating sample device was such that the goniometer would have required re-alignment each time that the diffractometer had to be used with conventional sample holders.

8.5.3.4.2. Stationary sample holders.

Various types of stationary sample holders were considered for use in the present study, as were also various sample loading techniques. These included the following:

(1) Gude and Hathaway (1961, p. 994) have suggested a sample holder for use with very small samples. This consists of a conventional aluminium sample holder with a rectangular opening (Philips holder) over which is laid a membrane substrate of plastic, made in a way similar to that in which substrates for electron microscopy are prepared. The sample is then sprinkled onto the membrane covering the opening in the sample holder. Whilst this technique is clearly suited to the qualitative study of small amounts of sample, it is equally clearly not suitable for quantitative analysis, and was not adopted for use in the present study.

(2) Tatlock (1966, p. 34) has suggested the use of a "back-loading" sample loading technique. This technique calls for a conventional Philips aluminium sample holder with its rectangular opening. A glass slide is taped to the one side of the opening and the sample is loaded from the back and compressed with a spatula until the sample is level with the back of the sample holder. A piece of stiff card or glass is then taped to the back of the holder, and the original glass slide is removed from the "front" of the holder, with this surface then being presented to the X-ray beam. This technique was tried out during the course of the present study, but was rejected because it was found that the sample orientation that resulted was not reproducible.

(3) Von Engelhardt (1955, p. 435) proposed the use of a so-called "side-loading" technique. This involved a modification of the conventional Philips holder, in which one edge of the sample holder was cut away, a glass plate was glued to the back of the holder and, after another glass slide had been clamped to the front of the holder, the sample was poured into the holder from the top edge. In this case the width of sample exposed to the X-ray beam was 11 mm and length 28 mm.

(4) Niskanen (1964, p. 709) has reported that he used the type of holder proposed by von Engelhardt with great success in his study of methods of reducing orientation effects in quantitative X-ray diffraction analysis of kaolin minerals. He found that the holder was satisfactory provided that care was taken to ensure that the sample was compacted in the holder in a reproducible manner. Niskanen proposed that a small frame should be used, in which the holder could drop from a constant height (in a manner best likened to the blade in a guillotine). A frame of this type was constructed for the present study, and was found to yield satisfactory results.

It soon became clear, however, that although the adoption of a side-loading technique was a definite step forward as regards the attainment of a more predictable degree of sample orientation, the size and construction of the sample holders used by von Engelhardt (1955, p. 435) and Niskanen (1964, p. 709) could be considerably improved upon. Before a new holder could be designed, however, the question of the optimum sample length had to be considered. Schoen (1962, p. 1390) has drawn attention to the fact that the intensities of X-ray diffraction peaks are obviously related to the area of sample irradiated, and that this is in turn related to the size of divergence slit used. (The question of the choice of divergence slit has been discussed in Section 8.5.2.6). As long as all the energy in the X-ray beam falls onto the sample, the intensity of one diffraction peak may be compared with that of another, but at low angles of θ part of the X-ray beam will pass above and below the sample, so that the sample is irradiated with less energy and peak heights are reduced from their true value. Choosing a narrower divergence slit will certainly overcome the problem of the X-ray beam passing above and below the sample, but this procedure has the drawback of decreasing the intensities of all the peaks by reducing the amount of energy falling on the sample. A more attractive and convenient method of ensuring that the energy all falls onto the sample without having to resort to continual changes of the divergence slits is to increase the size of the sample area to be irradiated. The relationship between sample length and the particular θ angle at which the X-ray beam will intercept that sample is given by the following equation (Schoen, 1962, p. 1390):

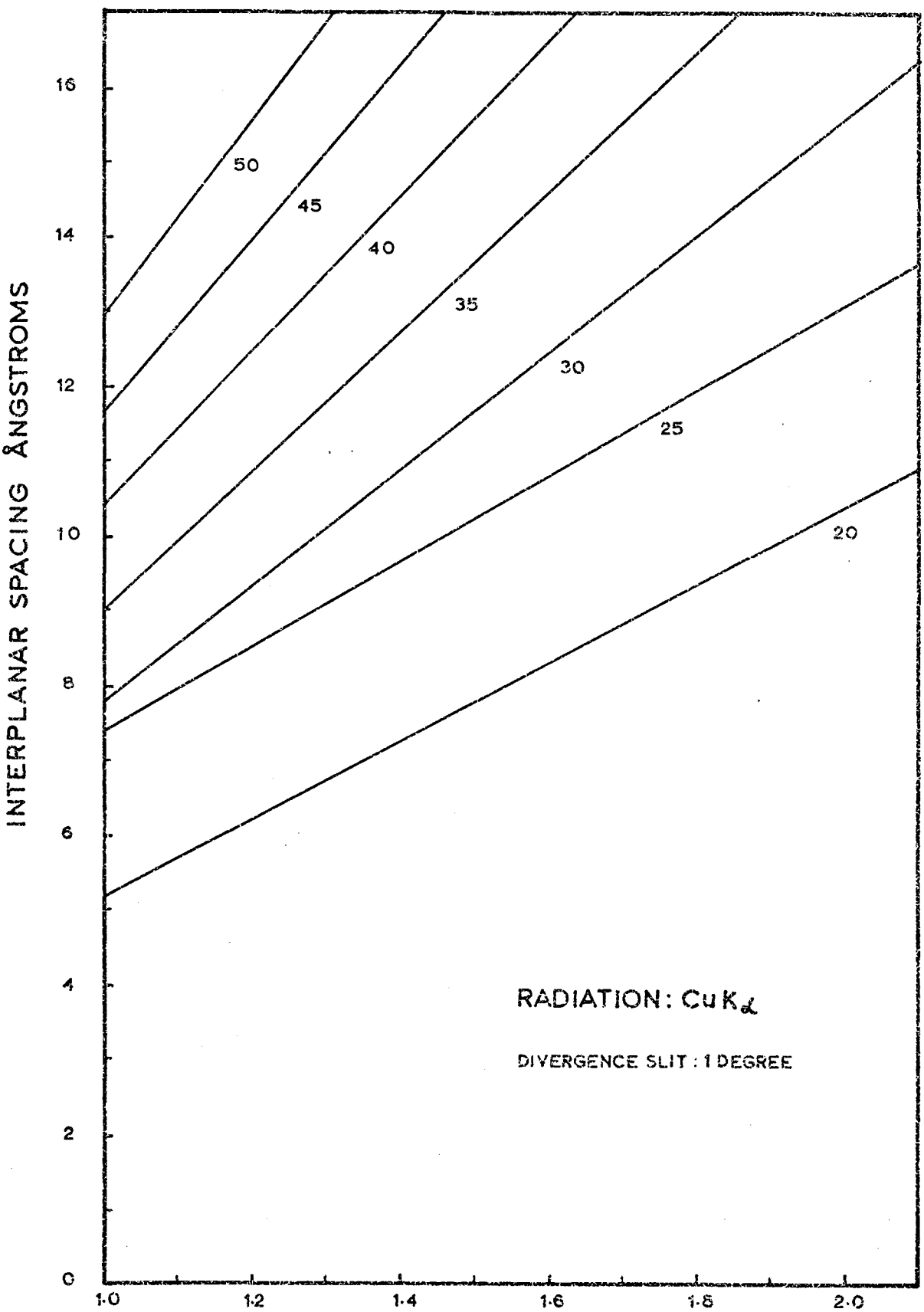


FIGURE 17 INTENSITY CORRECTION FACTOR

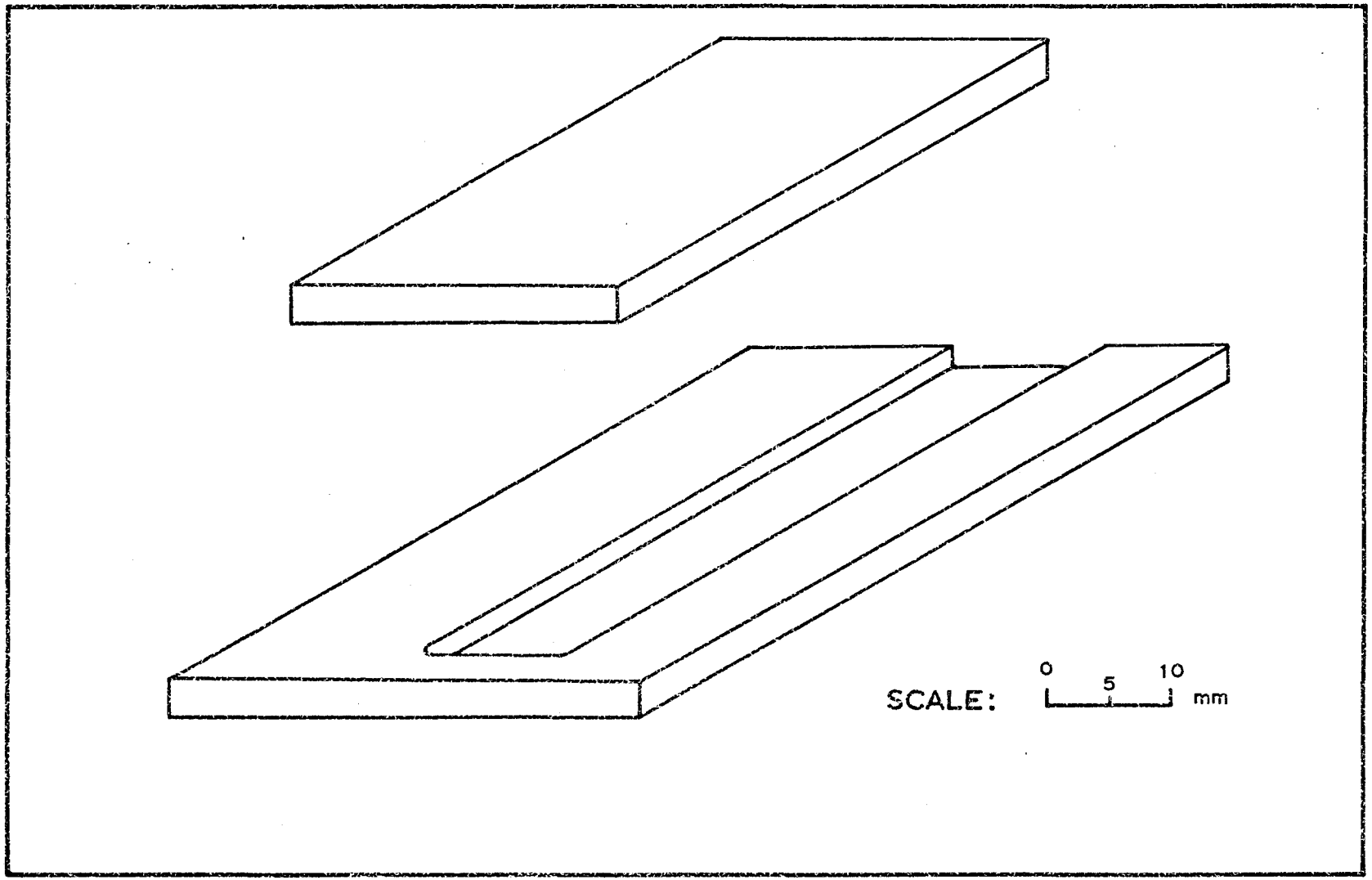


FIGURE 18 X-RAY SAMPLE HOLDER

$$L = \frac{\gamma}{57.3} \cdot \frac{R}{\sin\theta} \quad \text{Equation 7}$$

where γ is the angular aperture of the divergence slit in degress

L is the length of the sample in centimetres

R is the goniometer radius in centimetres

θ is the angle between the X-ray beam and the sample.

Solution of equation 7 (Schoen , 1962, p. 1390) indicates that a minimum 2θ angle of 7.4^{o} is required for a 1 degree divergence slit and a goniometer radius of 17.0 cm. For Cu K_{α} radiation, the 14 Å (001) chlorite peak at $2\theta = 6.3^{o}$ requires a sample length of 5.4 centimetres. Assuming that the energy is uniformly distributed throughout the X-ray beam but that a sample holder with a sample length of only 4.6 cm is used, the chlorite (001) peak heights would have to be increased by 15 per cent (4.6/5.4 = 0.85) to make them comparable in intensity with peaks received at angles greater than 7.4^{o}.

Unlike the sample holders described earlier, the holders manufactured for the present investigation did not involve the modification of commercial sample holders but rather the designing of completely new types of holders. The design was, however, influenced by the mechanical limitations imposed by the size of the X-ray chamber of the Philips goniometer used, so that the maximum sample length, for example, could not exceed 5.0 cm. With the aid of equation 7, however, it was possible to construct a nomogram (Figure 17) relating the angular setting of the goniometer (or interplanar spacing of the mineral, "d") to the length of sample used, from which it was possible to read off the correction factor that had to be applied to the diffracted intensity.

The holder manufactured for use in the present study was made of brass. Its design is shown in Figure 18. The sample is loaded from the end after the brass plate shown in the Figure has been securely clamped over the open groove. An essential feature of this design is that the two mating surfaces of sample holder and backing brass plate must be absolutely flat to ensure that the sample does not leak out during loading, and also that the sample surface is level with that of the sample holder. Brass was selected as the material for the backing plate because it was found that glass slides and plastics (as used by other investigators) tended to distort and also develop an electrostatic charge that tended to disrupt the sample surface when the plate was removed, leading to poor precision.

Although ideally, to minimize absorption errors, specimens should be made as thin as possible while remaining consistent with the equation of Alexander

and Klug (1948, p. 886) (equation 6, Section 8.5.3.3), it was found that a sample of this thinness could not be loaded properly. The prototypes of the sample holder had a groove with a depth of only 0.5 mm, but this resulted in poor precision as it was impossible to obtain uniformity of filling of the holder. It was found in practice that the depth of the groove in the sample holder had to be between 1 and 1.5 mm in order to enable the sample to be loaded satisfactorily. This thickness of 1.5 mm had the advantage of ensuring that the sample was thick enough to mask background noise contributed by the holder (see Section 8.5.3.2). The groove in the holder was widened to 12.5 mm to ensure that at no stage could the X-ray beam impinge upon the holder at the sides of the sample. Since, however, the overall length of the sample holder was 5.4 cm, the X-ray beam could, under certain conditions, irradiate the small area of brass below the groove. At angular settings greater than 6.8° 2θ Cu K_{α} (13Å) the small area of brass cannot be irradiated and therefore no background is contributed by the holder under these conditions. At angular settings below this (i.e., at settings greater than 13 Å), however, there will be some contribution from the background, but, as the area of holder irradiated is approximately 1/15 that of the sample, it can be considered negligible.

Gibbs (1965, p. 741) has reviewed several techniques of sample loading that are applicable to quantitative clay mineral analysis by X-ray diffraction. Unfortunately, however, none of these techniques could be used in the present study, as they were all designed for samples that had been sedimented to obtain only the 2 micron fraction of the samples and, as has been mentioned earlier (Section 8.5.3.1), any technique involving size fractionation cannot be used in the quantitative analysis of a whole rock powder as it renders the sample unrepresentative.

8.5.3.5. Preferred orientation and intensity measurements.

The platy morphology of the phyllosilicates makes it possible that they will sometimes adopt a preferred orientation during packing into a sample holder. If this occurs, it results in the intensity of the basal (00ℓ) reflections being raised at the expense of the non-basal reflections. In the case of the present study, the problem of preferred orientation was overcome by the fact that the specially-designed wider sample holder (described in Section 8.5.3.4.2), together with the end-loading technique adopted, produced samples with a reproducible degree of orientation.

Various authors have suggested overcoming the problem of preferred orientation by the addition of diluents to samples containing substances that are

likely to adopt a preferred orientation. Von Engelhardt (1955, p. 435) advocated the addition of finely-ground cork powder to the sample, while Brindley and Kurtossy (1961, pp. 1208 - 1209) suggested a technique that involved the mixing of samples with a thermoplasticorganic cement, the addition of Dioxane to dissolve the cement and the subsequent grinding of the mixture to a fine powder after drying. Both these techniques were considered unsuitable for use in the present study, for the following reasons:

(1) The addition of any diluent lowers the detection limits of the minerals present in the mixtures to be analysed.

(2) The proposed techniques call for considerable additional work to ensure that there is adequate mixing of the sample with the diluent, and at the same time carry with them the danger of contaminating the sample.

(3) The addition of a diluent alters the total mass absorption coefficient of the sample. Thus, if these techniques had been adopted, the mass absorption coefficients of all the samples would have had to be re-measured before the diffraction results could have been evaluated.

8.5.3.6. Mass absorption and peak intensities.

As was the case in quantitative X-ray fluorescence analysis (see Section 8.4.2), absorption effects are also extremely important in quantitative X-ray diffraction analysis and must be taken into account. A simple comparison of the diffraction patterns obtained from crushed whole rock powder samples (such as were examined in the present study) would not give a true reflection of the weight concentrations of the components present in the samples if the comparison was based only on the peak heights of the various components without suitable allowance being made for absorption effects. Klug and Alexander (1954, pp. 92 & 411) have drawn attention to the situation that arises when a mixture contains both a strong absorber (such as pyrite) and a weak absorber (such as quartz). The net effect is that the peaks of the weakly-absorbing material (quartz in this example) appear weaker, and those of the strong absorber (pyrite) appear stronger, than would have been expected from the linear relationship between concentration and peak intensity for each separate component.

Because of this situation, the quantitative analysis of any multicomponent mixture by means of X-ray diffraction presents considerable difficulties, in addition to problems caused by matters such as orientation and grain size. The difficulties presented by the quantitative X-ray diffraction analysis of multicompo-

nent systems have been confronted by numerous earlier investigators, but usually the scope of these investigations was confined to two- or three-component systems. In the case of the present study, however, it was necessary to develop techniques that would permit quantitative X-ray diffraction analysis for five major components (muscovite, pyrophyllite, chlorite, pyrite and "quartz", which was determined by difference) to be carried out on samples that often contained more than 10 components, although many of these other components were only present in minor amounts lying at, or just below, the detection limit. The summed effect of all these minor components on the total mass absorption coefficient of the sample could not be overlooked or dismissed, however, and it was thus necessary to ensure that the method of quantitative X-ray diffraction analysis developed for the purposes of the present study should take the total mass absorption coefficient of the sample into account.

8.5.4. Methods of quantitative X-ray diffraction analysis.

A brief discussion of some of the methods of quantitative X-ray diffraction analysis that have been proposed by earlier workers follows below. This precedes a description of the method finally adopted for use in the present study (see Section 8.5.5).

Klug and Alexander (1954, p. 412) have pointed out that the basic principle underlying the quantitative X-ray diffraction analysis of multicomponent mixtures is that the sample in question must be considered as being composed of just two components, the particular mineral that is to be analysed for and the sum of all the other minerals, which may be conveniently called the "matrix". The equation developed by Klug and Alexander (1954, pp. 411 - 415) for the analysis of any mixture is as follows:

$$I_1 = \frac{K_1 x_1}{\rho_1 [x_1(\mu_1^* - \mu_M^*) + \mu_M^*]} \quad . \; . \; . \quad \text{Equation 8}$$

where I_1 is the intensity diffracted by the component (component 1) that is being analysed for

K_1 is a constant that depends on the nature of component 1 and the geometry of the apparatus

x_1 is the weight fraction of component 1 in the mixture

μ_1^* is the mass absorption coefficient of component 1

μ_M^* is the mass absorption coefficient of the matrix

ρ_1 is the density of component 1

Although equation 8 provides the theoretical basis for all quantitative X-ray diffraction analysis of multicomponent mixtures, it is not easy to evaluate in practice.

When quantitative X-ray diffraction analysis is actually undertaken in practice, a method of countering absorption effects must be found, the method that is most commonly adopted involving the addition of an internal standard to the sample (Klug and Alexander, 1954, p. 426). In the case of the present study, however, it was again decided (as was earlier decided for quantitative X-ray fluorescence analysis -- Section 8.4.3.1) that the use of an internal standard method would not be advisable, since not only is the addition and proper blending of an internal standard time-consuming and difficult, but also the addition of an internal standard dilutes the sample, increases the number of measurements required and carries with it the danger of contaminating the sample.

Various authors have proposed methods of quantitative X-ray diffraction analysis that do not require the use of an internal standard. Williams (1959, pp. 1842 - 1843) has suggested a method that calls for a sample of finite thickness to be mounted on a copper specimen holder, with corrections for absorption effects being obtained from the intensity of a reflection from the specimen holder. This method involves the use of a rotating specimen holder and is unfortunately limited to samples with low mass absorption, or alternatively requires dilution to ensure that samples have low total mass absorption. It was not found possible to make use of this method in the case of the present study.

Leroux, Lennox and Kay (1953, p. 740) and Lennox (1957, p. 767) have also proposed methods of quantitative X-ray diffraction analysis that do not require the use of an internal standard. The basis of these methods is the following relationship, which was derived by the authors from the basic equation (equation 8):

$$x_1 = \left(\frac{I_1}{(I_1)_o}\right)\left(\frac{\mu_s^*}{\mu_1^*}\right) \quad \text{Equation 9}$$

where $(I_1)_o$ is the integrated intensity of pure component 1

I_1 is the integrated intensity of component 1 in the mixture

μ_s^* is the mass absorption coefficient of the sample

μ_1^* is the mass absorption coefficient of pure component 1

x_1 is the weight fraction of component 1 in the sample.

Niskanen (1964, p. 1268) developed a practical analytical procedure based on the methods proposed by Leroux and coworkers. He was able to obtain excellent quantitative results on a series of synthetic mixtures composed of kaolinite, quartz and calcite, the mean absolute error (defined as the difference between the X-ray results and the actual percentages) of his analytical results being only 1.5%. Niskanen made use of an external standard consisting of fine quartz powder moulded in Lucite to standardize the X-ray intensity so that comparable results could be obtained on a day-to-day basis. Niskanen estimated that, if his technique were to be used in the analysis of actual rock samples, the mean absolute error would be within 5%. For the purposes of the present study, however, Niskanen's method has a drawback in that it requires a knowledge of the intensity and mass absorption coefficient of the pure component (as can be seen from equation 9). In the case of the present study this data was not available, because of the virtual impossibility of obtaining samples of the phyllosilicates encountered in the Witwatersrand banket in a 100% pure form and because of the difficulty of obtaining "absolute" integrated values on samples of pure phyllosilicate when a phyllosilicate does happen to be available in a pure form (see Section 8.5.5.1), and thus Niskanen's method could not be used in the present investigation.

Black (1963, pp. 15 - 16) independently derived an equation of a form fundamentally similar to equation 9 (though with minor refinements) as the basis for his method for the analysis of bauxites. The application of Black's equation is, however, confined to those cases where the background on either side of the analytical peak in question can be expressed as a linear function of the reciprocal mass absorption coefficient of the material. As far as the present investigation is concerned, Black's method suffers from the same drawback as Niskanen's method inasmuch as it requires that pure component be available, in this case not only so that the "maximum" intensities can be determined but also to see how the backgrounds which are associated with all the chosen lines vary with absorption coefficient. The use of Black's method in the present investigation had thus to be ruled out.

Karlak and Burnett (1966, pp. 1742 - 1743) have proposed a method based on an interesting mathematical treatment of basic theory, but their method requires a knowledge of matrix theory for its application so that the likelihood of its general adoption is limited. From their work (Karlak and Burnett, 1966, p. 1744) one significant fact emerges, however, namely that when more than 3 components are to be analysed for in a mixture it is advisable to use intensity values obtained from binary calibration mixtures as an aid in the calculation of the results.

Tatlock (1966, p. 1) has developed an interesting technique for the analysis of felsic rocks. This method makes use of calibrated X-ray diffraction patterns established with the aid of standard powders, which consist preferably of minerals separated from the suite of rocks under study. Unfortunately the technique is limited to the analysis of rocks with relatively constant and restricted mineral assemblages. It is, however, interesting to note that Tatlock, like Niskanen (1964, p. 1268), makes use of the reflection obtained from quartz to adjust the instrument settings so that the data can be rendered comparable on a day-to-day basis.

An entirely new approach to the problem of multicomponent analysis has been made by Moore (1968, p. 325). This is based on the concept that the intensity of any given diffraction maximum is linearly affected by the relative amounts of the other mineralogical components present, or, put mathematically, that any mineral suite composed of n different components may be described by an n dimension linear manifold. The solution of such a system is facilitated by the principles of linear algebra, and statistical analysis may be applied through multiple linear regression. Moore has applied his method to the analysis of 2- and 3-component systems consisting of mixtures of quartz, fluorite, kaolinite, glauconite, illite and montmorillonite, and claims an accuracy of within 2 per cent for the method. Moore has pointed out (1968, p. 335) that in the analysis of binary mixtures the absolute percentage error, defined as $(X - X_1) \cdot 100$ where X is the concentration indicated and X_1 is the actual concentration of material in the binary mixture, is largest when the percentages of the two components are nearly equal. The error tends to zero as the proportions approach either single component end point.

8.5.5. Method of X-ray diffraction analysis adopted for the present study.

8.5.5.1. General considerations.

The method of quantitative X-ray diffraction analysis that was finally adopted for the present study is based on an equation published by Norrish and Taylor (1962, p. 99). This equation is of the same form as the one proposed by Reynolds (1967, p. 1500) that was used in the calculation of the X-ray fluorescence results of the present study (equation 5, see Section 8.4.4.2). The equation used in the calculation of the X-ray diffraction results of the present study is as follows:

$$x_1^u = \frac{I_1^u}{I_1^s} \cdot \frac{\mu^{*u}}{\mu^{*s}} \cdot x_1^s \quad . \quad . \quad . \quad . \quad \text{Equation 10}$$

where x_1^u is the unknown concentration of mineral 1 in the sample being analysed

x_I^s is the known concentration of mineral 1 in a standard mixture

I_1^u is the integrated area of reflection of mineral 1 in the sample

I_1^s is the integrated area of reflection of the same diffraction line of mineral 1 in the standard mixture

$\overset{*u}{\mu}$ is the mass absorption coefficient of the sample being analysed, containing mineral 1

$\overset{*s}{\mu}$ is the mass absorption coefficient of the standard mixture containing mineral 1.

The use of equation 10 as the basis of a method of analysis has the advantage of not requiring any internal standards or calibration charts, and, in addition, of making it possible for any diffraction peak produced by mineral 1 to be selected for the measurement of I_1. This latter fact is of considerable importance in the analysis of multicomponent systems such as rocks since, because of the complexity of patterns that may occur, any preselected line may suffer interference from adjacent or coincident lines, while in the case of the present technique the selection of a suitable line for measurement can be made after the diffractometer trace has been obtained. Another advantage of the technique adopted for the present study is that pure minerals are not required to act as standards, as they were in many of the methods discussed in Section 8.5.4, but that mixtures of known composition may be used instead. The use of pure minerals as standards is, of course, not precluded by equation 10, but in the case of the present study pure-mineral standards were considered to be impracticable for the reasons listed below:

(1) It was found to be virtually impossible to obtain samples of the phyllosilicates encountered in the Witwatersrand banket in a 100% pure form.

(2) Even when a pure phyllosilicate happened to be available for use as a standard, it was found that it was very difficult to obtain reliable "absolute" intensity values because of the orientation problems that arise when pure phyllosilicates are subjected to X-ray diffraction analysis. This was clearly illustrated by a test carried out in the course of the present investigation, in which a comparison was made between the precision of the results that could be obtained from a sample of pure muscovite and the precision obtainable from a quartz-muscovite mixture (consisting of 30 per cent quartz and 70 per cent muscovite). Both samples were endloaded 10 times andintegrated intensities for the quartz $(10\bar{1}0)$ peak and for the

muscovite (002) peak were obtained by means of the Disc Integrator. When the quartz ($10\bar{1}0$) peak produced by the quartz-muscovite mixture was measured, the coefficient of variation of the measurements was found to be 3.64%, while the coefficient of variation of measurements of the muscovite (002) peak was found to be 3.16% when the peak was produced by the quartz-muscovite mixture but 7.32% when the peak was produced by pure muscovite. The wider scatter of results obtained when measurements were made on pure muscovite may almost certainly be ascribed to the occurrence of a greater degree of preferred orientation in the muscovite when quartz was not present to act as a diluent. These findings indicate why the equation (equation 9) used by Leroux, Lennox and Kay (1953, p. 740), Niskanen (1964, p. 1268) and Black (1963, pp. 15 - 16) could not be used in the present study to calculate X-ray diffraction results, since equation 9 requires a knowledge of "absolute" intensity values measured on the pure component and it was apparent that little reliance could be placed on "absolute" intensity values measured on pure phyllosilicates (see Section 8.5.4).

It was thus clear that, in the present study, mixtures of known composition would have to be used as standards for quantitative X-ray diffraction analysis. As was mentioned in Section 8.5.4, Karlak and Burnett (1966, pp. 1742 - 1743) have stressed the advantages of using binary mixtures as standards in the analysis of multicomponent systems (in preference to multicomponent standard mixtures), and accordingly binary mixtures of known composition were prepared for use as standards in the present investigation.

8.5.5.2. The preparation of binary-mixture standards.

When standards are prepared for use in the quantitative X-ray diffraction analysis of a rock, the X-ray intensities of the minerals present in that rock should be simulated as closely as possible. Ideally, the minerals that are to be used as standards should be extracted from a sample of the actual rock that is to be analysed. When analysing samples from the Witwatersrand banket, however, it is seldom possible to extract minerals from the banket in a sufficiently high state of purity to permit them to be used in the preparation of standards, and minerals obtained from other sources must often be used instead. This unfortunately introduces some errors, because of differences in reflection intensities between minerals from different sources, but these errors cannot be avoided.

In the present study, five minerals (muscovite, pyrophyllite, chlorite, pyrite and quartz) were to be analysed for, and accordingly, high-purity samples of these five minerals were required for the preparation of standards.

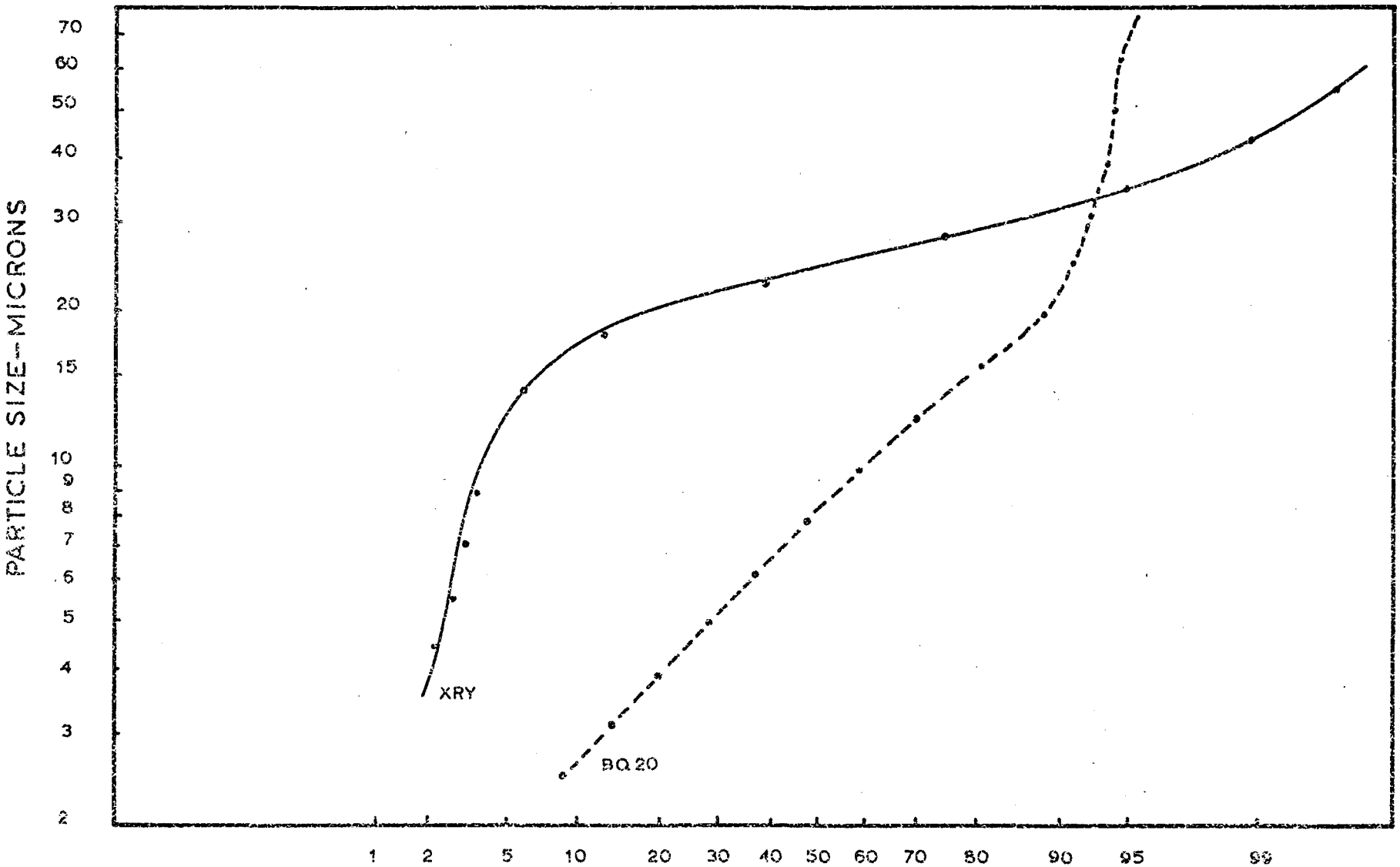


FIGURE 19 CUMULATIVE WEIGHT — PERCENT PROBABILITY

These high-purity samples were obtained in the following manner:

Muscovite: The muscovite used was one originally mined from a pegmatite in the Eastern Transvaal (Selati) and supplied in a "micronized" state. The median grain size was of the order of 5 microns and the purity greater than 99 per cent, based on the results of X-ray diffraction analysis and microscopic examination. The characterization of this muscovite is described in Part II of this thesis.

Pyrophyllite: The pyrophyllite used was obtained by the flotation of ore from the Loraine Gold Mine and was found to be 92 per cent pure, containing 7 per cent of quartz and 1 per cent of muscovite as impurities. The characterization of this pyrophyllite is also described in Part II of this thesis.

Chlorite: The chlorite used was obtained from the Ventersdorp Contact Reef at Venterspost and purified by heavy liquids. The chlorite was found to be 85 per cent pure and to contain 15 per cent of quartz as an impurity. Again, the characterization of this chlorite is described in Part II of this thesis.

Pyrite: The pyrite was obtained from Vogelstruisbult Mine on the East Rand, representing portion of a flotation concentrate prepared at the mine. The pyrite was further purified by heavy liquid and magnetic separations to yield a final concentrate that assayed over 98 per cent pure.

Quartz: The quartz powder used was obtained by grinding large optically-pure Brazilian quartz crystals in a Siebtechnik grinder for 90 seconds and air-elutriating the resulting powders to obtain an estimated particle size distribution of the order of less than 20 microns (XRY, see Figure 19). This was then further water-elutriated to yield a fraction with a median grain size of 8.4 microns, referred to as sample BQ 20 (see Figure 19).

The preparation of binary mixtures from these five minerals was carried out as follows:

The five "standard" minerals (muscovite, pyrophyllite, chlorite, pyrite and quartz) were first dried for 1 hour at 105^{o}C, and then, with the aid of an analytical balance, binary mixtures of muscovite-quartz, pyrophyllite-quartz, chlorite-quartz and pyrite-quartz were made up with due allowance for the presence of impurities in the components. The mixtures were then placed in screw-top glass bottles with two 1/4-inch steel ball bearings and violently agitated on a commercial flask shaker for 1 hour. All binary-mixture standards were prepared in duplicate, and care was taken to ensure that pairs of standards were always shaken simultaneously.

8.5.5.3. The determination of mass absorption coefficients for Witwatersrand samples and for binary-mixture standards.

When, as in the present investigation, a method of quantitative X-ray diffraction analysis based on the application of equation 10 is adopted, it then becomes necessary to determine the mass absorption coefficient of each sample (μ^{*u}) and each standard (μ^{*s}). This is a consequence of the fact that this method of X-ray diffraction analysis does not require any internal standards, since the use of internal standards in other analytical methods is essentially an indirect way of allowing for the term μ^{*u}/μ^{*s}. The mass absorption coefficients must be measured at the same wavelength as that used in the measurement of the diffracted intensities (I^u and I^s), as the use of any other wavelength could give rise to serious errors if an element with an absorption edge between the two wavelengths happened to be present. In the present investigation Cu K_α radiation was used for both absorption and diffraction measurements.

The method that was developed for the determination of mass absorption coefficients in the present study has been described in detail in Section 8.4.2.2. The value of the mass absorption coefficient (μ^{*u}) of each of the 143 Witwatersrand samples undergoing analysis was determined by this method at the time when these samples were being investigated with the aid of X-ray fluorescence techniques. In the case of the binary-mixture standards, however, a slightly different approach was adopted for the determination of μ^{*s}, in that mass absorption coefficient measurements were only carried out on certain of the binary-mixture standards while the mass absorption coefficients of the remaining binary-mixture standards were calculated from these measured coefficients with the aid of equation 2 (Section 8.4.2.1). Equation 2 states that the mass absorption coefficient of any mixture can be calculated in the following manner from the mass absorption coefficients of the pure components constituting the mixture and the weight fractions of the components in the mixture:

$$\mu^*_{sample} = W_A \cdot \mu^*_A + W_B \cdot \mu^*_B + \ldots\ldots + W_N \cdot \mu^*_N \quad \ldots\ldots\ldots \text{Equation 2}$$

where μ^*_{sample} is the total mass absorption coefficient of the mixture

W_N is the weight fraction of component N ($W_A+W_B+\ldots\ldots+W_N = 1$)

μ^*_N is the mass absorption coefficient of component N at the wavelength under consideration.

Thus, once the method of mass absorption coefficient measurement described in Section 8.4.2.2 had been used to determine the mass absorption coefficients of 100% pure quartz and of a binary-mixture standard of known composition where quartz was one of the two components, it became a simple matter to use equation 2 to calculate the mass absorption coefficient for any other binary mixture having the same two components but a different composition. This calculation could, of course, have been carried out manually, but in the present study, to save time, the computer programme NIMMNHNS, programme 7 listed in Section 9, was used to calculate the mass absorption coefficients over the whole range of binary mixtures involved, from the pure component on the one hand to a mixture of 1% component with 99% quartz on the other. This procedure greatly facilitated the determination of the term μ^{*s} for insertion in equation 10.

8.5.5.4. Procedure adopted for quantitative X-ray diffraction analysis.

8.5.5.4.1. Instrument settings.

A Philips wide range goniometer model PW 1050 was used for all the determinations. The instrumental settings used were as follows:

Radiation:	copper with nickel filter
X-ray generator output:	40kV, 20 mA
Goniometer scanning speed:	1 degree 2θ per minute
Slits:	1^{o} divergence, 0.1^{o} receiving, 1^{o} scatter
Ratemeter settings:	400 or 1000 counts per second
Time constant:	2 seconds
Detector:	proportional counter
Discriminator:	pulse height discrimination was used. The discriminator was set to give optimum peak-to-background ratio while still passing 90% of the energy due to copper radiation.
Chart-recorder paper speed:	26.5 mm per minute
Integration:	by means of Disc Integrator
Sample holder:	special design, see Section 8.5.3.4.2.

8.5.5.4.2. Choice of analytical peaks.

When any multicomponent mixture, such as a rock, is subjected to quantitative X-ray diffraction analysis, the selection of a suitable analytical peak is

to a great extent governed by the nature of the components of the matrix. The matrix components may, for example, cause the occurrence of peak interference in the region of the strongest line of the component that is being analysed for, or, in the case of rocks containing phyllosilicates, it may be found necessary to use basal reflections in the interests of increased precision of measurement, although the use of basal reflections entails special precautions to minimize any tendency to preferential orientation.

The peaks that were finally chosen for the analysis of the three phyllosilicates (muscovite, pyrophyllite and chlorite), pyrite and quartz in the present study are listed in Table XXXIV.

TABLE XXXIV

ANALYTICAL PEAKS CHOSEN FOR THE X-RAY DIFFRACTION ANALYSIS OF MUSCOVITE, PYROPHYLLITE, CHLORITE, PYRITE AND QUARTZ

MINERAL	ANALYTICAL PEAK
Muscovite	(002)
Pyrophyllite	(002)
Chlorite	(002)
Pyrite	(200)
Quartz	$(11\bar{2}0)$

8.5.5.4.3. Detection limits.

The detection limits, as defined by de Vries (1966, p. 5) (see Section 8.5.2.2), are set out in Table XXXV.

TABLE XXXV

X-RAY DIFFRACTION DETECTION LIMITS FOR MUSCOVITE, PYROPHYLLITE, CHLORITE, PYRITE AND QUARTZ

MINERAL	DETECTION LIMIT PER CENT
Muscovite	1
Pyrophyllite	2
Chlorite	2
Pyrite	3
Quartz	1

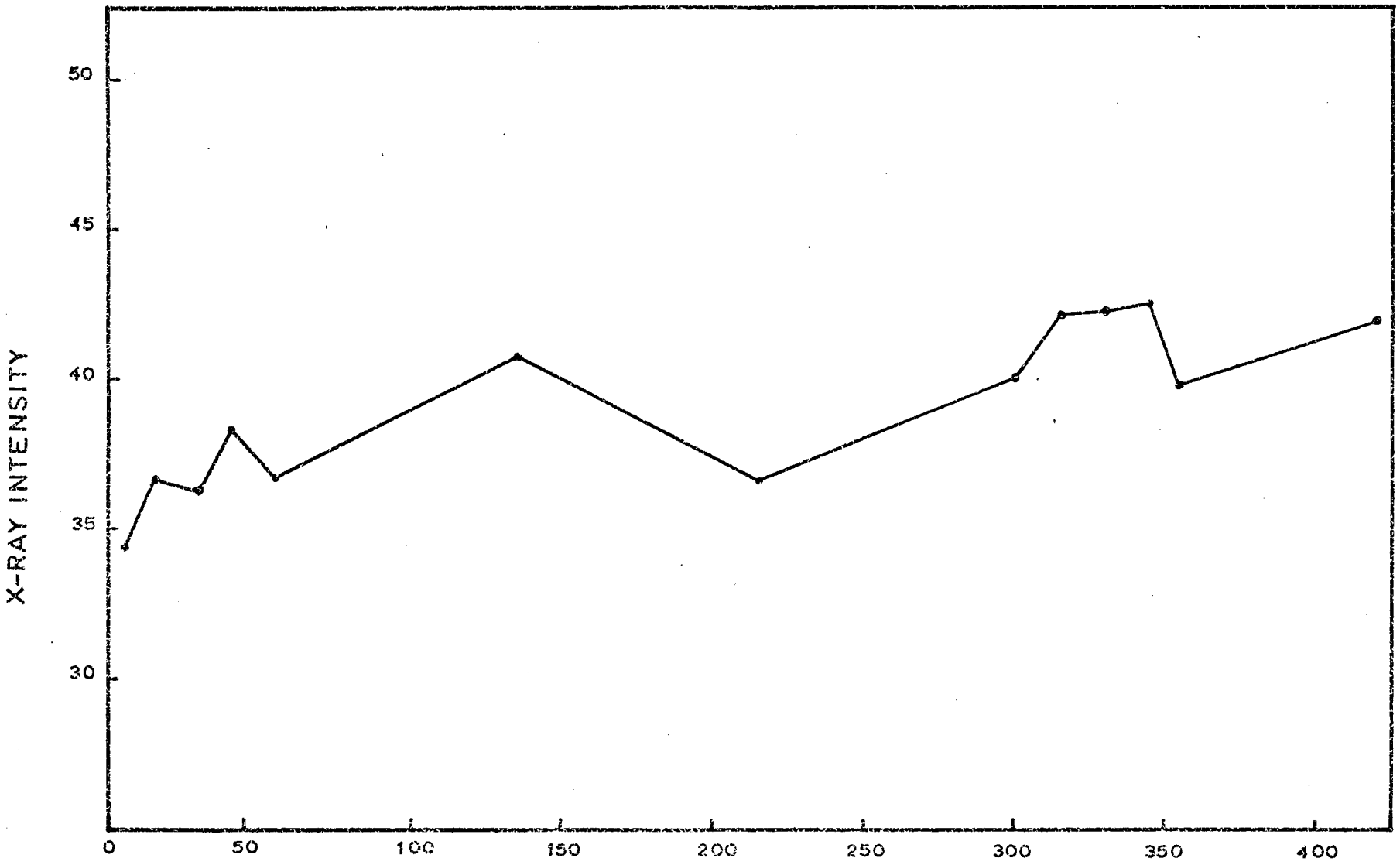

X-RAY INTENSITY
50
45
40
35
30
0
50
100
150
200
250
300
350
400
TIME—MINUTES

FIGURE 20

8.5.5.4.4. Precision of measurement.

In order to obtain some idea of the degree of reproducibility of peak intensity measurements on a day-to-day basis, various tests were carried out to investigate the stability of the instrument used in the present study. The results of these tests were as follows:

(1) A $3^{o}C$ rise in temperature of the instrument was found to result in an increase of less than 0.2% in the integrated intensity.

(2) Variations in diffracted intensity with respect to time were investigated by carrying out 160 consecutive measurements, at a scanning speed of 1^{o} 2θ per minute, on the quartz $(11\bar{2}0)$ peak produced by a sample of powdered quartz with a median grain size of 8.4 microns (sample BQ 20, see Section 8.5.5.2) set in a matrix of fibre-glass ground to a mirror-like flat finish with fine abrasives. The sample was moved between each set of 10 measurements. The changes in peak height over a period of 7 hours are shown in Figure 20. The peak heights were found to range from 34.7 to 42.7 (arbitrary units), with a mean of 39.6 and a coefficient of variation of 3.03%.

These results clearly indicated that it would be necessary to introduce some method of correction for short-term drift and random fluctuations in X-ray beam intensity, i.e., the need for the use of some external standard to enable comparable results to be obtained on a day-to-day basis became apparent. Two substances were considered for use as an external standard, the one being the quartz powder BQ 20 set in a matrix of fibreglass as described above and the other being a slab of novaculite, which is a very dense even-textured light-coloured cryptocrystalline siliceous rock similar to chert but characterized by a dominance of quartz rather than chalcedony (Tarr, 1937, pp. 18-47). When the suitability of these two substances was compared by carrying out 10 repeated observations of integrated intensity (using the Disc Integrator) on the quartz $(10\bar{1}0)$ peak produced by each substance, it was found that the coefficient of variation of the results was 0.82% when novaculite was used and 1.59% when quartz BQ 20 was used. It was thus clear that novaculite would be superior to quartz as an external standard.

8.5.5.4.5. Procedure adopted for the determination of diffracted intensities in Witwatersrand samples and binary-mixture standards.

The following analytical procedure was finally adopted for the determination of the diffracted intensities of the analytical peaks of each of the components being analysed for in the 143 Witwatersrand samples (I_1^u in equation 10) and

in the binary-mixture standards (I_1^s in equation 10):

Each sample was end-loaded into the specially-designed sample holder and scanned at 1^o 2 θ per minute, using the instrumental settings listed in Section 8.5.5.4.1. The integrated intensities of the analytical peaks of the minerals being analysed for were then determined with the aid of the Disc Integrator. Novaculite was used as an external standard to correct for short-term drift and random instrument fluctuations, and, after each sample had been run, the quartz $(11\bar{2}0)$ peak of novaculite was run and integrated in the identical way. The ratio of the integrated intensity of the analytical peak of the mineral being analysed for to the novaculite $(11\bar{2}0)$ peak was then calculated, and this corrected I_1^u was used in all subsequent calculations.

In the case of the binary-mixture standards, the analytical peaks selected for the components of the binary mixtures were, of course, the same as those chosen for the minerals in the banket samples (see Section 8.5.5.4.2). The loading and integration techniques adopted, and the instrumental settings used, were also identical to those used in the case of the Witwatersrand samples. Each standard was prepared in duplicate (as has been described in Section 8.5.5.2), and each of the duplicate standards was loaded and scanned three times, so that the integrated intensity of the analytical peak produced by a known quantity of the standard mineral was in fact determined six times. After each standard had been run, the quartz $(11\bar{2}0)$ peak of novaculite was run and integrated. The average value obtained for the integrated intensity of the analytical peak on the six standard runs was then divided by the average value obtained for the quartz peak on the six novaculite runs, and this corrected I_1^s was used in all subsequent calculations.

8.5.5.5. Calculation of results of quantitative X-ray diffraction analyses.

8.5.5.5.1. Preparation of calibration curves for binary-mixture standards.

As has been described in Section 8.5.5.2, the binary-mixture standards used in the present study were all mixtures of the analytical component (component 1 in equation 10) with quartz -- or, more specifically, the standards were mixtures of muscovite and quartz, pyrophyllite and quartz, chlorite and quartz, and pyrite and quartz. The exact composition of each standard mixture had to be selected on an arbitrary basis, and accordingly, in order to overcome any bias that might have been introduced by the selection of these particular standard mixtures, the following procedure was adopted:

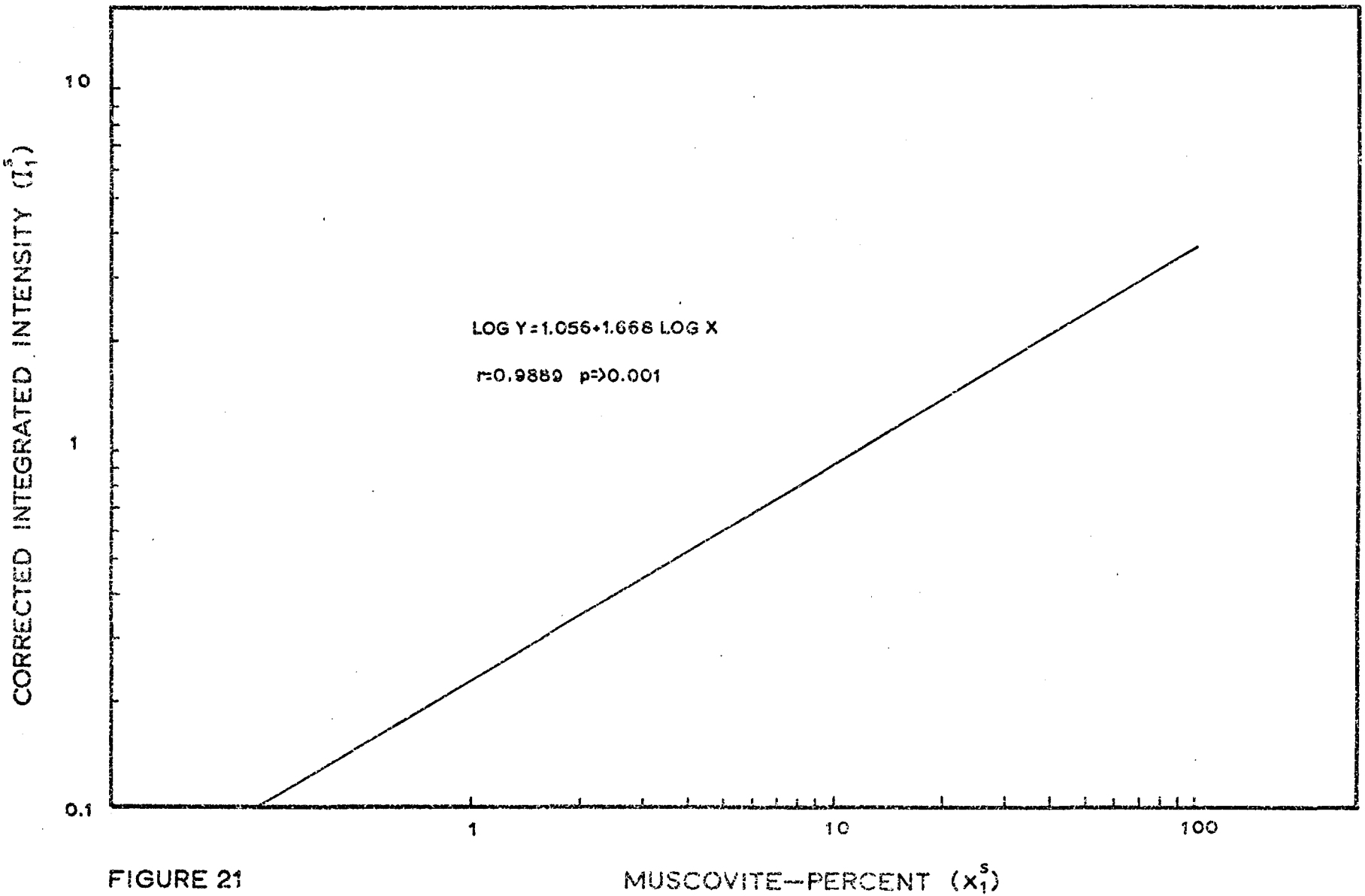

10
1
0.1
CORRECTED INTEGRATED INTENSITY (I_1^s)
LOG Y=1.056+1.668 LOG X
r=0.9889 p=>0.001
1
10
100
MUSCOVITE—PERCENT (x_1^s)

FIGURE 21

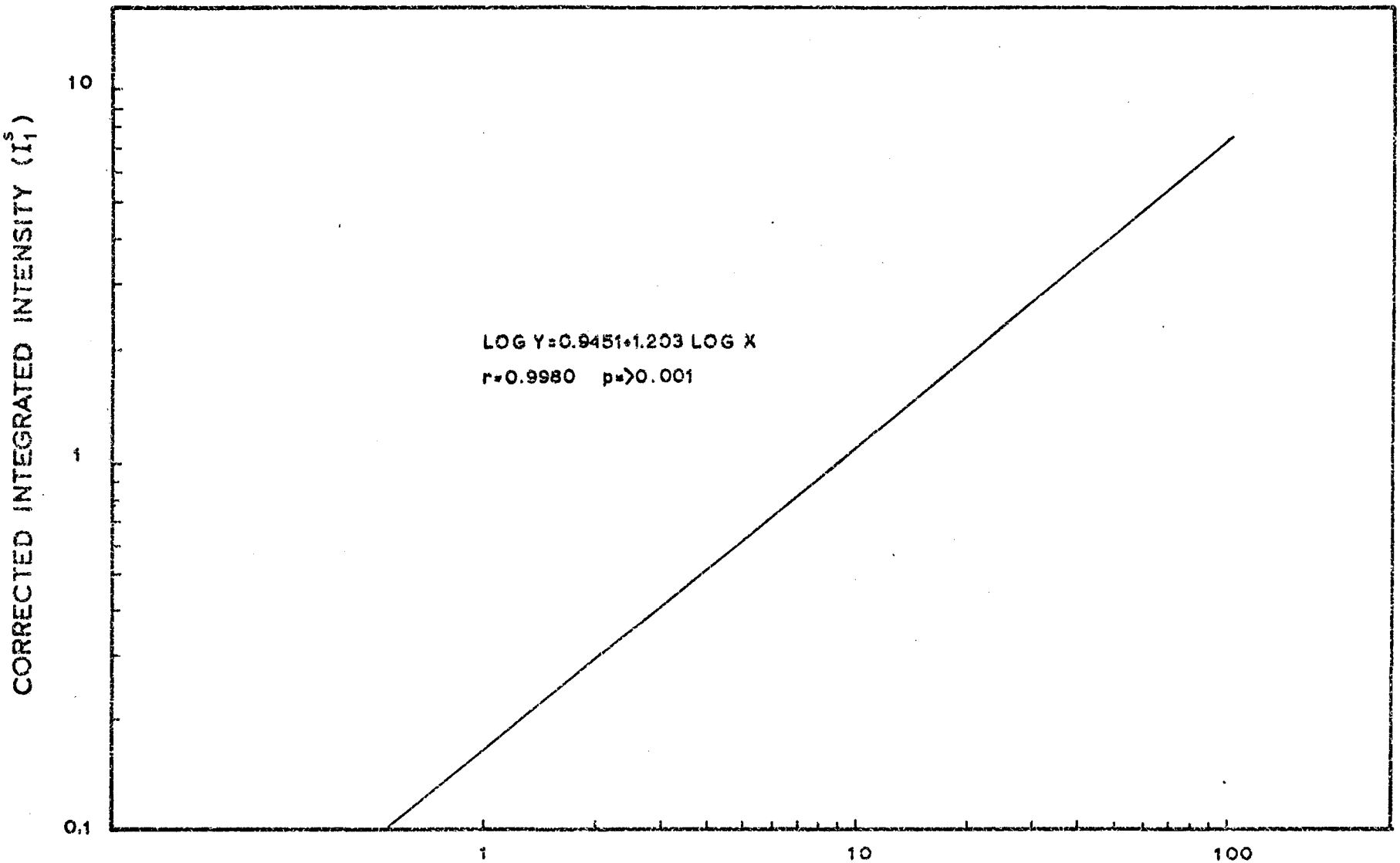


FIGURE 22 CHLORITE PERCENT (x_1^s)

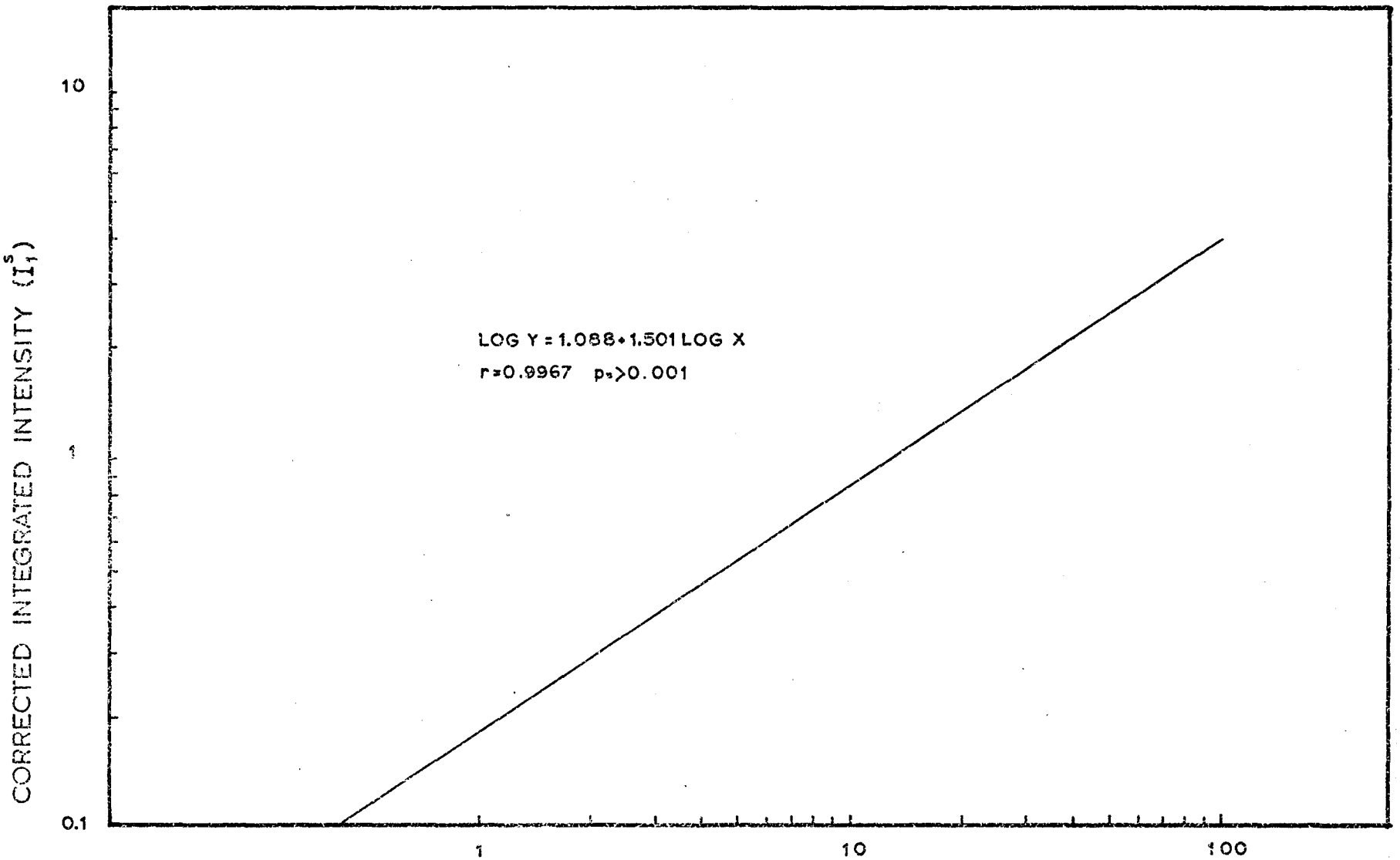


FIGURE 23 PYROPHYLLITE— PERCENT (x_1^s)

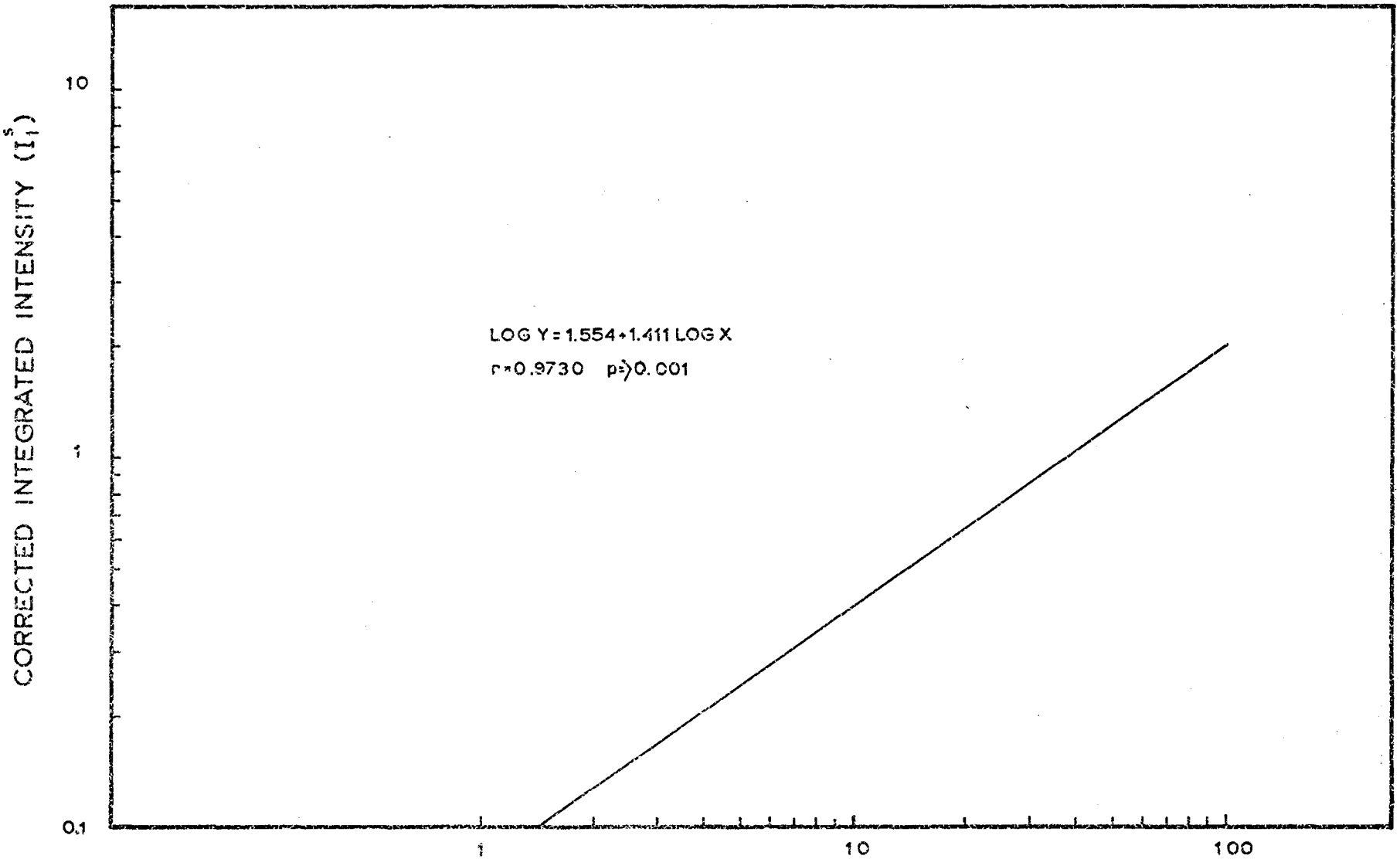


FIGURE 24 PYRITE- PERCENT (x_1^s)

Regression lines of "corrected integrated intensity" (corrected I_1^s) on the concentration of phyllosilicate or pyrite in the binary mixture (x_1^s) were fitted by least squares, using the computer programme DALKREG written by C. van Tonder of the National Institute for Metallurgy. These regression lines are shown in Figures 21, 22, 23, and 24. The correlation coefficients for the straight lines fitted ranged between 0.97 and 0.99, and the level of significance was in all cases greater than 0.1 per cent. From the graphs of the regression equations it was possible to read off the value of the integrated intensity of the analytical line produced by the phyllosilicate or pyrite in the binary mixture (I_1^s) for <u>any</u> concentration of the phyllosilicate or pyrite in the binary mixture (x_1^s). Alternatively, the actual regression equations produced by DALKREG could be used to calculate the value of I_1^s for any particular x_1^s, and this was the method finally adopted in the present study in view of the greater accuracy in determining I_1^s permitted by this latter method. As an aid in calculation, tables were constructed to show the value of I_1^s (calculated from the regression equations) at each 1% increment of x_1^s.

8.5.5.5.2. Evaluation of equation 10.

As was mentioned in Section 8.5.5.1, equation 10 states that:

$$x_1^u = \frac{I_1^u}{I_1^s} \cdot \frac{\mu^{*u}}{\mu^{*s}} \cdot x_1^s \quad \ldots\ldots\ldots \text{Equation 10}$$

where x_1^u is the unknown concentration of mineral 1 in the sample being analysed

x_1^s is the known concentration of mineral 1 in a standard mixture, in this case a mixture of mineral 1 and quartz

I_1^u is the corrected integrated area of reflection of mineral 1 in the sample (see Section 8.5.5.4.5)

I_1^s is the corrected integrated area of reflection of the same diffraction line of mineral 1 in the standard mixture (calculated from regression equations -- see Section 8.5.5.5.1)

μ^{*u} is the mass absorption coefficient of the sample being analysed, containing mineral 1 (see Section 8.5.5.3)

μ^{*s} is the mass absorption coefficient of the standard mixture containing mineral 1 (see Section 8.5.5.3)

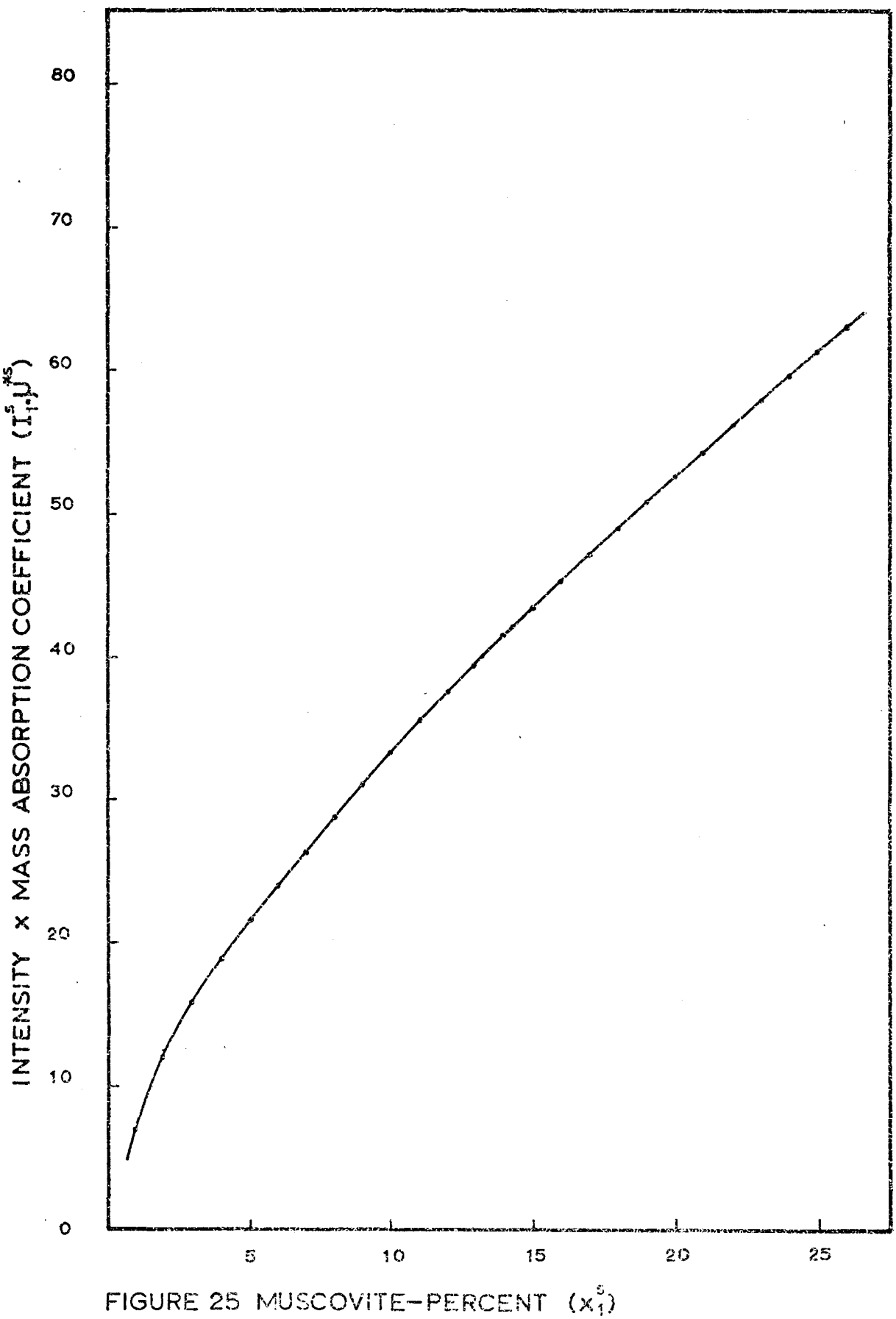


FIGURE 25 MUSCOVITE–PERCENT (x_1^5)

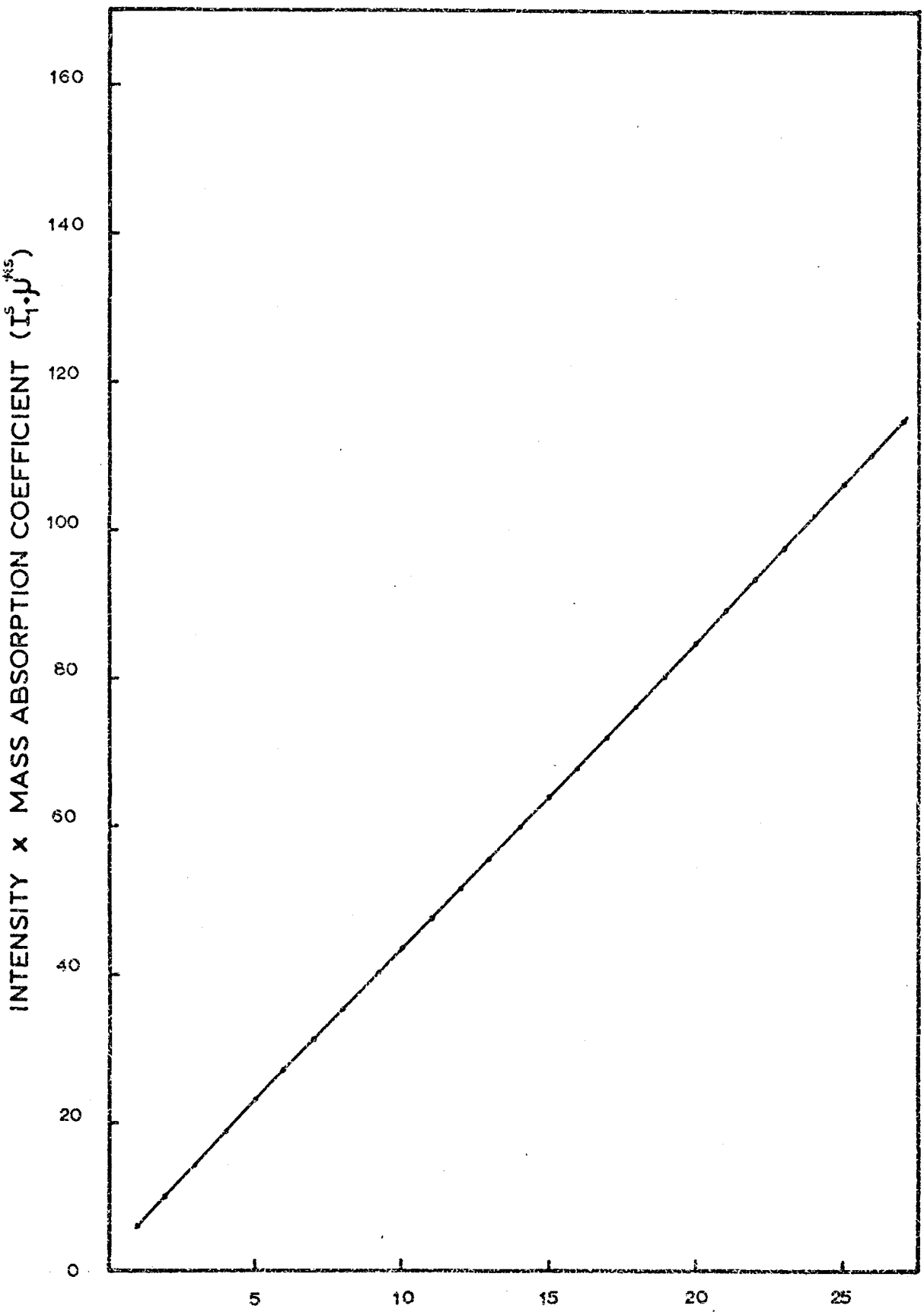


FIGURE 26 CHLORITE– PERCENT (x_1^S)

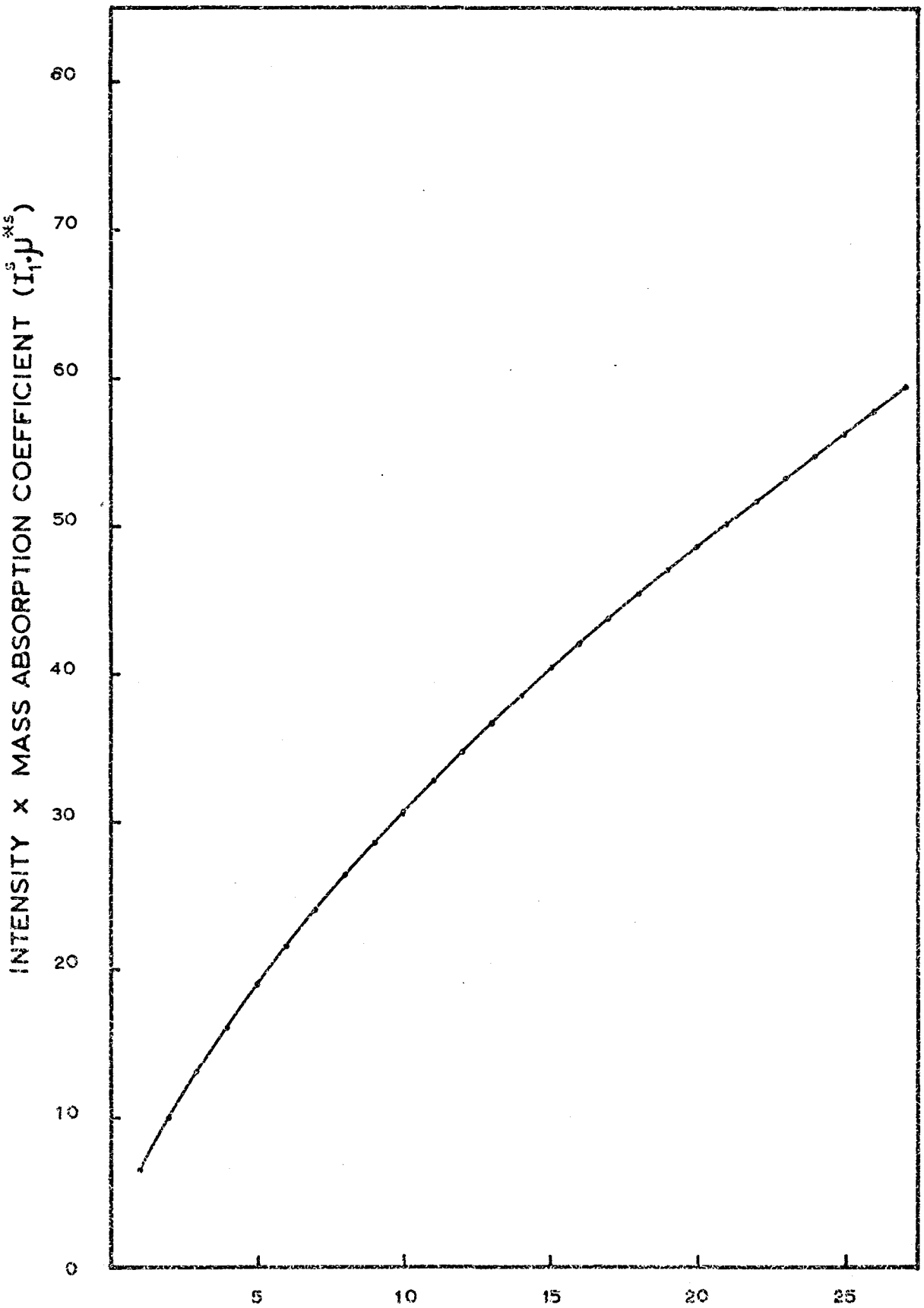


FIGURE 27 PYROPHYLLITE – PERCENT (x_1^s)

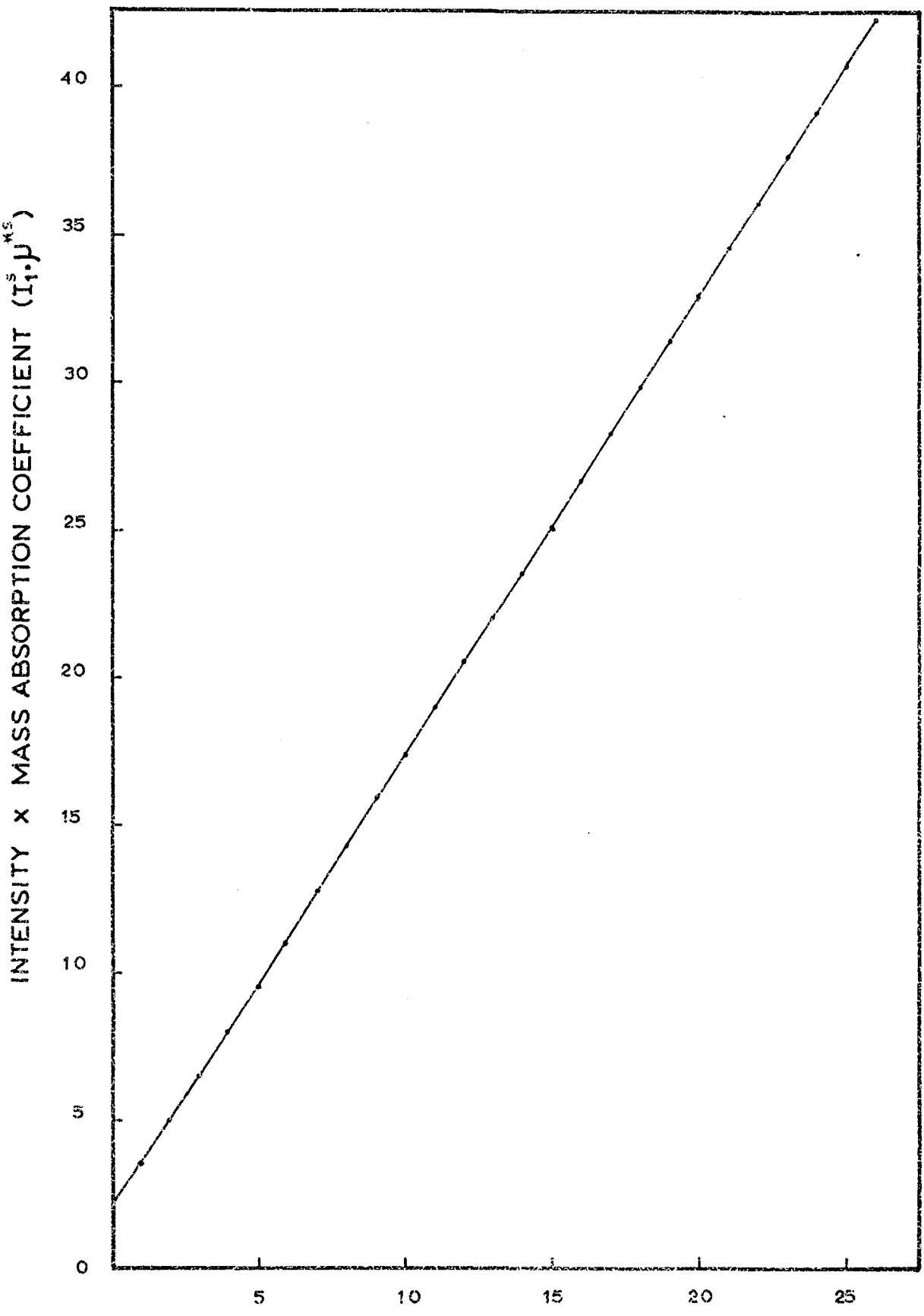


FIGURE 28 PYRITE-- PERCENT (x_1^s)

After the analytical procedures described in preceding paragraphs have been carried out, all the quantities on the right-hand side of equation 10 have been determined experimentally and the value of x_1^u can easily be calculated. In the case of the present study, however, it was found useful to adopt the procedure described below for the sake of added convenience in calculation:

The corrected integrated intensity produced by component 1 in a binary mixture (I_1^s) and the mass absorption coefficient of that binary mixture (μ^{*s}) were calculated at each 1% increment of the weight percentage of component 1 in that mixture (x_1^s). The product of each I_1^s and μ^{*s} was then plotted against each respective x_1^s. These curves relating $I_1^s \cdot \mu^{*s}$ to x_1^s for the binary-mixture standards muscovite-quartz, chlorite-quartz, pyrophyllite-quartz and pyrite-quartz (component 1 being respectively muscovite, chlorite, pyrophyllite and pyrite) are shown in Figures 25, 26, 27 and 28. Once these graphs have been plotted, the graph for each series of binary-mixture standards made up from a specific component 1 and quartz can be used to read off the value of the weight fraction (x_1^u) of component 1 in any sample (not necessarily a binary mixture) from the products of the integrated area of reflection produced by mineral 1 in the sample (I_1^u) and the mass absorption coefficient of that sample (μ^{*u}). Thus, when the results of the quantitative X-ray diffraction analyses of the 143 Witwatersrand samples were being calculated, the corrected value of I_1^u was first obtained (as described in paragraph 8.5.5.4.5), and this was then multiplied by the mass absorption coefficient μ^{*u} of the particular sample being analysed. From the resulting $I_1^u \cdot \mu^{*u}$, the concentration x_1^u of the component being analysed for (muscovite, chlorite, pyrophyllite or pyrite) was then read off from the graphs shown in Figures 25, 26, 27 and 28. "Quartz" (i.e., quartz plus all the other components of the banket sample that were not being analysed for) was then determined by difference after the amounts of muscovite, chlorite, pyrophyllite and pyrite in each sample had been calculated.

8.5.5.6. Check on the accuracy of the method of quantitative X-ray diffraction analysis adopted in the present study.

In order to evaluate the accuracy of the results obtainable by means of the method of quantitative X-ray diffraction analysis adopted in the present study, the following test was carried out:

Three different five-component mixtures, consisting of muscovite, chlorite, pyrophyllite, pyrite and quartz, were made up from the five high-purity

minerals in a manner identical to that used in the preparation of the binary-mixture standards (see Section 8.5.5.2). These three five-component mixtures of known composition were then treated as unknown samples and analysed by means of the X-ray diffraction method adopted in the present study. The results of these analyses are set out in Table XXXVI.

TABLE XXXVI

RESULTS OF QUANTITATIVE X-RAY DIFFRACTION ANALYSES CARRIED OUT ON THREE STANDARD MIXTURES CONSISTING OF MUSCOVITE, CHLORITE, PYROPHYLLITE, PYRITE AND QUARTZ

COMPONENT	TRUE CONC. %	INDICATED CONC. %	ABSOLUTE ERROR** %
Mixture No. 1 (μ^* = 45.32):-			
Muscovite	5.00	4.3	-0.70
Chlorite	5.00	5.6	+0.60
Pyrophyllite	5.00	5.6	+0.60
Pyrite	10.00	9.4	-0.60
"Quartz"	75.00	75.1 (by diff.)	+0.10
Mixture No. 2 (μ^* = 39.04):-			
Muscovite	10.11	8.8	-1.31
Chlorite	4.57	4.4	-0.17
Pyrophyllite	10.00	7.6	-2.40
Pyrite	5.00	5.6	+0.60
"Quartz"	70.32	73.6 (by diff.)	+3.28
Mixture No. 3 (μ^* = 50.97):-			
Muscovite	20.00	22.3	+2.30
Chlorite	0.00	---	-----
Pyrophyllite	20.00	20.00	0.00
Pyrite	15.00	14.6	-0.40
"Quartz"	45.00	43.1 (by diff.)	-1.90

** Absolute error = indicated concentration - true concentration

The last column of Table XXXVI, in which the absolute errors for the determination of the individual components are listed, provides an indication of the accuracy obtainable with the technique of quantitative X-ray diffraction analysis developed in the course of the present study. It can be seen that, on the whole, the absolute error of each determination compares very favourably with the mean absolute error of 1.5% which Niskanen (1964, p. 1270) obtained when he analysed synthetic mixtures by means of an X-ray diffraction technique that required pure components as standards (see Section 8.5.4). In fact, the mean absolute error of all the determinations listed in Table XXXVI is only 1.1%, which indicates that the accuracy of the binary-mixture-standard method of quantitative X-ray diffraction analysis used in the present study may be regarded as satisfactory.

8.6. The High-precision Determination of the Cell Parameters of Phyllosilicates.

8.6.1. General considerations.

In the course of the present study it was found necessary to carry out accurate determinations of the cell parameters of certain of the phyllosilicates present in the Vaal Reef and Ventersdorp Contact Reef samples, and also of certain other phyllosilicates which were examined for purposes of comparison with the phyllosilicates from the main suite of samples (see Part II of this thesis).

Various methods exist for obtaining high-precision values of cell constants and indexing the reflections obtained. In the case of the present study it was decided to use the diffractometer in preference to the Debye Scherrer camera in the interests of higher precision and resolution (Zussman, 1967, p. 281, and Brown 1961, p. 6). The use of the diffractometer also made it possible to obtain integrated intensities for the various reflections by means of the Disc Integrator attached to the recorder. A least squares refinement technique (Mirkin, 1964, p. 523) was regarded as the best approach for the calculation and refinement of the cell parameters. The reflections selected for least squares refinement were, as far as possible, reflections that could be indexed unambiguously. Usually more than 20 reflections were used for each computation, and, in view of the number of calculations involved, the results were evaluated with the aid of the IBM Model 360/50 digital computer at the University of the Witwatersrand.

Two computer programmes, CELFIT and GENRAT, were used to calculate the cell parameters and to index the diffraction peaks. The CELFIT

programme (Bracher, 1967), when supplied with sets of Miller indices (h, k, l), corresponding values of the Bragg angle (θ) and a set of approximate unit cell dimensions (a, b, c, α, β, γ), refines any or all of the latter by the method of least squares until the shifts in these parameters fall below specified limits. The GENRAT programme (Pistorius, 1968), when supplied with sets of unit cell dimensions, will generate all possible (h, k, l) reflections between two specified values of Bragg angle (θ). Reflections forbidden by space-group restrictions have then to be eliminated from the list by inspection. Both these programmes were rewritten into FORTRAN IV in order to be compatible with the IBM Model 360/50 computer, and are listed in Section 9 of this thesis as programme 1 (CELFIT) and programme 2 (GENRAT).

8.6.2. Sample preparation for cell parameter determinations.

Sodium chlorite (A.R. grade) was used as a standard to ensure angular accuracy of all measured diffraction peaks, the values accepted for sodium chlorite being those given by Mirkin (1964, p. 550). Although sodium chlorite is generally mixed with the sample and used as an internal standard, in the present case, where the lattice parameters of phyllosilicates had to be determined, it was used as an external standard since the addition of sodium chlorite would have led to a reduction of the often already small peak intensities with consequent loss of precision in the measurement of the angular position of the peaks.

The powdered phyllosilicate samples were end-loaded into the specially-designed brass sample holders (see Section 8.5.3.4.2), and a sample area approximately 50 mm long by 12.5 mm wide was presented to the X-ray beam. Integrated intensities were corrected for sample length with the aid of the nomogram shown in Figure 17. Instrumental settings were as listed in Section 8.5.5.4.1.

The δ correction (the angular discrepancy of the goniometer readings) for the specific diffractometer used was found to be as follows: from $+0.01^{\circ}$ 2θ at 20° 2θ, through 0.00 at 50° 2θ to -0.01° 2θ at 110° 2θ. This is of the same order as that determined by Chayes and MacKenzie (1957, p. 534), who found a difference of 0.0156° at 50° 2θ.

8.6.3. Measurement of angular position and intensity of peaks.

For all peaks the angular position was taken as a point in the centre of the peak, two thirds of the distance up from the base line. Intensity measurements were obtained by means of a Disc Integrator, with the strongest peak being taken as 100.

8.7. Infra-red Spectroscopy.

In the present study, infra-red absorption spectroscopy was used as an aid in the characterization of the phyllosilicates (see Part II of this thesis). The infra-red absorption spectra were obtained by means of the "alkali halide disc" technique in the following manner:

The concentration of powdered material embedded in potassium bromide was adjusted so that the level of absorption in the infra-red beam would produce an almost full-scale deflection in the region of interest. This meant that the concentration level of the analytical material was generally about 0.1 to 0.3 per cent.

Approximately 2 milligrams of preground sample material, with the grain size being less than 2.5 microns, was added to 1000 milligrams of Harshaw infrared-quality potassium bromide and blended in a Grindex or Wig-L-Bug dentists' amalgamator. Approximately 200 milligrams of the blended mixture was then weighed out and pressed in a vacuum die to form a suitably robust pellet or window. A pressure of 60 tons per square inch in a vacuum of less than 1 mm of mercury was found to be satisfactory in most cases, producing discs with a high percentage transmission (of the order of 85%).

The absorption curves were obtained by means of a Perkin Elmer Model 521 double-beam grating-type instrument. Linear wavenumber recording was used throughout at a scanning speed of 350 cm^{-1} per minute. Instrumental accuracy was assured by calibration against the water vapour spectrum and the spectrum of polystyrene.

9. COMPUTER PROGRAMMES.

Seven computer programmes used in the course of the present study are set out in subsequent pages. All the programmes were written in FORTRAN IV in order to be compatible with the IBM Model 360/50 digital computer.

Programme 1:

This programme, CELFIT, was used for the calculation of the cell parameters of the phyllosilicates (see Section 8.6.1 and Part II of this thesis).

Programme 2:

This programme, GENRAT, was used to index the reflections obtained during X-ray diffraction analysis of the phyllosilicates (see Section 8.6.1 and Part II of this thesis).

Programme 3:

This correlation covariance programme was used in the statistical evaluation of the results of the quantitative analyses carried out in the course of the present investigation (see Section 4 in Part I of this thesis).

Programme 4:

This programme was used in calculating the results of the quantitative X-ray fluorescence analyses (see Section 8.4.4.2). It makes use of Reynolds' formula to calculate the concentration of an element from analyses carried out with an international rock standard as an external reference standard. This programme was used where analyses had been performed with the aid of a flow counter, so that no dead time correction was required.

Programme 5:

This programme was used instead of programme 4 to calculate quantitative X-ray fluorescence results in those cases where a scintillation counter had been used in the analyses, so that a dead time correction was necessary. This programme incorporates the dead time correction of the scintillation counter used in the present study.

Programme 6:

This programme, NIMMNHMU, was used to calculate the mass absorption coefficient of any powdered material whose median grain size was less than 10 microns and which had been pressed into a disc (see Section 8.4.2.3). This programme makes use of equation 3 (see Section 8.4.2.2) and takes into consideration the dead time of the scintillation counter and the correction factor of 0.750 that had

to be applied for cellulose binder in the disc.

Programme 7:

This programme, NIMMNHNS, was used to calculate the mass absorption coefficient for a mixture composed of any two components whose mass absorption coefficients and relative concentrations are known (see Section 8.5.5.3).

```
LEVEL 16 ( 1 JULY 68)                    OS/360  FORTRAN H                              DATE  69.013/15.40.07

          COMPILER OPTIONS - NAME=  MAIN,OPT=02,LINECNT=56,SOURCE,BCD,NOLIST,NODECK,LOAD,MAP,NOEDIT,ID,NOXREF
1              C     CELFIT DEUR B.H.BRACHER
               C     VERTAAL DEUR D.C.MANDER.
   ISN 0002           SUBROUTINE PRELUD
   ISN 0003           COMMON PI,PIX,XIP,RA,RB,RC,RALP,RBET,RGAM,CELN
   ISN 0004           CELN=70000
   ISN 0005           RETURN
   ISN 0006           END
```

```
LEVEL 16 ( 1 JULY 68)                    OS/360  FORTRAN H                              DATE  69.013/15.40.25

          COMPILER OPTIONS - NAME=  MAIN,OPT=02,LINECNT=56,SOURCE,BCD,NOLIST,NODECK,LOAD,MAP,NOEDIT,ID,NOXREF
               C     IDENTITY , CELFIT
   ISN 0002           DIMENSION CELN(6),CELL(6),AMBDA(6),A(7,7),NOT(6),NUM1(7),NUM2(7),
                     1JH(1000),JK(1000),JL(1000),TTH(1000),SIG(1000),WTG(1000),SSO(1000
                     2),SSC(1000),O(7),SHT(6),B(6,6),TEM(6),FAM(6),TO(1000)
   ISN 0003           DOUBLE PRECISION TITLE(9)
   ISN 0004           COMMON PI,PIX,XIP,RA,RB,RC,RALP,RBET,RGAM,CELN
   ISN 0005         102 FORMAT(3I5,2F10.5,I5)
   ISN 0006         103 FORMAT(1HO,6F15.7,E12.5)
   ISN 0007         105 FORMAT(3I5,2F10.5,3F10.3)
   ISN 0008         106 FORMAT(7F15.4/15X,6F15.4/30X,5E15.4/45X,4F15.4/60X,3F15.4/75X,
                     12F15.4/90X,F15.4)
   ISN 0009         107 FORMAT(1H1/10HOITERATION,I3,4H  OF,5X,9AR///12H DIRECT CELL,
                     13F12.4,3F11.3/1X)
   ISN 0010         800 FORMAT(1H1/22HOFINAL O-CELL AND ESDS/2(///3F12.4,3F11.3))
   ISN 0011         801 FORMAT(1HO/4HO  H,4X,1HK,4X,1HL,2X,8H(1/D)**2,2X,
                     1 8H(1/D)**2,3X,7H  THETA,3X,7H  THETA,3X,7H  THETA)
   ISN 0012         802 FORMAT(20X,3HOBS,7X,4HCALC,6X,3HOBS,7X,4HCALC,4HDIFF)
   ISN 0013         803 FORMAT(1HO,9X,2HA*,13X,2HB*,13X,2HC*,11X,6HALPHA*,9X,
                     1 5HBETA*,10X,6HGAMMA*,4X,6HVOLUME)
   ISN 0014         805 FORMAT(1HO//7H MATRIX)
   ISN 0015         806 FORMAT(1HO//15H INVERSE MATRIX)
   ISN 0016         807 FORMAT(1HO//9H R-SHIFTS)
   ISN 0017         808 FORMAT(1HO/9H D-SHIFTS//6F13.6///7H D-CELL//6F13.6)
   ISN 0018             PI=3.1415926536
   ISN 0019             XIP=180.0/PI
   ISN 0020             PIX=PI/180.0
   ISN 0021             NPAR=6
   ISN 0022             MM=7
   ISN 0023         999 READ(5,809)(TITLE(I),I=1,9)
   ISN 0024         809 FORMAT(9A8)
   ISN 0025             READ(5,100)RA,RB,RC,RALP,RBET,RGAM
   ISN 0026         100 FORMAT(6F10.5)
   ISN 0027             IF (RA-1.0) 9,9,10
   ISN 0028          10 CALL RECIP
   ISN 0029             RA=CELN(1)
   ISN 0030             RB=CELN(2)
   ISN 0031             RC=CELN(3)
   ISN 0032             RALP=CELN(4)
   ISN 0033             RBET=CELN(5)
   ISN 0034             RGAM=CELN(6)
   ISN 0035           9 CONTINUE
   ISN 0036             READ(5,100)(AMBDA(I),I=1,6)
   ISN 0037             DO 111 I=1,6
   ISN 0038             IF (AMBDA(I)) 112,112,111
   ISN 0039         111 FAM(I)=(2.0/AMBDA(I))**2
   ISN 0040         112 READ (5,113)(NOT(I),I=1,6)
   ISN 0041         101 FORMAT(10I5)
   ISN 0042             DO 11 I=1,7
   ISN 0043             READ (5,101)(NUM1(I),NUM2(I)
   ISN 0044             IF (NUM1(I)) 12,12,11
   ISN 0045          11 CONTINUE
   ISN 0046          12 READ (5,100)AXINC,ANINC
```

```
ISN 0047          DO 14 I=1,1000
ISN 0048          READ(5,102)JH(I),JK(I),JL(I),THETA,SIG(I),IT
ISN 0049          WRITE(6,102)JH(I),JK(I),JL(I),THETA,SIG(I),IT
ISN 0050          IF (THETA) 15,15,16
ISN 0051       16 IQ(I)=IT
ISN 0052          SINTH=SIN(PIX*THETA)
ISN 0053          TTH(I)=THETA
ISN 0054          WTG(I)=1.0/(SIG(I)*FAM(IT)*SIN(2.0*PIX*THETA))
ISN 0055          SSQ(I)=FAM(IT)*SINTH*SINTH
ISN 0056       14 CONTINUE
ISN 0057       15 NREL=I-1
ISN 0058          CALL RECIP
ISN 0059          DO 19 I=1,6
ISN 0060       19 CELL(I)=CELN(I)
ISN 0061          NITER=0
ISN 0062       18 NITER=NITER+1
ISN 0063          WRITE(6,107)NITER,(TITLE(I),I=1,9),(CELL(I),I=1,6)
ISN 0064          DO 17 J=1,7
ISN 0065          DO 17 K=J,7
ISN 0066       17 A(J,K)=0.0
ISN 0067          COSA=COS(PIX*RALP)
ISN 0068          COSB=COS(PIX*RBET)
ISN 0069          COSG=COS(PIX*RGAM)
ISN 0070          SINA=SIN(PIX*RALP)
ISN 0071          SINB=SIN(PIX*RBET)
ISN 0072          SING=SIN(PIX*RGAM)
ISN 0073          S11=RA*RA
ISN 0074          S22=RB*RB
ISN 0075          S33=RC*RC
ISN 0076          S12=2.0*RA*RB*COSG
ISN 0077          S13=2.0*RA*RC*COSB
ISN 0078          S23=2.0*RB*RC*COSA
ISN 0079          DO 20 I=1,NREL
ISN 0080          FH=JH(I)
ISN 0081          FK=JK(I)
ISN 0082          FL=JL(I)
ISN 0083          SSC(I)=FH*FH*S11+FK*FK*S22+FL*FL*S33+FH*FK*S12+FH*FL*S13+FK*FL*S23
ISN 0084          D(7)=(SSQ(I)-SSC(I))*WTG(I)
ISN 0085          D(1)=(2.0*FH*(FH*RA+FK*RB*COSG+FL*RC*COSB))*WTG(I)
ISN 0086          D(2)=(2.0*FK*(FH*RA*COSG+FK*RB+FL*RC*COSA))*WTG(I)
ISN 0087          D(3)=(2.0*FL*(FH*RA*COSB+FK*RB*COSA+FL*RC))*WTG(I)
ISN 0088          D(4)=(-PI*FK*FL*RB*RC*SINA/90.0)*WTG(I)
ISN 0089          D(5)=(-PI*FH*FL*RA*RC*SINB/90.0)*WTG(I)
ISN 0090          D(6)=(-PI*FH*FK*RA*RB*SING/90.0)*WTG(I)
ISN 0091          DO 21 J=1,7
ISN 0092          IF(NUM1(J)) 22,22,23
ISN 0093       23 IT=NUM1(J)
ISN 0094          IK=NUM2(J)
ISN 0095       21 D(IK)=D(IK)+D(IT)
ISN 0096       22 DO 24 J=1,6
ISN 0097          IF (NOT(J)) 25,25,266
ISN 0098      266 IT=NOT(J)
ISN 0099       24 D(IT)=0.0
ISN 0100       25 DO 26 J=1,7
```



```
ISN 0101          DO 26 K=J,7
ISN 0102       26 A(J,K)=A(J,K)+D(J)*D(K)
ISN 0103       20 CONTINUE
ISN 0104          DO 199 I=1,6
ISN 0105          IF (NOT(I)) 198,198,197
ISN 0106      197 IT=NOT(I)
ISN 0107      199 A(IT,IT)=1.0
ISN 0108      198 WRITE(6,805)
ISN 0109          WRITE(6,106)((A(I,J),J=1,7),I=1,7)
ISN 0110          DO 200 I=2,NPAR
ISN 0111          L=I-1
ISN 0112          DO 200 J=1,L
ISN 0113      200 A(I,J)=0.0
ISN 0114          A(1,1)=1.0/SQRT(A(1,1))
ISN 0115          DO 202 I=2,NPAR
ISN 0116      202 A(1,I)=A(1,I)*A(1,1)
ISN 0117          DO 203 I=2,NPAR
ISN 0118          L=I-1
ISN 0119          DO 204 J=1,L
ISN 0120      204 A(I,I)=A(I,I)-A(J,I)*A(J,I)
ISN 0121          IF (A(I,I)) 998,998,997
ISN 0122      998 A(I,I)=.0001
ISN 0123          WRITE(6,996)
ISN 0124      996 FORMAT('*')
ISN 0125      997 A(I,I)=1.0/SQRT(A(I,I))
ISN 0126          LL=I+1
ISN 0127          DO 205 J=1,L
ISN 0128          DO 206 K=J,L
ISN 0129      206 A(I,J)=A(I,J)-A(K,I)*A(K,J)
ISN 0130      205 A(I,J)=A(I,J)*A(I,I)
ISN 0131          IF (I-NPAR) 222,203,222
ISN 0132      222 DO 207 J=LL,NPAR
ISN 0133          DO 211 K=1,L
ISN 0134      211 A(I,J)=A(I,J)-A(K,I)*A(K,J)
ISN 0135      207 A(I,J)=A(I,J)*A(I,I)
ISN 0136      203 CONTINUE
ISN 0137          DO 208 J=1,NPAR
ISN 0138      208 A(NPAR,J)=A(NPAR,J)*A(NPAR,NPAR)
ISN 0139          DO 210 I=2,NPAR
ISN 0140          MI=NPAR-I+1
ISN 0141          ATEMP=A(MI,MI)
ISN 0142          DO 210 J=1,MI
ISN 0143          L=I-1
ISN 0144          DO 209 K=1,L
ISN 0145          MK=NPAR-K+1
ISN 0146      209 A(MI,J)=A(MI,J)-A(MI,MK)*A(MK,J)
ISN 0147      210 A(MI,J)=A(MI,J)*ATEMP
ISN 0148          DO 213 I=2,NPAR
ISN 0149          L=I-1
ISN 0150          DO 213 J=1,L
ISN 0151      213 A(J,I)=A(I,J)
ISN 0152          DO 214 I=1,NPAR
ISN 0153          SHT(I)=0.0
ISN 0154          DO 214 J=1,NPAR
```

```
ISN 0155        214 SHT(I)=SHT(I)+A(I,J)*A(J,MM)
ISN 0156            DO 314 I=1,6
ISN 0157            IF (NUM1(I)) 315,315,316
ISN 0158        316 IT=NUM1(I)
ISN 0159            IK=NUM2(I)
ISN 0160        314 SHT(IT)=SHT(IK)
ISN 0161        315 WRITE(6,806)
ISN 0162            WRITE(6,106) ((A(I,J),J=1,7),I=1,7)
ISN 0163            WRITE(6,807)
ISN 0164            WRITE (6,106) (SHT(I),I=1,6)
ISN 0165            RA=RA+SHT(1)
ISN 0166            RB=RB+SHT(2)
ISN 0167            RC=RC+SHT(3)
ISN 0168            RALP=RALP+SHT(4)
ISN 0169            RBET=RBET+SHT(5)
ISN 0170            RGAM=RGAM+SHT(6)
ISN 0171            CALL RECIP
ISN 0172            DO 215 J=1,6
ISN 0173            SHT(J)=CELN(J)-CELL(J)
ISN 0174        215 CELL(J)=CELN(J)
ISN 0175            WRITE(6,808) (SHT(J),J=1,6),(CELL(J),J=1,6)
ISN 0176            DO 216 J=1,3
ISN 0177            IF (ABS(SHT(J))-ANINC) 216,216,18
ISN 0178        216 CONTINUE
ISN 0179            DO 217 J=4,6
ISN 0180            IF (ABS(SHT(J))-ANINC) 217,217,18
ISN 0181        217 CONTINUE
ISN 0182            DO 401 I=1,6
ISN 0183            IF (NOT(I)) 402,402,401
ISN 0184        401 CONTINUE
ISN 0185        402 FMMN=NREL-7+1
ISN 0186            RA=1001.0*RA/1000.0
ISN 0187            CALL RECIP
ISN 0188            RA=RA*1000.0/1001.0
ISN 0189            DO 403 I=1,6
ISN 0190        403 B(1,I)=(CELN(I)-CELL(I))*1000.0/RA
ISN 0191            RB=RB*1001.0/1000.0
ISN 0192            CALL RECIP
ISN 0193            RB=RB*1000.0/1001.0
ISN 0194            DO 404 I=1,6
ISN 0195        404 B(2,I)=(CELN(I)-CELL(I))*1000.0/RB
ISN 0196            RC=RC*1001.0/1000.0
ISN 0197            CALL RECIP
ISN 0198            RC=RC*1000.0/1001.0
ISN 0199            DO 405 I=1,6
ISN 0200        405 B(3,I)=(CELN(I)-CELL(I))*1000.0/RC
ISN 0201            RALP=RALP+0.01
ISN 0202            CALL RECIP
ISN 0203            RALP=RALP-0.01
ISN 0204            DO 406 I=1,6
ISN 0205        406 B(4,I)=(CELN(I)-CELL(I))*100.0
ISN 0206            RBET=RBET+0.01
ISN 0207            CALL RECIP
ISN 0208            RBET=RBET-0.01
```



```
ISN 0209            DO 407 I=1,6
ISN 0210        407 B(5,I)=(CELN(I)-CELL(I))*100.0
ISN 0211            RGAM=RGAM+0.01
ISN 0212            CALL RECIP
ISN 0213            RGAM=RGAM-0.01
ISN 0214            DO 408 I=1,6
ISN 0215        408 B(6,I)=(CELN(I)-CELL(I))*100.0
ISN 0216            DO 409 I=1,7
ISN 0217            IF (NUM1(I)) 410,410,411
ISN 0218        411 IT=NUM1(I)
ISN 0219            IK=NUM2(I)
ISN 0220            DO 409 J=1,6
ISN 0221        409 B(IK,J)=B(IK,J)+B(IT,J)
ISN 0222        410 DO 412 I=1,6
ISN 0223            IF (NOT(I)) 413,413,414
ISN 0224        414 IT=NOT(I)
ISN 0225            DO 412 J=1,6
ISN 0226        412 B(IT,J)=0.0
ISN 0227        413 FMMN=A(7,7)/FMMN
ISN 0228            DO 415 I=1,6
ISN 0229            SHT(I)=0.0
ISN 0230            DO 416 J=1,6
ISN 0231            TEM(J)=0.0
ISN 0232            DO 417 K=1,6
ISN 0233        417 TEM(J)=TEM(J)+A(J,K)*B(K,I)
ISN 0234        416 SHT(I)=SHT(I)+TEM(J)*B(J,I)
ISN 0235        415 SHT(I)=SQRT(SHT(I)*FMMN)
ISN 0236            DO 418 I=1,7
ISN 0237            IF (NUM1(I))419,419,420
ISN 0238        420 IT=NUM1(I)
ISN 0239            IK=NUM2(I)
ISN 0240        418 SHT(IT)=SHT(IK)
ISN 0241        419 WRITE(6,800)(CELL(I),I=1,6),(SHT(I),I=1,6)
ISN 0242            WRITE(6,803)
ISN 0243            COSA=COS(PIX*CELL(4))
ISN 0244            COSB=COS(PIX*CELL(5))
ISN 0245            COSG=COS(PIX*CELL(6))
ISN 0246            VOL=1.0-COSA*COSA-COSB*COSB-COSG*COSG+2.0*COSA*COSB*COSG
ISN 0247            VOL=CELL(1)*CELL(2)*CELL(3)*SQRT(VOL)
ISN 0248            WRITE(6,103)RA,RB,RC,RALP,RBET,RGAM,VOL
ISN 0249            WRITE(6,801)
ISN 0250            WRITE(6,802)
ISN 0251            DO 400 I=1,NREL
ISN 0252            IT=IO(I)
ISN 0253            XA=SQRT(1.0-SSC(I)/FAM(IT))
ISN 0254            XB=XIP*ARCOS(XA)
ISN 0255            DEL=TTH(I)-XB
ISN 0256        400 WRITE(6,105)JH(I),JK(I),JL(I),SSQ(I),SSC(I),TTH(I),XB,DEL
ISN 0257            GO TO 999
ISN 0258            STOP
ISN 0259            END
```

2

```
FORTRAN IV G LEVEL 1, MOD 3            MAIN              DATE = 69011          14/58/02              PAGE 0001

C     GENERAT
C     PROGRAM GENRAT(SR)
C     D.C.MANOER SC ADAPSIE.
C     PISTORIUS.
C  DATA CARDS.
C
C   1.  COLUMN 1.  1.
C       COLUMN 3.  IDEN,WHERE IDEN=1 FOR A CUBIC, TETRAGONAL, HEXAGONAL
C                                    OR ORTHORHOMBIC CRYSTAL.
C                                IDEN=2 FOR A MONOCLINIC CRYSTAL.
C                                IDEN=3 FOR A RHOMBOHEDRAL OR TRICLINIC
C                                    CRYSTAL.
C       COLUMN 5. K1    SEE DATA CARD 3.
C       COLUMN 7. K2    K2=1 - THE RESULTS WILL BE SORTED IN ORDER OF
C                              2*THETA VALUES BEFORE BEING PRINTED.
C                       K2=2 - NO SORTING BEFORE PRINTING.
C       COLUMN 9. K3    =1 FOR CUBIC, TETRAGONAL,HEXAGONAL AND RHOMBOHE-
C                         DRAL CRYSTALS K4 MAY BE EQUAL TO 1. THIS WILL
C                         ENSURE THAT RESULTS ARE PRINTED ONLY FOR THE
C                         FIRST OF A SET OF  H,K,L-VALUES WITH EXACTLY
C                         SIMILAR 2*THETA.
C                       =2 IF THIS FACILITY NOT WANTED
C                 N.B.    THIS FACILITY IS ONLY AVAILABLE IF K2=1  I.E.
C                         WHEN RESULTS ARE SORTED.
C       COLUMN 11-72.  ANY ALPHANUMERIC INFORMATION TO IDENTIFY PROBLEM.
C
C   2.  COLUMN   1- 8,   LAMDA.
C                9-11,   CUTT-OFF VALUE  2*THETA IN DEGREES.
C               12-14,   H-MAX.
C               15-17,   K-MAX.
C               18-20,   L-MAX.
C               21-23,   H-MIN.
C               24-26,   K-MIN.
C               27-29,   L-MIN.
C            ACCORDING TO FORMAT(F8.6,F3.0,6I3)
C
C   3. K1=1   A,B,C,D,E,F  ACCORDING  TO FORMAT 6F10.5
C      K2=2   AO,BO,CO,ALPHA,BETA,GAMMA ACCORDING TO FORMAT 6F10.5
C
0001            DIMENSION   IND1(1000),IND2(1000),IND3(1000),SSTH(1000)          MPC20030
0002            DIMENSION XNA(15)
0003       3    FORMAT(F7.3,F4.0,6I3,I1)
0004       4    FORMAT(6F9.6)                                                    MPC20040
0005       5    FORMAT(6F9.5)                                                    MPC20050
0006      92    FORMAT (///)                                                     MPC20060
0007            PII=3.1415926/2.                                                 MPC20070
0008      11    PI=3.1415926/180.                                                MPC20080
0009         10 READ(1,93,END=1000)IDEN,K1,K2,K3,(XNA(I),I=1,15)
0010            READ (1,3 ) FLAMDA,AAA,MH,MK,ML,MH,NK,NL
0011      200   FORMAT(6F10.4)
0012       93   FORMAT( 1H1,4(1X,I1),1X,15A4)
0013            CARL=0.                                                          MPC20090
0014            CUTOF=(SIN(AAA*PI/2.1))**2                                       PPC2
0015            IF(K1 -1)7,8,7

FORTRAN IV G LEVEL 1, MOD 3            MAIN              DATE = 69011          14/58/02              PAGE 0002

0016          7 READ (1,200) AO,BO,CO,ALPHA,BETA,GAMMA                           PPC2
0017            CA=COS(ALPHA *PI )                                               PPC2
0018            CB=COS ( BETA  *PI)
0019            CG=COS(GAMMA*PI)                                                 PPC2
0020            CCA=CA**2                                                        MPC20160
0021            CCB=CB**2                                                        MPC20170
0022            CCG=CG**2                                                        MPC20180
0023            X=(1.-CCA-CCB-CCG+2.*CA*CB*CG)*4./FLAMDA**2                      MPC20190
0024            A=(1.-CCA)/X/AO**2                                               MPC20200
0025            B=(1.-CCB)/X/BO**2                                               MPC20210
0026            C=(1.-CCG)/X/CO**2                                               MPC20220
0027            D=2.*(CA*CG-CB)/(X*BO*CO)                                        MPC20230
0028            E=2.*(CC*CA-CG)/(X*AO*CO)                                        MPC20240
0029            F=2.*(CA*CB-CG)/(X*AO*BO)                                        MPC20250
0030            GO TO 9                                                          MPC20260
0031          8 READ (1,200) A,B,C,D,E,F                                         PPC2
0032            X=2./FLAMDA                                                      MPC20310
0033            AA=SQRT(A) *Z                                                    PPC2
0034            BB=SQRT(B) *Z                                                    PPC2
0035            CC=SQRT(C) *Z                                                    PPC2
0036            Y=2./FLAMDA**2                                                   MPC20330
0037            CALP=D*Y/BB/CC                                                   MPC20340
0038            CBET=E*Y/CC/AA                                                   MPC20350
0039            CGAM=F*Y/AA/BB                                                   MPC20360
0040            ALP=PII-ARSIN(CALP)                                              PPC2
0041            ABET=PII-ARSIN(CBET)                                             PPC2
0042            AGAM=PII-ARSIN(CGAM)                                             PPC2
0043            SALP= SIN (ALP)                                                  PPC2
0044            SBET =SIN( ABET)
0045            SGAM=SIN( AGAM)                                                  PPC2
0046            CA=(CBET*CGAM-CALP)/(SBET*SGAM)                                  MPC20420
0047            CB=(CALP*CGAM-CBET)/(SALP*SGAM)                                  MPC20430
0048            CG=(CALP*CBET-CGAM)/(SALP*SBET)                                  MPC20440
0049            ALPHA = PII-ARSIN( CA)                                           PPC2
0050            BETA = PII-ARSIN ( CB)                                           PPC2
0051            GAMMA = PII-ARSIN ( CG)                                          PPC2
0052            ALPHA=ALPHA/PI                                                   MPC20460
0053            BETA=BETA/PI                                                     MPC20470
0054            GAMMA=GAMMA/PI                                                   MPC20480
0055            SB= SIN (BETA)                                                   PPC2
0056            SG= SIN (GAMMA)                                                  PPC2
0057            AO=1./(AA*SBET*SG)                                               MPC20520
0058            BO=1./(BB*SALP*SG)                                               MPC20530
0059            CO=1./(CC*SALP*SB)                                               MPC20540
0060            CCA=CA**2                                                        MPC20550
0061            CCB=CB**2                                                        MPC20560
0062            CCG=CG**2
0063          9 V=AO*BO*CO*SQRT(1.+2.*CA*CB*CG-CCA-CCB-CCG)
0064            WRITE (3,93) IDEN,K1,K2,K3,(XNA(I),I=1,15)                       PPC2
0065       32   FORMAT(//7H LAMDA=F10.6,8H  ASYNY=F5.0,4H  A=F11.8,4H  B=F11.8,4H MPC20610
              1 C=F11.8,4H  D=F11.8,4H  E=F11.8,4H  F=F11.8)
0066       33   FORMAT(//4H AO=F11.6,5H  BO=F11.6,5H  CO=F11.6,8H  ALPHA=F11.6,7H MPC20620
              1 BETA=F11.6,8H  GAMMA=F11.6,4H    V=F11.3)                      MPC20630
0067            WRITE (3,32) FLAMDA,AAA,A,B,C,D,E,F                              PPC2
```

```
FORTRAN IV G LEVEL 1, MOD 3            MAIN                DATE = 69011        14/08/02                PAGE 0003

0068              WRITE ( 3,33) A0,B0,C0,ALPHA,BETA,GAMMA,V                                    PP02
0069              WRITE (3,82)                                                                 PP02
0070         98   FORMAT(5H     H,5H     K,5H     L,10H    2*THETA,9H          D,17H        WP020660
                1       1/DD,20H       (SIN THETA)**2)                                        WP020670
0071              WRITE (3,99)                                                                 PP02
0072         99   FORMAT(//)                                                                   WP020690
0073              WRITE (3,93)                                                                 PP02
0074              IF(NL)37,17,37                                                               WP020700
0075         17   IF(NK)37,18,37                                                               WP020710
0076         18   IF(NH)37,16,37                                                               WP020720
0077         16   NL=NL+1                                                                      WP020730
0078         37   IF(IDEN-2)20,15,14                                                           WP020740
0079         20   DO24 I=1,1000                                                                WP020750
0080              IF(NH-MH)21,21,22                                                            WP020760
0081         22   IF(NK-MK)21,21,23                                                            WP020770
0082         23   IF(NL-ML)21,21,17                                                            WP020780
0083         21   IND1(I)=NH                                                                   WP020790
0084              IND2(I)=NK                                                                   WP020800
0085              IND3(I)=NL                                                                   WP020810
0086              AH=NH                                                                        WP020820
0087              AK=NK                                                                        WP020830
0088              AL=NL                                                                        WP020840
0089              SSTH(I)=A*AH**2+B*AK**2+C*AL**2+F*AK*AH                                      WP020850
0090              IF(SSTH(I)-CUTOF)25,25,26                                                    WP020860
0091         25   NL=NL+1                                                                      WP020870
0092              GO TO 24                                                                     WP020880
0093         26   IF(NL)27,28,27                                                               WP020890
0094         27   NK=NK+1                                                                      WP020900
0095              NL=0                                                                         WP020910
0096              GO TO 24                                                                     WP020920
0097         28   IF(NK)29,12,29                                                               WP020930
0098         29   NH=NH+1                                                                      WP020940
0099              NL=0                                                                         WP020950
0100              NK=0                                                                         WP020960
0101         24   CONTINUE                                                                     WP020970
0102              I=1000                                                                       WP020980
0103         12   IF(K2-1)31,30,31                                                             WP020990
0104         30   FORMAT(3I6,E12.9)                                                            WP021000
0105         31   DO35K=1,I                                                                    WP021010
0106              IF(SSTH(K)-CUTOF)81,81,35                                                    WP021020
0107         81   STH=SQRT (SSTH(K))                                                           PP02
0108              THETA=ARSIN (STH)                                                            PP02
0109              DTHETA=THETA*2./PI                                                           WP021040
0110              D=FLAMDA/2./STH                                                              WP021050
0111              DD=1./D**2                                                                   WP021060
0112              IF(K3-1)102,103,102                                                          WP021070
0113        103   IF (ABS(CARL-SSTH(K))-.00000001) 35,102,102                                  PP02
0114         36   FORMAT(3I5,4E14.8)                                                           WP021090
0115        102   WRITE (3,36)IND1(K),IND2(K),IND3(K),DTHETA,D,DD,SSTH(K)                      PP02
0116         35   CARL=SSTH(K)                                                                 WP021110
0117              IF(K-1000)79,40,79                                                           WP021120
0118         40   IF(IDEN-2)20,39,41                                                           WP021130
0119         15   N=0                                                                          WP021140
0120         39   DO60I=1,1000                                                                 WP021150

FORTRAN IV G LEVEL 1, MOD 3            MAIN                DATE = 69011        14/08/02                PAGE 0004

0121              IF(NH-MH)44,44,42                                                            WP021160
0122         42   IF(NK-MK)44,44,43                                                            WP021170
0123         43   IF(NL-ML)44,44,12                                                            WP021180
0124         44   IND1(I)=NH                                                                   WP021190
0125              IND2(I)=NK                                                                   WP021200
0126              IND3(I)=NL                                                                   WP021210
0127              AH=NH                                                                        WP021220
0128              AK=NK                                                                        WP021230
0129              AL=NL                                                                        WP021240
0130              SSTH(I)=A*AH**2+B*AK**2+C*AL**2+F*AH*AL                                      WP021250
0131         94   FORMAT(3I6,E12.6)                                                            WP021260
0132         96   IF(N)56,46,56                                                                WP021270
0133         46   IF(NH)59,47,59                                                               WP021280
0134         59   IF(NL)57,48,61                                                               WP021290
0135         61   NL=-NL                                                                       WP021300
0136              GO TO 60                                                                     WP021310
0137         47   IF(SSTH(I)-CUTOF)48,97,97                                                    WP021320
0138         97   IF(NL)52,50,52                                                               WP021330
0139         48   NL=NL+1                                                                      WP021340
0140              GO TO 60                                                                     WP021350
0141         57   IF(SSTH(I)-CUTOF)58,58,56                                                    WP021360
0142         58   NL=-NL+1                                                                     WP021370
0143              GO TO 60                                                                     WP021380
0144         56   N=N+1                                                                        WP021390
0145              IF(N-7)54,55,54                                                              WP021400
0146         54   NL=NL-1                                                                      WP021410
0147              GO TO 60                                                                     WP021420
0148         55   N=0                                                                          WP021430
0149         49   IF(NL+7)52,50,52                                                             WP021440
0150         52   NK=NK+1                                                                      WP021450
0151              NL=0                                                                         WP021460
0152              GO TO 60                                                                     WP021470
0153         50   IF(NK)51,12,51                                                               WP021480
0154         51   NH=NH+1                                                                      WP021490
0155              NK=0                                                                         WP021500
0156              NL=0                                                                         WP021510
0157         60   CONTINUE                                                                     WP021520
0158              I=1000                                                                       WP021530
0159              GO TO 12                                                                     WP021540
0160         14   N=0                                                                          WP021550
0161         41   DO 70I=1,1000                                                                WP021560
0162              IF(NH-MH)38,38,45                                                            WP021570
0163         45   IF(NK-MK)38,38,53                                                            WP021580
0164         53   IF(NL-ML)38,38,12                                                            WP021590
0165         38   IND1(I)=NH                                                                   WP021600
0166              IND2(I)=NK                                                                   WP021610
0167              IND3(I)=NL                                                                   WP021620
0168              AH=NH                                                                        WP021630
0169              AK=NK                                                                        WP021640
0170              AL=NL                                                                        WP021650
0171              SSTH(I)=A*AH**2+B*AK**2+C*AL**2+D*AK*AL+E*AH*AL+F*AH*AK                      WP021660
0172        101   IF(N)66,13,66                                                                WP021670
0173         13   IF(SSTH(I)-CUTOF)62,62,66                                                    WP021680
0174         62   IF(NL)64,65,63                                                               WP021690
```

```
FORTRAN IV G LEVEL 1, MOD 3            MAIN                DATE = 69011        14/09/52            PAGE 0035

0175        63    NL=-NL                                                                          WPC21530
0176              GO TO 70                                                                        WPC21540
0177        64    NL=-NL                                                                          WPC21550
0178        65    NL=NL+1                                                                         WPC21560
0179              GO TO 70                                                                        WPC21570
0180        66    N=N+1                                                                           WPC21580
0181              IF(N-7)67,68,67                                                                 WPC21590
0182        67    IF(NL)71,69,72                                                                  WPC21600
0183        71    NL=-NL                                                                          WPC21610
0184        69    NL=NL+1                                                                         WPC21620
0185              GO TO 70                                                                        WPC21630
0186        72    NL=-NL                                                                          WPC21640
0187              GO TO 70                                                                        WPC21650
0188        68    N=0                                                                             WPC21660
0189              IF(NL+3)74,73,74                                                                WPC21670
0190        73    IF(NK)78,12,78                                                                  WPC21680
0191        78    NK=NK+1                                                                         WPC21690
0192              NL=0                                                                            WPC21700
0193              GO TO 83                                                                        WPC21710
0194        74    IF(NK)75,76,77                                                                  WPC21720
0195        75    NK=-NK                                                                          WPC21730
0196        76    NK=NK+1                                                                         WPC21740
0197              GO TO 83                                                                        WPC21750
0198        77    NK=-NK                                                                          WPC21760
0199        83    NL=0                                                                            WPC21770
0200        70    CONTINUE                                                                        WPC21780
0201              I=1000                                                                          WPC21790
0202              GO TO 12                                                                        WPC21800
0203        79    GO TO 10                                                                        WPC21810
0204        30    J=I-1                                                                           WPC21820
0205               KI=I-1                                                                         WPC21830
0206              DO 92K=1,KI                                                                     WPC4183
0207              DO 91JAN=1,J                                                                    WPC4184
0208              IF(SSTH(JAN)-SSTH(JAN+1))91,91,90                                               WPC4185
0209        90    STOOR=SSTH(JAN)                                                                 WPC4186
0210              SSTH(JAN)=SSTH(JAN+1)                                                           WPC4187
0211              SSTH(JAN+1)=STOOR                                                               WPC4188
0212              INTER=IND1(JAN)                                                                 WPC4189
0213              IND1(JAN)=IND1(JAN+1)                                                           WPC4190
0214              IND1(JAN+1)=INTER                                                               WPC4191
0215              INTER=IND2(JAN)                                                                 WPC4192
0216              IND2(JAN)=IND2(JAN+1)                                                           WPC4193
0217              IND2(JAN+1)=INTER                                                               WPC4194
0218              INTER=IND3(JAN)                                                                 WPC4195
0219              IND3(JAN)=IND3(JAN+1)                                                           WPC4196
0220              IND3(JAN+1)=INTER                                                               WPC4197
0221        91    CONTINUE                                                                        WPC4198
0222              J=J-1                                                                           WPC4199
0223        92    CONTINUE                                                                        WPC4200
0224              GO TO 31                                                                        WPC4201
0225         1000 STOP                                                                            WPC4202
0226              END                                                                             WPC4203
```

3

```
FORTRAN IV G LEVEL 1, MOD 3            MAIN                DATE = 69030        15/47/21            PAGE 0001

              C     FORTRAN IV CORRELATION COVARIANCE PROGRAM                                      MAWK000
0001                REAL*8 XBAR(50),SD(90),COV(1500),SIG(50,50),DATA(50),COM                      MAWK001
0002                DIMENSION NMFAN(50),NCOV(1500),FMT(20),IDENT(20),COFFF(50)                    MAWK002
0003                DOUBLE PRECISION SDPRE ,DABS,DSORT                                            MAWK003
0004                EQUIVALENCE (SIG(1),COV(1)),(SIG(1501),NCOV(1)),(SD(1),COFFF(1))              MAWK004
0005                COMMON NOIN,NOVAR                                                             MAWK005
0006          888   READ (5,102,ERR=999) IDENT                                                    MAWK006
0007          102   FORMAT (20A4)                                                                 MAWK007
0008                WRITE(6,103)                                                                  MAWK008
0009          103   FORMAT ('1',T40,'CORRELATION/COVARIANCE PROGRAM')                             MAWK009
0010                WRITE (6,99) IDENT                                                            MAWK010
0011           99   FORMAT (T26,20A4,/)                                                           MAWK
0012                READ (5,101) NOIN,NOVAR,IZERO,IREG                                            MAWK011
0013                IF (IZERO .EQ. 0) IZERO=1                                                     MAWK012
0014                IF (NOVAR .EQ. 0) NOVAR=NOIN                                                  MAWK013
0015                IF (IREG .GT. 0) READ (5,101) IVAR,ISTART,ISTOP,INPRNT                        MAWK014
0016          101   FORMAT (16I5)                                                                 MAWK015
              C     INITIALIZE TO ZERO                                                            MAWK016
0017                NPTS=0                                                                        MAWK017
0018                NCOV=NOVAR*(NOVAR+1)/2                                                        MAWK018
0019                DO 1 I=1,NOVAR                                                                MAWK019
0020                XBAR(I)=0                                                                     MAWK020
0021           1    NMFAN(I)=0                                                                    MAWK021
0022                DO 2 I=1,NCOV                                                                 MAWK022
0023                COV(I)=0                                                                      MAWK023
0024           2    NCOV(I)=0                                                                     MAWK024
              C     COLLECT INPUT DATA, FORMAT FIRST                                              MAWK025
0025                READ (5,102) (FMT(I),I=1,20)                                                  MAWK026
              C     LOOP POINT FOR CARD READING                                                   MAWK027
0026           3    READ (5,FMT) (DATA(I),I=1,NOIN)                                               MAWK028
0027                IF (DATA(1).EQ.0.0.OR.DATA(2).EQ.0.0) GO TO 12                                MAWK029
0028                CALL TRANS(DATA)                                                              MAWK030
0029                WRITE (1,116) (DATA(I),I=1,NOVAR)                                             MAWK031
0030          116   FORMAT(1X,6D13.6)                                                             MAWK032
0031                NPTS=NPTS+1                                                                   MAWK033
0032                INDX=0                                                                        MAWK034
0033                GO TO (4,5),IZERO                                                             MAWK035
0034           4    CONTINUE                                                                      MAWK036
              C     ZEROES ARE VALID DATA                                                         MAWK037
0035                DO 6 I=1,NOVAR                                                                MAWK038
0036                CONS=DATA(I)                                                                  MAWK039
0037                XBAR(I)=XBAR(I)+CONS                                                          MAWK040
0038                DO 6 J=I,NOVAR                                                                MAWK041
0039                INDX=INDX+1                                                                   MAWK042
0040                COV(INDX)=COV(INDX)+CONS*DATA(J)                                              MAWK043
0041           6    CONTINUE                                                                      MAWK044
0042                GO TO 3                                                                       MAWK045
0043           5    CONTINUE                                                                      MAWK046
              C     ZEROES ARE MISSING INFORMATION                                                MAWK047
0044                DO 7 I=1,NOVAR                                                                MAWK048
0045                CONS=DATA(I)                                                                  MAWK049
0046                IF(CONS)8,9,8                                                                 MAWK050
0047           9    INDX=INDX+NOVAR-I+1                                                           MAWK051
0048                GO TO 7                                                                       MAWK052
0049           8    XBAR(I)=XBAR(I)+CONS                                                          MAWK053
0050                NMFAN(I)=NMFAN(I)+1                                                           MAWK054
0051                DO 10 J=I,NOVAR                                                               MAWK055
0052                COM=DATA(J)                                                                   MAWK056
```

```
0053              INDX=INDX+1                                                    HAWK057
0054              IF(CON)11,10,11                                                HAWK058
0055           11 NCOV(INDX)=NCOV(INDX)+1                                        HAWK059
0056              COV(INDX)=COV(INDX)+CON*CONS                                   HAWK060
0057           10 CONTINUE                                                       HAWK061
0058            7 CONTINUE                                                       HAWK062
0059              GO TO 3                                                        HAWK063
                C     PROCESSING SECTION                                       HAWK064
0060           12 CONTINUE                                                       HAWK065
0061              GO TO (13,14),IZERO                                            HAWK066
0062           13 CONTINUE                                                       HAWK067
0063              DO 15 I=1,NOVAR                                                HAWK068
0064           15 XBAR(I)=XBAR(I)/NPTS                                           HAWK069
0065              INDX=0                                                         HAWK070
0066              DO 16 I=1,NOVAR                                                HAWK071
0067              CONS=NPTS*XBAR(I)                                              HAWK072
0068              DO 16 J=I,NOVAR                                                HAWK073
0069              INDX=INDX+1                                                    HAWK074
0070              COV(INDX)=(COV(INDX)-CONS*XBAR(J))/(NPTS-1)                    HAWK075
0071           16 CONTINUE                                                       HAWK076
0072              GO TO 21                                                       HAWK077
0073           14 CONTINUE                                                       HAWK078
0074              DO 17 I=1,NOVAR                                                HAWK079
0075              IF(NMEAN(I)) 17,17,18                                          HAWK080
0076           18 XBAR(I)=XBAR(I)/NMEAN(I)                                       HAWK081
0077           17 CONTINUE                                                       HAWK082
0078              INDX=0                                                         HAWK083
0079              DO 19 I=1,NOVAR                                                HAWK084
0080              CONS=XBAR(I)                                                   HAWK085
0081              DO 19 J=I,NOVAR                                                HAWK086
0082              INDX=INDX+1                                                    HAWK087
0083              IF(NCOV(INDX))19,19,20                                         HAWK088
0084           20 COV(INDX)=COV(INDX)/NCOV(INDX)-CONS*XBAR(J)                    HAWK089
0085           19 CONTINUE                                                       HAWK090
0086           21 CONTINUE                                                       HAWK091
                C     OUTPUT PHASE                                             HAWK092
0087              GO TO (32,33), IZERO                                           HAWK093
0088           32 WRITE (6,109)                                                  HAWK094
0089              GO TO 34                                                       HAWK095
0090           33 WRITE(6,110)                                                   HAWK096
0091          109 FORMAT (T56,'ZEROES ARE VALID DATA')                          HAWK097
0092          110 FORMAT (T51,'ZEROES ARE MISSING INFORMATION')                 HAWK098
0093           34 CONTINUE                                                       HAWK099
0094              WRITE (6,104) NPTS,NOVAR                                       HAWK100
0095          104 FORMAT ('0',T54,'NUMBER OF READINGS',T74,I6/T54,'ORDER OF MATRIX', HAWK101
                   &T74,I6,///T58,'COVARIANCE MATRIX',//)                       HAWK102
                C     UNPACK COVARIANCE MATRIX                                 HAWK103
0096              INDX=NOCOV+1                                                   HAWK104
0097              DO 25 IPR=1,NOVAR                                              HAWK105
0098              I=NOVAR+1-IPR                                                  HAWK106
0099              DO 25 JPR=1,IPR                                                HAWK107
0100              J=NOVAR+1-JPR                                                  HAWK108
0101              INDX=INDX-1                                                    HAWK109
0102              SIG(J,I)=COV(INDX)                                             HAWK110
0103           25 CONTINUE                                                       HAWK111
0104              DO 26 I=1,NOVAR                                                HAWK112
0105              DO 26 J=1,I                                                    HAWK113
0106           26 SIG(J,I)=SIG(I,J)                                              HAWK114
```



```
                C     PRINT COVARIANCE MATRIX                                  HAWK115
0107              DO 27 I=1,NOVAR                                                HAWK116
0108              SD(I)=DSQRT(SIG(I,I))                                          HAWK117
0109              WRITE(6,105) (SIG(I,J),J=1,NOVAR)                              HAWK118
0110          105 FORMAT (7D17.6,/)                                              HAWK119
0111           27 CONTINUE                                                       HAWK120
                C     FORM AND PRINT CORR MATRIX                               HAWK121
0112              WRITE (6,107) (XBAR(I),I=1,NOVAR)                              HAWK122
0113              WRITE (6,115) (SD(I),I=1,NOVAR)                                HAWK123
0114          107 FORMAT ('1',T41,'MEAN VECTOR'//(T7,7D17.6,/))                  HAWK124
0115          115 FORMAT (///,T57,'STANDARD DEVIATIONS',//(T7,7D17.6,/))         HAWK125
0116              WRITE (6,108)                                                  HAWK126
0117          108 FORMAT ('1',T58,'CORRELATION MATRIX',//)                       HAWK127
0118              DO 28 I=1,NOVAR                                                HAWK128
0119              CONS=SD(I)                                                     HAWK129
0120              DO 29 J=1,NOVAR                                                HAWK130
0121           29 DATA(J)=SIG(I,J)/(CONS*SD(J))                                  HAWK131
0122              WRITE (6,106) (DATA(J),J=1,NOVAR)                              HAWK132
0123          106 FORMAT (T4,14F8.5,/)                                           HAWK133
0124           28 CONTINUE                                                       HAWK134
0125              IF (IREG.EQ.0) GO TO 46                                        HAWK135
0126              WRITE (6,114)                                                  HAWK136
0127          114 FORMAT ('1',T58,'REGRESSION SECTION'///)                       HAWK137
0128              DO 44 KK=ISTART,ISTOP                                          HAWK138
0129              COM=1./SIG(KK,KK)                                              HAWK139
0130              SIG(KK,KK)=1                                                   HAWK140
0131              DO 41 JJ=ISTART,ISTOP                                          HAWK141
0132           41 SIG(KK,JJ)=COM*SIG(KK,JJ)                                      HAWK142
0133              DO 44 II=ISTART,ISTOP                                          HAWK143
0134              IF(II-KK)42,44,42                                              HAWK144
0135           42 COM=-SIG(II,KK)                                                HAWK145
0136              SIG(II,KK)=0                                                   HAWK146
0137              DO 43 JJ=ISTART,ISTOP                                          HAWK147
0138           43 SIG(II,JJ)=SIG(II,JJ)+COM*SIG(KK,JJ)                          HAWK148
0139           44 CONTINUE                                                       HAWK149
0140              WRITE(6,111)IVAR,ISTART,ISTOP                                  HAWK150
0141          111 FORMAT (T38,'VARIABLE',I6,'  PREDICTED'//T38,'PREDICTORS',I6,'  -' HAWK151
                   &,I3/)                                                       HAWK152
0142              IF (MOD(INPRT,2) .EQ. 0) GO TO 51                              HAWK153
0143           52 WRITE(6,116)                                                   HAWK154
0144          116 FORMAT (///T58,'SUBMATRIX INVERSE'/)                           HAWK155
0145              DO 53 II=ISTART,ISTOP                                          HAWK156
0146              WRITE (6,117) (SIG(II,JJ),JJ=ISTART,ISTOP)                     HAWK157
0147          117 FORMAT(8(1X,E13.6))                                            HAWK158
0148           53 CONTINUE                                                       HAWK159
0149           51 CONTINUE                                                       HAWK160
0150              R=0                                                            HAWK161
0151              CONS=XBAR(IVAR)                                                HAWK162
0152              DO 39 II=ISTART,ISTOP                                          HAWK163
0153              COEFF(II)=0                                                    HAWK164
0154              DO 40 JJ=ISTART,ISTOP                                          HAWK165
0155           40 COEFF(II)=COEFF(II)+SIG(IVAR,JJ)*SIG(II,JJ)                    HAWK166
0156              R=R+SIG(IVAR,II)*COEFF(II)                                     HAWK167
0157              CONS=CONS-XBAR(II)*COEFF(II)                                   HAWK168
0158           39 CONTINUE                                                       HAWK169
0159              R=DSQRT(R/SIG(IVAR,IVAR))                                      HAWK170
0160              SDRR=DSQRT(DABS(SIG(IVAR,IVAR)*(1.-R**2)))                     HAWK171
0161              WRITE(6,112) R,SDRR                                            HAWK172
```

```
FORTRAN IV G LEVEL 1, MOD 3             MAIN            DATE = 63030        15/47/21            PAGE 0004

0162          117 FORMAT (T38,'MULTIPLE CORRELATION = ',F10.7//T38,'STANDARD DEVIATI HAWK172
                 &ON OF PREDICTION = ',F20.7,/)                                     HAWK173
0163              WRITE (6,119) CONS,(COEFF(J),J=ISTART,ISTOP)                      HAWK174
0164          119 FORMAT (T38,'CONSTANT = ',F14.6//T38,'REGRESSION COEFFICIENTS',(  HAWK175
                 &T44,F10.6//)                                                      HAWK176
0165              IF (INPRT.LT.31) GO TO 46                                         HAWK177
0166              WRITE (6,120)                                                     HAWK178
0167          120 FORMAT ('1',T54,'PREDICTED VALUE LISTING',//T54,'OBSERVED',T69,   HAWK179
                 &'PREDICTED',/)                                                    HAWK180
0168              REWIND 1                                                          HAWK181
0169              DO 46 I=1,NPTS                                                    HAWK182
0170              READ (1,116)(DATA(J),J=1,NOVAR)                                   HAWK183
0171              PRE=CONS                                                          HAWK184
0172              DO 47 J=ISTART,ISTOP                                              HAWK185
0173           47 PRE=PRE+COEFF(J)*DATA(J)                                          HAWK186
0174              WRITE (6,113)DATA(IVAR),PRE                                       HAWK187
0175          113 FORMAT (T52,F9.4,7X,F9.4)                                         HAWK188
0176           46 CONTINUE                                                          HAWK189
0177              REWIND 1                                                          HAWK190
0178              GO TO 888                                                         HAWK191
0179          999 WRITE (6,1000)                                                    HAWK192
0180         1000 FORMAT ('1')                                                      HAWK193
0181              STOP                                                              HAWK194
0182              END                                                               HAWK195

FORTRAN IV G LEVEL 1, MOD 3             TRANS           DATE = 63030        15/47/21            PAGE 0001

0001              SUBROUTINE TRANS(X)                                               HAWK196
0002              REAL*8 X(50)                                                      HAWK197
0003              COMMON NOIN,NOVAR                                                 HAWK198
0004              N1 = NOIN + 1                                                     HAWK199
0005              DO 1 J=N1,NOVAR                                                   HAWK200
0006            1 X(J) = DLOG(X(J-NOIN))                                            HAWK201
0007              RETURN                                                            HAWK202
0008              END                                                               HAWK203
```

FORTRAN IV G LEVEL 1, MOD 1 MAIN DATE = 68300 03/54/49 PAGE 0001

4

```
      C
      C CHROMIUM CONTENT OF WITWATERSRAND SAMPLES
      C REFERENCE SAMPLE USED WAS 01 NIM DUNITE WHICH CONTAINS 2750 PPM OF CR
      C FLOW COUNTER USED BUT NO DEAD TIME CORRECTION APPLIED
      C CORRECTED VALUES SHOWN ARE EXPRESSED IN PARTS PER MILLION.
      C USAMPL =UNCORRECTED INTENSITY OF SAMPLE
      C USAMBG =UNCORRECTED BACKGROUND INTENSITY OF SAMPLE
      C MUSAM =MASS ABSORBTION COEFFICIENT OF SAMPLE
      C USTAND = UNCORRECTED INTENSITY OF STANDARD
      C USTABG =UNCORRECTED BACKGROUND INTENSITY OF STANDARD
      C MUSTAN =MASS ABSORBTION COEFFICIENT OF STANDARD
      C CONSAM =CONCENTRATION OF ELEMENT IN SAMPLE
      C CONSTA =CONCENTRATION OF ELEMENT IN STANDARD
0001        REAL*8 USAMPL,USAMBG,MUSAM,USTAND,USTABG,MUSTAN,CONSAM,CONSTA,FINS
           1AM,FINSTA
0002        DIMENSION HEAD(20),DENT(2)
0003        READ (5,1000) HEAD
0004  1000  FORMAT (20A4)
0005        WRITE (6,1005) HEAD
0006  1005  FORMAT ('1',20A4)
0007        WRITE (6,1006)
0008  1006  FORMAT ('0CORRECTED VALUE    IDENTIFICATION',/)
0009        DO 1020 I=1,1000
0010        READ (5,1010,END=1040) USAMPL,USAMBG,MUSAM,USTAND,USTABG,MUSTAN,CO
           2NSTA,DENT
0011  1010  FORMAT (F6.0,2X,F6.0,2X,F6.3,2X,F6.0,2X,F6.0,2X,F6.3,2X,F6.0,2X,2A
           34)
0012        FINSAM = USAMPL-USAMBG
0013        FINSTA = USTAND-USTABG
0014        CONSAM = FINSAM/FINSTA*MUSAM/MUSTAN*CONSTA
0015  1020  WRITE (6,1030) CONSAM,DENT
0016  1030  FORMAT ('0',F11.3,13X,2A4)
0017  1040  STOP
0018        END
```

FORTRAN IV G LEVEL 1, MOD 3 MAIN DATE = 68316 22/37/54 PAGE 0001

5

```
      C THIS PROGRAM USES REYNOLD'S FORMULA TO CORRECT FOR MATRIX EFFECTS.
      C NICKEL CONTENT OF WITWATERSRAND SAMPLES.
      C REFERENCE SAMPLE USED WAS NIM DUNITE WHICH CONTAINS 2200 PPM OF NI
      C CORRECTED VALUES SHOWN ARE EXPRESSED IN PARTS PER MILLION.
      C USAMPL =UNCORRECTED INTENSITY OF SAMPLE
      C USAMBG =UNCORRECTED BACKGROUND INTENSITY OF SAMPLE
      C MUSAM =MASS ABSORBTION COEFFICIENT OF SAMPLE
      C USTAND = UNCORRECTED INTENSITY OF STANDARD
      C USTABG =UNCORRECTED BACKGROUND INTENSITY OF STANDARD
      C MUSTAN =MASS ABSORBTION COEFFICIENT OF STANDARD
      C CONSAM =CONCENTRATION OF ELEMENT IN SAMPLE
      C CONSTA =CONCENTRATION OF ELEMENT IN STANDARD
      C THIS IS WHERE THE DATA IS SPECIFIED.
0001        REAL*8 USAMPL,USAMBG,MUSAM,USTAND,USTABG,MUSTAN,CONSAM,CONSTA,FINS
           1AM,FINSTA
0002        DIMENSION HEAD(20),DENT(2)
0003        READ (5,1000) HEAD
0004  1000  FORMAT (20A4)
0005        WRITE (6,1005) HEAD
0006  1005  FORMAT ('1',20A4)
0007        WRITE (6,1006)
0008  1006  FORMAT ('0CORRECTED VALUE    IDENTIFICATION',/)
0009        DO 1020 I=1,1000
0010        READ (5,1010,END=1040) USAMPL,USAMBG,MUSAM,USTAND,USTABG,MUSTAN,CO
           2NSTA,DENT
0011  1010  FORMAT (F6.0,2X,F6.0,2X,F6.3,2X,F6.0,2X,F6.0,2X,F6.3,2X,F6.0,2X,2A
           34)
      C CALCULATION OF CORRECTION DUE TO DEAD TIME OF SCINTILLATION COUNTER.
0012        TRUSAM = USAMPL/(1.0-USAMPL*.2440D-06)
0013        TRUSBG = USAMBG/(1.0-USAMBG*.2440D-06)
0014        TRUSTA = USTAND/(1.0-USTAND*.2440D-06)
0015        TRUBAG = USTABG/(1.0-USTABG*.2440D-06)
      C THIS IS WHERE THE BACKGROUND IS SUBTRACTED FROM PEAK INTENSITY.
0016        FINSAM = TRUSAM-TRUSBG
0017        FINSTA = TRUSTA-TRUBAG
      C CALCULATION OF CONCENTRATION OF ELEMENT USING REYNOLD'S FORMULA
0018        CONSAM = FINSAM/FINSTA*MUSAM/MUSTAN*CONSTA
0019  1020  WRITE (6,1030) CONSAM,DENT
0020  1030  FORMAT ('0',F11.3,13X,2A4)
0021  1040  STOP
0022        END
```

6

```
c
c program nimmmns.
c this program is used to calculate the mass absorbtion coefficient of
c any powdered material,whose median grain size is less than 10 microns
c and which has been pressed into a disc.
c
c eyenul is the incident radiation falling on the scintillation counter
c with no pressed disc in the beam path.     (I0).
c eye is the radiation falling on the scintillation counter after it
c has passed through the pressed disc. (I).
c weight is the weight of the pressed disc weighed to 4 decimal places.
c truei0 is the incident radiation with no disc in the beam path and
c corrected for scintillation counter dead time losses.
c truei is the radiation after passing through a pressed disc and
c corrected for scintillation counter dead time losses.
c mu is the mass absorbtion coefficient of the substance.
      real*8 eyenul,eye,weight,truei0,truei,mu,final
      dimension head(20),dent(2)
      read (5,1000) head
1000  format (20a4)
      write (6,1005) head
1005  format ('1',20a4)
      write (6,1006)
1006  format ('0corrected value     identification',/)
      do 1020 i=1,1000
      read (5,1010,end=1040) eyenul,eye,weight,dent
1010  format (f6.6,4x,f6.0,4x,f5.4,5x,2a4)
c dead time correction factor of scintillation counter is .2440d-06
      truei0 = eyenul/(1.0-eyenul*.2440d-06)
      truei = eye/(1.0-eye*.2440d-06)
      mu = 1.267/weight*dlog(truei0/truei)
c 0.750 is an experimentally determined instrumental constant.
      final = mu/0.750
1020  write (6,1030) final,dent
1030  format ('0',f11.3,13x,2a4)
1040  stop
      end
/*
//go.sysin dd *
```

7

```
      c
      c program nimmhns.
      c this program calculates the mass absorbtion coefficient for a mixture
      c composed of any two components whose mass absorbtion coefficients
      c and relative concentrations are known.
      c
      c mu1 is the mass absorbtion coefficient of component 1
     c mu2 is the mass absorbtion coefficient of component 2
          real*4 mu1,mu2,muxc,mu
          integer outc1,outc2
         dimension comp1(5),comp2(5)
 1     read (5,900,end=1050) comp1,comp2
 900   format (2(5a4))
       read (5,1000) mu1,mu2
 1000  format (2f10.6)
       write (6,1010) mu1,mu2
 1010  format ('1results with mu 1 =',f6.2,'  and mu 2 = ',f6.2,/)
       write (6,1020)
 1020  format ('0',9x,'c1',21x,'c2',15x,'mu')
       write (6,1025) comp1,comp2
 1025  format ('0',5a4,3x,5a4,/)
       do 1030 i=1,101
       c1 = float(i-1)
       c2 = 100.0 - c1
       muxc = mu1*c1 + mu2*c2
       mu = muxc/100.0
       outc1 = ifix (c1)
       outc2 = ifix (c2)
       write (6,1040) outc1,outc2,mu
1030   continue
1040   format ('0',t11,i3,t34,i3,t49,f6.2)
       go to 1
1050   stop
       end
```

10. ACKNOWLEDGEMENTS.

I should like to express my appreciation and thanks to the Directorate of the National Institute for Metallurgy for permission to use, for thesis purposes, material gathered during the time that I was a member of the staff of the Mineralogy Section of the Institute.

Further, I should like to thank Dr. S.A. Hiemstra, Head of the Mineralogy Section, for the many informative discussions that I have had with him. I should like to express my gratitude to Mr. G.L.P. Urli, who contributed materially to this thesis by performing many of the analyses and computations required. I am indebted to Messrs. R.S. Birkill, J.C. van Tonder and P. Kritzinger of the Atomic Energy Board and National Institute for Metallurgy for guidance as regards computer programming. For statistical guidance I am indebted to the following members of the staff of the University of the Witwatersrand: Messrs. J. Pretorius of the Mining Department, P.A. Esselaar of the Economic Geology Research Unit and D. Hawkins of the Department of Statistics.

Finally, I should like to express my sincere appreciation to Dr. J.R. McIver, Acting Head of the Department of Geology at the University of the Witwatersrand, for the guidance that he has provided during the preparation of this thesis and for the many helpful discussions that I have had with him.

11. REFERENCES.

ABE, H. (1957) On the chlorite associated with gold ores. J. Jap. Ass. Miner. Petrol. econ. Geol., 41, 192-198.

ALBEE, A.L. (1962) Relationship between the mineral association, chemical composition and physical properties of the chlorite species. Am. Miner., 47, 851-870.

ALEXANDER, L. and KLUG, H.P. (1948) Basic aspects of X-ray absorption. Analyt. Chem., 20, 886-889.

ALEXANDER, L., KLUG, H.P. and KUMMER, E. (1948) Statistical factors affecting the intensity of X-rays diffracted by crystalline powders. J. appl. Phys. 19, 742-753.

ANDERSON, P.L. (1964) Installation and evaluation of the disc integrator for quantitative X-ray diffraction analyses. Norelco Reporter, 11, 12-13, 33, 40.

ARNOLD, R.G. (1969) Pyrrhotite phase relations below 304±6°C at less than 1 atmosphere total pressure. Econ. Geol., 64, 405-419.

BAILEY, S.W. and BROWN, B.E. (1962) Chlorite polytypism: I. regular and semi-random one layer structures. Am. Miner., 47, 819-850.

BAINES, C. (1966) Particle size effects. Proc. 5th Conf. on analytical methods. Swansea Symp., 118-121.

BEEVERS, J.R. (1967) A method for the determination of gold content of samples by solvent extraction and atomic absorption spectrophotometry. Econ. Geol., 62, 426-428.

BEUTELSPACHER, H. and VAN DER MAREL, H.W. (1968) Atlas of electron microscopy of clay minerals and their admixtures -- a picture atlas. Elsevier, Amsterdam, 333p.

BLACK, R.H. (1963) Quantitative diffractometric powder analysis of multicomponent mixtures. Norelco Reporter, 10, 14-18.

BOSCH, J.L. and ORTLEPP, R.J. (1966) An investigation of the applicability of zircon grain size as a parameter for indicating pay trends in certain Witwatersrand reefs. J.S. Afr. Inst. Min. Metall., 67, 122-131.

BRACHER, B.H. (1967) Celfit -- a computer programme to refine crystal unit cell dimensions. U.K. Atomic Energy Authority Res. Group Rpt. A.E.R.E.-5412.

BRAMMALL, A., LEECH, J.G.C. and BANNISTER, F.A. (1937) The paragenesis of cookite and hydromuscovite associated with gold at Ogufau, Carmarthenshire. Mineralog. Mag., 24, 507-516.

BRINDLEY, G.W. (1945) The effect of grain or particle size on X-ray reflections from mixed powders and alloys, considered in relation to the quantitative determination of crystalline substances by X-ray methods. Phil. Mag., 36, 347-369.

BRINDLEY, G.W. (1961) Chlorite minerals. Chapter 6 in Brown, G. Ed. The X-ray identification and crystal structures of clay minerals. Mineralog. Soc., London, 544 p.

BRINDLEY, G.W. (1965) Discussions and recommendations concerning the nomenclature of clay minerals and related phyllosilicates. Proc. 14th natn. Conf. on clay and clay minerals 1965, 27-34.

BRINDLEY, G.W. and GILLERY, F.H. (1956) X-ray identification of chlorite species. Am. Miner., 41, 169-186.

BRINDLEY, G.W. and KURTOSSY, S.S. (1961) Quantitative determination of kaolinite by X-ray diffraction. Am. Miner., 46, 1205-1215.

BROCK, B.B. and PRETORIUS, D.A. (1964) An introduction to the stratigraphy and structure of the Rand Goldfield. pp. 25-61 in Haughton, S.H. Ed. The geology of some ore deposits in Southern Africa. Geol. Soc. S. Afr., Johannesburg, 625 p.

BROWN, B.E. and BAILEY, S.W. (1963) Chlorite polytypism: II. Crystal structure of a one-layer Cr-chlorite. Am. Miner., 48, 42-61.

BROWN, G. (1951) X-ray identification and crystal structures of clay minerals. Mineralog. Soc., London, 345 p.

BROWN, G. (1955) The effect of isomorphous substitutions on the intensities of (00 ℓ) reflections of mica and chlorite-type structures. Mineralog. Mag., 30, 657-665.

BROWN, G. (1961) The X-ray identification and crystal structures of clay minerals. Mineralog. Soc. (Clay Minerals Group), London, 544 p.

BROWN, G. (1965) Significance of recent structure determinations of layer silicates for clay studies. Clay Minerals, 6, 73-82.

BROWN, G. and NORRISH, K. (1952) Hydrous micas. Mineralog. Mag., 29, 929-932.

BUERGER, M.J. and KENNEDY, G.C. (1958) An improved specimen holder for the focussing-type X- ray spectrometer. Am. Miner., 43, 756-757.

BURNS, A.F. and WHITE, J.L. (1963) Removal of potassium alters b dimension of muscovite. Science, N.Y., 139, 39-40.

BYSTRÖM-ASKLUND, A.M. (1966) Sample cups and a technique for sideward packing of X-ray diffractometer specimens. Am. Miner., 51, 1233-1237.

CHAKRABORTY, K.L. (1960) Geology and mineralogical characters of the Indian chromites. Econ. Geol., 60, 1660-1668.

CHAYES, F. and MACKENZIE, W.S. (1957) Experimental error in determining certain peak locations and distances between peaks in X-ray powder diffractometer patterns. Am. Miner., 42, 534-547.

COETZEE, F. (1965) Distribution and grain size of gold, uraninite, pyrite and certain other heavy materials in gold-bearing reefs of the Witwatersrand Basin. Trans. geol. Soc. S. Afr., 68, 61-89.

COUSINS, C.A. (1956) The value distribution of economic minerals with special reference to the Witwatersrand reefs. Trans. geol. Soc. S. Afr., 59, 95-121.

COOK, N.G.W., JOUGIN, N.C. and WIEBOLS, G.A. (1968) Rock cutting and its potentialities as a new method of mining. J. S. Afr. Inst. Min. Metall. 68, 435-454.

CROWLEY, M.S. and ROY, R. (1960) The effect of formation pressures on sheet structures -- a possible case of Al-Si ordering. Geochim. cosmochim. Acta, 18, 94-100.

CULLITY, B.D. (1956) Elements of X-ray diffraction. Addison-Wesley, Reading, Mass., 514 p.

DAVIES, D.N. (1949) The development and mineralization of the Ventersdorp Contact Reef at Venterspost. Unpub. M.Sc. Thesis, University Witwatersrand.

DEER, W.A., HOWIE, R.A. and ZUSSMAN, J. (1966) An introduction to the rock forming minerals. Longmans, London, 528 p.

DE KOCK, W.P. (1940) The Ventersdorp Contact Reef. Its nature, mode of occurrence and economic significance with special reference to the West Rand. Trans. geol. Soc. S. Afr., 43, 85-107.

DE KOCK, W.P. (1964) The geology and economic significance of the West Wits Line. In The geology of some ore deposits in Southern Africa. Vol. 1. Gold deposits of the Witwatersrand Basin. Geol. Soc. S. Afr., Johannesburg, 323-386.

DE VRIES, J.L. (1966) Counting strategy. Conf. X-ray Spectrosc., Swansea, 5 p.

FISHER, R.A. and YATES, F. (1957) Statistical tables for biological, agricultural and medical research. Oliver and Boyd, London, 138 p.

FLEISCHER, M. (1965) Summary of new data on rock samples G1 and W1, 1962-1965. Geochim. cosmochim. Acta, 29, 1263-1283.

FOSTER, M.D. (1956) Correlation of dioctahedral potassium micas on the basis of their charge relations. Bull. geol. Surv. U.S., 1036-D, 57-67.

FOSTER, M.D. (1962) Interpretation of the composition and classification of the chlorites. Prof. Pap. U.S. geol. Surv., 414A, 33 p.

FRANKEL, J.J. (1939) The green colour of the Hospital Hill Quartzites. Trans. geol. Soc. S. Afr., 42, 15-17.

FRANKEL, J.J. (1944) On silicates and dusts from the Witwatersrand gold mines. J. S. Afr. chem. metall. min. Soc., 44, 169-179.

FRANKEL, J.J. (1949) Dickite from the Witwatersrand gold mines. Mineralog. Mag., 28, 582-586.

FRONDEL, C. (1958) Systematic mineralogy of uranium and thorium. Bull. geol. Surv. U.S., 1064, 400 p.

FULLER, A.O. (1958) A contribution to the petrology of the Witwatersrand System. Trans. geol. Soc. S. Afr., 61, 19-45.

GARRETT, R.G. and NICHOL, I. (1969) Factor analysis as an aid in the interpretation of regional geochemical stream sediment data. Quart. Colorado School of Mines, 64, 245-263.

GAUDETTE, H.E., GRIM, R.E. and METZGER, C.F. (1966) Illite: a model based on the sorption behaviour of cesium. Am. Miner., 51, 1649-1656.

GIBBS, R.J. (1965) Error due to segregation in quantitative clay mineral X-ray diffraction mounting techniques. Am. Miner., 50, 741-751.

GIBBS, R.J. (1967) Quantitative X-ray diffraction analysis using only mineral standards extracted from the samples to be analysed. Clay Minerals, 7, 79-90.

GRIM, R.E. (1968) Clay mineralogy. McGraw-Hill, New York, 596 p.

GRIM, R.E., BRAY, R.H. and BRADLEY, W.F. (1937) The mica in argillaceous sediments. Am. Miner., 22, 813-829.

GUDE, A.J. and HATHAWAY, J.C. (1961) A diffractometer mount for small samples. Am. Miner., 46, 993-998.

HARMAN, H. (1960) Modern factor analysis. Univ. Chicago Press, Chicago, 469 p.

HAYASHI, H. and OINUMA, K. (1963) X-ray and infrared studies on the behaviour of clay minerals on heating. Clay Sci., 1, 8-28.

HAYASHI, H. and OINUMA, K. (1963) X-ray and infrared studies on the behaviour of clay minerals on heating. Clay Sci., 1, 134-154.

HAYASHI, H. and OINUMA, K. (1965) Relationship between infrared absorption spectra in the region 450-900 cm^{-1} and chemical composition of chlorite. Am. Miner., 50, 476-483.

HAYASHI, H. and OINUMA, K. (1967) Si-O absorption band near 1000 cm^{-1} and OH absorption bands of chlorite. Am. Miner., 52, 1206-1210.

HAYSLETT, H.T. (1968) Statistics made simple. W.H. Allen, London, 251 p.

HEINRICH, E.W. (1965) Further information on the geology of chromian muscovites. Am. Miner., 50, 758-762.

HEINRICH, E.W. and LEVINSON, A.A. (1955) Studies in the mica group: polymorphism among high-silica sericites. Am. Miner., 40, 983-995.

HENDRICKS, S.B. and JEFFERSON, M.E. (1939) Polymorphism of the micas. Am. Miner., 24, 729-771.

HEY, M.H. (1954) A new review of the chlorites. Mineralog. Mag., 30, 277-292.

HEYSTEK, H. (1955) Some hydrous micas in South African clays and shales: clays and clay minerals. Publs. natn. res. Coun. Can. No. 395, 337-354.

HIEMSTRA, S.A. (1968) The mineralogy and petrology of the uraniferous conglomerate of the Dominion Reefs Mine, Klerksdorp area. Trans. geol. Soc. S. Afr., 71, part I, 1-65.

HIEMSTRA, S.A. (1968) The geochemistry of the uraniferous conglomerate of the Dominion Reefs Mine, Klerksdorp area. Trans. geol. Soc. S. Afr., 71, part I, 67-100.

HIROSHI, A. (1957) On the chlorite associated with gold ores. J. Jap. Ass. Miner. Petrol. econ. Geol., 41, 192-198.

IMBRIE, J. (1963) Factor and vector analysis programs for analyzing geologic data. Tech. Rept. No.6 Contr. NONR. 1228(26). Off. Nav. Res. Geogr. Br.

IMBRIE, J. and VAN ANDEL, T.H. (1964) Factor analysis of heavy mineral data. Bull. geol. Soc. Am., 75, 1131-1155.

INGAMELLS, C.O. and SUHR, N.H. (1963) Chemical and spectrochemical analysis of standard silicate samples. Geochim. cosmochim. Acta, 27, 897-910.

JACKSON, W.W. and WEST, J. (1930) The crystal structure of muscovite $KAl_2(AlSi_3)O_{10}(OH)_2$. Zeit. Krist., 76, 211-227.

JACKSON, W.W. and WEST, J. (1933) The crystal structure of muscovite $KAl_2(AlSi_3)O_{10}(OH)_2$. Zeit. Krist., 85, 160-164.

JACOB, R.E. (1966) The geology of the Vaal Reefs Gold Mine, Western Transvaal. Unpub. M.Sc. Thesis, Rhodes Univ.

KARLAK, R.F. and BURNETT, D.S. (1966) Quantitative phase analysis by X-ray diffraction. Analyt. Chem., 38, 1741-1745.

KERRICK, D.M. (1968) Experiments on the upper stability limit of pyrophyllite at 1.8 Kilobars and 3.9 Kilobars water pressure. Am J. Sci., 26, 204-214.

KLUG, H.P. and ALEXANDER, L.E. (1954) X-ray diffraction procedures for polycrystalline and amorphous materials. Wiley, New York, 716 p.

KNOPF, A. (1929) The Mother Lode System of California. Prof. Pap. U.S. geol. Surv., 157, 38 p.

KODAMA, H. (1962) Interpretation of X-ray powder patterns of some hydromuscovites from Japan, with reference to their alkali contents. Clay Sci., 1, 88-99.

KODAMA, H, and OINUMA, K. (1962) Identification of kaolin minerals in the presence of chlorite by X-ray diffraction and infrared absorption spectra. Clays and Clay Minerals. Proc. 11th natn. Conf., 13, 236-249.

KOEN, G.M. (1956) Discussion of paper by Cousins, C.A. (1956), 115-117.

KOEN, G.M. (1961) The genetic significance of the size distribution of uraninite in Witwatersrand bankets. Trans. geol. Soc. S. Afr., 64, 23-55.

KRIGE, D.G. (1960) On the departure of ore value distributions from the lognormal model in South African gold mines. J.S. Afr. Inst. Min. Metall., 60, 231-244.

LAPHAM, D.M. and JARON, M.G. (1964) Rapid, quantitative illite determination in polycomponent mixtures. Am. Miner., 49, 272-276.

LENNOX, D.H. (1957) Monochromatic diffraction absorption technique for direct quantitative X-ray analysis. Analyt. Chem., 29, 766-770.

LEROUX, J., LENNOX, D.H. and KAY, K. (1953) Direct quantitative X-ray analysis. Analyt. Chem., 25, 740-743.

LEROUX, J. and MAHMUD, M. (1959) Influence of goniometric arrangement and absorption in qualitative and quantitative analysis of powders by X-ray diffractometry. Advances in X-ray analysis, 3, 337-347. Plenum Press, New York, 376 p.

LEVINSON, A.A. (1955) Studies in the mica group: polymorphism among illites and hydrous micas. Am. Miner., 49, 41 - 49.

LIEBENBERG, W.R. (1948) Rare minerals in the banket of the Witwatersrand System. U.S. Atomic Energy Com. NP 3992 (restricted).

LIEBENBERG, W.R. (1955) The occurrence and origin of gold and radioactive minerals in the Witwatersrand System, the Dominion Reef, the Ventersdorp Contact Reef and the Black Reef. Trans. geol. Soc. S. Afr., 58, 101-254.

LIEBENBERG, W.R. (1960) On the origin of uranium, gold and osmiridium in the conglomerates of the Witwatersrand goldfields. Neues Jb. Miner. Abh., 94, 831-867.

MACKENZIE, R.C. and MILNE, A.A. (1953) The effect of grinding on micas. I. Muscovite. Mineralog. Mag., 30, 178-185.

MALAN, S.P. (1959) The petrology and mineralogy of the rocks of the Dominion Reef System near Klerksdorp. Unpub. M.Sc. Thesis. Univ. Witwatersrand.

MARTIN, R.T. (1955) Reference chlorite characterization for chlorite identification in soil clays. Clays and Clay Minerals. Publs. natn. Res. Coun. Can., No. 395, 117-145.

MAXWELL, D.T. and HOWER, J. (1967) High-grade diagenesis and low-grade metamorphism of illite in the Pre-Cambrian Belt Series. Am. Miner., 52, 834-857.

MCLACHLAN, C. (1968) A grain size study of zircon and chromite in the Vaal Reef of the Klerksdorp Goldfield, Transvaal. Unpub. M.Sc. Thesis. Univ. Witwatersrand.

MIRKIN, L.I. (1964) Handbook of X-ray analysis of polycrystalline material. Consultants Bureau, New York, 731 p.

MOORE, C.A. (1968) Quantitative analysis of naturally occurring multicomponent mineral systems by X-ray diffraction. Clays and Clay Minerals, 16, 325-336.

MUNRO, A.H. (1966) A review of the use of statistical techniques in ore valuation. In Symposium on mathematical statistics and computer applications in ore valuation, March, 1966. J. S.Afr. Inst. Min. Metall., 3-12.

NEL, L.T., JACOBS, H., ALLAN, J.J. and BOZZOLI, G.R. (1937) "Wonderstone". Geol. Surv. Bull. Un. S. Afr., No. 8, 30 p.

NELSON, B.W. and ROY, R. (1958) Synthesis of chlorites and their structural and chemical composition. Am. Miner., 43, 707-725.

NISKANEN, E. (1964) Quantitative mineral analysis of kaolin-bearing rocks by X-ray diffraction. Analyt. Chem., 36, 1268-1271.

NISKANEN, E. (1964) Reduction of orientation effects in the quantitative X-ray diffraction analysis of kaolin minerals. Am. Miner., 49, 705-714.

NORRISH, K. and TAYLOR, R.M. (1962) Quantitative analysis by X-ray diffraction. Clay Minerals Bull.,5, 98-109.

OINUMA, K. and HAYASHI, H. (1965) Infrared study of mixed layer clay minerals. Am. Miner., 50, 1213-1227.

OINUMA, K. and HAYASHI, H. (1966) Infrared study of clay minerals from Japan. J. Tokyo Univ. (Nat. Sci.), 1-15.

OLIVER, W.M., TAYLOR, J.D., MALLETT, R.C. and STEELE, T.W. (1968) The determination of gold and silver in pyrite and banket by atomic absorption spectrophotometry. S. Afr. Nat. Inst. Metall. Rpt. 348, 6 p.

PAULING, L. (1930) The structure of chlorites. Proc. natn. Acad. Sci., 16, 578-582.

PETRUK, W. (1964) Determination of the heavy atom content in chlorite by means of the X-ray diffractometer. Am. Miner., 49, 61-71.

PHILLIPS, W.R. (1963) A differential thermal study of the chlorites. Mineralog. Mag., 33, 404-414.

PHILLIPS, W.R. (1964) A numerical system of classification for chlorites and septechlorites. Mineralog. Mag., 33, 1114-1124.

PISTORIUS, C.W.F.T. (1968) C.S.I.R., Pretoria, personal communication.

PRETORIUS, D.A. (1966) Conceptual geological models in exploration of gold mineralization in the Witwatersrand Basin. In Symposium on mathematical statistics and computer applications in ore valuation, March 1966. J. S. Afr. Inst. Min. Metall., 382 p.

RADOSLOVICH, E.W. (1960) The structure of muscovite $KAl_2(Si_3Al)O_{10}(OH)_2$. Acta crystallogr., 13, 919-932.

RADOSLOVICH, E.W. (1962) The cell dimensions and symmetry of layer-lattice silicates. II. Regression relations. Am. Miner., 47, 617-636.

RADOSLOVICH, E.W. and NORRISH, K. (1962) The cell dimensions and symmetry of layer-lattice silicates. I. Some structural considerations. Am. Miner., 47, 599-616.

RAMDOHR, P. (1958) New observations on the ores of the Witwatersrand in South Africa and their genetic significance. Akademie Verlag (Berlin). Trans. geol. Soc. S. Afr., 61, (annexure) 50 p.

REYNOLDS, R.C. (1963) Matrix corrections in trace element analysis by X-ray fluorescence: estimation of the mass absorption coefficient by Compton scattering. Am. Miner., 48, 1133-1143.

REYNOLDS, R.C. (1967) Estimation of mass absorption coefficients by Compton scattering: improvements and extensions of the method. Am. Miner., 52, 1493-1502.

RICHMOND, S.B. (1964) Statistical analysis. Ronald Press Co., New York, 633 p.

ROUBAULT, M., DE LA ROCHE, H. and GOVINDARAJU, K. (1966) Report on four geochemical rock standards: granites GR, GA, GH and basalt BR. Sci. de la Terre, 11, 107-121.

SAAGER, R. (1969) The relationship of silver and gold in the Basal Reef of the Witwatersrand System, South Africa. Mineral. Deposita (Berl.), 4, 93-113.

SAAGER, R. and ESSELAAR, P.A. (1969) Factor analysis of geochemical data from the Basal Reef, Orange Free State Goldfield, South Africa. Econ. Geol., 64, 445-451.

SAKSENA, B.D. (1964) Infrared hydroxyl frequencies of muscovite, phlogopite and biotite micas in relation to their structures. Trans. Faraday Soc., 60, 1715-1725.

SCHIDLOWSKI, M. (1965) Eine bemerkenswerte Verwachsung von Uranpecherz und Gold aus den Witwatersrand-Konglomeraten. Naturwissenschaften, 52, 1-2.

SCHIDLOWSKI, M. (1966) Mineralbestand und Gefügebilder in Faseraggregaten von kohliger Substanz ('Thucholith') aus den Witwatersrand Konglomeraten. Contr. Miner. Petrol., 12, 365-380.

SCHIDLOWSKI, M. (1966) Beitrage zur Kenntnis der radioaktiven Bestandteile der Witwatersrand-Konglomerate. II. Brannerit und 'Uranpecherzgeister'. N. Jb. Miner. Abh., 105, 310-324.

SCHIDLOWSKI, M. (1968) The gold fraction of the Witwatersrand conglomerates from the Orange Free State goldfield (South Africa). Mineralium Deposita (Berl.), 3, 344-363.

SCHLIEPHAKE, R.W. (1965) Direkte Bestimmung des Massenschwächungs-koeffizienten für die röntgenographische Phasenanalyse. Neues Jb. Miner. Abh., 2, 192-203.

SCHMALZ, R.F. (1958) A technique for quantitative modal analysis by X-ray diffraction and its application to modern sediments of the Peru-Chile trench. Ph.D. Thesis. Harvard University, Cambridge, Mass.

SCHOEN, R. (1962) Semi-quantitative analysis of chlorites by X-ray diffraction. Am. Miner., 47, 1384-1392.

SCHWEIGART, H. and VON RAHDEN, H. (1964) Oolithische Strukturen in Pyriten des Ventersdorp-Contact-Reefs, Süd Afrika. Geol. Rundschau, 54, 1143-1148.

SHARP, J.W.N. (1949) The economic auriferous bankets of the Upper Witwatersrand beds and their relationship to sedimentation features. Trans. geol. Soc. S. Afr., 52, 265-288.

SHIROZU, H. (1958) X-ray patterns and cell dimensions of chlorites. Mineralog. J. Sapporo, 2, 209-223.

SHIROZU, H. (1962) Thermal reaction of iron chlorites. Clay Sci., 1, 108-113.

SHIROZU, H. (1963) Structural changes of some chlorites by grinding. Mineralog. J. Sapporo, 4, 1-11.

SIMPSON, D.J. (1951) Some results of radiometric logging in the boreholes of the Orange Free State gold fields and neighbouring areas. Trans. geol. Soc. S. Afr., 54, 99-133.

SMITH, J.V. and YODER, H.S. (1956) Experimental and theoretical studies of the mica polymorphs. Mineralog. Mag., 31, 209-235.

SNYMAN, C.P. (1965) Possible biogenic structures in Witwatersrand thucholite. Trans. geol. Soc. S. Afr., 68, 225-235.

SPEARMAN, C. (1904) General intelligence, objectively determined and measured. Ann. Jour. Psych., 15.

STUBICAN, V. and ROY, R. (1961) Isomorphous substitution and infra-red spectra of the layer-lattice silicates. Am. Miner., 46, 32-51.

STUCKEY, J.L. (1925) The pyrophyllite deposits of the Deep River region of North Carolina. Econ. Geol., 20, 442-463.

SWANSON, H.E., MORRIS, M.C., STINCHFIELD, R.P. and EVANS, E.H. (1962) Standard X-ray diffraction powder patterns. Nat. Bur. Stand. Monogr. 25, sect 1.

TARR, W.A. (1937) Terminology of the chemical siliceous sediments. Nat. Res. Council Rpt. Comm. on sedimentation, 1937-1938, 18-47.

TATLOCK, D.B. (1966) Rapid modal analysis of some felsic rocks from calibrated X-ray diffraction patterns. Bull. geol. Surv. U.S., No. 1209, 41 p.

TUDDENHAM, W.M. and LYON, R.J.P. (1959) Relation of infrared spectra and chemical analysis for some chlorites and related minerals. Analyt. Chem., 31, 377-380.

VELDE, B. (1965) Experimental determination of muscovite polymorph stabilities. Am. Miner., 50, 436-449.

VELDE, B. and HOWER, J. (1963) Petrological significance of illite polymorphism in Paleozoic sedimentary rocks. Am. Miner., 48, 1239-1254.

VILJOEN, R.P. (1964) Petrographic and mineragraphic aspects of the Main Reef and Main Reef Leader of the Main Bird Series, Witwatersrand System. Unpub. M.Sc. Thesis. Univ. Witwatersrand.

VOLBORTH, A. (1963) X-ray spectrographic determination of all major oxides in igneous rocks, and precision and accuracy of a direct pelletizing method. Nevada Bur. Min. Rep. No. 6, A1-A71.

VOLBORTH, A. (1965) Dual grinding and X-ray analysis of all major oxides in rocks to obtain true composition. Appl. Spectrosc., 19, 1-7.

VON ENGELHARDT, W. (1955) Möglichkeiten der quantitativen Phasenanalyse von Tonen mit Röntgenstrahlen. Z. Kristallogr., 106, 430-459.

VON RAHDEN, H.V.R. (1964) A detailed mineralogical investigation of the Ventersdorp Contact Reef at Venterspost and Libanon Gold Mines, West Rand, with special reference to the mode of mineralization of this horizon. Unpub. M.Sc. Thesis. Univ. Witwatersrand.

VON RAHDEN, H.V.R. (1968) A literature survey of the vertical distribution of gold and uranium in various auriferous reefs. S. Afr. Nat. Inst. Metall., Rep. 269, 12 p.

VON RAHDEN, H.V.R. and HIEMSTRA, S.A. (1967) A preliminary mineralogical investigation of pyrite from the Kimberley and Main Reefs, Vogelstruisbult Gold Mine. S. Afr. Nat. Inst. Metall., Rep. 140, 10 p.

VON RAHDEN, H.V.R. and HIEMSTRA, S.A. (1967) The mineralogy of uranium in Western Areas ores. S. Afr. Nat. Inst. Metall., Rep. 237.

WEAVER, C.E. (1956) A discussion on the origin of clay minerals in sedimentary rocks. Publs. Natn. Res. Coun. Can., No. 566, 159-173.

WEAVER, C.E. (1958) The effect and geological significance of potassium "fixation" by expandable clay minerals derived from muscovite, biotite, chlorite and volcanic material. Am. Miner., 43, 839-861.

WEBBER, G.R. (1965) Second report of analytical data for CAAS syenite and sulphide standards. Geochim. cosmochim. Acta, 29, 229-248.

WEISKIRCHNER, W. (1960) Zur Bestimmung des Massenschwächungskoeffizienten. Neues Jb. Miner. Mh., 60, 257-265.

WHITESIDE, H.C.M. (1941) An unusual suite of minerals from a vug in a quartz vein in the Kimberley Series, Daggafontein Mines Ltd. Trans. geol. Soc. S. Afr., 44, 121-126.

WILLIAMS, P.P. (1959) Direct quantitative diffractometric analysis. Analyt. Chem., 31, 1842-1844.

WILSON, N.L., OOSTHUIZEN, D.H., BRINK, W.C.J. and TOENS, P.D. (1964) The geology of the Vaal Reef Basin in the Klerksdorp area. pp. 399-416 in Haughton, S.H. Ed. The geology of some ore deposits in Southern Africa. Geol. Soc. S. Afr., Johannesburg, 625 p.

WINCHELL, A.N. (1936) A third study of the chlorites. Am. Miner., 21, 642-651.

YODER, H.S. and EUGSTER, H.P. (1955) Synthetic and natural muscovites. Geochim. cosmochim. Acta, 8, 225-280.

ZUSSMAN, J. (1967) Physical methods in determinative mineralogy. Academic Press, London, 514 p.

ZVYAGIN, B.B. (1967) Electron-diffraction analysis of clay mineral structures. Plenum Press, New York, 364 p.